PAGES 1397–1516

ISSN 0003–2654

ROYAL SOCIETY OF CHEMISTRY

The Analyst

A monthly international journal dealing with all branches of the theory and practice of analytical chemistry, including instrumentation and sensors, and physical, biochemical, clinical, pharmaceutical, biological, environmental, automatic and computer-based methods

Vol.115 No.11 November 1990

The Analyst

The Analytical Journal of The Royal Society of Chemistry

Editorial Manager, Analytical Journals: Judith Egan

Editor, *The Analyst*
Harpal S. Minhas
The Royal Society of Chemistry,
Thomas Graham House, Science Park,
Milton Road, Cambridge CB4 4WF, UK
Telephone 0223 420066.
Fax 0223 423623. Telex No. 818293 ROYAL.

US Associate Editor, *The Analyst*
Dr J. F. Tyson
Department of Chemistry,
University of Massachusetts,
Amherst MA 01003, USA
Telephone 413 545 0195
Fax 413 545 4490

Senior Assistant Editor
Paul Delaney

Assistant Editors
Brenda Holliday, Paula O'Riordan, Sheryl Whitewood

Editorial Secretary: Claire Harris

Advertisements: Advertisement Department, The Royal Society of Chemistry, Burlington House, Piccadilly, London, W1V 0BN. Telephone 071-437 8656. Telex No. 268001. Fax 071-437 8883.

The Analyst (ISSN 0003–2654) is published monthly by The Royal Society of Chemistry, Thomas Graham House, Science Park, Milton Road, Cambridge CB4 4WF, UK. All orders accompanied with payment should be sent directly to The Royal Society of Chemistry, The Distribution Centre, Blackhorse Road, Letchworth, Herts. SG6 1HN, England. 1990 Annual subscription rate UK £220.00, EEC £233.00, Rest of World £253.00, USA $493.00. Purchased with *Analytical Abstracts* UK £476.00, EEC £520.00, Rest of World £547.00, USA $995.00. Purchased with *Analytical Abstracts* plus *Analytical Proceedings* UK £561.00, EEC £611.00, Rest of World £645.00, USA $1187.00. Purchased with *Analytical Proceedings* UK £279.00, EEC £296.50, Rest of World £321.00, USA $626.00 Air freight and mailing in the USA by Publications Expediting Inc., 200 Meacham Avenue, Elmont, NY 11003.
USA Postmaster: Send address changes to: *The Analyst,* Publications Expediting Inc., 200 Meacham Avenue, Elmont, NY 11003. Second class postage paid at Jamaica, NY 11431. All other despatches outside the UK by Bulk Airmail within Europe, Accelerated Surface Post outside Europe. PRINTED IN THE UK.

Information for Authors

Full details of how to submit material for publication in *The Analyst* are given in the Instructions to Authors in the January issue. Separate copies are available on request.

The Analyst publishes papers on all aspects of the theory and practice of analytical chemistry, fundamental and applied, inorganic and organic, including chemical, physical, biochemical, clinical, pharmaceutical, biological, environmental, automatic and computer-based methods. Papers on new approaches to existing methods, new techniques and instrumentation, detectors and sensors, and new areas of application with due attention to overcoming limitations and to underlying principles are all equally welcome. There is no page charge.

The following types of papers will be considered:

Full papers, describing original work.

Short papers: the criteria for originality are the same as for full papers, but short papers generally report less extensive investigations or are of limited breadth of subject matter.

Communications, which must be on an urgent matter and be of obvious scientific importance. Rapidity of publication is enhanced if diagrams are omitted, but tables and formulae can be included. Communications receive priority and are usually published within 5–8 weeks of receipt. They are intended for brief descriptions of work that has progressed to a stage at which it is likely to be valuable to workers faced with similar problems. A fuller paper may be offered subsequently, if justified by later work.

Reviews, which must be a critical evaluation of the existing state of knowledge on a particular facet of analytical chemistry.

Every paper (except Communications) will be submitted to at least two referees, by whose advice the Editorial Board of *The Analyst* will be guided as to its acceptance or rejection. Papers that are accepted must not be published elsewhere except by permission. Submission of a manuscript will be regarded as an undertaking that the same material is not being considered for publication by another journal.

Regional Advisory Editors. For the benefit of potential contributors outside the United Kingdom, a Panel of Regional Advisory Editors exists. Requests for help or advice on any matter related to the preparation of papers and their submission for publication in *The Analyst* can be sent to the nearest member of the Panel. Currently serving Regional Advisory Editors are listed in each issue of *The Analyst.*

Manuscripts (four copies typed in double spacing) should be addressed to:

Harpal S. Minhas, Editor, *The Analyst,*
Royal Society of Chemistry,
Thomas Graham House,
Science Park, Milton Road,
CAMBRIDGE CB4 4WF, UK *or:*

Dr. J. F. Tyson
US Associate Editor, *The Analyst*
Department of Chemistry
University of Massachusetts
Amherst MA 01003, USA

Particular attention should be paid to the use of standard methods of literature citation, including the journal abbreviations defined in Chemical Abstracts Service Source Index. Wherever possible, the nomenclature employed should follow IUPAC recommendations, and units and symbols should be those associated with SI.

All queries relating to the presentation and submission of papers, and any correspondence regarding accepted papers and proofs, should be directed to the Editor, *The Analyst* (address as above). Members of the Analytical Editorial Board (who may be contacted directly or via the Editorial Office) would welcome comments, suggestions and advice on general policy matters concerning *The Analyst.*

Fifty reprints are supplied free of charge.

Use of X-ray Fluorescence Spectrometry for the Direct Multi-element Analysis of Coal Powders

Bill C. Pearce, John W. F. Hill and Ian Kerry
British Coal Corporation, Scientific Services Laboratory Technical Department, Ashby Road, Stanhope Bretby, Burton on Trent, Staffordshire DE15 0QD, UK

The evaluation of automated X-ray fluorescence (XRF) spectrometry for the elemental analysis of UK coals is described. The XRF determination of chlorine is now used for coal pricing purposes and phosphorus levels are reported routinely in order to monitor the quality of coal. The data on elemental composition which can be generated rapidly by direct XRF analysis of pressed coal powders enable values of slagging and fouling indices to be determined with acceptable accuracy. Such factors have wide application in industry for predicting the combustion characteristics of coal, including slagging and fouling propensities. The relative standard deviations for the elements chlorine, sulphur and phosphorus and the calculated slagging index and fouling factor are less than 7%. The accuracy of the method when compared to standard reference coals is acceptable with detection limits which range from 0.04 and 0.05% m/m for the major elements Al and Si, respectively, 0.01% m/m for minor elements and 0.002% m/m for the trace element phosphorus.

Keywords: *Coal analysis; automated X-ray fluorescence analysis; slagging and fouling indices; chlorine and phosphorus determination*

The use of X-ray fluorescence (XRF) spectrometry for the analysis of coal powders is extremely attractive for the following reasons. (*i*) It is a multi-element technique; (*ii*) it provides good sensitivity down to trace concentrations in coal; (*iii*) only minimal and non-destructive sample preparation is required; (*iv*) absorption is low because the matrix is basically carbon; and (*v*) the technique is highly suitable for automation and provides a high throughput of samples.

The increasing demands for improved efficiency for coal analysis without loss of precision and accuracy have resulted in investigations into instrumental methods as alternatives to British Standard (BS) procedures.[1] The BS tests require lengthy digestion procedures, for example the determination of sulphur involves fusion of the coal with Na_2CO_3 - MgO to convert all of the sulphur into sulphate followed by gravimetric determination of the precipitated barium sulphate. Such procedures take several hours per sample and are very labour intensive. Elemental composition is normally determined by first ashing the coal at 815 °C and digesting the ash either in hydrofluoric acid or sodium hydroxide. The solutions are then analysed by classical methods or by atomic absorption and colorimetric techniques. (For a more detailed appraisal see reference 1.)

The use of XRF for coal analysis is not new and has been utilised by British Coal for many years to determine ash content.[2,3] The methods, however, were only applicable to a single source of coal and required frequent updating as the coal matrix changed. The technique has been assessed by Kiss[4] for the determination of sulphur, chlorine and other elements in American brown coal. However, the concentrations reported for sulphur and chlorine were very much lower than those typically found in coals mined in the UK. Kuhn and Henderson[5] have reported a successful wavelength dispersive XRF system to determine some 21 minor and trace elements in coal. Pearce[6] and Thorne *et al.*[7] have described multi-element XRF analysis using multi-variable regression procedures for the automated analysis of coal. The use of XRF for production and quality control monitoring in other fields is already well established[8,9] and its suitability for automation accepted.[10] X-ray fluorescence analysis in metallurgical and mineral analysis has been shown to be both precise and accurate.[11]

A problem with accurate quantitative XRF analysis is that observed X-ray emission intensities must be corrected for matrix effects that cause absorption or enhancement of the X-ray signal.[12–14] Synthetic matrix-matched standards for coal are extremely difficult to produce.[15] This is primarily due to the great variation in the forms of bonding of the elements found in coal. For example, sulphur can exist as pyrites, organic sulphur bound to the coal substance and sulphates all of which produce widely different X-ray emissions for the same mass concentration. The proportions in coal of the three forms are also extremely variable, hence, a calibration set would require a wide range to cover all of the sulphur compounds. The particle sizes of the mineral species present are also variable and affect the intensity values obtained.

The use of a "fundamental parameters" approach to calculate theoretical correction constants[16] is complex and would require extensive chemical analysis and computation of data. Therefore, in order to establish accurate XRF analysis of powders, particle size effects[17–19] and mineralogical effects[12,20] need to be considered. Alternatively, some workers,[21,22] have suggested the use of thin films for coal analysis using XRF techniques in order to avoid complications with matrix effects. The current daily determinations required on coal samples supplied to the National Laboratory of the British Coal Corporation at Bretby are in excess of 5000. The use of automated XRF spectrometry for the accurate determination of chlorine, phosphorus and elements used to calculate coal combustion parameters[23,24] is described in this paper. The results have been validated using certified reference materials and comparison with coals analysed by British Standard methods[1] and currently accepted standard methods.

Experimental

Apparatus

The following apparatus was used: an Applied Research Laboratories (ARL) Model 72000S simultaneous, vacuum X-ray fluorescence spectrometer fitted with a 3-kW rhodium anode end-window tube, controlled by a DEC PDP 11-03 computer; a microprocessor-controlled scanner covering the wavelength range 0.085–0.72 nm; and monochromators for the elements carbon, sodium, magnesium, aluminium, silicon, phosphorus, sulphur, chlorine, potassium, calcium, titanium, manganese, iron and rhodium. The detector flow gases used were: 90% argon - 10% methane for sodium and 21% carbon dioxide - 79% helium for carbon, other detectors sealed. A 36-

sample autochanger with a sample rotation facility to take steel sample rings with a 40-mm outside diameter, 35-mm internal diameter and 14-mm depth [Fisons Instruments, Applied Research Laboratories (ARL), Crawley, Sussex, UK]; mains voltage stabiliser, 220 V, 42 A (Watford Control Instruments, Watford, UK); a recirculating water cooler, Model IC20 (Flowcool Systems, Somercotes, Derbyshire, UK); a pelletising press and tool for the above steel rings, Model HTP-40 (Herzog, Osnabrück, FRG); a planetary ball mill (Christison, Team Valley, Gateshead, UK); a Malvern laser particle sizing instrument (Malvern Instruments, Malvern Link, Malvern, Worcestershire, UK); and a top-pan balance to weigh up to 20 ± 0.05 g were also used. The room was air conditioned to 21 ± 2 °C.

Reagents

Lithium tetraborate flux (*Spectroflux* 100). (Johnson Matthey, Royston, Hertfordshire, UK.)

AnalaR grade chemicals. (BDH, Poole, Dorset, UK.)

Sample Selection

There are very few coals with certified elemental concentrations which can be used for calibration of the XRF spectrometer. It was therefore necessary to select and analyse a calibration set of coals. The ARL software used can accommodate up to 99 samples to produce calibration equations and interference corrections. It was decided that a maximum number of standards should be used where possible to cover the wide range of elemental concentrations found in clean coals of less than 5% m/m ash and coal blends used for electricity generation which have up to 25% m/m ash content.

For the calibration of chlorine, 99 coals covering the commercial outputs of the Nottinghamshire and Derbyshire coalfields were initially chosen. A wider selection of 88 coals from the Southern, Northern and Midland coalfields in the UK were selected for the remaining elements to give a broader coal sample selection and wider rank range. The resulting calibration algorithms were evaluated by analysing a further 99 coals of the Southern coalfields, National Institute of Standards and Technology Standard Reference Material (NIST SRM) 1632a Trace Elements in Coal (Bituminous) and three Alpha Resources certified coals.

Sample Preparation

The coal samples were air-dried and ground to less than 212 μm. Air-dried coal is necessary as the inherent moisture appears to act as a binding agent. In addition chlorine in coal is volatile and thus could be lost in any forced drying process. A portion of this air-dried coal (8 ± 0.05 g) was weighed on the top-pan balance. This was transferred into the steel sample ring and placed on the pressing tool of the Herzog pelletising press. The clean tool head was placed in position and the coal powder pelletised under a load of 16 tonnes for 25 s. The tool head was polished to better than a 1 μm finish and re-polished after every thousand pressings to maintain the smooth surface of the pressed coal pellet.

Lithium tetraborate beads were prepared by fusion in the accepted way using various additions of AnalaR grade reagents to produce eight beads containing a low and a high X-ray intensity for each element. These beads were used to adjust day to day spectrometer drift utilising a two-point correction. Carbon was drift-corrected using a perspex bottom standard and a polythene top standard. The elemental constituents in each of the beads are given in Table 1.

Instrument Conditions

The rhodium X-ray tube was operated at 50 kV, 40 mA with re-circulating water cooling to stabilise the X-ray output. The counting time was regulated by an internal titanium target for 12×10^6 counts which gives approximately 35 s per analysis. The spectrometer was thermostatically stabilised at 30.5 ± 0.5 °C and the instrument sited in an air conditioned room at 21 ± 2 °C. The above criteria are necessary to maintain accurate calibrations for long periods, *i.e.*, to give maximum routine analysis throughputs. The vacuum in the spectrometer was maintained at <100 μm of Hg with a sample pre-vacuum of up to 100 μm of Hg.

The details of the monochromator used for each element are given in Table 2. Two unusual monochromators are required for sulphur and chlorine which use an NaCl crystal in preference to the general LiF crystal because it has better reflectivity for sulphur and chlorine X-rays, particularly in light element matrices. However, the chlorine background is poorer due to secondary emission from the crystal.

The carbon total reflection monochromator overcomes the problem of detecting low energy X-rays by using a crystal that allows some higher energy X-rays to be reflected which are eliminated using magnets. X-rays of lower energy than carbon are also reflected but these are absorbed prior to the crystal by a polypropylene film in the primary slit. Two further features of this monochromator are the use of activated alumina to improve the local vacuum, and He - CO_2 flow gas rather than the normal Ar - CH_4.

Calibration

The set of calibration coals were thoroughly analysed chemically by the following methods. Chlorine determination using BS 1016[1] Eschka mixture fusion; sulphur determination with the Leco SC132 sulphur analyser. The ash elements were determined after hydrofluoric acid digestion of the coal ash using inductively coupled plasma optical emission spec-

Table 1. Make up of beads for drift correction

	Bottom standard		Top standard	
Bead	Monochromators	Compounds added	Monochromators	Compounds added
A ..	C	Perspex	—	—
B ..	Na, K	Na_2CO_3, K_2CO_3	Rh	Na_2CO_3, K_2CO_3
C ..	Mg, Al, P, Ca, Ti, Fe	MgO, Al_2O_3, $Ca_3(PO_4)_2$, TiO_2, Fe_2O_3	Si	SiO_2
D ..	Si, S, Cl	SiO_2, K_2SO_4,	Na, Mg	Na_2CO_3, MgO
E ..	Rh	LiCl	P, S	$Ca_3(PO_4)_2$, K_2SO_4
F ..	—	—	C	Polythene
G ..	—	—	Al, K, Ca, Ti, Fe	Al_2O_3, K_2SO_4, $Ca_3(PO_4)_2$, TiO_2, Fe_2O_3
H ..	—	—	Cl	LiCl

Table 2. Monochromator details

Element	Crystal	X-ray line	Wavelength/nm
C	—*	K	4.4
Na	TlAP†	K	1.1909
Mg	ADP‡	K	0.9889
Al	PET§	K	0.8339
Si	PET	K	0.7126
P	PET	K	0.6155
S	NaCl	K	0.5373
Cl	NaCl	K	0.4729
K	LiF_{200}	K	0.3742
Ca	LiF_{200}	K	0.3360
Ti	LiF_{200}	K	0.2750
Fe	LiF_{200}	K	0.1937
Rh	LiF_{200}	Compton K	—
Scanner	LiF_{200}	—	0.085–0.350
Scanner	PET	—	0.180–0.720

* Total reflection monochromator.
† Thallium hydrogen phthalate.
‡ Ammonium dihydrogen phosphate.
§ Pentaerythritol.

trometry (ICP-OES).[25] The ash content was determined using the incineration method of BS 1016.[1] The elemental composition of the coal can be calculated from the determined ash analysis using the equation:

$$\text{Element (\% m/m) air-dried coal basis} = \frac{\text{elemental oxide in the ash (\% m/m)} \times \text{ash (\% m/m) air-dried basis}}{100 \times \text{factor converting elemental oxide into element}}$$

Previous work[6] has shown that the amount of coal used to press the pellet affected the X-ray intensity. For the range of elements determined there was an increase of between 0.4 and 3% and for rhodium backscatter an increase of 30% in the mass range 4–12 g. This increase was greatest up to 8 g with a linear increase up to 12 g. This is because the lower X-ray energies of the elements determined up to iron have an effective layer thickness of <1 mm. Hence an increase in over-all thickness has a negligible effect on the intensities of these elements from 4 g upwards. However, rhodium K backscatter radiation would be expected to increase up to its effective layer thickness of approximately 10 mm in a carbon-based matrix. This is greater than the typical depth of 3 mm of an 8-g pellet.

As rhodium backscatter is used in the elemental correction procedure, a constant mass for the coal pellet is essential. A mass of 8 g was selected because at this mass the backscatter change becomes linear and in practice 8 g of coal are as much as can be transferred accurately into the steel ring. The sample rotation facility was used for the bead standard analysis to overcome inhomogeneity problems produced by the fusion procedure. However, it was found unnecessary for this to be used for coal samples because they gave virtually identical intensities irrespective of whether they were rotated. The coals were therefore analysed without rotation.

The sets of calibration coals were pelletised and the spectrometer was drift-corrected using the bead standards. The coals were then analysed twice consecutively and the average intensities for each element stored in a regression file. Nominal concentrations for the above coals were then matched with the stored intensities. From these data the calibration was performed using the Multi-Variable Regression (MVR) program provided by the manufacturer which allows for various mathematical correction models and polynomials to be assessed. The model used was the Lucas-Tooth - Pyne intensity model[26] illustrated simply below.

$$c_a = (A_0 + A_1 I_a + A_2 I_a^2)(1 + K_i I_i + L_i I_i^2)$$

where c_a = the concentration of the element affected; I_a = intensity of the element affected; A_0, A_1, A_2 = the coefficients of the polynomial calibration graph; I_i = intensity of interfering elements; and K_i, L_i = the coefficients of the polynomial for interfering elements. The effect of interfering elements was calculated from the MVR software using a selection of elements which included silicon or rhodium backscatter intensity. These elements generally give good absorption corrections as they reflect the ash content of the coal. Mineralogical effects in coal were also corrected, *e.g.*, iron and sulphur in pyrites, and calcium and sulphur in gypsum.

Table 3. Calibration graphs listing interfering elements (SEE = standard error of the estimate)

Element	Interfering element	SEE, % m/m
Na	Si	0.012
Mg	Si	0.016
Al	Fe, Rh backscatter	0.109
Si	Al, Ca	0.133
P	Si	0.003
S	Mg, Ca, Fe, Rh backscatter	0.072
Cl	Si	0.018
K	Al, Rh backscatter	0.024
Ca	Mg, Rh backscatter	0.022
Ti	Si	0.006
Fe	Rh backscatter	0.056
(Ash)	C, K, Ca, Fe, Rh backscatter	0.61

Table 4. Mean size of coal during grinding in a planetary ball mill

Grinding time/min	Mean particle size/μm: Coal G1	Coal G2	Coal G3	Coal G4	Coal G5
0	38	57	59	62	55
5	26	36	32	31	33
10	22	27	24	28	29
15	19	24	22	24	28
20	19	22	20	22	28
30	18	20	18	21	28
60	20	20	18	23	28

The calibration was initially assessed using a calculated standard error of the estimate (SEE) of the differences between nominal and calculated values using the equation:

$$\text{SEE} = \sqrt{\frac{(c_N - c_c)}{n - 2}}$$

where c_N = the nominal concentration of the element; c_c = the calculated concentration of the element; and n = the number of samples. The interfering elements used are listed in Table 3. The calibration and correction equations were stored in the coal analysis program file together with the necessary data for drift corrections. Several other coal combustion parameters can be derived from the XRF elemental analysis such as slagging and fouling propensities.[23] These are discussed in more detail below.

Ash content is broadly proportional to silicon concentration and a regression of silicon counts *versus* nominal ash content was evaluated. The base : acid ratio is the ratio of basic to acidic oxides in the ash.

$$\text{Base : acid ratio} = \frac{Fe_2O_3 + CaO + Na_2O + MgO + K_2O}{SiO_2 + Al_2O_3 + TiO_2}$$

This gives an indication of the potential melting-point of coal ash on combustion particularly in the secondary superheater and economiser tubes. Such fouling deposits impede gas flows and dramatically reduce efficiency and are related according to the equation:

$$\text{Fouling factor} = \text{base : acid ratio} \times Na_2O \text{ (\% m/m) in the ash.}$$

The base : acid ratio is also useful for determining the slagging characteristics of ash material. Such material is difficult to remove from the combustion zone of the boiler and its

accumulation provides an insulating layer preventing efficient heat exchange taking place:

Slagging index = base : acid ratio × sulphur content of coal (% m/m) (dry basis)

Particle Size Effects

It has been established that particle size has a considerable effect on X-ray intensity.[17–19] To determine the magnitude of the effect, five coals were ground in duplicate for up to 1 h in a planetary ball mill. The resulting mean particle size of the coal was determined by laser diffraction. The results are given in Table 4 and the mean size is plotted in Fig. 1. They show that the particle size reaches a minimum after about 20 min of grinding. The values obtained were between 18 and 28 μm. Further reduction in size is prevented by "plating" (one particle coalescing with another) of coal particles. In fact grinding for long periods (a few hours) begins to produce an increase in particle size because of this effect.

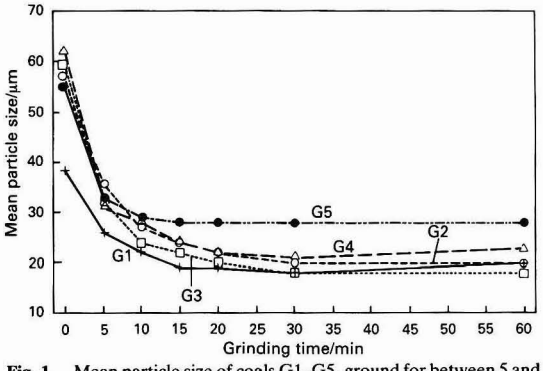

Fig. 1. Mean particle size of coals G1–G5, ground for between 5 and 60 min in a planetary ball mill

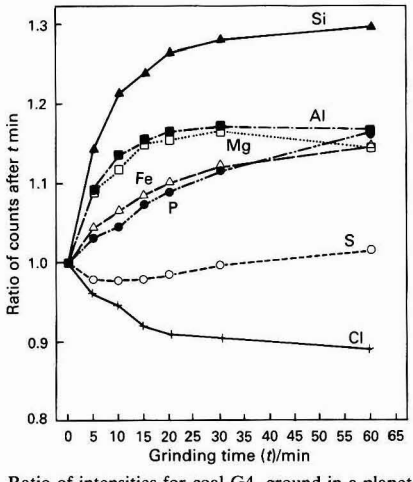

Fig. 2. Ratio of intensities for coal G4, ground in a planetary ball mill for between 5 and 60 min, to unground coal

Table 5. Comparison of SEEs for ground and, planetary ball mill, finely ground coals

Element	SEE, % m/m: Ground coal	Finely ground coal
Na	0.013	0.012
Mg	0.016	0.014
Al	0.109	0.085
Si	0.133	0.116
P	0.003	0.002
S	0.072	0.070
Cl	0.018	0.019
K	0.024	0.022
Ca	0.022	0.016
Ti	0.006	0.006
Fe	0.056	0.054

The ground coals were pressed and their intensities measured. A typical graph of intensity *versus* grinding time is shown in Fig. 2. This shows an increase of up to 30% for silicon, 10–20% for the other ash elements, a slight decrease followed by a small increase for sulphur and a 10% decrease in chlorine intensity. Fig. 2 also shows that the intensities were constant after about 40 min of grinding which is twice the time necessary to achieve an apparent minimum particle size. This suggests coal minerals are still being ground to a smaller particle size after 20 min but that "plating" of discrete coal particles may be occurring.

A plausible explanation for the reduction in sulphur and chlorine intensities after prolonged grinding might be loss of the volatile components of these elements. However, great care was taken in grinding to eliminate "hot-spots" and BS 1016 Eschka analysis of the ground coals before and after grinding confirmed no loss of these elements. The reduction in intensity for sulphur and chlorine is more likely to be explained by increased absorption as a result of a reduction in particle size of minerals present in coal, *e.g.*, iron pyrites and marcasite.

This study proved that the XRF intensity is particle size dependent. The effect of particle size was evaluated by grinding 10 g of the calibration set (99 samples) for 20 min and then an 8-g portion was pressed. The coals were used for calibration and compared with the SEE for the 99 unground coals. The results are given in Table 5. Silicon, aluminium and calcium show a significant improvement whereas the other elements show only a marginal improvement. This indicates that ground coals would give better results for the determination of silicon, aluminium and calcium. However, the time involved to fine grind and clean out the mill after each sample does not allow for rapid analysis of large numbers of samples. Therefore, the use of such grinding procedures has not been justified.

The rhodium Compton backscatter is affected by the thickness of the pellet which decreases very slightly when the coal is finely ground because of increased packing density. However, the SEEs of elements, using rhodium as an interfering element, do not all improve significantly, suggesting this is not an important factor in the fine grinding of coals.

Precision and Accuracy of XRF Method

The precision of the XRF method for determining chlorine, sulphur, phosphorus and rhodium backscatter is given in Table 6. These results indicate a mean relative standard deviation (RSD) of 0.31% for chlorine, 0.20% for sulphur, 3.7% for phosphorus and 0.88% for rhodium backscatter. Table 7 indicates the precision of the XRF method for the determination of ash, the silica ratio, base : acid ratio, slagging index and fouling factor. The RSDs for all these parameters are less than 6%, the lowest being for the silica ratio (0.4%) and highest for the fouling factor (5.5%).

The accuracy of the method for elemental analysis was evaluated by comparison with certified reference materials (Table 8) and also by comparison with ICP-OES, Leco and BS 1016 elemental analysis (Table 9). Scatter diagrams of chlorine and phosphorus determinations *versus* accepted values are given in Figs. 3 and 4. The XRF results presented indicate, that with the exception of sodium, there is excellent agreement with certified reference values and analyses of coal using currently accepted methods of elemental analysis (including BS 1016[1] methods).

Table 6. Reproducibility of analysing ten different pellets for two selected coals X and Y

	Chlorine, % m/m		Sulphur, % m/m		Phosphorus, % m/m		Silicon-based ash, % m/m	
Pellet No.	X	Y	X	Y	X	Y	X	Y
1	0.193	0.302	2.110	1.464	0.0601	0.0041	18.272	2.867
2	0.193	0.301	2.115	1.460	0.0598	0.0042	18.209	2.916
3	0.193	0.300	2.109	1.458	0.0602	0.0039	18.123	2.867
4	0.193	0.299	2.116	1.457	0.0594	0.0038	18.155	2.822
5	0.192	0.299	2.110	1.455	0.0591	0.0035	18.172	2.852
6	0.192	0.300	2.121	1.457	0.0592	0.0044	18.139	2.826
7	0.193	0.300	2.109	1.454	0.0603	0.0040	18.398	2.877
8	0.193	0.299	2.109	1.456	0.0597	0.0042	18.170	2.820
9	0.192	0.298	2.112	1.458	0.0601	0.0037	18.316	2.844
10	0.193	0.300	2.113	1.460	0.0594	0.0040	18.445	2.810
Mean	0.1927	0.2998	2.1124	1.4579	0.05973	0.00398	18.240	2.850
SD	0.000483	0.00113	0.00395	0.00288	0.000437	0.000266	0.000483	0.0326
RSD, %	0.25	0.38	0.19	0.20	0.73	6.67	0.62	1.14
Chemical value*	0.18	0.29	2.41	1.52	0.060	0.003	19.13	2.86

* See reference 1.

Table 7. Analysis of a typical coal sample to evaluate the precision of the method

Coal pressing	Ash, % m/m	Silica ratio	Base : acid ratio	Slagging index	Fouling factor
1	15.18	77.46	0.264	0.484	0.621
2	15.86	77.07	0.267	0.500	0.601
3	15.77	76.93	0.269	0.508	0.600
4	16.32	76.69	0.270	0.521	0.546
5	15.75	76.93	0.269	0.506	0.594
6	15.75	76.84	0.268	0.501	0.582
7	15.80	76.77	0.270	0.509	0.608
8	15.21	77.09	0.268	0.494	0.651
9	16.36	76.39	0.273	0.525	0.564
10	15.87	77.11	0.266	0.505	0.575
Mean	15.79	76.93	0.268	0.505	0.594
Range	15.18–16.36	76.39–77.46	0.264–0.273	0.484–0.525	0.546–0.651
SD	0.38	0.29	0.002	0.012	0.030
95% Confidence limit	15.79 ± 0.76	76.93 ± 0.58	0.268 ± 0.004	0.505 ± 0.024	0. 594 ± 0.060
RSD, %	2.4	0.4	0.7	2.4	5.5

Table 8. Comparison of XRF values with certified or reference values

Sample	Value, % m/m	Na	Mg	Al	Si	P	S	Cl	K	Ca	Ti	Fe	(Ash)
NIST SRM 1632a	Certified	0.08	0.10*	2.97*	5.9*	0.028*	1.62 (1.45)*	0.08*	0.42	0.23	0.16*	1.11	ND†
	XRF	0.09	0.12	2.61	5.59	0.025	1.42	0.09	0.40	0.27	0.15	1.07	ND
		0.09	0.12	2.61	5.61	0.025	1.42	0.09	0.41	0.27	0.15	1.08	ND
		0.10	0.12	2.61	5.60	0.025	1.41	0.09	0.41	0.27	0.15	1.08	ND
	Mean XRF	0.09	0.12	2.61	5.60	0.025	1.42	0.09	0.41	0.27	0.15	1.08	ND
Alpha 2753‡	Certified	0.01	0.04	1.07	1.96	0.014	ND	ND	0.15	0.04	0.06	0.36	7.3
	XRF	0.05	0.04	0.94	2.00	0.018	0.82	0.05	0.15	0.07	0.06	0.34	6.7
		0.05	0.04	0.94	2.00	0.018	0.82	0.05	0.15	0.07	0.06	0.34	6.6
		0.04	0.04	0.94	2.01	0.018	0.82	0.05	0.15	0.07	0.06	0.34	6.6
	Mean XRF	0.05	0.04	0.94	2.00	0.018	0.82	0.05	0.15	0.07	0.06	0.34	6.6
Alpha 2757‡	Certified	0.05	0.08	1.34	3.14	0.004	ND	ND	0.31	0.12	0.08	1.46	12.5
	XRF	0.07	0.11	1.42	3.12	0.010	2.79	0.04	0.32	0.16	0.07	1.47	12.1
		0.08	0.11	1.42	3.10	0.010	2.79	0.04	0.31	0.16	0.07	1.47	12.2
		0.07	0.11	1.42	3.11	0.010	2.79	0.04	0.32	0.16	0.07	1.48	12.3
	Mean XRF	0.07	0.11	1.42	3.11	0.010	2.79	0.04	0.32	0.16	0.07	1.47	12.2
Alpha 2751‡	Certified	0.31	0.10	0.52	0.77	0.010	ND	ND	0.03	0.60	0.03	0.30	5.2
	XRF	0.20	0.13	0.43	0.49	0.012	0.51	0.03	0.01	0.70	0.03	0.31	4.1
		0.20	0.13	0.43	0.49	0.012	0.49	0.03	0.01	0.67	0.03	0.29	4.0
		0.20	0.13	0.43	0.49	0.012	0.49	0.03	0.01	0.66	0.03	0.29	3.9
	Mean XRF	0.20	0.13	0.43	0.49	0.012	0.50	0.03	0.01	0.68	0.03	0.30	4.0

* Values determined by Gladney, see reference 27.
† ND = Not determined.
‡ Alpha Resources Inc., Stevensville, MI, USA.

Table 9. Statistical summary of comparison of XRF coal analysis and ICP ash analysis, Leco sulphur elemental analysis and BS 1016 elemental analysis

	Concentration (air-dried coal basis), % m/m										
	Na	Mg	Al	Si	P	S	Cl*	K	Ca	Ti	Fe
Range	0.03–0.31	<0.01–0.45	0.52–4.34	0.30–7.75	0.002–0.053	0.95–2.87	0.08–0.79	0.01–1.05	0.07–1.00	0.02–0.17	0.26–2.09
Mean XRF	0.128	0.134	1.648	2.813	0.018	1.617	0.332	0.317	0.329	0.066	1.064
Mean ICP and BS 1016	0.110	0.136	1.666	2.819	0.018	1.575	0.337	0.333	0.317	0.066	1.095
Average difference, XRF − ICP; $n = 99$	0.018	−0.002	−0.017	0.004	0.0005	0.041	−0.006	−0.016	0.011	<0.001	−0.032
Standard deviation of difference	0.014	0.029	0.124	0.273	0.0046	0.118	0.018	0.029	0.028	0.013	0.092
95% Confidence limit	±0.028	±0.058	±0.248	±0.546	±0.0092	±0.236	±0.036	±0.058	±0.056	±0.026	±0.184

* BS 1016 Eschka determination on the coal.

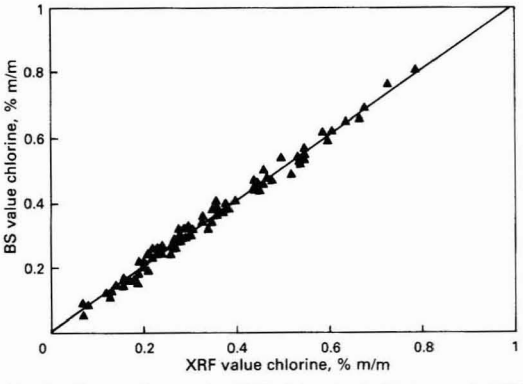

Fig. 3. Scatter diagram for XRF determined chlorine against BS chlorine determination for 99 test coals

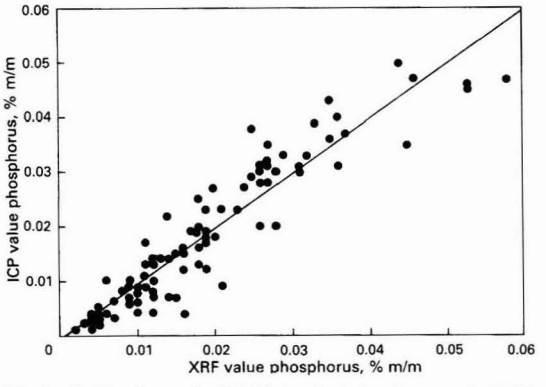

Fig. 4. Scatter diagram for XRF determined phosphorus against ICP values for 99 test coals

Table 10. Comparison of XRF coal analysis with BS ash content and derived ash parameters

	Ash (air-dried basis), % m/m	Silica ratio	Base : acid ratio	Slagging index	Fouling factor
Range	3.3–31.9	48.5–84.0	0.20–0.61	0.18–1.12	0.11–3.14
Mean XRF	12.540	70.770	0.334	0.538	0.681
Mean ICP and BS1016	12.299	70.474	0.334	0.558	0.647
Average difference, XRF − ICP, $n = 99$	0.16	0.27	0.004	−0.015	0.039
Standard deviation of difference	0.64	1.87	0.031	0.084	0.164
95% Confidence limit	±1.28	±3.74	±0.062	±0.168	±0.328

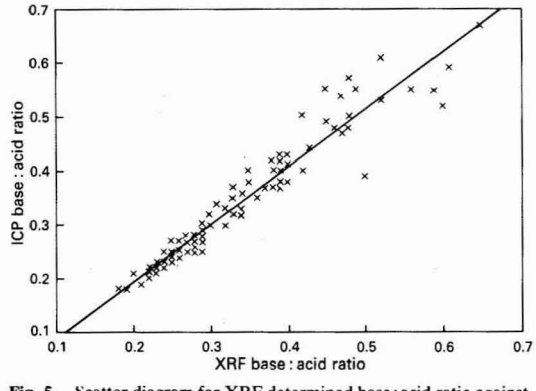

Fig. 5. Scatter diagram for XRF determined base : acid ratio against ICP values for 99 test coals

Table 10 shows the results for XRF determinations of ash, silica ratio, base : acid ratio, slagging index and fouling factor. The scatter diagram for base : acid ratio *versus* ICP values is given in Fig. 5. The values presented for 99 coal samples show good agreement for all of the parameters with the exception of the fouling factor. This can be largely attributed to the inaccuracies in the XRF determination of sodium. The detection limits for the elemental analysis of coal by XRF are given in Table 11. This shows detection limits range from 0.04 and 0.05% m/m for the major elements aluminium and silicon, respectively, to 0.01% m/m for the minor elements and 0.002% m/m for the trace element phosphorus.

Conclusions

X-ray fluorescence spectrometry has been applied successfully to rapid elemental determinations of pressed coal powders. In addition, XRF elemental analyses have been utilised successfully to calculate coal combustion parameters such as slagging

Table 11. Detection limits of elements for XRF coal analysis

Element	Na	Mg	Al	Si	P	S	Cl	K	Ca	Ti	Fe
Detection limit, % m/m	0.01	0.01	0.04	0.05	0.002	0.01	0.01	0.01	0.01	0.01	0.01

and fouling indices. Such parameters are finding applications by coal scientists for the efficient utilisation of coal in combustion processes. The precision of the method for major, minor and trace elements in coal is good. The RSDs obtained being <7% in all instances. The accuracy of the method is acceptable and has been established by the use of certified reference coals and standard coals whose compositions have been verified by an independent laboratory. The limits of detection found range from 0.04 and 0.05% m/m for the major elements aluminium and silicon, respectively, to 0.01% m/m for the minor elements chlorine, magnesium, sodium, potassium, calcium, iron and titanium and 0.002% m/m for the trace element phosphorus.

The authors thank C. T. Massey, Head of Technical Department, W. E. Hindmarsh, Head of Major Projects and Mine Services, and D. J. Stephenson, Scientific Services Manager, for allowing this work to be published. Professor L. Ebdon, Director Polytechnic South West, is also acknowledged for his advice and encouragement in producing the manuscript.

The comments and conclusions are those of the authors and do not necessarily represent the view of The British Coal Corporation.

References

1. British Standard 1016, parts 1–21, Methods for the Analysis and Testing of Coal and Coke, British Standards Institution, London, 1977.
2. Cammack, P., and Balint, A., *Soc. Min. Eng. AIME, Trans.*, 1976, **260**, 361.
3. Page, D., and Piggins, T., Use of Lab-X Analyser for the Routine Laboratory Determinations of Ash Content of Coal Parts 1 and 2, National Coal Board North East Area Scientific Department, Internal Report Nos. A/2717 and A/2725, 1981.
4. Kiss, L. T., *Anal. Chem.*, 1966, **38**, 1731.
5. Kuhn, J. K., and Henderson, L. R., *Am. Chem. Soc., Div. Fuel Chem. Prepr. Pap.*, 1977, **22**, 68.
6. Pearce, W. C., *PhD Thesis*, Sheffield City Polytechnic, 1984.
7. Thorne, L., McCormick, G., Downing, B., and Price, B., *Fuel*, 1983, **62**, 1053.
8. Price, B. J., *Int. Lab.*, 1981, **11**, 80.
9. Clewer, P. J., *Int. Lab.*, 1982, **12**, 54.
10. Harvey, P. K., and Atkin, B. P., *Inst. Min. Metall., Trans., Sect. A*, 1982, **91**, 17.
11. Hughes, H., *Metall. Mater. Technol.*, 1984, 137.
12. Bertin, E. P., "Principles and Practice of X-ray Spectrometric Analysis," Plenum Press, New York, 1970.
13. Jenkins, R., "An Introduction to X-ray Spectrometry," Heyden, London, 1976.
14. Jenkins, R., Gould, R. W., and Gedike, D., "Quantitative X-ray Spectrometry," Marcel Dekker, New York, 1981.
15. Gorbusskus, M. F., and Wong, J., *X-ray Spectrom.*, 1983, **12**, 118.
16. Jenkins, R., Goke, J. F., Niemann, R. L., and Westberg, R. G., *Norelco Rep.*, 1976, **23**, 32.
17. Bernstein, F., Proceedings of the 11th Annual Conference on Application of X-ray Analysis, Denver, August 1961, p. 436.
18. Kuhn, J. K., Horfst, W. F., and Shimp, N. F., *Adv. Chem. Ser.*, 1975, **141**, 66.
19. Frigge, J., *Erdoel Kohle, Erdgas, Petrochem.*, 1972, **25**, 447.
20. Tertian, R., and Claisse, F., "Principles of Quantitative X-ray Fluorescence Analysis," Heyden, London, 1982, p. 311.
21. De Kalbe, E. L., and Fossol, V. A., Proceedings of ERDA Symposium on X-ray and Gamma Ray Sources, Appl. Univ. of Mich. Ann Arbor, Conf 760539, 1976.
22. Orlić, I., Pavlić, M., Rendić, D., Marijanović, P., Valković, B., Budnar, M., and Cindro, L., paper presented at the International Congress of Analytical Techniques in Fusion Chemistry, Barcelona, 1981.
23. Winegartner, E. C., *Editor*, "Coal Fouling and Slagging Parameters," American Society of Mechanical Engineers Committee on Corrosion and Deposits From Combustion Gases, 1974.
24. Jones, A. R., An Appraisal of the Applicability of Common Slagging Indices to British Coals, Central Electricity Generating Board, Technology Planning and Research Division, Marchwood, Southampton, 1987.
25. Pearce, W. C., Thornewill, D., and Marston, J., *Analyst*, 1985, **110**, 625.
26. Lucas-Tooth, H. J., and Pyne, E. C., *Adv. X-ray Anal.*, 1964, **7**, 523.
27. Gladney, E. S., *Anal. Chim. Acta*, 1980, **118**, 385.

Paper 0/01674H
Received April 17th, 1990
Accepted July 27th, 1990

Rapid Acid Extraction of Bituminous Coal for the Determination of Phosphorus

Kenneth W. Riley, Harry N. S. Schafer and Helen Orban
CSIRO Division of Coal and Energy Technology, P.O. Box 136, North Ryde, NSW 2113, Australia

A rapid acid extraction method for the determination of phosphorus in coal is described. Coal is weighed into polypropylene bottles, hydrofluoric and hydrochloric acids are added and the resulting mixture is heated in a microwave oven. Boric acid is then added to complex the fluoride. Phosphorus is determined by spectrophotometry, as the molybdovanadate complex, in an aliquot of the acid extract. This method is a rapid alternative to the commonly used methods, which require the prior oxidation of coal. A comparison of results for the analysis of 22 coals by this method and a standard method indicate that the proposed method is accurate.

Keywords: *Coal analysis; phosphorus determination; microwave oven digestion*

A number of standard methods[1-3] are available for the determination of phosphorus in coal. These methods require the oxidation of coal, either in a furnace or with nitric and sulphuric acids, before spectrophotometric measurement of phosphorus as the reduced molybdophosphate complex. Standard methods are also available for the determination of phosphorus in coal ash. The ash is fused with lithium tetraborate,[4] digested with sulphuric, hydrofluoric and nitric acids[5] or decomposed with hydrochloric and hydrofluoric acids in a bomb or sealed bottle;[6] the phosphorus is then determined as the molybdovanadate complex. The time required for the determination of phosphorus in coal could be significantly shortened if the time consuming oxidation step were to be avoided.

A rapid, alternative method, involving the use of a mixture of hydrochloric and hydrofluoric acids to dissolve most of the mineral matter in coal without oxidising the carbonaceous matter, has been devised. The coal is heated with the acids in a sealed polypropylene bottle in a microwave oven. Extraction of phosphorus is complete in a matter of minutes. The phosphorus in solution is subsequently determined by spectrophotometry as the yellow phosphomolybdovanadate.

Experimental

The method used to determine the phosphorus in bituminous coal samples is described below.

Acid Extraction

Sub-samples (1 g) of coal (crushed to ≈212 μm) were weighed into autoclavable polypropylene bottles (Nalgene, 125 ml capacity, Cat. No. 2006-0004). The total mass of each coal sample plus bottle was noted. Concentrated hydrochloric acid (1 ml) and hydrofluoric acid (40%, m/m) (4 ml) were added and the bottles were sealed and shaken to wet the coal. Six bottles at a time were placed in a sealed plastic container and heated for 45 s at 500 W in a microwave oven, equipped with a turn-table. This digestion time was established by trial and error. Care must be taken to balance the loading of the oven with the heating time and energy output to avoid overheating and overpressurising the polypropylene bottles. The use of microwave ovens for acid digestion, and the precautions to be taken, have been discussed in the literature.[7-9]

The bottles were cooled, opened in a fume cupboard, and 40 ml of 4% (m/v) boric acid solution were added. The bottles were again sealed, placed in the plastic container and heated for a further 60 s. On cooling, the mass of solution was adjusted to 100.0 g with distilled water. An aliquot of each solution, free from suspended coal, was obtained by centrifuging or by filtration through a dry filter-paper (Whatman No. 40). A reagent blank was submitted to the same procedure.

Calibration

A standard phosphorus solution (1 ml ≡ 0.1 mg of P) was prepared by dissolving 0.2197 g of dried (at 110 °C) potassium dihydrogen phosphate in distilled water and adjusting the volume to 500 ml. Calibration solutions were prepared by transferring aliquots (2, 4 and 6 ml) of this standard solution into polypropylene bottles, together with the amounts of hydrochloric, hydrofluoric and boric acids used to extract the coal. The mass of each calibration solution was adjusted to 100.0 g. A blank reference solution containing the acids was prepared similarly.

Determination of Phosphorus

Aliquots (10 ml) of each of the reference, calibration, sample and blank solutions were transferred into 25-ml calibrated flasks. To each was added 5 ml of molybdovanadate solution[6] [1 l of this solution was prepared by dissolving 1.25 g of NH_4VO_3 in 400 ml of dilute (1 + 1) nitric acid, then adding, with stirring, 400 ml of a solution containing 50 g of $(NH_4)_6Mo_7O_{24}.4H_2O$ and diluting to volume]. The complexed solutions were diluted to 25 ml, and the molybdovanadate complex was allowed to form for 10 min before the absorbance of each was measured at 430 nm, in 40 mm cells, against the complexed reference solution (blank). A Unicam SP 500 Series 2 spectrophotometer was used. A calibration graph was prepared by plotting absorbance *versus* the phosphorus content of the calibration solutions, the concentrations of phosphorus in the sample solutions were read from the graph, and the concentrations in the coal samples were calculated.

Of the 22 coals analysed by this method, only one produced a yellow extract before complexation. This is caused either by Fe^{3+} or soluble organic matter and can, of course, cause an error in the spectrophotometric measurement. This was compensated for by taking a second aliquot of the uncomplexed acid extract, diluting to 25 ml and reading the absorbance. This reading was used to correct for the apparent concentration of phosphorus in that sample.

If the amount of phosphorus in a sample aliquot was greater than that of the highest calibration solution, a smaller aliquot was taken and the volume of this was adjusted to 10 ml with the blank solution, before the addition of the molybdovanadate.

Table 1. Comparison of acid-extraction procedure with standard method (results are expressed as percentage of P, dry basis)

Coal	Acid extraction	Standard method
A	0.002, 0.001	0.002, 0.002
B	0.005, 0.005	0.004, 0.004
C	0.076, 0.079	0.078, 0.079
D	0.151, 0.158	0.155, 0.152
E	0.584, 0.611	0.587, 0.574
ASCRM 009* ..	0.031, 0.032	0.033, 0.033

* Australian Standard Coal Reference Material 009, 0.032% P certified.

Table 2. Comparison of different acid extractions and standard method (results are expressed as percentage of P, dry basis)

Coal	Microwave oven	Water-bath	Standard method
A	0.002	0.002	0.002
B	0.005	0.004	0.004
F	0.028	0.030	0.033
I	0.064	0.066	0.068

Comparison With Standard Method

The same coals were analysed using the Australian standard method[1] (dry oxidation procedure), which is similar to the British[2] and ISO[3] standard methods. The coals were ashed and the ash was dissolved in sulphuric and hydrofluoric acids. Aliquots of the resulting digests were taken, and the reduced molybdophosphate complex was formed by the addition of ammonium molybdate, antimony tartrate and ascorbic acid solutions. The absorbance of each solution, together with a standard solution, was measured at 710 nm and the concentrations of phosphorus present in the coals were calculated.

Results and Discussion

Typical results obtained on a number of the coals, analysed by the direct acid-extraction method and the standard method, are listed in Table 1. The individual results for each of these coals, analysed in duplicate, are given to indicate the repeatability of the method. The results obtained are in excellent agreement with those obtained by use of the standard method. The least-squares regression of the two sets of analyses of 22 coals with phosphorus contents between 0.002 and 0.6% is

$$y = 1.029x - 0.003 \ (R^2 = 0.999)$$

where y = result (mean) using proposed method and x = result (mean) using standard method.

However, if the result for coal E, which is unusually high in phosphorus, is removed from the data set, the regression is

$$y = 1.002x - 0.001 \ (R^2 = 0.998)$$

This is the regression of 21 results ranging from 0.002 to 0.16% of phosphorus; eight results of <0.05%, six between 0.05 and 0.10%, and seven >0.1%.

The use of the microwave oven allows the very rapid acid extraction of the coal. However, concerns have been expressed on the safety[7] of using microwave ovens not designed for laboratory use for this purpose. As an alternative to heating in a microwave oven, the coals can be extracted by using a heated water-bath or ultrasonic bath[10] although the extraction time is lengthened.

A number of samples were extracted in a water-bath at 90 °C for 2 h and then heated further for 1 h after the addition of boric acid. These times are recommended for the digestion of coal ash[6] and it is probable that these could be reduced. The results for the analysis of four coals using the microwave oven and water-bath digestions and of the standard method are given in Table 2. The agreement between the methods is good.

Conclusion

Phosphorus can be determined by spectrophotometry after the direct acid extraction of bituminous coal. This is a rapid alternative to the commonly used methods, which require the coal to be ashed in a furnace or oxidised with acids before determination of the phosphorus. The time of acid extraction can also be significantly shortened if the coal - acid mixture is heated in a microwave oven.

The accuracy of the method is excellent, as indicated by the very good agreement between the results obtained with this method and those of the Australian standard method.

References

1. "Phosphorus in Coal and Coke," Australian Standard 1038, Part 9, 1977, Standards Association of Australia, North Sydney, 1977.
2. "Phosphorus in Coal and Coke," BS 1016: 1977: Part 9, British Standards Institution, London, 1977.
3. "Solid Mineral Fuels—Determination of Phosphorus Content —Reduced Molybdophosphate Photometric Method," International Standard 622, 1981, International Organization for Standardization, 1981.
4. American Society for Testing and Materials, "Major and Minor Elements in Coal and Coke Ash by Atomic Absorption," ASTM D 3682-78, Annual Book of ASTM Standards, Volume 05.05, American Society for Testing and Materials, Philadelphia, PA, 1987.
5. American Society for Testing and Materials, "Analysis of Coal and Coke Ash," ASTM, D 2795-84, Annual Book of ASTM Standards, Volume 05.0.5, American Society for Testing and Materials, Philadelphia, PA, 1987.
6. "Analysis of Higher Rank Coal Ash and Coke Ash," Australian Standard 1038, Part 14.2, 1985, Standards Association of Australia, North Sydney, 1985.
7. Kingston, H. M., and Jassie, L. B., *in* Kingston, H. M., and Jassie, L. B., *Editors*, "Introduction to Microwave Sample Preparation: Theory and Practice," American Chemical Society, Washington, DC, 1988, pp. 231–243.
8. Gilman, L., and Grooms, W., *Anal. Chem.*, 1988, **60**, 1624.
9. Aysola, P., Anderson, P. W., and Langford, C. H., *Anal. Chem.*, 1988, **60**, 1625.
10. Riley, K. W., and Godbeer, W. C., *Analyst*, 1990, **115**, 865.

Paper 0/02624G
Received June 12th, 1990
Accepted July 4th, 1990

Automated Flow Injection Measurement of Photographic Dyes in Gelatin at Elevated Temperatures

Richard H. Taylor, Gregory D. Clark,* Jaromir Růžička and Gary D. Christian
Center for Process Analytical Chemistry, Department of Chemistry, BG-10, University of Washington, Seattle, WA 98195, USA.

A method of measuring spectrophotometrically the concentrations of photographic dyes is described. The problems of analysing the highly concentrated, non-aqueous dyes when dispersed in a highly viscous gelatin matrix were solved by the use of a flow injection analysis system which performed automated dissolution and dilution using the split zone - gradient chamber method at elevated temperatures with dimethyl sulphoxide as the system carrier stream. The requirement of maintaining the matrix in which the dyes are located at an elevated temperature was met by housing the fluid bearing portion of the system within an incubator oven, with remote computer control and remote detection via optical fibres. The precision of the dilutions gave a relative standard deviation of 2% or better for dilutions up to 2000-fold of the injected sample. When compared with manual dilution and measurement, agreement was within 5% for all samples.

Keywords: *Visible spectrophotometry; flow injection; automated dilution; photographic dyes*

In the analysis of many process streams the necessity of sample pre-treatment makes the use of on-line analysis impractical. The sample handling required for pre-treatment also introduces possible sources of error and presents a problem when the sample is toxic, radioactive or requires a specific physical environment.

The use of flow injection analysis (FIA) is a way to address these problems. The FIA method has been shown to perform effectively with non-aqueous systems as with aqueous systems.[1-4] It allows for remote control and, by the use of optical fibres, remote spectrophotometric detection. This enables the solution bearing portion of the FIA apparatus to be isolated and maintained in a specific environment or to be at a distant location.

One example of the types of samples encountered in process streams is that of photographic dyes, which are dispersed at very high concentrations in gelatin media and which must be maintained at elevated temperatures in order to avoid gelation. It is necessary to dilute the process stream samples of these dyes up to several thousand times prior to spectrophotometric analysis. Several automatic dilution systems, such as zone sampling, gradient chamber dilution, dual-stage gradient chamber dilution and the cascade dilution system have been developed.[5-8]

In this study, photographic dyes in gelatin matrices were measured spectrophotometrically after using an FIA automated dilution system at elevated temperatures. The split zone - gradient chamber technique was selected for this study because large dilutions could be reproduced accurately and the degree of dilution could be changed without physically altering the system.[9] This technique, due to the mechanical stirring in the gradient chamber, is independent of the sample viscosity up to fairly high viscosity levels. The dye samples must be maintained at an elevated temperature for the gelatin media in which they are dispersed to remain in the liquid state. This requirement is met by enclosing the solution bearing sections of the FIA system within an incubator oven where a constant elevated temperature can be maintained.

Principle

The split zone - gradient chamber technique for automated dilution[9] is based on the reproducible dispersion that occurs when a sample is injected into an FIA system, *i.e.*, each injection of a similar analyte will disperse in an identical manner.[10] A portion of the trailing edge of the sample zone, can be re-directed, or split off, to obtain a dilution of the injected sample. This re-direction, or zone splitting, can be accomplished with a pump and a T-piece and is made reproducible through appropriate control of the pump. The trailing zone is the portion of the sample that is detected. The height and area of the detected peak can be measured and each parameter can be related to the sample concentration.

The dilution that occurs in the system can be defined in terms of the inverse mole ratio, introduced by Whitman and Christian.[8] The ratio of the number of moles injected, n^0, to the number of moles detected, n_{det}, is the inverse mole fraction, x^{-1}, such that:

$$x^{-1} = n^0/n_{det}$$

As the area of the detected peak is proportional to the number of moles then x^{-1} can be written as:

$$x^{-1} = kA^0/A_{det}$$

where A^0 is the area of the k-fold manually diluted calibration standard and A_{det} is the area of the peak of the same standard solution after dilution by zone splitting.

The gradient chamber is the primary dispersing component in the system and causes the system to perform in a way similar to a single mixing chamber system, which changes the shape of the peak to be skewed and hence produces a more pronounced trailing edge. This increases the amount of control over the extent of the dilution and enhances the precision.[6]

Experimental

Reagents

The carrier used in all experiments was ACS spectroscopic grade dimethyl sulphoxide (DMSO) (J. T. Baker). Two different photographic dyes, magenta and yellow, in gelatin media were provided by the Polaroid Corporation. All manual dilutions of the dyes provided were performed with the same grade DMSO.

Apparatus

A split zone dilution system with an in-line gradient chamber was used (Fig. 1). The pumps were Alitea CT-4 peristaltic pumps with remote Alitea Model SC controllers. A Rheodyne Type 5701 pneumatic actuator was used with a Rheodyne Type 50 4-way injection valve employing a 25-μl sample loop.

* Present address: Department of Laboratory Medicine, SB-10, University of Washington, Seattle, WA 98195, USA.

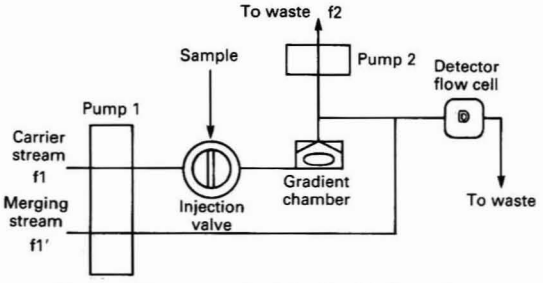

Fig. 1. Split zone - gradient chamber dilution system

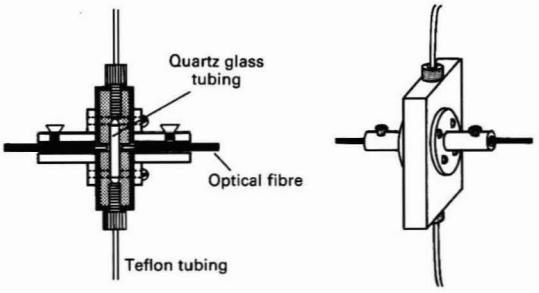

Fig. 3. Flow cell for split zone - gradient chamber dilution system

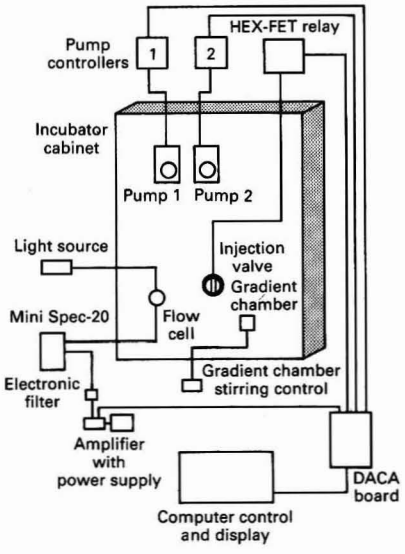

Fig. 2. System set-up for control and sample isolation for FIA split zone - gradient chamber dilution system

The tubing was poly(tetrafluoroethylene) (PTFE) with an internal diameter of 0.51 mm; the pump tubing was Norprene Tubing. Stirring in the gradient chamber was performed by means of a magnetic stirrer. The gradient chamber was constructed of PTFE and had a volume of 680 μl, when the stirring bar was in place.

The system manifold and pumps were housed inside a Lab Line Imperial III incubator oven. The pump controllers and the injection valve actuator were controlled by and data were collected using an IBM Data Acquisition and Control Adapter (DACA) in conjunction with an IBM XT computer (Fig. 2).

The detector used was a Bausch & Lomb Spectronic Mini 20 spectrophotometer. The output was directed to an electronic low pass filter and a linear amplifier and then through the DACA board to the computer where the transmittance signal was converted into an absorbance value. An external laboratory-built light source with a variable intensity control was used. The external light source and spectrophotometer were connected to the flow cell in the incubator oven via 100-μm acrylic optical fibres (General Fiber Optics). The flow cell (Fig. 3) uses quartz-glass tubing with an internal diameter of 2.0 mm. Stray light was prevented from affecting the measurement by the design of the optical fibre mounting flanges of the flow cell. It was supported in the system set-up by a bracket in which the flanges rested.

General Procedure

The flow-rates of the carrier stream (f1) and the merging stream (f1′) were 3.22 ml min^{-1} and the flow-rate of the splitting line (f2) was 4.31 ml min^{-1}. With these flow-rates, the flow of the splitting stream was greater than the flow of the carrier stream (f1 < f2) while the sum of the flows of the carrier and merging streams was greater than the flow of the splitting stream (f1 + f1′ > f2). With both pumps running, the flow from the gradient chamber was via the splitting stream; the flow of the merging stream passed to both the gradient chamber and through the detector flow cell, thus providing a continuous flow through the flow cell. At the appropriate time after the injection of the sample pump 2 was stopped and the remaining sample in the gradient chamber was pumped, with further dilution by the merging stream, through the detector flow cell.

The temperature of the incubator oven was maintained above 40 °C to ensure that the gelatin media of the dyes remained liquid. The incubator temperature was maintained between 41 and 44 °C for the entire period of the study. No fluctuation of the absorbance value was observed at any temperature in this range. No adverse effects were observed with the materials or in the operation of the system.

The system was controlled by the IBM XT computer through the use of the general FIA system control program of Clark *et al.*[11]

The wavelengths used for the detection of the magenta and yellow dyes were 553 and 459 nm, respectively.

Results and Discussion

Initially a series of samples of the magenta dye were injected into the system and the area of the absorbance profiles determined with no zone splitting (corresponding to a delay time of zero). The areas were plotted with respect to sample concentration (Fig. 4). This indicated that the amount of detected sample must be reduced by a factor of *ca.* 25 by zone splitting in order to bring the undiluted dye sample within the linear part of the Beer's law response curve.

The degree of splitting which would be obtained at a specific delay time was determined by measuring a single concentration of the dye at various delay times and calculating the inverse mole fraction, x^{-1}. The inverse mole ratio, as a ratio of the areas of the detected peaks, gives an indication of the fraction of the injected sample that is detected. The resultant graph (Fig. 5) indicates that a delay time of 60 s would produce a splitting off of 1/50 of the injected sample for measurement.

Using a delay time of 60 s, magenta dye samples at concentrations up to and including that of the undiluted dye were injected into the system and analysed. The areas of the absorbance profiles of all the samples, including the undiluted dye sample, produced a linear graph with respect to concentration (Fig. 6). The equation for this line was $A = 0.356c - 1.10$, where c is the concentration in g l^{-1}, with a correlation

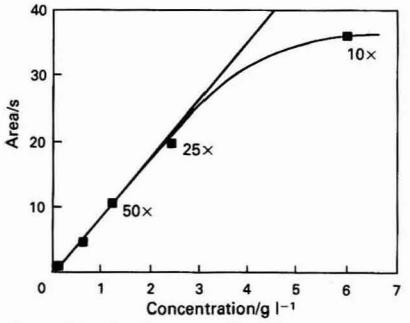

Fig. 4. Area of the absorbance profile with respect to concentration of magenta dye at a delay time of zero

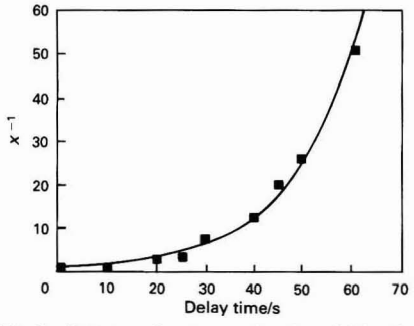

Fig. 5. Inverse mole ratio as a function of delay time

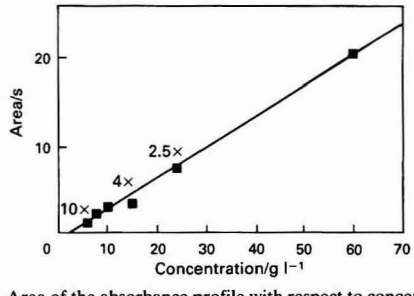

Fig. 6. Area of the absorbance profile with respect to concentration of magenta dye at a delay time of 60 s

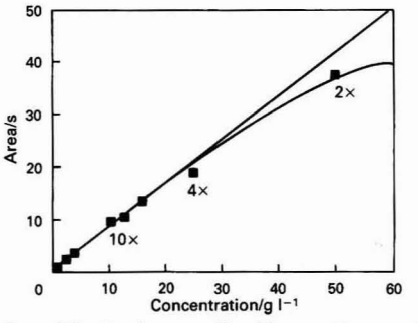

Fig. 7. Area of the absorbance profile with respect to concentration of yellow dye at a delay time of zero

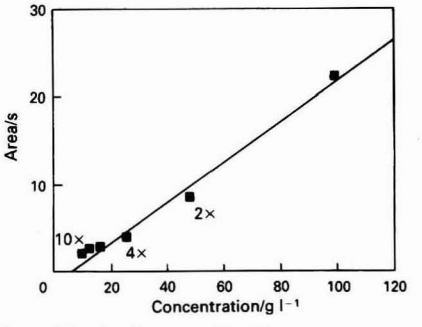

Fig. 8. Area of the absorbance profile with respect to concentration of yellow dye at a delay time of 30 s

Table 1. Concentration of photographic dyes in gel media as determined by automated FIA dilution and conventional manual dilution

	Concentration/g l^{-1}		
Sample	FIA method	Manual method	$\Delta x/x$,* %
1	51.0	53.1	−4.0
2	40.2	41.4	−2.9
3	57.2	55.4	+3.2
4	56.5	59.3	−4.7
		Average	−2.1

* Difference of the two measurements divided by the average of the two measurements.

coefficient of 0.993. Note that the absorbance profile is the absorbance measured during the time the sample is being detected, therefore the area (the product of time and absorbance) has units of time in seconds. The non-zero intercept is believed to be caused by the gelatin matrix in which the dye was dissolved. Unfortunately, no samples of the gelatin media without a dissolved dye were available as controls. The maximum peak absorbance of all the samples also produced a linear graph with respect to concentration, with the maximum peak absorbance of the undiluted dye at an absorbance value of 0.82. The equation of this line was $A = 0.0141c - 0.0242$ with a value of 0.995 for the correlation coefficient.

The same procedure was followed using the yellow dye. By using a zero delay time, the graph of the area of the absorbance profile with respect to concentration (Fig. 7) for a series of dye samples, indicated that an additional reduction by a factor of at least 6 achieved by zone splitting would be required to bring all the samples within the linear part of the measurement range. By using the graph given in Fig. 5 a delay time of 30 s was chosen to produce the desired degree of dilution. Analysing the same samples at a delay time of 30 s produced a graph in which the areas of the absorbance profiles were linear with respect to the concentration of the sample (Fig. 8). This line had a correlation coefficient of 0.992 and the equation $A = 0.236c - 1.82$.

In order to test the accuracy of the dilution system, a set of five magenta dye samples with various concentrations were analysed by both the FIA procedure and by a conventional technique using manual dilution and a diode array spectrophotometer. A set of standards was made by the appropriate manual dilution of one dye sample; the remaining four undiluted samples were measured relative to these standards. The standards and the samples were analysed with a delay time of 60 s. Calibration graphs were prepared from the

standards for both methods and used to calculate the concentrations of the unknown samples. When compared with each other, the results of the two methods agreed to within 5% for all of the samples (Table 1). This shows that the method of dilution and measurement by FIA is an acceptable alternative to manual dilutions and measurement.

Multiple measurements (≥ 3) were made for all analyses. The relative standard deviation was found to be 2.0% or less for all samples at concentrations above 1/1000 of that of the undiluted dye when analysed with a delay time of 60 s.

This study shows that the split zone - gradient chamber method of automated dilution is adaptable for use with samples encountered in the process environment. The ability to remotely control and monitor the system, points to its use in applications in which either isolation or a specific environment is required, for example, the elevated temperature required here. The system dilutes and measures with a single injection of sample, thus incorporating the pre-treatment of the sample into the analysis. The high reproducibility of the dilution step, the lack of sample handling required and the reduction in the time required for analysis, indicate the advantages of this system over the manual dilution and measurement technique. The most outstanding feature of the system is the ability to change the degree of dilution selectively by the manipulation of only one system pump; no physical alteration of the system is required.

The financial support of the Polaroid Corporation is gratefully acknowledged. We thank T. Tougas for providing the dye samples, and Y. Fraticelli and M. Riebe for helpful discussions.

References

1. Christian, G. D., and Attiyat, A. S., *Anal. Chem.*, 1984, **56**, 429.
2. Attiyat, A. S., *J. Flow Injection Anal.*, 1987, **4**, 26.
3. Attiyat, A. S., *Can. J. Spectrosc.*, 1987, **32**, 118.
4. Whiteside, I. R. C., Worsfold, P. J., Lynes, A., and McKerrell, E. H., *Anal. Proc.*, 1988, **25**, 60.
5. Reis, B. F., Jacintho, J., Moratatti, J., Krug, F. J., Zagatto, E. A. G., Bergamin Fo, H., and Pessenda, L. C. R., *Anal. Chim. Acta*, 1981, **123**, 221.
6. Gisen, M., Thommen, C., and Mansfield, K. F., *Anal. Chim. Acta*, 1986, **179**, 149.
7. Garn, M. B., Gisin, M., Gross, H., King, P., Schmidt, W., and Thommen, C., *Anal. Chim. Acta*, 1988, **207**, 225.
8. Whitman, D. A., and Christian, G. D., *Talanta*, 1989, **36**, 205.
9. Clark, G. D., Růžička, J., and Christian, G. D., *Anal. Chem.*, 1989, **61**, 1773.
10. Růžička, J., and Hansen, E. H., *Anal. Chim. Acta*, 1980, **114**, 19.
11. Clark, G. D., Christian, G. D., Růžička, J., van Zee, J. A., and Anderson, G. F., *Anal. Instrum.*, 1989, **18**, 1.

Paper 0/01233E
Received March 21st, 1990
Accepted May 4th, 1990

On-line Dilution, Steady-state Concentrations by Tandem Injection and Merging Stream. Application to Inductively Coupled Plasma Atomic Emission Spectrometry Sequential Multi-element Soil Analysis

Yecheskel Israel and Ramon M. Barnes
Department of Chemistry, Lederle Graduate Research Center, University of Massachusetts, Amherst, MA 01003-0035, USA

Recently developed flow injection on-line dilution methods, *i.e.*, the merging stream and tandem injection, which yield steady-state concentrations, have been applied to the analysis of reference soil sample digests by inductively coupled plasma atomic emission spectrometry. Direct or on-line dilution determinations were applied, with dilutions ranging from 1.8 to 15 for both dilution methods. Higher dilutions are not feasible, especially when trace elements are involved. A variable speed peristaltic pump was used to limit the total flow-rate by the merging-stream dilution method to 2 ml min^{-1}. This permitted the design of a flow module with one set of coils and a flow configuration suitable for all dilutions. Varying the dilution required only the variation of the peristaltic pump flow tube diameters. Selecting the required dilution for the tandem injection method was carried out with no manual operations and involved only pre-programming of the injection time and the injection cycle period. The results obtained exhibit comparable accuracy and precision for major and minor elements to those obtained by direct determination. By varying the dilution for the determination of trace elements, screening the optimum dilution(s) suitable for the determination of each trace element is possible.

Keywords: *Flow injection; on-line dilution; soil analysis; inductively coupled plasma atomic emission spectrometry*

Various on-line dilution methods have been developed for analysis using flow injection (FI),[1–5] which in every instance yields a transient concentration profile. Israel *et al.*[6] recently developed on-line dilution methods with steady-state concentrations by exploiting flow injection configurations. These methods were intended for application to sequential, multi-element analysis with inductively coupled plasma atomic emission spectrometry (ICP-AES) or mass spectrometry (ICP-MS) instruments, and also for general purpose on-line dilution.

A novel approach was adopted,[6] employing tandem injection, whereby a discrete sample volume, V_i, is injected in tandem into a flowing diluent. For medium to high dispersion conditions and varying V_i and the diluent volume, V_D, diverse dilutions could be achieved to produce steady-state concentrations of the diluted sample. The appearance of signal (*i.e.*, concentration) ripples hampered the exploitation of the tandem injection method for on-line dilution, except over a limited dilution range. On the other hand, when tandem injection was coupled with a single, or especially a double, confluence with the diluent then low, medium and high dilutions were achieved yielding steady-state concentrations without temporal signal variations.

The merging stream principle alone can provide low dilutions with steady-state concentrations.[6] Coupling this technique with the tandem injection principle permits a wide dilution range and easily varied dilution for a specific flow configuration. For a time-based flow system, this variable dilution is achieved simply by re-programming the ratio of the sample injection time, t_i, to the injection cycle period, t_{TI}. The latter is the sum of t_i, and the diluent flow time between consecutive injections, t_D.

In order to evaluate the linearity of the steady-state concentration in the previous study,[6] the intensity - time relationship was determined for a single element (*e.g.*, Co or Sc) at the emission intensity peak with either ICP-AES or ICP-MS. Adequate linearity was demonstrated with a precision which in every instance was similar to that obtained by direct nebulisation of a pre-diluted sample.

In an earlier study,[7,8] several marker elements present in soils were determined sequentially by ICP-AES. The sample was fused with lithium metaborate and subsequently digested with dilute nitric acid. Mainly owing to the presence of major constituents and to the high salt matrix content, the samples were pre-diluted prior to multi-element determinations. Varying the pre-dilution was sometimes necessary in order to secure optimum results for some trace elements. A considerable time-saving can result from adopting on-line dilution methods for this analysis.

This paper examines the application of on-line dilution methods with steady-state concentrations to the ICP-AES sequential multi-element analysis of soil samples to adapt them for the analysis of practical samples without pre-dilution. This investigation also seeks to apply various dilutions to screen the optimum dilution required for the determination of specific minor or trace elements. Ten major, minor and trace elements were determined in reference soil samples.

On-line Steady-state Dilution Using FI Configurations

This section summarises the relationships developed previously,[6] expressing the dependence of the dilution factor, d, on the applied method of dilution. Equations 1–5 permit the calculation of the dilution factor for each on-line dilution method.

The dilution factor for tandem injection alone is

$$d_{TI} = (V_i + V_D)/V_i = V_{TI}/V_i \quad \ldots \quad (1)$$

where V_{TI} is the volume of the sample and the diluent for each injection cycle period, t_{TI}. When time-based flow systems are employed, d_{TI} is conveniently re-defined in terms of t_{TI} and t_i.

$$d_{TI} = t_{TI}/t_i = (t_i + t_D)/t_i \quad \ldots \quad (2)$$

The merging stream dilution factor, d_{MS}, is defined in terms of the flow-rates of the sample, U_S, and the diluent, U_D. For a single confluence of the sample and diluent,

$$d_{MS} = (U_S + U_D)/U_S \quad \ldots \quad (3)$$

For multiple confluence of the sample with the diluent, the sum of the diluent stream flow-rates is substituted for U_D in equation (3).

For the combination of tandem injection and merging stream dilution, the over-all dilution factor is

$$d_T = d_{TI}d_{MS} \quad (4)$$

or

$$d_T = (t_i + t_D)(U_S + U_D)/(t_iU_S) \quad (5)$$

As only the combination of tandem injection with merging stream dilution instead of tandem injection alone will be employed in this investigation, for convenience the technique henceforth will be referred to as tandem injection.

Experimental

ICP-AES Detector

A sequential ICP-AES system (Perkin-Elmer Plasma II), with the specifications and operating parameters as listed in Table 1, was coupled with a flow injection on-line dilution apparatus for the determination of Al, Ba, La, Mn, Si, Ti, V, Y, Yb and Zr in reference soil samples.

The operation of the Plasma II emission spectrometer was controlled completely by the system software of the PE 7500 computer. Two 1-m Ebert monochromators were utilised covering the wavelength range from 160 to 800 nm (*cf.* Table 1). Sequential multi-element analyses were performed with the Myers - Tracy signal compensation system employing an Sc internal reference standard. This arrangement permitted simultaneous correction for the instantaneous intensity variation of each element to that of the internal reference readings.

The demountable torch assembly (Perkin-Elmer Plasma II) includes a chemically resistant Ryton (Philips) cross-flow nebuliser. The argon flow to the nebuliser is controlled by a thermostated mass-flow controller.

Table 1. ICP-AES system specifications and operating parameters

Radiofrequency (r.f.) generator—

Frequency/MHz	27.12
R.f. induction coil	Water cooled, 4 turns $\frac{1}{8}$ in, copper
R.f. generator power/W	1000

Monochromators—

Monochromator	Ruling density/ lines mm^{-1}	Bandpass/ nm	Wavelength range/ nm	Linear dispersion/ nm mm^{-1}
A	3600	<0.009	160–400	0.229
B	1800	<0.018	160–800	0.527

Monochromator parameters—

Selected monochromator	A	B
Signal compensation	Yes	Yes
PMT gain/V	600	600
Sampling time/ms	100	100
Survey window/nm	0.050	0.100
Peak window/nm	0.040	0.100
Background correction	Off	Off
Photomultiplier	Hamamatsu R787	
Viewing height/mm	15 mm above load coil	
Slits/μm	20, curved	

Argon flow-rates/l min^{-1}—

Plasma	15
Auxiliary	1.0
Nebuliser	1.0
Peristaltic pump flow-rate/l min^{-1}	1.0
Equilibrium time/s	15

ICP-AES Measurement

The operational conditions for the sequential determination of elements by ICP-AES are listed in Table 2 which are the same as those recommended by the manufacturer, although independent optimisation for each element is possible.

The most prominent emission line[9] was chosen for each element, except for Al and V, to avoid the influence of the background emission of neighbouring OH lines. The wavelengths of all of the elements were calibrated prior to analysis in order to avoid wavelength shift. Only one standard solution was prepared containing standard concentrations of the sequentially determined elements, the Sc internal reference and $LiBO_2$. This standard solution contained exactly the same concentration of fused $LiBO_2$ and Sc as the soil reference sample solutions, while the blank contained only $LiBO_2$ (fused before dissolution, without Sc). Except for trace elements, an attempt was made to match the concentration of each element in the standard solution with the concentration range of the same elements in soil solutions (*cf.* Table 2). For each element, the wavelength, detection limit, concentration range in the reference soil sample digests and concentration in the standard solution are listed in Table 2.

On-line Dilution Apparatus

Dilutions of approximately 2–15 are feasible for on-line dilution of reference soil samples. However, from the range of concentrations for the sample solutions listed in Table 2, a dilution of 15 will result in concentrations of La and Yb, for all samples and of V and Y for some samples, being lower than the detection limit. Both the merging stream and the tandem injection dilution techniques were applied to obtain this dilution range.

Manifold for merging stream dilution

A four-channel variable speed peristaltic pump, P_1, (Rainin Rabbit) coupled with a flow manifold was used for merging stream on-line dilution (Fig. 1). Three channels of P_1 are employed for the sample (S) and diluent streams (D_1 and D_2) and are connected to a laboratory-built flow module, which in turn is connected to the nebuliser peristaltic pump, P_2. The flow module tubing [Fisherbrand Accu-Rated poly(vinyl chloride) (PVC)] was used with Y-connectors for confluence junctions and a T-connector for stream flow splitting (SFS). This expression is preferred over zone splitting,[6] as a uniform solution exists in the present arrangement. Stream splitting is

Table 2. Spectrometric operating conditions, detection limits, range of concentrations of elements in reference soil digests and the concentration of the elements in the standard solution

Element and line	Wavelength/ nm	c_l*/ μg ml^{-1}	Soil digests concentration range/ μg ml^{-1}	Standard solution concentration/ μg ml^{-1}
Al I	396.152	0.028	94–186	100
Ba II	455.403	0.0013	0.32–2.0	2
La II	379.478	0.010	0.034–0.11	0.1
Mn II	251.610	0.0014	1.08–1.7	2
Si I	251.611	0.012	316–640	400
Ti II	334.941	0.0038	4–17	10
V II	292.402	0.0075	0.08–0.3	1
Y II	371.030	0.0035	0.03–0.08	0.2
Yb II	328.937	0.0018	0.004–0.008	0.1
Zr II	343.823	0.0071	0.16–1.6	2

* c_l = limit of detection, *i.e.*, the concentration equivalent to three times the SD of the blank. See reference 10.

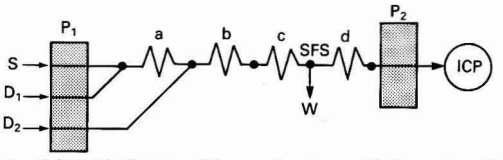

Fig. 1. Schematic diagram of the merging stream dilution system: P_1, variable speed peristaltic pump with flow-rates in ml min^{-1} at 100% motor speed (in parentheses); S, soil sample digest (0.6 or 1.2); D_1 and D_2, diluent 5% HNO_3. D_1 (0.45, 0.6 or 1.2), and D_2 (0.6 or 1.2). Coils (length in cm/i.d. in mm): a, 50/0.7; b, 40/1.5; c, 50/0.7; and d, 40/1.0. P_2, Plasma peristaltic pump (1 ml min^{-1}); SFS, stream flow splitting T-connector; W, waste; and ICP, plasma detector

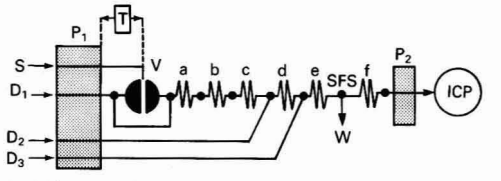

Fig. 2. Schematic diagram of the tandem injection dilution system: P_1, constant speed peristaltic pump; S, soil sample digest with 1.2 ml min^{-1} flow-rate; D_1, D_2 and D_3, diluent 5% HNO_3 flowing at equal rates of 0.45 ml min^{-1}; V, injection valve and T, timer. Coils (length in cm/i.d. in mm): a, 40/1.4; b, 50/0.5; c, 50/0.7; d, 50/0.7; e, 40/1.0; and f, 40/1.0. SFS, stream flow splitting T-connector; W, waste; P_2, plasma peristaltic pump with a flow-rate of 1.0 ml min^{-1}; and ICP, plasma detector

necessary to drive to waste the excess of diluted sample that does not flow through P_2. This arrangement provides a perfect interface of the flow system with the plasma detector. The flow-rates in the peristaltic pump tubes are measured at 100% motor speed to allow calculation of the expected dilutions using equation (3). The dilution was usually determined from intensity measurements of the Sc II line at 357.635 nm of standard solutions in the same manner as was performed previously.[6] The total flow-rate, U_T, at 100% motor speed was chosen to exceed 1 ml min^{-1}, the flow-rate used for P_2. However, if U_T has also exceeded 2.0 ml min^{-1}, the motor speed was accordingly decreased to confine the flow-rate below 2.0 ml min^{-1}.

This arrangement is advantageous in facilitating the selection of a single set of coils to provide effective mixing for any of the required dilutions. The flow module was fastened into a plastic channel 60 cm in length. This unit is ready for transfer and/or operation with any ICP detector by connecting the flow module on both sides to P_1 and P_2.

On-line dilutions of up to 5-fold were realised using merging stream dilution. For example, a dilution factor of three is obtained with three equal flow-rate merging streams.

FI apparatus for tandem injection dilution

A commercial flow injection instrument used for tandem injection on-line dilution (Tecator FIAstar 5020 analyser) has been described previously.[10] A time-based injection valve permits the choice of a variable injection time, t_i, with a 200-µl injection loop. The selection of the injection cycle period, t_{TI}, is microprocessor controlled, and for the same sample can be repeated up to 99 times. A schematic diagram of the flow apparatus used for tandem injection dilution, which involves two confluence junctions with the diluent, is given in Fig. 2. Essentially the same manifold was used in a previous study[6] except for minor coil modifications.

Pump speed is constant in this flow injection apparatus. The flow configuration was designed to yield medium to high axial dispersion,[6] therefore a low flow-rate for D_1 is used (typically 0.45 ml min^{-1}). An attempt was made also to restrict U_T to less than 2.0 ml min^{-1}. Various dilutions can be obtained conveniently with tandem injection by selecting a constant flow configuration and varying t_i and t_{TI}. The over-all dilution by tandem injection is calculated from equation (5). If for example, equal flow-rates for D_1, D_2 and D_3 are selected and t_{TI} is set constant, equal to 20 s, then the over-all dilution factors, d_T, of 4, 6, 7.5, 12 and 15, are attained by programming t_i to values equal to 15, 10, 8, 5 and 4 s, respectively. Tandem injection dilution was used to obtain dilutions from approximately 8 to 15.

Reagents and Standards

Analytical-reagent grade citric and nitric acids were used. Stock standard solutions containing 1000 mg l^{-1} of Al, Ba, La, Mn, Sc, Y, Yb and V were prepared from analytical-reagent grade compounds of pure metals. These solutions and commercial 1000 mg l^{-1} Si, Ti and Zr stock standard solutions (Custom Standard, Inorganic Ventures) were used for the preparation of multi-element standard solutions (*cf.* Table 2). Scandium standard solution (1000 mg l^{-1}) was prepared by dissolving 0.7669 g of Sc_2O_3 in 10 ml of 1 + 1 v/v HNO_3 in a microwave digestion apparatus (CEM, Model MDS 81D) at 80% power for 1 min and 35% power for 10 min. If the solution was not completely clear, the dissolution programme was repeated. The solution was diluted to 500 ml with 5% v/v nitric acid.

The diluent used was 5% HNO_3. However, when digests of soil devoid of Sc were analysed routinely, 50 mg l^{-1} of Sc were also added to the diluent as an internal reference element. Doubly distilled, de-ionised water was used throughout.

Canadian reference soil samples [Canada Centre for Mineral and Energy Technology (CANMET)], Regosolic Clay Soil, SO-1, Podzolic B Horizon Soil, SO-2, Calcareous C Horizon Soil, SO-3, Chenozemic A Horizon soil, SO-4 and International Atomic Energy Agency (IAEA) Certified Reference Material Soil 7 were used to assess the validity of using on-line dilution methods.

Sample Preparation

Essentially the same fusion and digestion procedures were used as described in a previous study,[7] except that for fusing, 0.20 g of reference soil sample was used instead of 0.25 g and Sc was employed, instead of Co, as the internal reference standard.

Results and Discussion

Sequential multi-element ICP-AES analysis was performed either directly or after various on-line dilutions of reference soil digests. Two digests of each sample were prepared, and each was analysed in triplicate. The mean and the standard deviation (SD) of three results for every element in each digest were calculated and are reported in Table 3. These results are compared with the recommended elemental concentration data for IAEA CRM Soil 7 and with the recently compiled elemental data[11] for CANMET soils SO-1 to SO-4. Details of the method of computing the recommended elemental means and the associated SDs are given in the original paper.[11]

Direct analysis of sample digests was made possible by the use of a torch assembly which tolerated analytes with high salt content. However, to avoid nebuliser clogging, thorough rinsing with dilute 5% HNO_3 was adopted between two consecutive digest analyses. The SD obtained by direct determination of Al, Ba, Mn, Si and Ti did not exceed 2.1%. Direct determination of La and Yb in soil digests was not carried out, but the SDs for the direct determination of V, Y and Zr were high. However, the use of direct analysis of soil digests for routine applications is inadequate, particularly when a normal cross-flow nebuliser and torch assembly is used.

Table 3. Direct and on-line dilution determination of elements in reference soil samples digests by sequential ICP-AES. Values are given in μg g^{-1} except where percentages are indicated. Values of SD are given in parentheses

Element	Recommended value	Direct	On-line dilution factor 1.8	5.0	15.3*
SO-1—					
Al, %	9.31 (0.23)	9.50 (0.02)	9.35 (0.12)	9.27 (0.06)	9.39 (0.06)
		9.42 (0.02)	9.37 (0.06)	9.28 (0.10)	9.25 (0.02)
Ba	870 (70)	876 (2)	862 (4)	844 (21)	876 (14)
		894 (12)	867 (4)	846 (20)	869 (7)
La	54 (2)	ND†	56 (2)	56 (1)	54 (4)
		ND	56 (2)	54 (3)	50 (15)
Mn	890 (40)	914 (18)	867 (12)	850 (2)	877 (15)
		902 (12)	869 (6)	860 (2)	874 (12)
Si, %	25.70 (0.29)	25.95 (0.2)	26.30 (0.2)	25.44 (0.2)	25.74 (0.2)
		25.73 (0.0)	26.06 (0.4)	25.70 (0.1)	25.80 (0.4)
Ti	5200 (200)	5230 (20)	5250 (30)	5220 (15)	5180 (50)
		5170 (10)	5290 (60)	5170 (45)	5260 (20)
V	133 (4)	120 (8)	130 (4)	135 (1)	130 (20)
		114 (12)	128 (2)	131 (1)	120 (30)
Y	24.5 (1.4)	22.9 (0.7)	18.0 (1.0)	27.0 (2.9)	40.0 (4.6)
		22.8 (0.5)	17.7 (0.6)	26.5 (3.0)	44.3 (6.2)
Yb	2.24 (0.25)	ND	2.29 (0.23)	4.05 (0.6)	3.70 (2.3)
		ND	2.39 (0.16)	3.53 (0.4)	4.00 (3.1)
Zr	84 (10)	86.2 (2.4)	74.8 (3.2)	95.4 (25)	166 (46)‡
		85.8 (1.6)	71.3 (6.0)	91.0 (14)	178 (6)
SO-2—					
Al, %	7.99 (0.26)	8.05 (0.08)	7.91 (0.03)	7.90 (0.03)	7.69 (0.11)
		7.93 (0.06)	7.91 (0.08)	7.83 (0.07)	7.79 (0.06)
Ba	1000 (110)	1045 (9)	1002 (7)	985 (23)	973 (18)
		1023 (5)	992 (11)	968 (25)	990 (8)
La	46.5 (0.7)	ND	55.5 (2.9)	43.9 (5.3)	39.2 (8)
		ND	57.2 (1.1)	41.8 (7)	36.8 (12)
Mn	720 (20)	709 (1)	683 (5)	706 (1)	705 (15)
		705 (5)	677 (7)	690 (3)	665 (25)
Si, %	24.97 (0.29)	25.05 (0.03)	25.47 (0.19)	25.30 (0.13)	25.05 (0.5)
		24.83 (0.13)	25.12 (0.36)	25.05 (0.10)	24.57 (0.5)
Ti	8600 (500)	8350 (25)	8410 (40)	8360 (160)	8410 (120)
		8430 (15)	8560 (30)	8450 (140)	8370 (174)
V	57 (4)	67.0 (4.0)	58.8 (2.6)	62.9 (9.3)	63.5 (35.2)
		66.4 (2.4)	61.0 (3.0)	69.0 (5.2)	77.5 (34.0)
Y	40 (2)	40.0 (0.5)	32.4 (0.2)	40.8 (0.3)	46.6 (5.1)
		36.8 (2.1)	33.1 (0.3)	42.0 (0.5)	48.4 (4.5)
Yb	3.5 (0.4)	ND	4.04 (0.1)	4.65 (1.0)	5.30 (3.0)
		ND	4.21 (0.5)	4.55 (0.2)	4.90 (2.6)
Zr	760 (60)	590 (9.2)	390 (76)	240 (40)	860 (30)‡
		546 (4.4)	237 (15)	172 (24)	854 (28)‡
SO-3—					
Al, %	3.07 (0.16)	3.07 (0.04)	3.09 (0.03)	3.10 (0.08)	3.11 (0.02)
		3.05 (0.02)	3.05 (0.03)	3.04 (0.04)	3.14 (0.02)
Ba	290 (40)	292 (4)	277 (4.0)	271 (5.3)	286 (4.1)
		286 (2)	273 (0.8)	268 (6.6)	278 (4.3)
La	16.9 (1.3)	ND	35.4 (1.4)	23.0 (7.2)	—§
		ND	33.1 (0.9)	20.1 (2.8)	—§
Mn	540 (30)	536 (2.8)	510 (3.2)	558 (15)	539 (11)
		522 (7.2)	504 (4.2)	539 (9.2)	535 (9)
Si, %	15.76 (0.16)	16.25 (0.01)	16.26 (0.06)	16.22 (0.20)	16.29 (0.21)
		16.02 (0.01)	16.08 (0.14)	16.04 (0.13)	16.06 (0.17)
Ti	2000 (200)	2040 (15)	2060 (6)	2040 (40)	2130 (20)
		2010 (5)	2030 (14)	2100 (20)	2070 (10)
V	36 (4)	48.0 (5.0)	46.2 (4.2)	48.5 (7.5)	—§
		49.4 (2.8)	41.3 (3.0)	41.5 (4.5)	—§
Y	16.4 (1.7)	16.9 (1.1)	13.2 (0.8)	17.5 (2.5)	30.1 (4.7)
		16.3 (0.7)	13.7 (0.5)	19.3 (2.6)	34.7 (1.5)
Yb	1.67 (0.18)	ND	1.87 (0.12)	4.3 (3.0)	—§
		ND	1.73 (0.26)	3.7 (2.1)	—§
Zr	156 (13)	181 (7.3)	172 (3.6)	185 (24)	266 (26)‡
		178 (6.6)	174 (4.5)	179 (15)	252 (22)‡
SO-4—					
Al, %	5.41 (0.20)	5.42 (0.07)	5.39 (0.04)	5.38 (0.08)	5.29 (0.03)
		5.46 (0.03)	5.35 (0.02)	5.28 (0.12)	5.44 (0.07)
Ba	700 (40)	754 (1.4)	740 (9.2)	702 (11)	742 (6)
		750 (0.6)	738 (4.2)	694 (17)	740 (8)
La	28.2 (1.7)	ND	37.5 (2.2)	—§	18.9 (10.5)
		ND	35.0 (5.6)	—§	22.2 (16.2)
Mn	600 (30)	605 (2.5)	594 (11.5)	612 (9.5)	582 (16)
		601 (1.5)	571 (5.5)	604 (6.5)	603 (14)

Table 3—*continued*

Element	Recommended value	Direct	On-line dilution factor 1.8	5.0	15.3*
SO-4—					
Si, %	31.96 (0.31)	31.11 (0.16)	32.06 (0.24)	31.93 (0.14)	32.26 (0.62)
		30.83 (0.36)	31.18 (0.45)	31.53 (0.16)	32.34 (0.35)
Ti	3340 (240)	3510 (60)	3560 (40)	3460 (30)	3530 (50)
		3470 (20)	3560 (60)	3520 (50)	3450 (43)
V	85 (5)	88.0 (7.4)	88.2 (4.0)	91.7 (20)	83.6 (7.7)
		86.8 (4.0)	85.6 (2.4)	88.2 (14)	79.7 (9.6)
Y	22 (2)	21.8 (0.4)	18.7 (0.3)	23.0 (1.8)	30.3 (2.7)
		21.0 (0.8)	18.3 (0.2)	27.2 (2.7)	29.0 (4.6)
Yb	2.1 (0.4)	ND	2.80 (0.36)	—§	—§
		ND	2.83 (0.48)	—§	—§
Zr	270 (15)	287 (2.8)	303 (7.3)	302 (30)	328 (16)‡
		269 (2.0)	279 (3.2)	291 (22)	338 (26)‡
Soil 7—					
Al, %	4.4–5.1	4.80 (0.03)	4.65 (0.03)	4.74 (0.07)	4.78 (0.03)
		4.75 (0.01)	4.62 (0.05)	4.72 (0.09)	4.84 (0.03)
Ba	131–196	162 (1.8)	147 (1.0)	140 (3.2)	156 (2.2)
		154 (1.0)	149 (0.9)	142 (2.8)	163 (2.6)
La	27–29	ND	39.6 (1.8)	36.0 (25.0)	18.8 (12.2)
		ND	36.6 (1.3)	31.2 (17.2)	24.4 (18.8)
Mn	604–650	628 (11)	604 (13)	627 (4.8)	628 (6.5)
		644 (15)	604 (11)	612 (3.3)	634 (7.4)
Si, %	16.9–20.1	17.50 (0.07)	17.16 (0.17)	17.55 (0.22)	17.43 (0.27)
		17.46 (0.12)	17.12 (0.24)	17.37 (0.18)	17.48 (0.18)
Ti	2600–3700	3102 (14)	3105 (15)	3080 (45)	3280 (34)
		3084 (10)	3140 (10)	3120 (35)	3180 (20)
V	59–73	70.8 (4.7)	68.5 (7.6)	79.7 (2.6)	53.8 (10.5)
		69.3 (3.4)	72.3 (3.5)	83.8 (1.8)	68.7 (8.7)
Y	15–27	21.2 (0.3)	23.6 (0.8)	24.6 (1.8)	38.0 (2.5)
		23.4 (0.5)	23.7 (1.1)	25.5 (1.3)	40.2 (1.6)
Yb	1.9–2.6	ND	2.58 (0.27)	2.93 (0.97)	—§
		ND	2.39 (0.22)	2.57 (0.73)	—§
Zr	180–201	186 (5.5)	202 (11.5)	187 (6.8)	255 (26.8)‡
		190 (4.5)	210 (8.4)	193 (5.3)	248 (13.4)‡

* On-line dilution by tandem injection.
† ND = not determined.
‡ 0.2 g of citric acid was added to a 100-ml sample digest.
§ The standard deviation was higher than the value.

The mean results obtained by direct determination for the same five elements (*cf.* Table 3) can also be compared with the recommended data of elemental concentrations. Except for the relative deviation of Mn (6.6%) and Ba (maximum 7.7%) in three soil samples, the error did not exceed 3.5%. However, the results obtained generally fall within the specified range of recommended concentrations and exhibit acceptable deviations when compared to ICP-AES results reported by others.[7,12]

On-line dilutions between 1.8 and 15.3 were applied in the determination of soil samples. Three dilutions (1.8, 3.0 and 5.0) were made by the merging stream and three (8.0, 12.0 and 15.3) by the tandem injection techniques. Two digests of each soil were prepared, and each digest was determined in triplicate. The mean and SD of three readings for each element in a digest were calculated. The results of three representative dilutions are reported in Table 3.

The effectiveness of the on-line dilution procedures in generating steady-state concentrations can be assessed mainly from the SD of the results from major and minor elements obtained by replicate determinations. These results (combined with the accuracy of determination) can be compared with those obtained by direct determination. For all of the dilutions given in Table 3, and also for others not reported, the SD of data for Al, Si and Ti, did not exceed 2.7%. The SD for Ba and Mn at all dilutions was less than 3%, reaching this upper level for Mn at a dilution of 15.3. The percentage deviation of Al, Ba and Ti for all reference samples at all dilutions was within the range of the recommended concentrations. However, the determination of Mn and Si in soils SO-2 and SO-3 at some dilutions yielded results that were very slightly lower for Mn and higher for Si, compared with the recommended concentrations (*cf.* Table 3). Nevertheless, these deviations agree with other results obtained for ICP-AES soil analysis[7,12] and by the direct determination method used in this work. Therefore, the results obtained for these five major and minor elements clearly indicate that the on-line dilution methods are adequate for sequential ICP-AES analysis of soil samples.

In a previous study of sequential multi-element analysis of soils,[7] La and Yb were not determined, and ICP-MS was understood to be more accurate and precise than ICP-AES for the determination of V, Y and Zr. In the present study the influence of various on-line dilutions on the accuracy and precision of the results was examined for the determination of La, V, Y, Yb and Zr in reference soil samples using ICP-AES (*cf.* Table 3). The results are dependent on the reference soil sample, and the results obtained for each element using ICP-AES are discussed below. However, as these elements are trace constituents, deviations of up to 20% from the recommended values are considered adequate, particularly when the SD does not exceed 15%.

Lanthanum

Addition of $LiBO_2$ to the lanthanum standard solution increased the background emission and resulted in a decrease of the signal to background ratio. Dilution of the SO-3, SO-4 and Soil 7 digests by 6 and SO-1 and SO-2 by 10 lowered the concentration of La below its detection limit.

Direct determination of La was not performed. The results obtained for La in SO-1 were satisfactory at all dilutions, but the deviation of the results for the concentration of La in SO-2 was about ±20%. On the other hand, the lanthanum results in SO-3, SO-4 and Soil 7 when dilutions of less than or equal to 5 were used exhibit either significant deviation or a very poor precision. Even at a dilution of 1.8, large errors were obtained for all three samples.

The use of high-purity $LiBO_2$, which has a lower La background emission, might improve both the accuracy and precision of La determination in soil digests. However, to obtain satisfactory results, separation and pre-concentration of La, prior to ICP-AES determination, has been suggested.[13,14]

Vanadium

Adequate precision resulted from the direct determination of V in all of the soil samples, and the accuracy was acceptable for SO-4 and Soil 7. However, the deviation of the V results for SO-1, SO-2 and SO-3 was high (−12, 17 and 35%, respectively). The most suitable results for V were obtained at a dilution of 1.8 for all of the soils analysed, except for a deviation of 19% which was obtained for SO-3 (containing the lowest V concentration). Although some of the results are acceptable for other dilutions also, a dilution of 15.3 reduces the concentration of V either close to the detection limit or below it. However, a dilution of 5.0 did not yield adequate results for all of the samples. Therefore, a dilution of 1.8 is recommended for the determination of V.

Yttrium

Adequate precision and accuracy were demonstrated for the direct determination of Y in all of the soil samples. Except for SO-2 the Y concentration at a dilution of 15.3 is lower than the detection limit. At this dilution the deviation from the recommended values exceeded 35%, except for SO-2 for which only 19% deviation was obtained. The SD was satisfactory for all samples at all dilutions. Long-term variation of the blank emission can be responsible for introducing a bias that influences the accuracy of results to a greater extent than its precision, especially at the detection limits or lower. Fairly accurate results were exhibited for dilutions of 1.8 and 5.0.

Ytterbium

Direct determinations were not performed for this element. Dilutions of 5.0 and higher reduced the Yb concentration to below the detection limit. Only the results obtained at a dilution of 1.8 were satisfactory, but the results for SO-2 and SO-4 were about 20 and 35% higher, respectively, than the recommended values.

Zirconium

In previous studies[7] citric acid was added to aid the digestion of Zr from the fused SO-2 sample (containing the highest concentration of Zr); otherwise, very low results were obtained. The results also deteriorated for aged solutions. This observation was verified in the present work, which indicated that only in the presence of citric acid could a stable Zr solution be obtained for SO-2 even after storage for several months. Direct determination of Zr in the absence of citric acid was satisfactory for the other soil samples except for the slightly high mean results obtained for SO-3 (about 15%) and SO-4 (about 10%). The need to add citric acid to SO-2 to form Zr-stable digests is peculiar to its composition. When compared with the composition of the other test soils, SO-2 was found to contain the highest concentration of Zr and Ti (*cf.* Table 3) and also phosphate (0.3% P, approximately 3- to 6-fold the concentration of the other soils).

Fusion of soil samples leads to the formation of lithium zirconate, which is fairly insoluble in water but is soluble in acid.[15] In spite of this, zirconium phosphates (including zirconium pyrophosphate) and zirconium hydroxide under special conditions are acid insoluble. However, the precipitation of zirconium hydroxide is inhibited by the presence of tartrates or citrates, because these form soluble complexes that are stable even in basic solution.[15]

Satisfactory results were obtained for Zr at dilutions of 1.8 and 5.0. At a dilution of 15.3 for which citric acid was added, the results obtained for Zr were especially high for SO-1 and SO-3. This result is not clearly understood, but it was not pursued, as the addition of citric acid to these samples is not mandatory.

Conclusions

On-line dilution methods constitute an important step in the automation of analytical processes. Their application obviates the time consuming operation of pre-dilution and dispenses with the need for additional laboratory glassware for dilution. Cleaning glassware can also be a source of contamination of sample solutions, especially when trace constituents are involved.

Pre-dilution is required for routine analysis of soil digests, even with the use of a torch assembly that tolerates analytes with a high salt content, as otherwise thorough cleaning must be adopted between consecutive analyses. In spite of these precautions, deterioration of the signal is common.

Use of the merging stream, or the tandem injection, technique is adequate for on-line dilution of reference soil sample digests. For major and minor elements accurate and reproducible results were obtained. They compare well with the results obtained by direct analysis of soil digests and are in good agreement with the recommended values. Furthermore, on-line dilution enables decisions to be made concerning the dilutions that are most suitable for the determination of some trace elements in soil samples. Similarly, this approach may provide other applications, for example, multiple dilutions corresponding to different matrix compositions.

Both of the steady-state on-line dilution methods have utilised a merging stream configuration, which supplies a continuously flowing diluent. This arrangement prevents clogging of the nebuliser capillaries, especially with high salt content solutions. This improves the nebuliser operation and contributes to plasma stability. The continuously flowing stream is not hindered by the introduction of air as the samples are changed, especially when a suitable SFS device is included. In addition to providing a suitable interface of the flow system with the plasma detector, SFS is also capable of diminishing pressure build-up and partially or completely discharging air bubbles to waste.

The merging stream configuration also allows the introduction of reagents. An internal reference standard is often added to the diluent stream, for example,[16] and the approach was applied in the routine analysis of soil sample digests devoid of an internal reference standard.

The over-all effect of on-line dilution methods saves time by avoiding pre-dilution. However, on-line dilutions involve some measurement delay until a steady-state concentration is obtained. For ICP-AES determinations, data acquisition is delayed by 3 min for the merging stream and 3.5 min for the tandem injection techniques. However, flow of the next sample can be initiated 1 min before the termination of data acquisition of the first, a practice which was adopted for the present study. In addition, this delay includes the interval required for plasma equilibration and the period involved in

rinsing the nebuliser between consecutive sample analyses. The delay for the on-line dilution techniques does not exceed 1.5–2.0 min for each analysis of one sample digest.

A new design of the merging stream on-line dilution apparatus was examined. The variable speed peristaltic pump with a flow manifold module facilitated a flow-rate of <2.0 ml min^{-1} for all dilutions. Thus, one set of mixing coils can be effective for all dilutions. The only requirement in selecting the desired dilution is to configure the flow-rates of the peristaltic pump flows using equation (3). Dilutions between 1.8 and 5 were useful for demonstrating the application of the merging stream on-line dilution method. However, the entire range of dilutions up to 15 is feasible for the ICP-AES sequential analysis, which can easily be carried out with the merging stream dilution approach.

The tandem injection method was applied for dilutions from 8 to 15. This technique is especially suited for high dilutions, but in principle, it may also be used for low dilutions. Only one flow configuration, involving equal flow-rates for all channels, has permitted the variation of the applied dilution by merely changing t_i with a constant t_{TI} of 20 s. No other operation was required to achieve the desired dilutions.

The use of the Myers - Tracy signal compensation method with Sc as the internal reference element permitted simultaneous correction for short-term variations of the plasma source, which appears to yield satisfactory results for major and minor elements in reference soil samples.

Both of the steady-state dilution methods applied here are adequate for application to the multi-element sequential analysis of reference soil samples.

This research was supported by the *ICP Information Newsletter*.

References

1. Mindegaard, J., *Anal. Chim. Acta*, 1979, **104**, 185.
2. Reis, B. F., Jacintho, A. O., Mortatti, J., Krug, F. J., Zagatto, E. A. G., Bergamin, F. H., and Pessenda, L. C. R., *Anal. Chim. Acta*, 1981, **123**, 221.
3. Gisin, M., Thommen, C., and Mansfield, K. F., *Anal. Chim. Acta*, 1986, **179**, 149.
4. Bysouth, S. R., and Tyson, J. F., *J. Anal. At. Spectrom.*, 1987, **2**, 217.
5. Garn, M. B., Gisin, M., Gross, H., King, P., Schmidt, W., and Thommen, C., *Anal. Chim. Acta*, 1988, **207**, 225.
6. Israel, Y., Lásztity, A., and Barnes, R. M., *Analyst*, 1989, **114**, 1259.
7. Wang, X., Lásztity, A., Viczián, M., Israel, Y., and Barnes, R. M., *J. Anal. At. Spectrom.*, 1989, **4**, 727.
8. Lásztity, A., Wang, X., Viczián, M., Israel, Y., and Barnes, R. M., *J. Anal. At. Spectrom.*, 1989, **4**, 737.
9. Winge, R. K., Peterson, V. J., and Fassel, V. A., *Appl. Spectrosc.*, 1979, **33**, 206.
10. Israel, Y., *Anal. Chim. Acta*, 1988, **206**, 313.
11. Gladney, E. S., and Roelandts, I., *Geostand. Newsl.*, 1989, **13**, 217.
12. Kanda, Y., and Taira, M., *Anal. Chim. Acta*, 1988, **207**, 269.
13. Broekaert, J. A. C., and Hormann, P. K., *Anal. Chim. Acta*, 1981, **124**, 421.
14. Brenner, I. B., Watson, A. E., Steele, T. W., Jones, E. A., and Goncalves, M., *Spectrochim. Acta, Part B*, 1981, **36**, 785.
15. Hahn, R. B., *in* Kolthoff, I. M., and Elving, P. J., *Editors*, "Treatise On Analytical Chemistry," Part II, Volume V, Wiley-Interscience, New York, 1961, p. 78.
16. Barnes, R. M., Israel, Y., and Bakowska, E. G., Paper presented at the XXVI Colloquium Spectroscopicum Internationale, Sofia, Bulgaria, July 2–9, 1989.

Paper 0/00749H
Received February 19th, 1990
Accepted June 8th, 1990

Flow Injection Spectrophotometric Determination of 4-Aminophenazone Based on Diazotisation and Coupling Reactions

AbdulAziz M. Alwehaid
Chemistry Department, College of Science, King Saud University, P.O. Box 2455, Riyadh-11451, Saudi Arabia

The flow injection spectrophotometric determination of 4-aminophenazone (4-aminoantipyrine), based on the diazotisation of *p*-nitroaniline with nitrite and coupling with 4-aminophenazone, is developed. The coupling reaction takes place in a 250-cm reaction coil, and the resulting azo-compound is quantified by spectrophotometry at 380 nm. A linear calibration graph is obtained for increasing concentrations up to 50 μg ml^{-1}. The experimental limit of detection (three times the noise signal) is 0.05 μg ml^{-1} (200 μl), and the relative standard deviation is 0.61 and 0.27% for 4 and 50 μg ml^{-1} (ten injections), respectively. The sampling rate is 50 h^{-1} and the over-all dispersion of the system is 1.96.

Keywords: *4-Aminophenazone; flow injection; diazotisation and coupling; spectrophotometry*

The pyrazolone-derivative analgesics are longer acting than aspirin. They exert an antipyretic effect in some situations in which aspirin is not completely effective, *e.g.*, in Hodgkin's disease with fever unresponsive to salicylates or chemotherapy.[1] They are, however, more toxic,[2] a factor that restricts their use and makes their identification and determination of great importance. One of these pyrazolone derivatives is 4-aminophenazone (4-amino-2,3-dimethyl-1-phenyl-3-pyrazolin-5-one or 4-aminoantipyrine), and it appears that there are very few spectrophotometric methods available for its determination.[3,4] It can be determined by coupling with diazotised *p*-nitroaniline and producing a yellow azo dye that is quantified by spectrophotometry at 380 nm.[5] In general, rapid, accurate, precise, simple and cost-effective procedures are favourable methods for routine analysis. Flow injection (FI) is a well known technique that satisfies most of these requirements.

In this paper, the advantages of FI (simplicity, high precision, rapidity and low reagent consumption) are combined with the benefits of the diazotisation and coupling reactions for the spectrophotometric determination of 4-aminophenazone. The chemical reaction variables, and also the FI variables, were optimised on the basis of sensitivity, sampling rate and reagent consumption.

Experimental

Reagents

All chemicals were of analytical-reagent grade and were used without further purification. Distilled de-ionised water was used throughout.

4-Aminophenazone stock solution (1000 μg ml^{-1}). Prepared by dissolving 0.5 g of 4-aminophenazone in water in a 500-ml calibrated flask, the solution being made up to volume with water. Working standards were prepared by appropriate dilution with water.

p-Nitroaniline solution (3×10^{-3} M). Prepared by dissolving 0.1036 g of *p*-nitroaniline in about 50 ml of hot water. The solution was cooled and transferred into a 250-ml calibrated flask and made up to volume with water.

Sodium nitrite solution (0.02 M). Prepared by dissolving 0.345 g of sodium nitrite in water in a 250-ml calibrated flask, the solution being made up to volume with water.

Hydrochloric acid solution (0.5 M). Prepared by dilution of concentrated hydrochloric acid and standardised by titrimetry against various amounts of sodium carbonate. A 0.1 M solution was prepared by appropriate dilution.

Dye-forming reagent (1×10^{-3} M). In a 100-ml calibrated flask, 33.33 ml of the above *p*-nitroaniline solution, 7 ml of 0.1 M hydrochloric acid and about 50 ml of water were mixed and the mixture was stirred; 5 ml of 0.02 M nitrite were then added and the solution was made up to volume with water. After 10–15 min the small amount of precipitate formed was filtered off.

Interferent solutions (5000 μg ml^{-1}). Prepared by dissolving the appropriate amount of interferent in cold water, hot water or ethanol and diluting to volume with water.

Apparatus

A Gilson Minipuls 3 (four channels) peristaltic pump was used. Samples were introduced via a Rheodyne RH-5020 injection valve with interchangeable loops of different volumes. The reaction coil was of PTFE tubing (0.5 mm i.d.) as was the remainder of the manifold tubing. The absorbance of the azo dye formed was measured at 380 nm with an LKB Ultrospec II 4050 spectrophotometer equipped with a Helma 18-μl flow cell and attached to an MSE Princess 80 multi-range chart recorder.

FI Manifold

The FI manifold used is outlined in Fig. 1. It consists of two channels. The sample solution (200 μl) is introduced via the injection valve (I) into the water stream and is pumped at a flow-rate of 1.5 ml min^{-1} while the reagent is pumped through the other channel at a flow-rate of 0.5 ml min^{-1}. The two streams are mixed at a T-junction and the coupling reaction takes place in a 250-cm reaction coil (C). The resulting dye is then monitored by spectrophotometry at 380 nm, and the peaks are recorded by the chart recorder (Re).

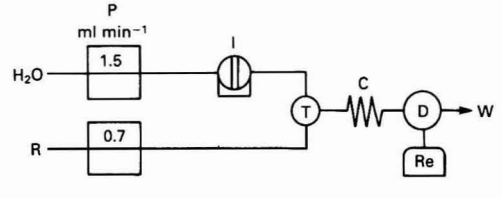

Fig. 1. Schematic diagram of the FI manifold used. P, Peristaltic pump; R, dye-forming reagent consisting of 33.33 ml of 3×10^{-3} M *p*-nitroaniline, 7 ml of 0.1 M HCl and 5 ml of 0.02 M NO_2^- in 100 ml of water; I, injection valve (200 μl); T, T-junction; C, reaction coil (250 cm); D, detector; Re, recorder; and W, waste

Procedure

By using the FI manifold described above, inject the sample solution (1–50 μg ml^{-1} of 4-aminophenazone, 200 μl) and read the maximum absorbance obtained and/or record the signals on the chart recorder.

Results and Discussion

Nitrite ions react with *p*-nitroaniline in an acidic medium to form the diazonium ion, which, in turn, is coupled with 4-aminophenazone to form the dye to be measured. The reaction variables and also the FI variables were optimised in terms of sensitivity, precision, sampling rate and reagent consumption.

Influence of Reaction Variables

Reagent concentration

The influence of the concentration of the diazotised *p*-nitroaniline was investigated by injecting 200 μl of a 50 μg ml^{-1} solution of 4-aminophenazone into the water stream pumped at 1.5 ml min^{-1}. Different concentrations of the diazotised *p*-nitroaniline were prepared, in the same manner as described under Reagents, with various volumes of *p*-nitroaniline and nitrite solutions. The concentration of hydrochloric acid was 7×10^{-3} M in the final volume of each solution. Each solution was then pumped through the reagent channel at a flow-rate of 0.7 ml min^{-1}. The results obtained are shown in Fig. 2. A maximum peak-height absorbance was obtained with 1×10^{-3} M of diazotised *p*-nitroaniline. This concentration gave reproducible results for at least 1 week at room temperature and was, therefore, used in all further experiments.

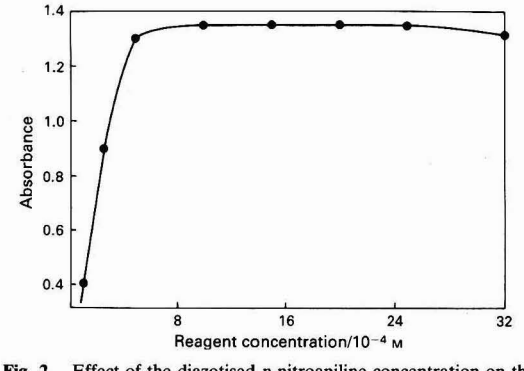

Fig. 2. Effect of the diazotised *p*-nitroaniline concentration on the absorbance of a 50 μg ml^{-1} 4-aminophenzone solution. Flow-rates, sample volume and reaction coil length are as given in Fig. 1.

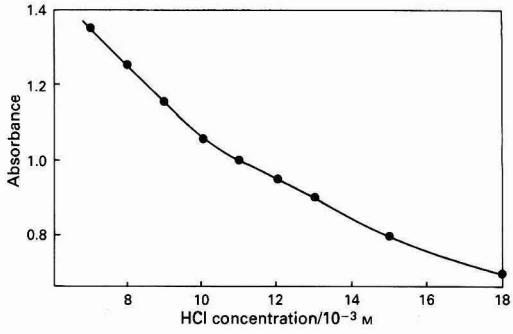

Fig. 3. Influence of HCl concentration on peak-height absorbance of a 50 μg ml^{-1} 4-aminophenazone solution. All FI variables are as shown in Fig. 1

Effect of hydrochloric acid concentration

The effect of the hydrochloric acid concentration was found to be critical and, therefore, had to be carefully controlled as small changes in its concentration in the final volume could easily have led to appreciable changes in the peak-height absorbance for the same 4-aminophenazone sample solution. Fig. 3 shows the results obtained with different concentrations of hydrochloric acid in a fixed concentration of the diazotised *p*-nitroaniline reagent, *i.e.*, 1×10^{-3} M. The peak-height absorbance of a 50 μg ml^{-1} sample solution increased with decreasing concentrations of hydrochloric acid down to 7×10^{-3} M. Use of concentrations of $<7 \times 10^{-3}$ M resulted in a large background absorbance (approximately 2.7) and an extremely unstable baseline, when compared with the background absorbance (about 0.04), which led to the very stable baseline, obtained when a 7×10^{-3} M solution was employed. This concentration was chosen in optimising the FI parameters.

Influence of FI Parameters

Sample volume

Increasing the sample volume injected will lead to an increase in the sensitivity obtained until a steady-state signal is attained when the equilibrium reaches its maximum. For the manifold shown in Fig. 1, the influence of the sample volume was evaluated for a 50 μg ml^{-1} solution of 4-aminophenazone, and the results obtained are presented in Fig. 4. An increase in the peak-height absorbance was obtained by increasing the injected sample volume up to 200 μl, above which the increase in absorbance was not significant. This sample volume was, therefore, considered to be the optimum.

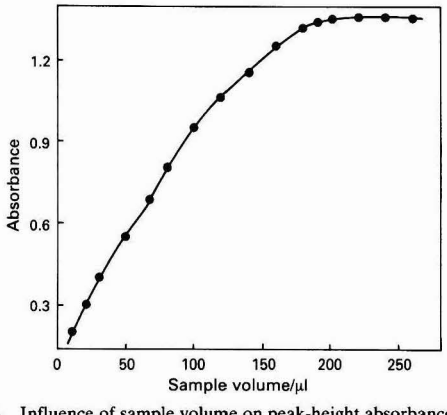

Fig. 4. Influence of sample volume on peak-height absorbance of a 50 μg ml^{-1} 4-aminophenazone solution. All other FI variables are as shown in Fig. 1

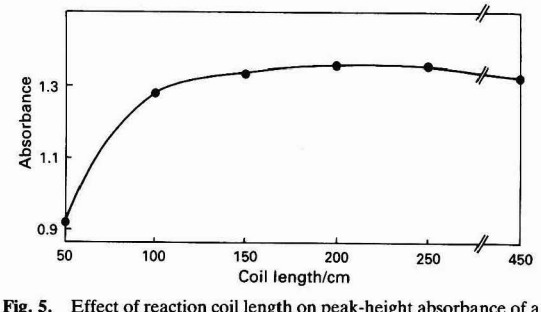

Fig. 5. Effect of reaction coil length on peak-height absorbance of a 50 μg ml^{-1} sample solution. All other FI variables are as shown in Fig. 1

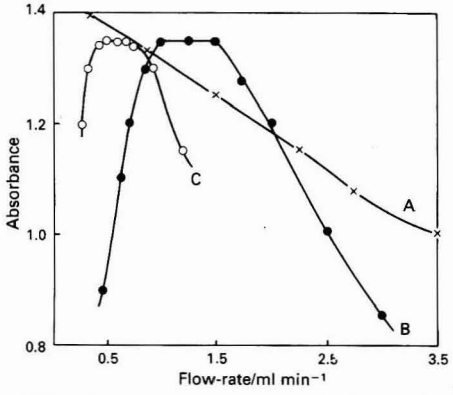

Fig. 6. Effect of flow-rate on absorbance of a 50 μg ml^{-1} sample solution; A, total flow-rate; B, sample stream; and C, reagent stream

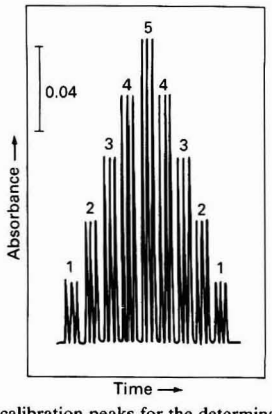

Fig. 7. Typical calibration peaks for the determination of 4-aminophenazone. The concentrations are shown on the peaks in μg ml^{-1}

Reaction coil length

By using the FI parameters shown in Fig. 1, the effect of reaction coil length on the peak-height absorbance of a 50 μg ml^{-1} sample solution was evaluated. Various coils with increasing lengths were placed between the T-junction and the detector. The results obtained (Fig. 5) show that maximum dye production was achieved with coil lengths of 200–300 cm. This can be explained as follows: as the reaction coil length increases more dye is produced, up to 200 cm, above which a constant absorbance is obtained, owing to the balance between the increase in the dye production and the dispersion effect up to 300 cm. At longer coil lengths, dispersion decreases the absorbance. A 200-cm coil length was, therefore, chosen as the optimum.

Total flow-rate

The influence of total flow-rate was evaluated, at a flow-rate ratio (sample to reagent) of 1 : 1, by increasing the pump speed and injecting a 50 μg ml^{-1} sample solution at different total flow-rates. The results shown in Fig. 6 (curve A) indicate that maximum absorbance was obtained at the lowest possible flow-rate. However, the peaks were broadened and sample throughput was very low, hence it was decided to evaluate sample and reagent flow-rates individually.

Sample and reagent flow-rates

The effect of sample flow-rate was evaluated over the range 0.45–3.0 ml min^{-1} at a reagent flow-rate of 0.7 ml min^{-1}. It was found that increasing the sample flow-rate from 0.45 to 1.0 ml min^{-1} resulted in an increase in sensitivity (Fig. 6, curve B) and sample throughput. The sensitivity at higher flow-rates remained constant, up to 1.5 ml min^{-1}, above which it decreased. The reason for this effect was explained previously[6] by using a similar FI manifold to that shown in Fig. 1 and injecting a dye. It was shown that when the flow-rates in both channels are similar, reproducible and fast mixing is achieved in the T-junction. As the sample flow-rate decreases, however, its flow into the exit stream is restricted, leading to drawn-out peaks; this explains the decrease in curve B (Fig. 6) as the flow-rate decreases. Therefore, increasing the flow-rate improves the sensitivity. This effect, however, is in conflict with the dispersion effect as the flow-rate increases, leading to a constant sensitivity over the range 1.0–1.5 ml min^{-1}. Higher flow-rates resulted in poorer sensitivity, owing to dispersion and the decrease in the time allowed for dye formation.

The reagent flow-rate was investigated at a sample flow-rate of 1.5 ml min^{-1}. The results obtained (Fig. 6, curve C) show that maximum sensitivity was obtained at a reagent flow-rate of 0.7 ml min^{-1}. Lower flow-rates resulted in poorer sensitivity, owing to insufficient reagent being delivered, while higher flow-rates merely increased the dispersion. The total flow-rate under the optimised conditions was 2.2 ml min^{-1}.

Table 1. Effect of some possible interfering species on FI determination of 10 μg ml^{-1} of 4-aminophenzone.

Interferent	Concentration/ μg ml^{-1}	Error,%
Alanine	100	3
Antipyrine	100	2
Amidopyrine	100	7
Aminobenzoic acid	100	30
Aminobenzoic acid	50	10
Aminoacetophenone	100	15
Arginine	100	1
Benzoic acid	100	0
Indole	100	187
Indole	50	98
2-Aminonaphthalene-4-sulphonic acid	100	164
2-Aminonaphthalene-4-sulphonic acid	50	89
α-Naphthol	100	213
α-Naphthol	50	160
1-Aminonapthalene	100	0
Salicyclic acid	100	0
Uracil	100	0

Determination of 4-Aminophenazone

Calibration graphs for the determination of 4-aminophenazone were established under the optimised experimental conditions shown in Fig. 1. The calibration graph was linear for up to 50 μg ml^{-1} with a correlation coefficient (9 points) of 0.9997. Typical recorded calibration peaks, covering the range 1–5 μg ml^{-1} are shown in Fig. 7. The least-squares equation for this graph is peak-height absorbance = $0.028c - 1 \times 10^{-3}$, where c is the concentration of 4-aminophenazone in μg ml^{-1}. The experimental limit of detection was obtained by comparing the magnitude of the signal of the injected sample with a signal equal to three times the noise signal caused by the pulsation of the peristaltic pump. It was found to be 0.05 μg ml^{-1}. The calculated limit of detection,[7] using the statistical information obtained from the graph shown in Fig. 7, was found to be 0.1 μg ml^{-1} (twice the noise signal). The relative standard deviation was 0.61% for a 4 μg ml^{-1} sample solution and 0.27% for a 50 μg ml^{-1} solution (ten injections of each). The sampling rate was 50 h^{-1} and the over-all dispersion of the system was 1.96.

Interference

Table 1 summarises the effects of some possible interfering species and shows that indole, 2-aminonaphthalene-4-sulphonic acid and α-naphthol interfere in the determination of 10 μg ml^{-1} of 4-aminophenazone.

Conclusion

The FI method described above for the determination of 4-aminophenazone in aqueous solution, based on diazotisation and coupling reactions, provides a precise, simple and rapid technique that satisfies most of the requirements in routine analysis.

The author thanks M. Demashki for assistance, and the Research Centre of the College of Science for financial support (Project No. Chem/1408/05).

References

1. Meyers, F. H., Jawetz, E., and Goldfien, A., "Review of Medical Pharmacology," Sixth Edition, Lange Medical Publications, Los Altos, CA, 1976, p. 290.
2. Reynolds, J. E. F., and Prasad, A. B., "Martindale, The Extra Pharmacopoeia," Twenty-eighth Edition, The Pharmaceutical Press, London, 1982, p. 272.
3. Zanin, V. V., Musael'yants, V. Ya., Savel'eva, T. A., and Ponomarev, V. D., *Farmatsiya (Moscow)*, 1982, **31**, 77; *Anal. Abstr.*, 1982, **43**, 5E38.
4. Zanin, V. V., Smirnov, E. V., Papikyan, N. N., and Ponomarev, V. D., *Farmatsiya (Moscow)*, 1979, **28**, 33; *Anal. Abstr.*, 1980, **38**, 4E45.
5. Al-Abachi, M. Q., Al-Delami, A. M. S., and Al-Najafi, S., *Analyst*, 1988, **113**, 1661.
6. Al-Wehaid, A., and Townshend, A., *Anal. Chim. Acta*, 1987, **198**, 45.
7. Miller, J. C., and Miller, J. N., "Statistics for Analytical Chemistry," Ellis Horwood, Chichester, 1986, p. 96.

Paper 0/00189I
Received January 12th, 1990
Accepted June 26th, 1990

Determination of Light Hydrocarbon Gases in Sea Water Using Three Variants of Static "Equilibrium" Headspace Analysis

Alexander P. Bianchi
Environmental Laboratory, Exxon Chemical Company, Cadland Road, Hythe, Southampton, Hampshire SO4 6NP, UK

Three methods for the determination of the light hydrocarbon gases methane, ethane, ethene, propane, propene, butane, 2-methylpropane and butenes in coastal sea water are described. The first two methods are based on manual equilibration of the headspace vapours in glass vessels, followed by injection into the gas chromatograph. The third method uses a commercial semi-automatic, pneumatically controlled headspace device interfaced to the gas chromatograph. Analysis is then performed using both packed and capillary column chromatography, followed by flame-ionisation detection. The limit of detection is below 2×10^{-5} ml l^{-1} v/v for method variant I and below 5×10^{-6} ml l^{-1} v/v for method variants II and III.

Keywords: *Light hydrocarbon gas; surface water; coastal sea water; static headspace; gas chromatography with flame-ionisation detection*

Reports of oil pollution in the marine environment have received considerable attention recently. Spills of oil and volatile chemicals into coastal sea water represent potentially significant environmental and ecological threats to marine ecosystems. However, the more visible effects of oil in sea water have masked interest in the disposition and behaviour of the more soluble components of petroleum, particularly the dissolved gaseous hydrocarbons. Marine chemists have long recognised that these compounds do not all evaporate following spillage, and may be transported down into the water column via turbulent mixing of water masses and laterally via currents.[1]

Equally, little attention has been devoted to assessing the occurrence and importance of low-level inputs of biogenically derived hydrocarbon gases within productive coastal estuaries.[2] Taken individually, or together, these hitherto unexplored processes lead to various concentrations of dissolved gases in water which in turn provide information about polluting or biological activities. For example, in a recent study of marine pollution caused by shoreside marina developments in the UK, exceptionally high levels of light hydrocarbons were found in nearby waters.[3]

There have been few reports of low relative molecular mass hydrocarbons in open-ocean waters or in rivers and estuaries. Swinnerton and Linnenbom[4] reported the first *in situ* measurements of the C_1–C_4 hydrocarbon content of sea water from the Atlantic and the Gulf of Mexico. This was shortly followed by a study of the distribution of methane and carbon monoxide between the atmosphere and the sea water surface.[5] There are no published references to similar studies of light hydrocarbons in any UK rivers, estuaries or coastal waters. Therefore, it is impossible to assess the likelihood of their occurrence or potential contribution to levels of dissolved organic carbon in natural waters. A common theme in this type of work is that the relevant data are not available because suitable methods and equipment have not been developed for the study of these compounds. The absence of data, in turn, forestalls judgement and leads to the exclusion of these compounds from scientific assessments of estuarine quality.

Until comparatively recently, very few simple analytical methods have been available for the determination of trace levels of dissolved light hydrocarbons in water. Early techniques developed in the USA[1] involved continuous stripping of large volumes of sea water (*i.e.*, 6 l min^{-1}) followed by vacuum collection of the stripped gas inside glass funnels. The stripped gas was then injected into a gas chromatograph via a 1.76-ml sample loop at 5-min intervals. Limits of detection for the C_1–C_4 hydrocarbon gases down to 1×10^{-7} ml l^{-1} were reported for the method.

Two simpler methods for detecting C_1–C_4 hydrocarbons in water have been developed by UK water authority laboratories.[6] These variants include direct aqueous injection and vacuum de-gassing of water samples in a glass vessel, followed by displacement of the gas into a gas-sampling loop. Both methods utilise packed column chromatography and flame-ionisation detection. Direct aqueous injection was found to be unsatisfactory in the laboratory for routine analysis of moderately contaminated sea water samples. High levels of suspended matter and salt deposits were observed to collect in the chromatograph injection liner causing contamination and "memory" effects. The vacuum de-gassing method overcame these difficulties but provided unreliable repeatability in regular use. This was because many water samples frequently contained varying levels of viscous oils, acids and suspended solids (*i.e.*, >100 mg l^{-1}) which rapidly abrade glass joints and precipitate leakages.

Equilibrium headspace methods overcome these problems and have been used successfully for the determination of volatile compounds in both surface water and "hostile" sample matrices. Manual "static" headspace techniques have been reported by Croll *et al.*[7] for trihalomethanes in surface waters and by Bianchi and Varney[8] for volatile aromatics in estuarine sediments Both methods provide low limits of detection (*i.e.*, <1.0 μg l^{-1}) and have relative standard deviations (RSDs) of less than 2%.

Experimental

Apparatus and Instrumentation

Three different static headspace methods were investigated for the determination of light hydrocarbons in surface waters. The basic approaches are summarised below.

Variant I. Indirect gas-syringe sampling

Equilibration and sampling were carried out using a simple syringe-pump arrangement. The apparatus is illustrated in Fig. 1. In this arrangement, a 500-ml syringe was interfaced to a stainless-steel tube (3 mm o.d.) connected to the inlet of a six-port gas sampling valve (2-ml sampling loop capacity). The sampling bottle was connected by a glass stopcock - metal connection to the outlet tubing of the gas sampling valve. The sample vessel (containing 800 ml of sample and 200 ml of purified helium head-gas) was immersed in a 5-l water-bath. The sample bottle was agitated every 10 min. Gas chromatographic analysis was carried out using a packed column.

Variant II. Direct gas-syringe sampling

Equilibration and sampling were carried out using a similar technique to that described for variant I. This variant is shown in Fig. 2. The syringe has a fabricated water sheath lining, permitting water at the same temperature as the equilibration temperature to be passed through the sheath. A 20-ml head-gas sample was drawn from the equilibration bottle into the syringe and injected into the gas chromatograph via a gas-sampling valve. A PLOT fused-silica capillary column was used for the chromatographic separation.

Variant III. Pneumatic, semi-automatic injection

The manual injection techniques descibed in variants I and II were substituted by a commercial semi-automated headspace sampling instrument (Perkin-Elmer HS-6) permanently attached to the gas chromatograph. Water samples were equilibrated and injected *in situ*. The HS-6 unit consists of a rotating temperature-controlled magazine with six recesses for 6-ml glass vials and a control unit for programming the time and temperature of the sampling. The magazine is mounted on the injector panel of the chromatograph. The operating principle involves controlled heating of the sample vials within the magazine [see Fig. 3(*a*)]. After the heating and equilibration period, the magazine is pushed upwards on a spigot. This step causes a fixed sampling needle to penetrate the septum of the headspace vial [see Fig. 3(*b*)]. The penetration of the needle is followed by pneumatic introduction of a predetermined aliquot of equilibration gas. The gas develops a pressure inside the headspace of the vial greater than that at the inlet of the chromatographic column. After a programmed time interval, the pressurised sample vapour is flushed from the sampling needle into the capillary column. The three stages of equilibration, pressurisation and sampling are shown schematically in Fig. 4.

The operating conditions for each of the three variants are presented in Table 1.

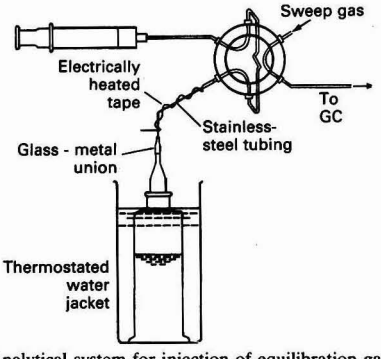

Fig. 1. Analytical system for injection of equilibration gas using a simple syringe-pump principle onto a stainless-steel packed column

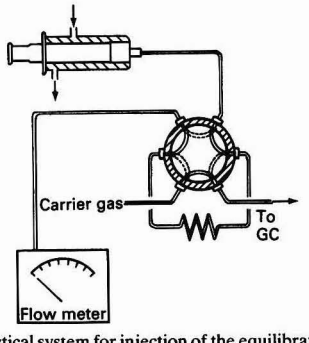

Fig. 2. Analytical system for injection of the equilibration gas from a variable-volume sampling device onto a PLOT fused-silica capillary column

Reagents and Glassware

"Blank" sea water was prepared by solvent extraction of sea water taken from an unpolluted coastal site. After the extraction of solvent extractable organics into re-distilled dichloromethane, the sea water was purged in a stream of ultrapure nitrogen. Secondary blank sea water was prepared by spiking AnalaR-grade distilled water with a heat-treated, dehydrated sea-salt mixture (Instant-ocean, Aquarium Systems, OH, USA) to simulate natural sea water [salinity = 30 ± 3 p.p.t. (parts per thousand)] and brackish estuarine water (salinity = 15 ± 3 p.p.t.).

Calibrated flasks fitted with modified stoppers for the insertion of hypodermic syringe needles were washed and dried before use. Glass tubing and glass - metal fixtures were cleaned before use. Glass gas-bulbs for gas standard preparation were stored under nitrogen.

Standard Preparation

Gas and aqueous standards were prepared according to protocols described by Brooks and Sackett,[1] Thain[9] and Grob and Kaiser.[10] Briefly, this involves the dilution of gas mixtures in water using 1- and 2-l calibrated flasks (at room temperature and pressure) containing blank sea water. Injections were conducted according to the protocols described by Kolb *et al.*[11]

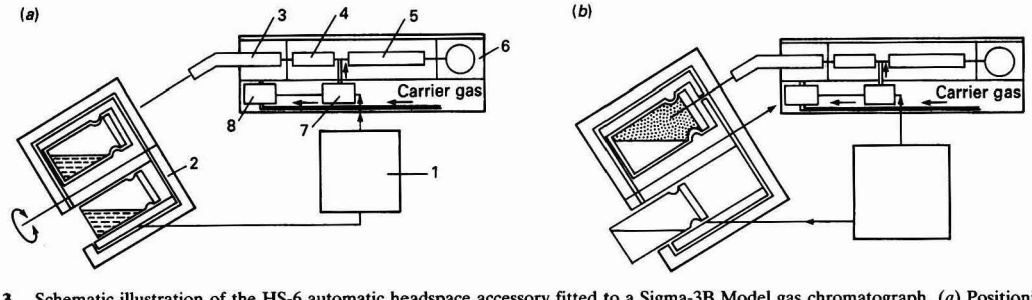

Fig. 3. Schematic illustration of the HS-6 automatic headspace accessory fitted to a Sigma-3B Model gas chromatograph. (*a*) Positioning of the sample vial and (*b*) sampling position. 1, Control unit of the headspace sampling accessory; 2, temperature-controlled magazine to hold the vials; 3, gas chromatograph injector; 4, pre-column (optional); 5, chromatographic column; 6, detector (flame ionisation for hydrocarbons); 7 and 8, electronically controlled gas-control valves. Reproduced with permission from Perkin-Elmer

Results and Discussion

Evaluation of the Analytical Variants

The chromatographic separation of standard component peaks on the packed column (variant I) is shown in Fig. 5(*a*). A corresponding analysis of an actual sample taken from the river Itchen is shown in Fig. 5(*b*). Although individual peaks are discernible, the separation is poor and the analysis time fairly long. The improved chromatography obtained using the capillary columns in variants II and III are shown for comparison in Fig. 6(*a*) and (*b*).

Simple experiments were conducted in order to determine the effect of temperature and ionic strength on the recoverability of light hydrocarbons from spiked standard mixtures. Using variants I and II, experiments to determine an optimum sample volume were carried out. By comparison, the semi-automated headspace equipment (HS-6) is designed such that the upper limit is approximately 6 ml. Further work was attempted to define the lower limits of detection and the RSDs of the analytical techniques.

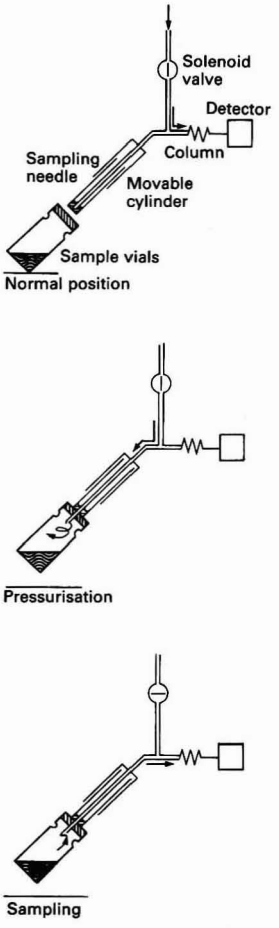

Fig. 4. Schematic diagram of the three principal stages of the HS-6 headspace analyser system. Reproduced with permission from Perkin-Elmer

Effect of temperature

Raising the temperature of the sample matrix decreases the solubility of many organic compounds in water, and proportionally enriches the gas phase. The Clausius - Clapeyron equation demonstrates how the partial pressure of components is increased by an increase in

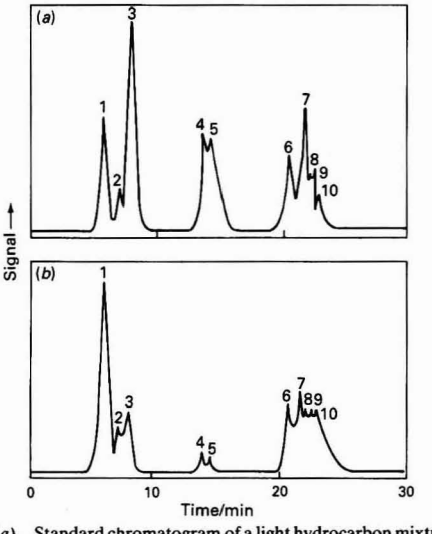

Fig. 5. (*a*) Standard chromatogram of a light hydrocarbon mixture in water run on a Porapak-Q packed column: range ×1 and attenuation ×1. (*b*) Sample chromatogram showing light hydrocarbons in a surface water sample from the River Itchen on a Poropak-Q column: range ×1 and attentuation ×1. Components: 1, methane; 2, ethene; 3, ethane; 4, propene; 5, propane; 6, 2-methylpropane; 7, butene; 8, butane; 9, *cis*-but-2-ene; and 10, *trans*-but-2-ene

Table 1. Operating conditions for variants I, II and III

	Variant I	Variant II	Variant III
Sample equilibration:			
Equilibration temperature/°C	50	50	70
Equilibration time/min	45	45	4
Gas chromatography:			
GC column	2 m × 3 mm o.d. stainless steel packed with 80–100 mesh Porapak-Q	50 m × 0.32 mm i.d. Al_2O_3/KCl PLOT	50 m × 0.32 i.d. Al_2O_3/KCl PLOT
Carrier gas	Helium	Helium	Helium
Column flow/ml min^{-1}	35	1	1
Initial temperature/°C	50 (isothermal)	70	70
Initial time/min	—	0	5
Ramp rate/°C min^{-1}	—	4	7.5
Final temperature/°C	—	160	160
Injector temperature/°C	75	70	70
Detector temperature/°C	175	200	200

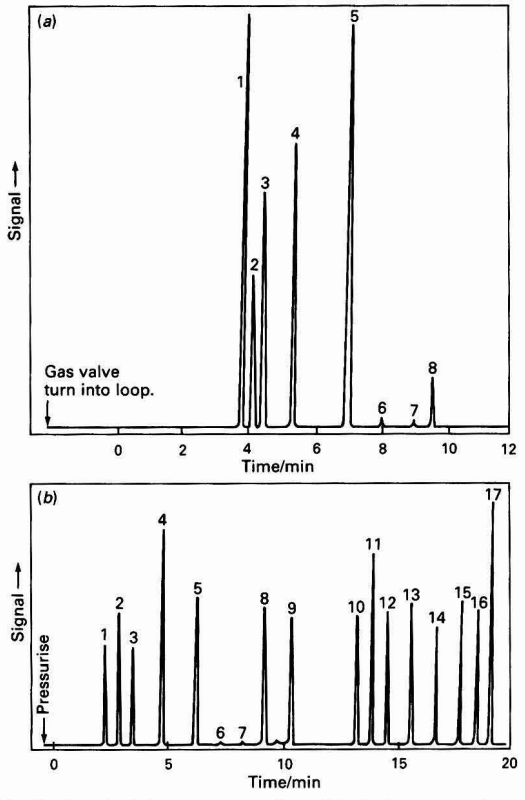

Fig. 6. Standard chromatograms of two light hydrocarbon mixtures in water run on PLOT fused-silica capillary columns. (*a*) Standard (approximately 2×10^{-3} ml l^{-1} for components 1–5) using the direct gas-syringe technique, *i.e.*, variant II. (*b*) Standard (approximately 1×10^{-3} ml l^{-1} per component) using the HS-6 headspace device, *i.e.*, variant III (see text for details). Components: 1, methane; 2, ethane; 3, ethene; 4, propane; 5, propene; 6, ethyne; 7, alkyne (propadiene?); 8, 2-methylpropane; 9, butane; 10, *trans*-but-2-ene; 11, but-1-ene; 12, 2-methylpropene; 13, *cis*-but-2-ene; 14, 2-methylbutane; 15, propyne; 16, pentane; and 17, 1,3-butadiene

temperature: $d\ln p_i/dT = L/RT^2$, where T is the temperature, L the latent heat of vaporisation of component i, and R the gas constant.

Standards containing approximately equal volumes of methane, ethane, ethene, propane, propene, butane and 1,3-butadiene (about 1×10^{-4} ml l^{-1}) were equilibrated at 25, 50 and 75 °C, using variants I and II. The results, normalised to the values obtained at 25 °C and quoted as ± one standard deviation, are presented in Table 2. They represent the recovery dependence of both variants, because, experimentally, there was found to be <5% difference between them. This suggests that temperature variations have an almost identical effect on recovery. However, inspection of the data shows that at temperatures above 50 °C the standard deviation of the means increases significantly. Despite the virtual doubling in response, this disproportionate effect is probably due to condensation effects inside the sampling system and the gas sample valve pipework. Although the use of heated tape minimises this effect, the collection of large amounts of water vapour inside the sampling system is undesirable.

A similar experiment was performed on variant III (the HS-6 system). As the sample volume is considerably less, the problem of water vapour condensation is expected to be less pronounced. The experimental data are shown in Table 3. As before, the values are normalised to those obtained at 30 °C, and tabulated as ± one standard deviation.

Table 2. Effects of equilibration temperature on relative recovery for both variants I and II ± one standard deviation

	Equilibration temperature/°C		
	30	50	75
Methane	1.00 ± 0.01	1.59 ± 0.03	1.96 ± 0.55
Ethane	1.00 ± 0.02	1.33 ± 0.02	1.99 ± 0.43
Ethene	1.00 ± 0.02	1.45 ± 0.04	2.01 ± 0.65
Propane	1.00 ± 0.02	1.34 ± 0.04	2.10 ± 0.63
Propene	1.00 ± 0.03	1.44 ± 0.05	2.01 ± 0.64
2-Methylpropane	1.00 ± 0.02	1.40 ± 0.05	2.44 ± 0.54
1,3-Butadiene	1.00 ± 0.01	1.75 ± 0.05	2.57 ± 0.73

Table 3. Effects of equilibration temperature on relative recovery using the HS-6 headspace device ± one standard deviation

	Equilibration temperature/°C		
	30	50	70
Methane	1.00 ± 0.01	1.89 ± 0.03	2.43 ± 0.05
Ethane	1.00 ± 0.01	1.58 ± 0.02	2.02 ± 0.06
Ethene	1.00 ± 0.02	1.69 ± 0.03	2.30 ± 0.03
Propane	1.00 ± 0.02	1.45 ± 0.04	2.03 ± 0.03
Propene	1.00 ± 0.03	1.64 ± 0.03	2.05 ± 0.03
2-methylpropane	1.00 ± 0.03	1.57 ± 0.03	2.38 ± 0.04
1,3-Butadiene	1.00 ± 0.04	1.74 ± 0.04	2.47 ± 0.04

Table 4. Effect of ionic strength on the relative recovery of light hydrocarbons from water using variants I and II ± one standard deviation

	Salinity, p.p.t.		
	10	30	66
Methane	1.00 ± 0.01	1.00 ± 0.01	1.02 ± 0.40
Ethane	0.99 ± 0.01	1.00 ± 0.01	1.03 ± 0.43
Ethene	0.99 ± 0.01	1.00 ± 0.02	1.02 ± 0.32
Propane	0.99 ± 0.01	1.00 ± 0.02	1.02 ± 0.30
Propene	1.00 ± 0.02	1.00 ± 0.02	1.03 ± 0.24
2-Methylpropane	1.00 ± 0.03	1.00 ± 0.01	1.07 ± 0.47
1,3-Butadiene	1.00 ± 0.03	1.00 ± 0.01	1.09 ± 0.35

A key observation arising from the HS-6 data is the much smaller increase in standard deviation with temperature compared with variants I and II. This is further evidence that the larger amounts of water vapour, and hence the greater potential for condensation, are the main cause of the increase in standard deviation. However, as the HS-6 is an automatic device, whereas variants I and II are manually controlled, some element of operator error may also be a contributing factor. Variant II utilises a capillary column, which suggests that the use of a packed column rather than the high-performance fused-silica capillary column is not a major source of variation in this particular application. The use of the higher equilibration temperature (*i.e.*, 70 °C) is therefore a worthwhile strategy considering the increase in peak area recovery it affords.

Effect of salinity

Increasing the ionic strength of the sample matrix will enhance the concentration of organic compounds found in the gas phase. As the blank matrix was sea water (rather than distilled water), no correction for the increased solubility exhibited by organic compounds in distilled water was necessary.

However, as the salinity of estuarine waters can range from virtually zero to that of sea water (about 33 p.p.t.) some assessment of the influence of varying salinity was required. A standard sea water matrix spiked with equal volumes of methane, ethane, ethene, propane, propene, 2-methylpropane and 1,3-butadiene was used. Their concentrations were approximately 1×10^{-4} ml l^{-1} each. Standards were prepared

at salinities of 10, 30 and 66 p.p.t. The hypersaline solution was prepared from a mixture of sodium sulphate and sodium chloride (AnalaR, BDH, Poole, Dorset, UK). The salinities of 10 and 30 p.p.t. were prepared using the synthetic sea-salt mixture and pre-stripped distilled water. An equilibration temperature of 50 °C was selected for this work. Again, the data obtained using variants I and II were within 5%, and are quoted together (see Table 4). The results were normalised to the salinity of 30 p.p.t. for comparison. Equivalent data obtained using the HS-6 system (variant III) are presented for comparison in Table 5. There are only marginal variations in relative recoveries across a wide range of salinity. Comparing the data in Tables 4 and 5 shows that, when using larger sample volumes as in variants I and II, standard deviations at higher salinities are greater than those encountered with variant III. These results, together with those from the previous section, show that, over the range of temperatures and salinities examined, variations due to salinity are of minor importance and equilibration temperature has a much greater effect on method performance.

Effect of sample volume

Basic experiments to evaluate the influence of sample volume on the manual headspace variants I and II were carried out. A standard sea water mixture with a salinity of 30 p.p.t. was spiked with equal volumes containing 1×10^{-4} ml l^{-1} of methane, ethane, propane, propene, 2-methylpropane and 1,3-butadiene. Sample volumes were varied from 200 to 1000 ml. Peak-area recovery was measured and is quoted relative to an 800-ml water volume. The data are presented in Table 6.

Clearly, as sample volume is progressively increased, so relative recoveries are also increased. This general observation is true of any water - equilibration gas system as the ratio of water phase to gas increases. However, as predicted by Kolb *et al.*,[11] this effect will not be as pronounced for compounds with a high partition coefficient. Further, as can be seen from Table 6, precision will also decrease (slightly) as sample volume increases. The time required for temperature equilibrium to be reached also increases with sample volume, and the potential for leakages, water vapour production and re-condensation also increases. As it is often necessary to have non-standard water vessels for water volumes in excess of 1 l, it can be seen that there are several practical advantages in keeping sample-handling apparatus to standard dimensions.

The optimum sample volume is a balance between the maximum amount of sample that can be handled (which lowers the limits of detection and hence increases the analytical sensitivity) and the variation of precision with volume. The data in Table 5 show that, when using water volumes between 200 and 800 ml, the precision of component recoveries varies only slightly *i.e.*, ±0.02. When the water volume is increased to 1000 ml, there are approximately 2-fold increases in precision. Hence, a sample volume of 800 ml was chosen as the optimum volume to work with when using manual sampling techniques.

Detection limits and relative standard deviation

The lower detection limit in gas chromatographic analysis is generally considered to be that amount of analyte which gives a peak area response three times the standard deviation of the response obtained from the blank. In equilibrium headspace experiments developed to detect trace amounts of organochlorine compounds in effluent water, Pizzie[12] defined the lower detection limit mathematically as: $DL = 3\sigma_b/m$, where σ_b is the standard deviation of the blank response and m

Table 5. Effect of ionic strength on the relative recovery of light hydrocarbons from water using the HS-6 headspace analyser ± one standard deviation

	Salinity, p.p.t.		
	10	30	66
Methane	1.00 ± 0.01	1.00 ± 0.01	1.03 ± 0.01
Ethane	0.99 ± 0.01	1.00 ± 0.01	1.02 ± 0.01
Ethene	1.00 ± 0.01	1.00 ± 0.01	1.02 ± 0.01
Propane	1.00 ± 0.01	1.00 ± 0.01	1.01 ± 0.02
Propene	1.00 ± 0.02	1.00 ± 0.02	1.00 ± 0.02
2-Methylpropane	1.00 ± 0.01	1.00 ± 0.02	1.01 ± 0.02
1,3-Butadiene	1.00 ± 0.01	1.00 ± 0.02	1.02 ± 0.02

Table 6. Effect of sample volume on the relative recovery of light hydrocarbons from water. Results are normalised to an 800-ml sample volume ± one standard deviation

	Sample volume/ml			
	200	600	800	1000
Methane	0.94 ± 0.02	0.96 ± 0.03	1.00 ± 0.02	1.04 ± 0.06
Ethane	0.93 ± 0.02	0.97 ± 0.02	1.00 ± 0.04	1.05 ± 0.07
Ethene	0.93 ± 0.02	0.97 ± 0.03	1.00 ± 0.04	1.04 ± 0.08
Propane	0.92 ± 0.03	0.98 ± 0.03	1.00 ± 0.03	1.03 ± 0.04
Propene	0.93 ± 0.03	0.98 ± 0.03	1.00 ± 0.03	1.03 ± 0.05
2-Methylpropane	0.94 ± 0.03	0.98 ± 0.03	1.00 ± 0.03	1.03 ± 0.06
1,3-Butadiene	0.95 ± 0.04	0.99 ± 0.04	1.00 ± 0.04	1.05 ± 0.07

Table 7. Lower detection limits (DL) and RSD(%) for light hydrocarbons in sea water using three static headspace methods (six replicates). All results expressed as ml $l^{-1} \times 10^{-6}$

	Variant method					
	Indirect gas syringe (I)		Direct gas syringe (II)		HS-6 pneumatic(III)	
	DL	RSD, %	DL	RSD, %	DL	RSD, %
Methane	11.0	4.5	<0.1	1.4	0.1	1.9
Ethane	12.9	3.4	<0.1	1.3	1.9	1.4
Ethene	13.8	3.4	0.4	1.4	2.7	1.3
Propane	13.7	3.1	0.5	1.1	3.1	1.3
Propene	12.9	3.0	<0.1	1.3	1.3	0.9
2-Methylpropane	14.3	2.9	0.4	1.1	1.0	1.3
Butane	15.6	2.8	0.4	0.5	0.9	0.5
2-Methylpropene	12.3	3.2	0.2	0.4	1.3	0.8
1,3-Butadiene	8.1	4.3	<0.1	0.7	0.5	0.9

Table 8. Typical dissolved light hydrocarbon concentrations in water samples from the estuaries of Southampton and the Beaulieu river. Results expressed as ml $l^{-1} \times 10^{-6}$

	Southampton water (Hythe)	Beaulieu river
Methane	1040	1790
Ethane	75	25
Ethene	95	15
Propane	120	10
Propene	45	15
2-Methylpropane	255	40
Butane	300	20
2-Methylpropene	175	10
Butene	125	<5
1,3-Butadiene	40	<5

is the slope (or sensitivity) of the calibration graph for the analyte in question.

The lower limits of detection and the RSD(%) for C_1–C_4 light hydrocarbons using variants I, II and III are shown in Table 7. These detection limits reflect, in part, the lower sensitivity obtained using packed column chromatography (variant I) compared with the high-performance fused-silica capillary PLOT columns (used in variants II and III). Manual systems of equilibration and injection can be considered much less efficient than the semi-automatic, pneumatic system (variant III). Even though variant II is capable of lower limits of detection, variant III, combined with capillary column chromatography, offers a limit of detection comparable to variant II, but uses much less sample. Variants II and III generate repeatable data to within an RSD of 2%. Variant I, however, exhibited higher RSD values between 2.8 and 4.5%, largely due to the use of a packed column. It ought to be recognised that this performance will be satisfactory for many laboratories that wish to carry out less precise determinations of light hydrocarbons in water.

Sample Data—A Case Study

The methods described were used to study the variation in levels of light hydrocarbons with time in Southampton water. The existence of the estuary has led to the intense commercial and residential development of its shores where it supports a number of industries varying from oil refining and merchant shipping to boat building and fishing. Large tracts of shoreline have also been converted to marina complexes over the last 5 years. The Beaulieu river, a smaller estuary, is located a further 15 miles to the west along the Solent coastline. This rural waterway remains largely undeveloped and is therefore considerably less subject to inputs of anthropogenic volatile carbon compounds. Typical sample data from surface water in both estuaries are shown in Table 8 for comparison.

The data suggest that, although methane is largely of biogenic origin, the industrialised Southampton estuary contains up to ten times higher concentrations of C_2–C_4 hydrocarbons than the rural Beaulieu estuary. Previous research[3,13,14] has suggested that spillages of marine fuels, atmospheric fallout and untreated sewage wastes are a major and increasingly growing source of these hydrocarbons relative to many of the "traditional" inputs associated with local chemical-processing industries.

Conclusion

As a major reason for studying light hydrocarbons was to examine anthropogenic inputs to surface water, these limits were compared with the concentrations found in uncontaminated open-ocean water by Brooks and Sackett.[1] These workers quoted levels of approximately 5×10^{-5} ml l^{-1} for methane, 3×10^{-6} ml l^{-1} for ethane plus ethene, 1×10^{-6} ml l^{-1} for propane and about 1×10^{-1} ml l^{-1} for C_4 hydrocarbons in open-ocean surface waters. Table 7 shows that only variants II and III are suitable for monitoring light hydrocarbons in the estuary by this criterion.

However, all three methods offer a significant degree of flexibility to the analytical chemist working in this field. All three techniques can be used with relatively clean waters or with contaminated wastewaters. They do not involve the use of cumbersome or highly expensive and complex apparatus. Further, these methods have facilitated the monitoring of light hydrocarbon gases in estuarine and coastal waters and provided exclusive quantitative data on the occurrence and behaviour of these compounds as water pollutants.

The author thanks M. S. Varney (Oceanography Department, University of Southampton) and A. J. Phillips (Earth Sciences, Open University) for their valuable comments made during the preparation of the manuscript.

References

1. Brooks, J. M., and Sackett, W. M., *J. Geophys. Res.*, 1973, **78**, 5248.
2. Knap, A. H., *PhD Thesis*, University of Southampton, 1984.
3. Bianchi, A. P., Bianchi, C. A., and Varney, M. S., *Oil Chem. Pollut.*, 1989, **5**, 477.
4. Swinnerton, J. W., and Linnenbom, V. J., *J. Gas Chromatogr.*, 1967, **5**, 570.
5. Swinnerton, J. W., and Linnenbom, V. J., *Environ. Sci. Technol.*, 1969, **3**, 838.
6. "The Determination of Methane and Other Hydrocarbon Gases in Water, 1988," HM Stationery Office, London, 1988.
7. Croll, B. T., Sumner, M. E., and Leathard, D. A., *Analyst*, 1986, **111**, 73.
8. Bianchi, A., and Varney, M. S., *Analyst*, 1989, **114**, 47.
9. Thain, W., "Monitoring Toxic Gases in the Atmosphere for Hygiene and Pollution Control," Pergamon Press, New York, 1980.
10. Grob, R. L., and Kaiser, M. A., "Environmental Problem Solving Using Gas - Liquid Chromatography," *Journal of Chromatography Library Volume* 21, Elsevier, Amsterdam, 1982.
11. Kolb, B., Kraub, H., and Auer, M., "Perkin-Elmer Applications Paper 21/1978/HSA-21," Perkin-Elmer, Buckinghamshire, 1978.
12. Pizzie, R., *PhD Thesis*, University of Southampton, 1984.
13. Bianchi, A., and Varney, M. S., *Water Waste Treat.*, 1988, **31**, 14.
14. Bianchi, A., Varney, M. S., and Phillips, A. J., *J. Chromatogr.*, 1989, **467**, 111.

Paper 0/01352H
Received March 28th, 1990
Accepted July 25th, 1990

Application of High-performance Size-exclusion Liquid Chromatography to the Study of Copper Speciation in Waters Extracted From Sewage Sludge Treated Soils

Andrew R. Morrisson and John S. Park
School of Applied Sciences, RGIT, St. Andrews Street, Aberdeen, UK
Barry L. Sharp
Analytical Division, Macaulay Land Use Research Institute, Craigiebuckler, Aberdeen, UK

A simple linear relationship has been established between the ionic strength and electrical conductivity of soil solutions. This relationship allows the preparation of an eluent for high-performance liquid chromatography which resembles the soil solution in terms of pH and ionic strength without requiring a complete ionic analysis of the sample. High-performance size-exclusion chromatography has been used in conjunction with ultraviolet detection for the molecular species and graphite furnace atomic absorption spectrometry for copper. A TSK G3000 SW column was used with an eluent consisting of Na_2HPO_4 - NaH_2PO_4. The analysis of soil solutions extracted by centrifugation using this system enabled the separation of the soluble organic matter into fractions of high and low relative molecular mass. The determination of copper in these fractions revealed that 60–80% of the copper is bound to humic and fulvic acids and is unavailable for plant uptake. The proportion of copper complexed with organic matter of high relative molecular mass was found to be affected by the drainage status of the soil.

Keywords: *Chemical speciation; graphite furnace atomic absorption spectrometry; high-performance size-exclusion chromatography; soil solution; sewage sludge treated soil*

In recent years there has been considerable concern regarding the disposal of sewage sludges on agricultural land. This concern is related to the high concentrations of potentially toxic heavy metals that may be present in such effluents.[1] The toxicity of these heavy metals is governed by their physico-chemical form or speciation.[2] However, because there is a lack of analytical methods capable of providing a convenient assessment of this speciation, regulatory agencies have defined upper limits for the loading of soils in terms of the extractable contents using the classical diagnostic reagents employed to determine plant "availability." A recent Council for European Communities (CEC) directive laid down upper limits for heavy metal concentrations in sewage sludge used in agriculture.[3]

For copper, the apparently high level permitted in the soil arises because a large proportion of the metal is organically bound in forms that are not available to the plant. This is thought to be the result of complexation with the higher relative molecular mass humic substances.[4] Humic substances have been defined as a "general category of naturally occurring, biogenic, heterogeneous organic substances that can generally be characterised as being yellow to black in colour, of high molecular weight and refractory."[5] Humic substances can be split into two main classes, *i.e.*, humic and fulvic acids, with fulvic acid generally being of lower relative molecular mass. The addition of such ligands to a polluted soil has been shown to cause a decrease in the plant-available copper.[6]

Copper is also known to form complexes with lower relative molecular mass ligands, *e.g.*, citric acid.[7] The lower relative molecular mass copper complexes are potentially available to a greater extent to plants and it is already known that, for example, copper - citrate complexes are highly toxic to the alga *Selenastrum capricornutum*.[8] For inorganic copper there is considerable evidence that the free Cu^{2+} ion is the most toxic form, but that simple inorganic species, *e.g.*, $CuCl_2$ are also extremely toxic.[2]

Heavy metals in soil solutions undergo complex equilibria which are very easily disturbed. Conventional methods used for assessing plant availability involve the use of chemical extractants.[1,9] However, the addition of any extractant to a soil will have a disruptive effect on the soil equilibria and it has been shown that the correlation between extractable copper and plant-available copper is very low.[10] The diversity and poorly defined properties of naturally occurring aqueous organic material still constitutes a major drawback for copper speciation studies. A division between defined low relative molecular mass organic substances and diversified high relative molecular mass humic substances is perhaps the clearest distinction that can be made.[5] A much lower proportion of the copper is present as Cu^{2+} or simple inorganic complexes, *e.g.*, $CuCl_2$.

The criteria for an analytical method to investigate the partitioning between the plant-available and non-available forms are that it should provide a separation based primarily on molecular size/mass, such that the natural speciation should not be significantly altered by the preparation chemistry or interactions with the column packing and that it should be convenient to run on a routine basis. These requirements suggested the use of size-exclusion chromatography (SEC). It was then necessary to establish that a satisfactory separation could be achieved at a pH and total ionic strength (I) equivalent to that of the extracted solutions in order that the original speciation was preserved.

The total ionic strength of a solution can be determined by a complete analysis of the component ionic species. This is appropriate for the initial investigation of an analytical method, but would be too time consuming to carry out on every sample. For this reason, the relationship between total ionic strength and electrical conductivity (EC) of the extracted solutions was investigated and a model was established, which agrees well with that previously proposed by Griffin and Jurinak.[11] Hence simple measurements of the solution conductivity and pH indicate directly an appropriate composition for the eluent. The resulting model was also applied to real soil solutions in order that an estimate of the degree of complexation of the major ionic species could be obtained.

Experimental

Apparatus

Soils were centrifuged using an MSE Mistral 3000 centrifuge (Fisons Scientific Equipment, Loughborough, Leicestershire,

UK). The resultant solutions were analysed for cationic content by flame emission spectrometry (Na and K) on a Corning 400 photometer (Corning, Halstead, Essex, UK) and by atomic absorption spectrometry (AAS) (Ca, Mg and Cu) on either a Varian 1275 (Varian Associates, Walton on Thames, Surrey, UK) or a Perkin-Elmer 560 (Perkin-Elmer, Beaconsfield, Buckinghamshire, UK) instrument. Anions were determined by high-performance ion chromatography (Cl^- and SO_4^{2-}) on a Dionex 4000 chromatograph (Dionex UK, Camberley, Surrey, UK) and by flow injection colorimetry (HCO_3^-, NO_3^- and PO_4^{3-}) on a Tecator FIAstar 510 instrument (Perstorp Analytical, Bristol, UK).

The high-performance liquid chromatography (HPLC) separation was carried out with a TSK (Toyo Soda, Tokyo, Japan) G3000 SW SEC column (8 × 300 mm) fitted with a TSK GSW (8 × 40 mm) guard column. All HPLC apparatus used was manufactured by LKB (Bromma, Sweden) and consisted of: a 2152 HPLC controller, a 2158 UV cord SD, (λ = 284 nm) 2150 HPLC pump and a 11300 Ultrograd mixer driver. Samples were injected via a Valco C6W injection valve fitted with a 200-μl injection loop. Fractions of the eluate (0.25 ml) were collected and an aliquot (5 μl) was analysed by graphite furnace AAS (GFAAS) using a Pye Unicam SP9 atomic absorption spectrometer fitted with a PU 9090 data graphics system, a PU 9095 video furnace programmer and an SP 9 furnace power supply. The furnace conditions employed were as given in Table 1.

Reagents

Model soil solutions were prepared from AnalaR-grade chemicals (BDH, Poole, Dorset, UK). In order that copper contamination could be minimised, the HPLC eluent was prepared from high-purity Aristar-grade chemicals (BDH).

A humic acid standard (50 mg dm^{-3}) was made by dilution of a 200 mg dm^{-3} stock solution prepared by dissolving 0.2 g of humic acid powder in 1 cm^3 of 0.2 mol dm^{-3} NaOH and diluting with water. A fulvic acid standard (50 mg dm^{-3}) was prepared by dissolving fulvic acid powder in distilled water. This solution was then filtered to remove any particulate matter. The humic and fulvic acids were extracted from soil of the Insch Association sampled at Greenhall Farm, Insch. Unless stated otherwise, all other reagents were prepared from AnalaR-grade chemicals.

All glassware was soaked overnight in 2% Decon, rinsed, washed three times with 1 + 4 v/v HNO_3 and finally rinsed three times with water. All water used was purified by de-ionisation and distillation.

Table 1. Furnace conditions for the Pye Unicam SP9 atomic absorption spectrometer at λ = 324.8 nm

Temperature/°C	75	100	350	700	1800	2650
Time/s	20	25	25	25	5	5

Table 2. Laverock Brae Soil, map reference NJ 921111

Parent material . .	Glacial till	Till derived from mixed acid igneous, acid metamorphic and basic igneous rocks
Soil association . .	Tarves	Brown forest soil
Soil series	Thistlyhill	
Drainage	Imperfect	
Vegetation	Rotational by pasture based on rye grass	

Procedure

Preparation of model soil solutions

Eighteen model soil solutions were prepared with similar ionic concentrations to the soil extracts studied by Griffin and Jurinak.[11] The use of model solutions ensured that their ionic content was known accurately. It was decided that the use of data obtained from the analysis of soil extracts would introduce errors into the derivation of a conductivity - ionic strength relationship for the following reasons: experimental errors would be introduced during the extraction and subsequent analysis; the experimental methods used by Griffin and Jurinak measured total concentrations and not the free ionic fraction which contributes to the ionic strength. This would lead to an overestimation of the ionic strength of the soil extract.

Additionally, five model solutions were prepared with similar ionic concentrations to the field of interest (Laverock Brae Farm, Aberdeen, UK). This field has a history of sewage sludge application and its characteristics are shown in Table 2. Soil samples were taken from the Ap horizon (the 0–20 cm ploughed surface layer of the soil) of the field. The soil solutions were extracted by centrifugation of the wet soil (2 × 250-g samples) at 2000 *g* for 1 h. The centrifuge tubes were specially constructed and were similar to those used by Elkhatib *et al.*[12]

The conductivities of the 23 model solutions were measured at 25 °C. The calculated total ionic strength was then corrected for ion-pair formation.[13] A linear regression analysis was then carried out on the *EC versus I* data.

HPLC analysis of soil solutions

The soils were sampled and centrifuged as before, except that the soil solutions were filtered using a Gelman LC3A 0.45-μm filter to remove any particulate matter before analysis. The soil solutions were injected on to the HPLC column with a carrier flow-rate of 0.75 ml min^{-1}. The mobile phase used consisted of Na_2HPO_4 and NaH_2PO_4. A computer program BUFFER was written which enabled the correct concentration of each of the two components to be calculated so that the resulting buffer had the same ionic strength and pH as the soil solution under investigation.

Results and Discussion

The data obtained from the total ionic analysis of the soil solution are shown in Table 3.

Table 3. Soil solution concentrations. In each instance the first value in the pair of values is concentration in p.p.m. and the second is concentration in mmol dm^{-3}

Sample site	Cl^-	HCO_3^-	NO_3^-	PO_4^{3-}	SO_4^{2-}	Ca^{2+}	Cu^{2+}	K^+	Mg^{2+}	Mn^{2+}	Na^+
1	38.132	39.101	16.713	0.205	8.073	1.1948	0.313	2.253	0.16	0.0041	24.26
	1.074	0.641	0.269	0.00216	0.0841	0.0298	0.000489	0.0577	0.0067	0.000075	1.0547
2	27.538	34.9	26.733	0.198	11.97	2.093	0.0178	1.994	0.17	0.0067	16.29
	0.776	0.57	0.431	0.0021	0.124	0.0523	0.000278	0.0511	0.00709	0.000122	0.708
3	35.465	12.86	28.429	0.155	7.31	2.330	0.02	2.399	0.10	0.0184	10.67
	0.999	0.211	0.458	0.00163	0.076	0.0583	0.000313	0.0615	0.00417	0.000335	0.464
4	29.77	24.91	15.215	0.104	10.35	1.506	0.0179	2.54	0.06	0.0087	13.98
	0.839	0.408	0.245	0.00109	0.108	0.0377	0.000279	0.0651	0.0025	0.000158	0.608
5	23.31	49.77	8.574	0.0073	4.510	0.96	0.0157	1.15	0.06	0.023	16.04
	0.657	0.816	0.141	0.00076	0.047	0.024	0.000245	0.0295	0.0025	0.000418	0.697

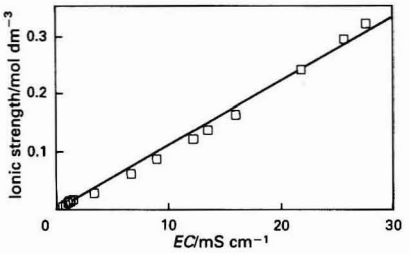

Fig. 1. Graph of *I versus EC* for model solutions of soil waters

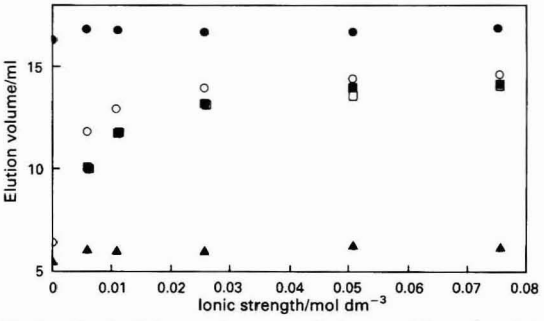

Fig. 2. Graph of elution volume *versus* ionic strength for various test samples: ●, acetone; ○, citric acid; ■ fulvic acid; □, humic acid; and ▲, blue dextran

The linear relationship between ionic strength and electrical conductivity of the 23 model solutions was found to have a high degree of correlation. The relationship found was very similar to that reported by Griffin and Jurinak,[11] but the gradient was slightly lower. An explanation for this, as indicated previously, is that some of the analytical techniques employed by Griffin and Jurinak to measure the ionic content of soil extracts measure the total concentration of a particular ion. As a result such methods will include organically complexed and adsorbed forms of the ion in question. These forms do not contribute to the ionic strength of the solution and as a consequence the total ionic strength will be overestimated. The relationship between ionic strength and conductivity is shown in Fig. 1. The correlation coefficient found in this work is significantly higher than that reported by Griffin,

$$I = 0.0127\ EC$$
$$r = 0.996$$

where r is the correlation coefficient, I the ionic strength in mol dm^{-3} and EC the electrical conductivity in mS cm^{-1}. The use of this relationship to predict the ionic strength of a soil solution will produce a reliable estimate of I in order that a suitable HPLC column eluent can be prepared.

The use of SEC techniques in the study of humic substances has been widely reported.[14–16] The column chosen for this work was a TSK G3000 SW, as the use of such columns has been previously reported.[14–16] One problem with this type of column arises from coulombic repulsion between the column packing and the sample when distilled water is used as an eluent. In such instances, the test samples are eluted at the column void volume and no separation is achieved. To overcome this problem, some workers have employed high ionic strength eluents[14] (up to 0.1 mol dm^{-3} NaCl). An eluent with such a high ionic strength is obviously unsuitable for soil solution speciation studies.

The column was tested over a wide range of ionic strengths using humic, fulvic and citric acids, as test samples because these compounds reflected the relative molecular mass range of interest in soil solutions. Blue dextran (a high relative

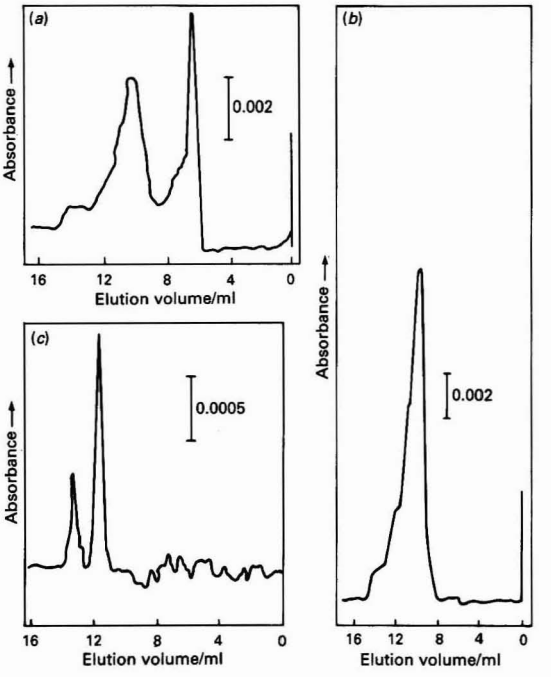

Fig. 3. Size-exclusion chromatograms obtained with a mobile phase consisting of Na_2HPO_4 - NaH_2PO_4 (0.0058 mol dm^{-3}) at pH 5.8. (*a*) Humic acid; (*b*) fulvic acid; and (*c*) citric acid

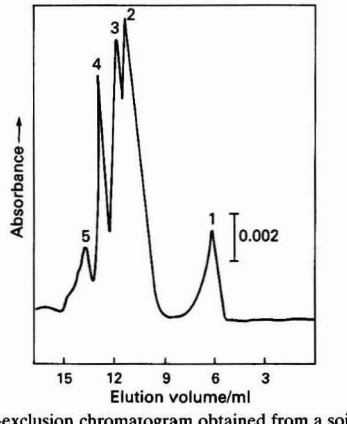

Fig. 4. Size-exclusion chromatogram obtained from a soil solution. Mobile phase: Na_2HPO_4 - NaH_2PO_4 (0.0058 mol dm^{-3}) pH 5.8

molecular mass polysaccharide) was used to determine the column void volume V_0. Similarly acetone was used to find the totally included volume V_i. The results were plotted as a graph of V (where V = elution volume) *versus* ionic strength in mol dm^{-3} (Fig. 2). It was noticeable that at higher ionic strengths there was very little separation between the high relative molecular mass humic substances and low relative molecular mass citric acid. This was also true at zero ionic strength where all the polar samples were eluted at the column void volume as a result of coulombic repulsion. Fig. 3(*a*), (*b*) and (*c*) shows the chromatograms obtained for humic, fulvic and citric acids, respectively, when the test samples were run at an ionic strength comparable to that of a soil solution. Humic acid can be seen to be present as two very different relative molecular mass fractions, one of which is above the fractionation range of the column (relative molecular mass >300 000) as it occurs

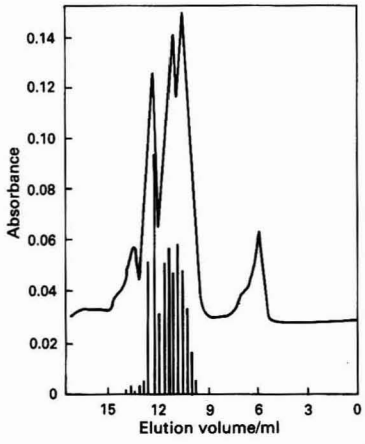

Fig. 5. Size-exclusion chromatogram obtained for sample site Lab 1-A. Mobile phase: Na_2HPO_4 - NaH_2PO_4 (0.0058 mol dm^{-3}) pH 5.8

Table 4. Results obtained for the determination of total soil solution copper by ICP-OES

	Humic materials		Low relative molecular mass ligands	
	Amount of total Cu		Amount of total Cu	
Soil sampling site	%	p.p.m.	%	p.p.m.
Lab 1-A	67.0	0.106	33.0	0.052
Lab 1-B	63.2	0.099	26.8	0.041
Lab 1-C	83.0	0.094	16.6	0.019

at the void volume and one of much lower relative molecular mass. Fulvic acid occurs as just one fraction with an elution volume almost identical with the lower relative molecular mass humic acid fraction. Similar splitting of humic acid peaks was found by Vaughan and Ord[17] when they attempted to separate humic and fulvic acids by gel filtration on Sephadex G-75. They also encountered a second humic acid peak which co-eluted with fulvic acid. Although humic acid is generally classed as being soluble in alkali it usually contains a water-soluble fraction which has very similar properties, including relative molecular mass, to fulvic acid. It is this fraction which co-elutes with fulvic acid. Citric acid also occurs as two peaks, the reason for this is unclear. It is unlikely that it is due to impurities as the citric acid was of AnalaR-grade and should, therefore, contain no noticeable impurities. Indeed the same sample has been tested on a reversed-phase column and was found to contain no impurities. One possible explanation for the second peak is that some of the citric acid may have interacted with the sodium ions in the eluent, resulting in the formation of the sodium salt of citric acid.

It was noted that at low ionic strengths the degree of separation between citric acid and the humic substances was much greater than at either zero ionic strength or high ionic strengths. It may be that the column was not separating the compounds on relative molecular mass alone, and some coulombic repulsion was occurring. This coulombic repulsion seemed to affect the humic substances to a much greater extent than citric acid and hence permitted a clear separation between the low relative molecular mass organic ligands and the humic and fulvic fractions.

A soil solution was analysed under the same conditions and the resulting chromatogram is shown in Fig. 4. The chromatogram can be seen to consist of five distinct peaks. Peak 1 is due to the high relative molecular mass humic acid fraction normally present in soils. Peak 2 is thought to be due to the low relative molecular mass humic acid fraction and also fulvic acid, as the elution volume was identical with that of the test samples. Similarly, peak 4 has an elution volume similar to that of citric acid and was, therefore, due to the low relative molecular mass organic ligands in the soil solution. Peak 3 lies in between those due to citric acid and the lower relative molecular mass humic substances and it is most likely that this peak is due to a splitting of the latter peak. Peak 5 may be due to splitting of the low relative molecular mass organic acid peak. Again this may be due to interactions with the sodium ions in the eluent, or ultraviolet absorbing inorganic ligands, *e.g.*, NO_3^-, which also elute at this volume.

Duplicate soil samples were taken from each sampling site and the soil solutions were extracted as before. The samples were run using HPLC and 0.25-ml fractions were collected and analysed for copper by GFAAS. The resulting absorbances were superimposed on the chromatogram (Fig. 5). It is evident that the majority of the copper (67%) is complexed with the humic substances which is, as expected, due to the abundance of humic materials in soils. A significant amount of copper is complexed with low relative molecular mass ligands (33%).

Another two samples were taken from different locations and the total soil solution copper was determined by inductively coupled plasma optical emission spectrometry (ICP-OES). The results are presented in Table 4.

It is apparent that in this soil the majority of the copper is present as complexes with humic substances but that a significant amount is present as complexes with low relative molecular mass ligands, *e.g.*, citric, malic and lactic acids. The specific nature of these low relative molecular mass ligands will be investigated in future work. From the results it is evident that samples taken from sites Lab 1-A and Lab 1-B were similar in the amounts of copper bound by humic materials. Sampling site Lab 1-C, however, showed a much greater proportion of the copper bound to humic material. This site was different from the previous two in that the soil had a much higher moisture content. In fact this part of the field tended to collect water and was often waterlogged. In contrast sites 1-A and 1-B were on a much greater gradient and subsequently water tended to drain off rapidly. From these results it seems evident that if soil water is allowed time to equilibrate with the soil particles then the soil solution copper will be predominantly in the form of copper - humic or copper - fulvic acid complexes.

We are grateful to the Science and Engineering Research Council for their financial support. We thank M. L. Berrow for his assistance with sampling and providing background information on the Laverock Brae soil. We also thank A. Hepburn (Soils Division, Macaulay Land Use Research Institute, Aberdeen, UK) for providing the humic and fulvic acid samples.

References

1. Burridge, J. C., and Berrow, M. L., *in* "Proceedings of the International Conference on Environmental Contamination," London, July 1984. CEP Consultants Ltd., Edinburgh, 1984, pp. 215–224.
2. Florence, T. M., *Trends Anal. Chem.*, 1983, **2**, 162.
3. Council of European Communities, 1986, "Council Directive on the Protection of the Environment, and in Particular of the Soil when Sewage Sludge is used in Agriculture." CEC 86/278/EEC.
4. Saunders, J. R., and Bloomfield, C., *J. Soil Sci.*, 1980, **31**, 53.
5. Ohman, L. O., and Sjöberg, S., *in* Kramer, J. R., and Allen, H. E., *Editors*, "Metal Speciation: Theory, Analysis and Practice," Lewis 1988, pp. 1–33.

6. Piccolo, A., *Sci. Total Environ.*, 1989, **81**, 607.
7. Brown, L., Haswell, S. J., Rhead, M. M., O'Neill, P., and Bancroft, K. C. C., *Analyst*, 1983, **108**, 1511.
8. Florence, T. M., *Analyst*, 1986, **111**, 489.
9. Mclaren, R. G., and Crawford, D. V., *J. Soil Sci.*, 1973, **24**, 171.
10. Gunn, A. M., Winnard, D. A. and Hunt, D. T. E., *in* Kramer, J. R., and Allen, H. E., *Editor*, "Metal Speciation: Theory, Analysis and Practice," Lewis, 1988, p. 261.
11. Griffin, R. A., and Jurinak, J. J., *Soil Sci.*, 1973, **116**, 26.
12. Elkhatib, E. A., Hern, J. L., and Staley, T. E., *Soil Sci. Am. J.*, 1987, **51**, 578.
13. Adams, F., *Soil Sci. Soc. Am. Proc.*, 1971, **35**, 420.
14. Baham, J., Ball, N. B., and Sposito, G., *J. Environ. Qual.*, 1978, **7**, 181.
15. Saito, Y., and Hayano, S., *J. Chromatogr.*, 1979, **177**, 390.
16. Adamic, M. L., and Bartak, D. E., *Anal. Chem.*, 1984, **57**, 279.
17. Vaughan, D., and Ord, B. G., *J. Exp. Bot.*, 1981, **32**, 679.

Paper 0/01018I
Received March 6th, 1990
Accepted July 27th, 1990

Analytical Methodology for the Determination of Aflatoxins in Peanut Butter: Comparison of High-performance Thin-layer Chromatographic, Enzyme-linked Immunosorbent Assay and High-performance Liquid Chromatographic Methods*

M. P. K. Dell and S. J. Haswell†
School of Chemistry, Thames Polytechnic, Wellington Street, London SE18 6PF, UK
O. G. Roch
School of Pharmacy and Biomedical Sciences, Portsmouth Polytechnic, King Henry I Street, Portsmouth PO1 2DZ, UK
R. D. Coker, V. F. P. Medlock and K. Tomlins
Mycotoxin Section, Natural Resources Institute, Chatham Maritime, Chatham, Kent ME6 4TB, UK

High-performance thin-layer chromatography (HPTLC) was applied to the separation and quantification of aflatoxin in 300 jars of "crunchy" peanut butter. A critical evaluation of the proposed HPTLC method has been carried out by statistical comparisons with a commercially available enzyme-linked immunosorbent assay (ELISA) kit and a high-performance liquid chromatographic (HPLC) method. The statistical tests indicated that whilst the distributions of the data sets obtained with each method were similar, the HPLC method was found to be biased. Over-all results indicated that the HPTLC method gave more consistent data, relatively lower standard deviations and lower coefficients of variation. The ELISA kit was found to be less precise than the HPTLC and HPLC methods and prone to some loss of sensitivity caused by matrix interference.

Keywords: *Aflatoxin determination; peanut butter; high-performance thin-layer chromatography; enzyme-linked immunosorbent assay; high-performance liquid chromatography*

Aflatoxin B_1 is a highly toxic carcinogenic fungal metabolite that may play a key role in the epidemiology of human liver cancer and other diseases.[1] Aflatoxins are produced in foodstuffs and feedstuffs by the fungi *Aspergillus flavus* and *Aspergillus parasiticus*, at higher temperatures and relative humidities than those normally found in the UK.[2] However, there is considerable evidence showing the presence of aflatoxins in commodities imported into the UK, including confectionery nuts and nut-based food products such as peanut butter.[3] Owing to the inevitable health risks to man and livestock from this mycotoxin, many countries have introduced regulations and legislation which stipulate the maximum levels of aflatoxin permitted in foods and feeds.[4] An upper legal limit of 10 μg kg^{-1} is proposed for the UK, for the total level of aflatoxin permitted in individual retail packs of finished nuts and nut products.[3]

Simple, sensitive and rapid methods of analysis are required if such regulations are to be efficiently implemented and the exposure of the UK population to aflatoxin properly investigated. Currently, thin-layer chromatography (TLC)[5–7] and high-performance liquid chromatography (HPLC) are widely used for the quantification of aflatoxins and several HPLC methods for peanut butter analysis have been published.[8–15] Recently a number of enzyme-linked immunosorbent assays (ELISA) for peanut butter have been described, demonstrating the many advantages they have over conventional analytical procedures.[16–23] Some of these studies have been devoted to optimising and improving the ELISA protocol by decreasing the analytical time involved[17,20,21] and by increasing the specificity and sensitivity using monoclonal antibodies.[16] An improved ELISA test has also been used as a routine technique in the assay of aflatoxin B_1 in peanut butter.[21] Peanut butter is marketed as "smooth" and "crunchy" forms, with the crunchy peanut butter containing particles up to approximately 1 mm in diameter. A study carried out in 1986 on aflatoxin levels in peanut butter showed that out of the 129 jars examined, 6% exceeded a concentration of 10 μg kg^{-1}, 8% contained <10 μg kg^{-1} and 86% of the samples were below the limit of detection.[21] Studies in 1982, 1983 and 1984[10] indicated that the aflatoxins were particularly associated with samples of peanut butter in the crunchy form.

In the present study 300 jars of crunchy peanut butter have been analysed by high-performance thin-layer chromatography (HPTLC)[24,25] and the results recorded have been statistically compared to those obtained using both a commercial ELISA kit and an HPLC method.

Experimental

Apparatus

The Bond-Elut clean-up equipment supplied by Jones Chromatography consisted of a vacuum manifold (Vacelut), disposable 500-mg phenyl bonded phase cartridges (PH), solvent reservoirs (4, 25 and 75 ml), polyethylene porous frits (20 μm), adapters and luer stopcocks. The HPTLC aluminium-backed plates, 20 × 20 cm (Merck 5547), were cut to a 10 × 20-cm size, pre-conditioned by immersion in methanol for 60 min and oven-dried for 2–3 min at 100 °C; the pre-conditioned plates were then stored in a desiccator. The HPTLC experiments were performed using a fluorodensitometer (TLC scannerII: Camag 76610), an electronic integrator (TLC integrator SP 4270: Camag 76650) and an Apricot PC operating with Link-up software (Quadrant Scientific). An automated TLC sampler (Camag 27200) was also used.

Absorbance measurements of the ELISA kits were recorded on a Dynatech MR600 microplate reader. A Gilson 222-401 autosampler was used for the automatic dilution and transfer of the crude sample extracts on to the micro-titration plates.

The HPLC equipment consisted of a Waters 6000A pump fitted with a Rheodyne 7125 injection valve (200-μl loop). The analytical column used was a reversed-phase Spherisorb 5 ODS, 25 × 4.6 cm (Technicol), with a mobile phase of water - acetonitrile - methanol (60 + 30 + 10) pumped at a

* Presented at SAC 89, the 8th SAC International Conference on Analytical Chemistry, Cambridge, UK, 30 July–5 August, 1989.
† To whom correspondence should be addressed.

flow-rate of 0.7 ml min^{-1}. Detection was achieved using a Kratos spectrofluorimeter (FS 970 LC) with excitation and emission wavelengths of 363 and 418 nm, respectively.

Reagents and Materials

Aflatoxin standards

Stock solutions of each of the aflatoxins B_1, B_2, G_1 and G_2 (purchased from Aldrich) were prepared by the addition of 100 ml of spectroscopic grade solvent [benzene - acetonitrile (98 + 2)] to each 10 mg of crystalline material to give an estimated concentration of 100 μg ml^{-1}. These solutions were further diluted to contain approximately 10 μg ml^{-1} and their exact concentrations were determined by ultraviolet (UV) absorbance measurements using a Perkin-Elmer Lambda 3 UV - visible spectrophotometer.[26] The standard solution used for HPTLC contained aflatoxins B_1, B_2, G_1 and G_2 with a total concentration of 3 μg ml^{-1} (corresponding to 1 μg ml^{-1} of aflatoxins B_1 and G_1 and 0.5 μg ml^{-1} of aflatoxins B_2 and G_2) and was stored at −20 °C in benzene - acetonitrile (98 + 2). A standard solution containing approximately 1 μg ml^{-1} of each of the four aflatoxins was then used as an external standard for HPLC determinations. An aliquot (1 ml) of the mixed solution was transferred into a vial and evaporated to dryness at 40 °C, under nitrogen, using a sample concentrator. Conversion of aflatoxins B_1 and G_1 into the hemiacetals[27] (aflatoxins B_{2a} and G_{2a}, respectively) was achieved by the addition of trifluoroacetic acid (50 μl) to the vial and, after about 1 min, removing the excess of acid in a stream of nitrogen; the residue was then dissolved in 4 ml of water - acetonitrile (90 + 10). The resulting solution provided a standard containing about 25 ng per 100 μl of each aflatoxin in a satisfactory injection solvent.

All inorganic chemicals and organic solvents were of AnalaR or HPLC grade. Distilled water was used throughout.

Procedure

Samples

Peanut butter samples (approximately 311 g) were systematically collected from the production line of a 3.6-tonne batch (11 400 jars), at 57-s intervals over an 8-h shift. The complete contents (approximately 311 g) of each of 300 jars of naturally contaminated peanut butter were used in the analysis.

Sample preparation

All of the following sample preparation steps were carried out in parallel for a set of ten samples. The complete, weighed contents of each jar were blended with water (1 + 1.5 m/v) in a 2-l Waring blender, at low speed for 1 min, followed by 2 min at high speed. Immediately after blending, two 100-g portions of the homogeneous slurry were taken using a plastic ladle. The portions were labelled as slurry A and slurry B.

Acetone (200 ml) was added to slurry A and the mixture was blended in a 1-l Waring blender at high speed for 3 min. After filtration through a Whatman No. 1 filter-paper, an aliquot (about 50 ml) was taken for Bond-Elut clean-up for both HPTLC and HPLC analysis.

Acetonitrile (100 ml) and water (40 ml) were added to slurry B. The mixture was blended and filtered; an aliquot (100 μl) was diluted with a commercial diluent (2.4 ml) that was provided with the ELISA kit; diluted aliquots (50 μl) were then applied to micro-titration plates either manually or by using an autosampler (Gilson) and subsequently analysed.

Sample clean-up

Using the Vacelut manifold 10–12 samples were prepared simultaneously. Fig. 1 shows a diagram of the stages used in this procedure using a combination of PH columns and reservoirs. The phenyl bonded columns (PH, 500 mg) were

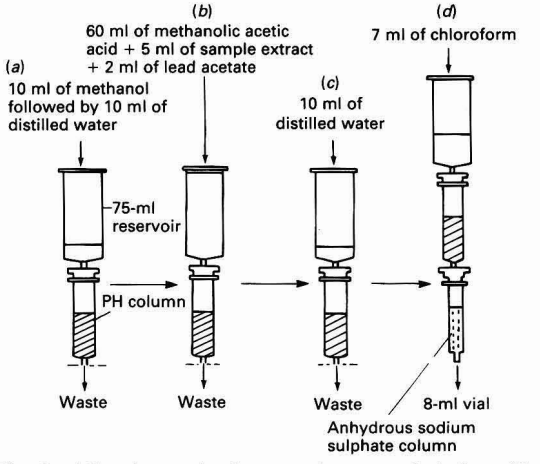

Fig. 1. Aflatoxin sample clean-up using pre-packed disposable phenyl bonded columns. (*a*) Wetting the column; (*b*) isolation of aflatoxins; (*c*) rinsing the column; and (*d*) elution of aflatoxins

firstly solvated with methanol and then with water, ensuring that the column sorbent was not allowed to dry. Aliquots of methanolic acetic acid solution [60 ml of water - acetic acid - methanol (92.3 + 1 + 6.7)], sample filtrate (5 ml) and lead acetate solution (2 ml) were mixed in the reservoir and pulled through the solvated PH cartridges under vacuum at a rate of approximately 10 ml min^{-1}.

The lead acetate solution was prepared using 100 g of lead acetate trihydrate dissolved in 300 ml of water, to which 1.5 ml of acetic acid had been added, and made up to a final volume of 500 ml with water. The lead acetate solution was used to aid in the clean-up by precipitating colloidal material from the sample extract. The cartridges were washed with distilled water (10 ml) and then dried by passing air through them for 5 min. A 4-ml reservoir, containing about 3 g of granular anhydrous sodium sulphate, was connected to the bottom, and a 25-ml reservoir was fitted to the top, of each PH cartridge. Chloroform (7 ml) was added to the cartridge and eluted at a rate of approximately 1 ml min^{-1}. The eluate was collected and evaporated to dryness on a heating block at 40 °C, under a gentle stream of nitrogen.[25,28,29]

HPTLC Analysis

Residues from the peanut butter extracts were dissolved in 200 μl of benzene - acetonitrile (98 + 2) and transferred into a polypropylene micro-vial. An automated TLC sampler was used to apply the external standard and sample solutions (50–10000 nl) on to the adsorbent layer of the HPTLC plate as a row of spots 5 mm apart positioned 20 mm from the bottom of the plate. Bi-directional development of the plate was carried out using a previously described method.[30] The aflatoxins were quantified by UV fluorescence in the reflectance mode using a monochromatic densitometer and electronic integrator. The concentration of aflatoxin in each sample was determined by converting the density value obtained from the fluorodensitometer into a peak-height measurement, using a valley to valley integration method. Fig. 2(*a*) and (*b*) shows the HPTLC traces of a standard and a sample, respectively.

ELISA Kit for Total Aflatoxin Assay

A commercial ELISA kit (Biokits) was used in this study. The kit contained six double column sensitised micro-strips (96 assay wells, coated with a pre-determined aflatoxin B_1 preparation, and dried), aflatoxin assay diluent concentrate,

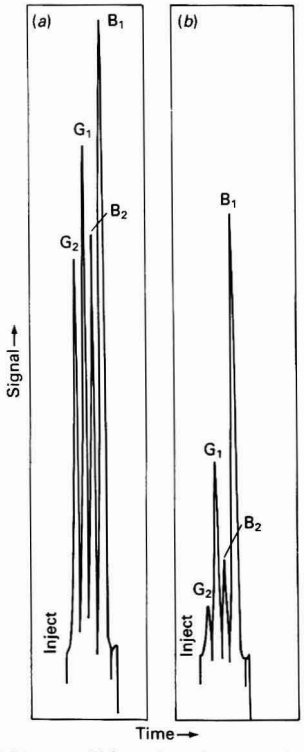

Fig. 2. HPTLC traces of (*a*) an aflatoxin standard and (*b*) a peanut butter sample. Densitometer light source: high-pressure mercury lamp. Wavelength, 366 nm; and scan speed, 0.5 mm s^{-1}. Bi-directional plate development: the first solvent, anhydrous diethyl ether, was used to remove interfering compounds. The plate was rotated through 180° and developed twice with chloroform - xylene - acetone (6 + 3 + 1) for 20 min

rat anti-aflatoxin, wash solution concentrate, antibody - enzyme conjugate, 2,2′-azino-di(3-ethylbenzylthiazoline sulphonic acid-6) diazonium salt (ABTS) concentrate and peroxide - citrate buffer and stop solution (1.5% m/v sodium fluoride in distilled water).

A series of standard solutions of aflatoxin B_1 (in the range 20–2000 pg ml^{-1}), together with the diluted sample extracts, were added to the appropriate wells of the plate, followed by 50-μl aliquots of rat anti-aflatoxin. The plate was constantly agitated and incubated at room temperature for 2 h, timed from the first addition of rat anti-aflatoxin. After washing five times with diluted wash solution, using a Nunc 8 probe micro-well washer, aflatoxin assay peroxidase conjugate (100 μl) was added, and the plate was further incubated for 30 min at room temperature with constant mixing. Finally, after further washing, 100 μl of the substrate solution were added and the plate was incubated for a further 30 min at room temperature until the absorbance of the maximum binding well had reached approximately 1.5 at 410 nm. The enzyme reaction was terminated by the addition of 50 μl of stop solution. The absorbance of each well was measured at 410 nm using the micro-plate reader.

A standard calibration graph was constructed by plotting the measured signal against $\log_{10}$ of the aflatoxin concentration (pg ml^{-1}). The total aflatoxin concentration in the samples was then estimated by reference to the calibration graph which had a sigmoidal function. In the direct competitive form of ELISA used here for total aflatoxin determination, the aflatoxin concentration varies inversely with the colour intensity of the substrate.

HPLC Analysis

The peanut butter residues obtained from the clean-up procedure were treated with trifluoroacetic acid (50 μl) and, after removal of excess of acid, 125 μl of injection solvent [water - acetonitrile (90 + 10)] were added. This solution (100 μl) was injected manually into the HPLC system and the concentration of aflatoxin in each sample, in μg kg^{-1}, was determined by a comparison of peak areas using a calibration sample of known concentration.

Results and Discussion

HPTLC Method

The efficiency and performance of the combined PH bonded phase - bi-directional HPTLC method were assessed in a reproducibility study and compared with those obtained for the ELISA and HPLC methods.

Ten replicate peanut butter extracts were spiked at various levels of aflatoxin (5, 10, 20 and 50 μg kg^{-1} total aflatoxin). The precision of the HPTLC procedure decreases with concentration. At lower concentrations the coefficient of variation (CV) increased, *e.g.*, 8.5% for the 5 μg kg^{-1} level, compared with variations at the higher levels of 4.7% for the 10 μg kg^{-1} level, 3.3% for the 20 μg kg^{-1} level and 2.4% for the 50 μg kg^{-1} level. The HPLC method was assessed as having CV values of 12.9% for the 5 μg kg^{-1} level, 5.2% for the 10 μg kg^{-1} level, 3.7% for the 20 μg kg^{-1} level and 2.8% for the 50 μg kg^{-1} level of total aflatoxin. The performance of the ELISA kit was assessed for peanut butter extracts using a previously described methodology.[21] The CV was found to be 14.6% for extracts containing a spiked B_1 value of 5 μg kg^{-1}, 12.8% for the spiked B_1 level of 10 μg kg^{-1}, 11.4% for the spiked B_1 level of 20 μg kg^{-1} and 10.5% for the spiked B_1 level of 50 μg kg^{-1}.

The combined PH bonded phase - bi-directional HPTLC procedure was found to have a detection limit of 2.0 μg kg^{-1} for B_1, 2.6 μg kg^{-1} for B_2, 2.5 μg kg^{-1} for G_1 and 2.7 μg kg^{-1} for G_2. These limits of detection were found to be below the proposed legal limit of 10 μg kg^{-1} for finished nuts and nut products. For the aflatoxin standards, 1.006 μg kg^{-1} B_1, 0.259 μg kg^{-1} B_2, 0.501 μg kg^{-1} G_1 and 0.255 μg kg^{-1} G_2, the CV for the HPTLC method was found to be less than 1.5% for B_1 and G_1 and 3% for B_2 and G_2 using fluorescence detection for the toxins.

Peanut Butter Study

In this study the aflatoxin concentration of 300 jars of peanut butter was determined by HPTLC, ELISA and HPLC and a summary of the analysis is shown in Table 1. The large numbers of samples used represent a more detailed study than any reported in the literature to date.[10,21] Good agreement can be seen to exist between the HPTLC and ELISA results for values of less than 6 μg kg^{-1}. This trend was also true in general for concentrations greater than 6 μg kg^{-1}, however, one sample gave a value of 44.7 μg kg^{-1} by ELISA whereas higher values of 95.8 and 83.1 μg kg^{-1} were recorded by the HPTLC and HPLC assays, respectively. The distribution profile (Fig. 3) obtained for the 300 samples (HPTLC method) clearly identified that the batch of peanut butter analysed contained local "hot-spots" of aflatoxin which remained even after processing.

Statistical Evaluation of Results

A statistical evaluation of the aflatoxin data was performed using box and whisker plots, scatterplots, the maximum likelihood functional relationship (MLFR) technique and the Wilcoxon signed rank test.

A box and whisker plot from the 300 sample set (Fig. 4) was used to display the raw data distribution. The plots showed the

Table 1. Analysis of 300 crunchy peanut butter samples

Method	Clean-up	Type of aflatoxin	Number of samples in the total aflatoxin concentration range (μg kg^{-1}) <2	2–5	6–10	11–30	31–100	>100	Maximum	Average
HPTLC	PH Bond-Elut	B_1, B_2, G_1, G_2	1	107	125	50	16	1	170.8	10.3
ELISA	No clean-up	Total aflatoxin	3	104	127	49	16	1	165.2	10.2
HPLC	PH Bond-Elut	B_1, B_2, G_1, G_2	45	123	77	43	11	1	117.4	7.9

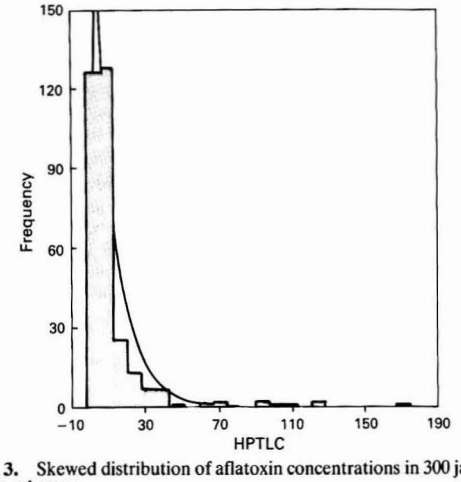

Fig. 3. Skewed distribution of aflatoxin concentrations in 300 jars of peanut butter

	Minimum	25th Percentile	Median	75th Percentile	Maximum
HPTLC	1.70	4.30	6.20	9.50	170.80
ELISA	1.30	4.40	6.00	9.80	165.20
HPLC	0.30	2.60	4.30	8.30	117.40

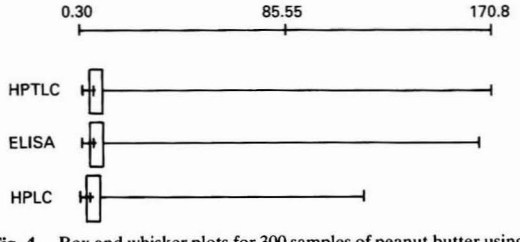

Fig. 4. Box and whisker plots for 300 samples of peanut butter using the Tukey five number summary

minimum value, the lower quartile (25th percentile), the median, the upper quartile (75th percentile), and the maximum value, and indicate that all three methods had a similar asymmetric distribution with little apparent difference between the sets of raw data.

Pairwise scatterplots were used to examine the relationship between the methods. On inspection of these scatterplots one observes that there is a rotational bias between all the methods [Fig. 5(*a*) and (*b*)], however, the HPTLC - ELISA scatterplot showed less bias than the HPTLC - HPLC scatterplot. Hence, these plots suggest that the HPTLC - ELISA methods give a better agreement than the HPTLC - HPLC methods. It is also clear that the ELISA data have more experimental variation or scatter than the HPTLC or HPLC data.

It is evident from Fig. 3 that the distribution of the aflatoxins in the 300 peanut butter samples is skewed. Conventional regression methods assume a normally distributed *y*-variable and no random variations in the *x*-variable. Hence linear regression does not offer a valid approach for the comparison

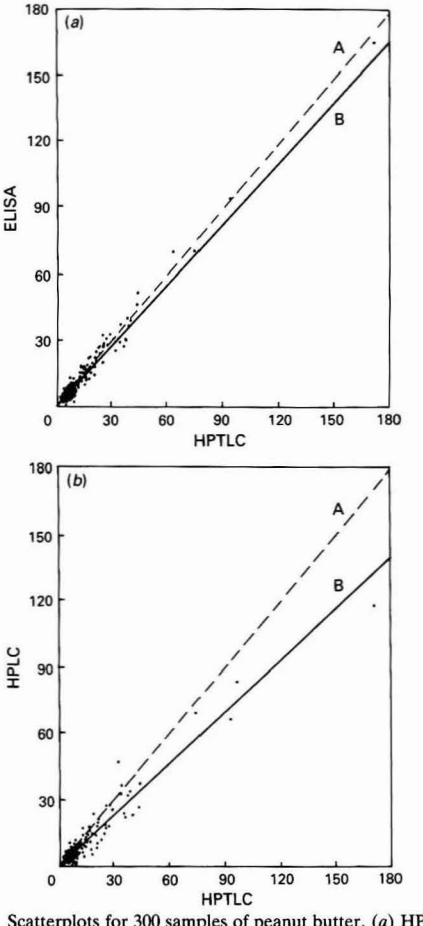

Fig. 5. Scatterplots for 300 samples of peanut butter. (*a*) HPTLC - ELISA scatterplot; and (*b*) HPTLC - HPLC scatterplot. A, Line of perfect agreement; and B, regression line

Table 2. Wilcoxon signed rank test

Test parameter	HPTLC - ELISA	HPTLC - HPLC
Number of samples	300	300
No. of positive differences	144	240
Average rank	142.608	156.681
No. of negative differences	150	57
Average rank	144.15	101.211
Sample test statistic *z*	0.785846	11.0424

of these methods, although such techniques are still widely used. To overcome these problems the transformation of the *x* and *y* variables (*i.e.*, use of a log scale) or the use of an alternative regression method such as the MLFR technique can be used.[31]

The MLFR technique assumes that there is variance on both axes and it provides unbiased estimates of the intercept (*a*)

and the slope coefficient (b) with their respective standard errors [se(a) and se(b)]. A FORTRAN program for the MLFR technique was used to determine the functional relationship between the methods (the program was obtained from Professor B. D. Ripley). The results for the HPTLC - ELISA methods were: intercept = −0.1894 with a standard error of 0.2241, slope = 0.9969 with a standard error of 0.02607, whilst the results for the HPTLC - HPLC methods were: intercept = 0.2724 with a standard error of 0.08488, slope = 0.7828 with a standard error of 0.0665. These results indicate that there is a measurable bias between the HPTLC - HPLC methods which is not apparent between the HPTLC - ELISA methods.

The Wilcoxon signed rank test was also used on the data sets of the three methods to confirm the trends identified by the MLFR technique. This test indicated that the data from the HPTLC - ELISA methods were in good agreement (Table 2) giving 144 positive differences with an average rank of 142.61, whilst the 150 negative differences showed an average rank of 144.15. The calculated test statistic (z = 0.79) was not considered significant, leading to the conclusion that the two sample sets, from the HPTLC - ELISA methods, may have medians that are not significantly different. However, the calculated test statistic for the HPTLC - HPLC set was 11.04, hence at the 1% level of significance the null hypothesis was rejected as the test statistic was greater than 2.58.

Conclusions

The results showed that many advantages are gained by using HPTLC as a routine method for the analysis of peanut butter. The HPTLC method is robust and can handle a high sample throughput; 36 samples may be separated simultaneously and scanned at a rate of at least one sample per minute.

"Poisoning" of the adsorbent layer of the disposable HPTLC plate with residual contaminants does not represent a problem. However, some manual skill is required for developing plates if reproducible densitometer readings are to be obtained. The aflatoxins are naturally fluorescent and, therefore, can be detected easily by HPTLC in the low picogram range. The choice of detector is not restricted because all samples are detected *in situ*, in the absence of the developing solvent. Furthermore, the amount of solvent used [20 ml of chloroform - xylene - acetone (6 + 3 + 1)] is much less than that required for the analysis of a comparable number of samples by HPLC. The PH Bond-Elut column clean-up was found to be simple to use and gave satisfactory results in all respects.

The ELISA kits offer a rapid, cheap and potentially sensitive method of detecting aflatoxins; however, the assay is still prone to some loss of sensitivity caused by matrix interferences at lower toxin levels and a loss of precision. However, it is worth noting that the extraction procedure for the kit was very simple and no clean-up was found to be necessary.

The HPLC method used in this study (manual injection and pre-column derivatisation) was found to be precise but biased. The pre-column derivatisation step was thought to be a possible source of this apparent systematic bias.

The statistical tests also indicated that whilst the distributions of the data sets obtained by each method were similar, the HPLC method was found to be biased. However, over-all results showed that the HPTLC method gave more consistent data, relatively lower standard deviations and lower coefficients of variation for a range of aflatoxin concentrations.

This research project was funded by SERC and NRI. P. Goodwin of Cortecs Diagnostics is thanked for providing the ELISA kits and the technical assistance that went with it. Professor B. D. Ripley, Department of Mathematics, University of Strathclyde, Glasgow G1 1XH, UK, is thanked for sharing his MLFR program. The authors also thank Dr. C. Gay of NRI for his helpful advice on the statistical interpretation of results.

References

1. Peers, F. G., Gilman, G. A., and Linsell, C. A., *Int. J. Cancer*, 1976, **17**, 167.
2. Diener, U. L., and Davis, N. D., *J. Stored Prod. Res.*, 1969, **5**, 251.
3. Ministry of Agriculture, Fisheries and Food, Survey of Mycotoxins in the United Kingdom: Fourth Report of the Steering Group on Food Surveillance, Working Party on Mycotoxins. Food Surveillance Paper No. 4, HM Stationery Office, London, 1980, p. 5.
4. Van Egmond, H. P., *Food Addit. Contam.*, 1989, **6**, 139.
5. Altenkirk, B., *J. Chromatogr.*, 1972, **65**, 456.
6. Beljaars, P. R., Verhulsdonk, C. A. H., Paulsch, W. E., and Liem, D. H., *J. Assoc. Off. Anal. Chem.*, 1973, **56**, 1444.
7. Trucksess, M. W., Brumley, W. C., and Nesheim, S., *J. Assoc. Off. Anal. Chem.*, 1984, **67**, 973.
8. Campbell, A. D., Francis, O. J., Beebe, R. A., and Stoloff, L., *J. Assoc. Off. Anal. Chem.*, 1984, **67**, 312.
9. Francis, O. J., Lipinski, L. L., Gaul, J. A., and Campbell, A. D., *J. Assoc. Off. Anal. Chem.*, 1982, **65**, 672.
10. Gilbert, J., and Shepherd, M. J., *Food Addit. Contam.*, 1985, **2**, 171.
11. Hurst, W. J., and Toomey, P. B., *J. Chromatogr. Sci.*, 1978, **16**, 372.
12. Jansen, H., Jansen, R., Brinkman, U. A. Th., and Frei, R. W., *Chromatographia*, 1987, **24**, 555.
13. Pons, W. A., and Franz, A. O., *J. Assoc. Off. Anal. Chem.*, 1978, **61**, 793.
14. Tarter, E. J., Hanchay, J.-P., and Scott, P. M., *J. Assoc. Off. Anal. Chem.*, 1984, **67**, 597.
15. Thiel, P. G., Stockenstrom. S., and Gathercole, P. S., *J. Liq. Chromatogr.*, 1986, **9**, 103.
16. Candlish, A. A. G., Stimson, W. H., and Smith, J. E., *Food Microbiol.*, 1987, **4**, 147.
17. Chu, F. S., Fan, T. S., Zhang, G.-S., Xu, Y.-C., Faust, S., and McMahon, P. L., *J. Assoc. Off. Anal. Chem.*, 1987, **70**, 854.
18. El-Nakib, O., Pestka, J. J., and Chu, F. S., *J. Assoc. Off. Anal. Chem.*, 1981, **64**, 1077.
19. Fan, T. S. L., and Chu, F. S., *J. Food Prot.*, 1984, **47**, 263.
20. Morgan, M. R. A., Kang, A. S., and Chan, H. S. W., *J. Sci. Food Agric.*, 1986, **37**, 908.
21. Mortimer, D. N., Shepherd, M. J., Gilbert, J., and Morgan, M. R. A., *Food Addit. Contam.*, 1987, **5**, 127.
22. Ram, B. P., Hart, P., Cole, R. J., and Pestka, J. J., *J. Food Prot.*, 1986, **49**, 792.
23. Mortimer, D. N., Shepherd, M. J., Gilbert, J., and Clarke, C., *Food Addit. Contam.*, 1988, **5**, 601.
24. Tosch, D., Waltking, A. E., and Schlesier, J. F., *J. Assoc. Off. Anal. Chem.*, 1984, **67**, 337.
25. Dell, M. P. K., Haswell, S. J., and Coker, R. D. (in preparation).
26. Coker, R. D., Jones, B. D., Nagler, M. J., Gilman, G. A., Wallbridge, A. J., and Panigrahi, S., "Mycotoxin Training Manual," National Resources Institute, London, 1984, Section B:2.
27. Takahashi, D. M., *J. Chromatogr.*, 1977, **131**, 147.
28. Hurst, W. J., Snyder, K. P., and Martin, R. A., *J. Chromatogr.*, 1987, **409**, 413.
29. Tomlins, K. I., Jewers, K., and Coker, R. D., *Chromatographia*, 1989, **27**, 67.
30. Coker, R. D., Jewers, K., Tomlins, K. I., and Blunden, G., *Chromatographia*, 1989, **27**, 49.
31. Thompson, M., *Anal. Chem.*, 1989, **61**, 1942.

Paper 9/02102G
Received May 18th, 1989
Accepted July 13th, 1990

Determination of Selenium by Gas Chromatography and Comparison With Graphite Furnace Atomic Absorption Spectrometry*

A. F. Al-Attar† and G. Nickless
Department of Inorganic Chemistry, School of Chemistry, The University, Bristol BS8 1TS, UK

Selenium(IV) reacts with 3-bromo-5-trifluoromethyl-1,2-diaminobenzene to form 4-bromo-6-trifluoromethylpiazselenol, which is detected by means of a gas chromatograph equipped with an electron-capture detector. A rapid and sensitive method for the determination of total selenium in plant samples thus developed, is described. A comparison of gas - liquid chromatography with electron-capture detection and graphite furnace atomic absorption spectrometry for the determination of selenium in plant samples, showed no difference between the two methods at the 99% level of confidence. The synthesis and characterisation of substituted 1,2-diaminobenzenes used as reagents for selenium determination is also reported. These reagents, namely 3-chloro-5-trifluoromethyl-1,2-diaminobenzene and 4-chloro-5-fluoro-1,2-diaminobenzene, are very sensitive and have short retention times. Their applicability to the determination of total selenium in National Institute of Standards and Technology Standard Reference Materials was therefore evaluated. The detection limit was 2.2 ng ml^{-1} and the minimum detectable amount was about 5 pg of selenium. The detection limits were evaluated using statistical methods.

Keywords: *Selenium determination; method comparison; gas - liquid chromatography; graphite furnace atomic absorption spectrometry*

The discovery of selenium as an essential trace element for animals and humans[1] has resulted in an increased interest in this element. Initial attention lay in its potential toxicity, but subsequent studies have shifted because of its importance in biochemistry.[2]

Selenium is an important element in relation to human health and disease because the safety margins between deficiency, nutrition and toxic doses are very narrow.[3]

Selenium is widely distributed in the Earth's crust, but occurs at low concentrations (0.05 p.p.m.); the primary sources are volcanic emanations and metallic sulphides associated with igneous activity. Secondary sources are biological sinks in which the element has accumulated.[4]

The determination of selenium is still a major challenge. Many problems that complicate its determination have been reported,[5] *i.e.*, severe matrix effects, digestion or extraction difficulties and the volatility of the element.

A number of analytical methods are now available for the determination of selenium at trace levels (ng g^{-1}) using the different detection techniques that have been developed.[5–12] Generally, gas - liquid chromatography with electron- capture detection (GLC-ECD) and atomic absorption [hydride generation and graphite furnace atomic absorption spectrometry (GFAAS)] are the most popular methods for the determination of selenium in biological and environmental samples.

1,2-Diaminobenzene (*o*-phenylenediamine) and its derivatives react selectively and quantitatively with selenium(IV) to form piazselenols that are volatile and stable. Trace levels of selenium in materials as diverse as biological tissues, high-purity metals and natural waters have been determined successfully as piazselenols by means of gas chromatography with ECD.[3,11,13,14]

The use of AAS has increased during the last two decades and now covers a large proportion of the total number of selenium determinations in various materials.[6,8,9,10,15]

Graphite furnace atomic absorption spectrometry is especially suitable for direct analysis because of its high sensitivity (detection limit 90 pg of selenium), but it is neither simple, nor free from interferences or losses through volatilisation.[10]

Nakashima and Toei[16] first used the GLC-ECD method for the determination of selenium using 4-chloro-1,2-diaminobenzene and reported a minimum detectable amount of 40 ng of selenium. Shimoishi[14] studied 13 derivatives of 1,2-diaminobenzene, and found the sensitivity of the derivatives varied with the nature of the substituents in the order $H < Cl < Br < NO_2$. 4,6-Dibromopiazselenol had the highest sensitivity and could be used to detect 1 ng of selenium.

Dilli and Sutikno[17] prepared and investigated two fluorinated reagents, namely the 4-fluoro- and 4-trifluoromethyl-1,2-diaminobenzenes. Al-Attar and Nickless[3] investigated the properties of 3-bromo-5-fluoro-1,2-diaminobenzene and 3-bromo-5-trifluoromethyl-1,2-diaminobenzene as reagents for the determination of selenium using GLC-ECD. They proved to be superior to previously reported systems.

The purpose of the present work has been to investigate the possibility of finding more sensitive reagents for the determination of selenium by GLC-ECD. This paper also compares the results of two different methods for the determination of selenium in a series of plant samples by GLC-ECD using 3-bromo-5-trifluoromethyl-1,2-diaminobenzene and by GFAAS.

Experimental

Reagents and Materials

All glassware was washed with detergent solution, rinsed with tap water followed by distilled water, and placed in 40% v/v nitric acid (concentrated) (analytical-reagent grade) for at least 48 h before use. The glassware was then rinsed with distilled water and doubly distilled water and oven-dried at 60 °C.

AnalaR hydrochloric, nitric, perchloric and sulphuric acids, AnalaR magnesium nitrate hexahydrate and selenious acid standard solution (SpectrosoL; for atomic spectrometry) and analytical-reagent grade selenium dioxide were obtained from BDH (Poole, Dorset, UK). 4-Fluoro-5-chloro-1,2-diaminobenzene, 3-chloro-5-trifluoromethyl-1,2-diaminoben-

* Presented at SAC 86, the 7th SAC International Conference on Analytical Chemistry, Bristol, UK, 20–26 July, 1986.

† Present address: Petroleum and Petrochemicals Research Institute, King AbdulAziz City for Science and Technology, P.O. Box 6086, Riyadh-11442, Saudi Arabia.

zene and 1,2-dinitro-3,4,5,6-tetrachlorobenzene were obtained from Maybridge Chemicals (Trevillet, Tintagel, Cornwall, UK).

The following reagents were prepared:

1,2-*Diamino*-3,4,5,6-*tetrachlorobenzene hydrochloride*. This was synthesised from 1,2-dinitro-3,4,5,6-tetrachlorobenzene (10.71 g, 0.035 M) by reduction with iron (metal) powder in the presence of hydrogen (BDH) in ethanol containing ammonium chloride. The resultant crude precipitate was dissolved in diethyl ether and hydrogen chloride gas was passed through the solution to obtain the hydrochloride salt. The yield was 7.1 g (63.6%) as a white crystalline solid with m.p. 212–214 °C (decomposed).

3,5-*Dinitro*-1,2-*diaminobenzene* This reagent was synthesised as described in the following scheme:

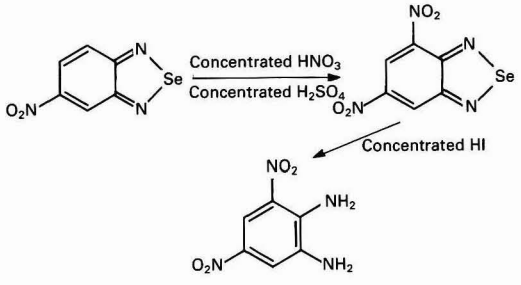

5-Nitropiazselenol (20 g, 0.088 M) was dissolved in concentrated sulphuric acid (160 ml) and fuming nitric acid (sp. gr. 1.5; 120 ml) was added. The solution was heated slowly to 90 °C and, after 15 min, cooled and poured on to crushed ice. The precipitate was filtered off, dried and recrystallised from acetic acid to yield pale yellow needles of 4,6-dinitropiazselenol (17.3 g, 72%), m.p. 210–212 °C.[18,19]

4,6-Dinitropiazselenol (4.1 g, 0.015 M) was mixed with 55% hydriodic acid (sp. gr. 1.7; 35 ml) and heated at 50 °C for 2 h under refluxing conditions. The cooled mixture was treated with sodium hydrogen sulphite to remove iodine, and made alkaline with 30% m/v sodium hydroxide solution and extracted with diethyl ether. The crude product was recrystallised from acetic acid[19] to give brick-red needles of 3,5-dinitro-1,2-diaminobenzene (1.8 g, 60%) with m.p. 216–218 °C.

Purification of 1,2-diamines and the preparation of their solutions were carried out following previously reported procedures.[3]

Piazselenols For the synthesis of piazselenol standards, equimolar amounts of 0.04 M diamine hydrochloride salt and selenium(IV) (as selenium dioxide or selenious acid) were mixed in 0.2 M HCl (the corresponding piazselenol was immediately precipitated). The mixture was allowed to stand at room temperature for at least 2 h. The solid piazselenols were filtered off through a glass-fibre paper and the damp solids recrystallised from ethanol - acetone (95 + 5).[3,14]

Instrumentation

Gas - liquid chromatography (GLC) was carried out with a Pye Unicam Series 104 chromatograph equipped with a ^{63}Ni electron-capture detector in the pulse mode (150 μs), a detector oven controller and a column oven controller. Extracts were separated on a 150 × 0.3 cm i.d., 0.6 cm o.d., Pyrex glass column. The column was packed with 5% OV-17 on Chromosorb W-AW-DMCS (80–100 mesh). The column and detector temperatures were maintained at 200 and 300 °C, respectively, and the nitrogen flow-rate was 30 ml min^{-1}.

A Varian AA 775 atomic absorption spectrometer fitted with a Model GTA 95 graphite tube atomiser was used for all absorption measurements. Absorption signals were obtained with the N_2 stopped-flow method. A hollow-cathode lamp was employed for selenium at a current of 5 mA. All analyses were performed at 196.0 nm using a 1.0-nm bandpass (slit-width). Pyrolytic graphite coated graphite tubes (Varian) were employed. The deuterium lamp background corrector was employed to correct for non-specific absorption observed during atomisation. The furnace operating parameters are shown in Table 1. The instrument was calibrated with standard solutions using the concentration mode.

Table 1. Atomic absorption furnace operating parameters

Step No.	Temperature/ °C	Time/s	N_2 flow/ l min^{-1}	Read command
1	90	5	3	—
2	120	60	3	—
3	300	10	3	—
4	500	5	3	—
5	500	5	3	—
6	500	2	0	—
7	2700	1.1	0	*
8	2700	2	0	*
9	2700	2	3	—

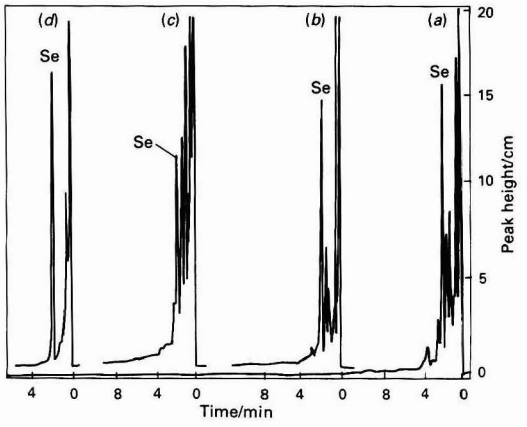

Fig. 1. Electron-capture detector responses showing peaks in chromatograms of 5-chloro-6-fluoropiazselenol extracts and effects of clean-up. (*a*) 0.2 ng of selenium(IV) + 1,2-diamino-4-chloro-5-fluorobenzene without clean-up; (*b*) 0.2 ng of selenium(IV) + 1,2-diamino-4-chloro-5-fluorobenzene + washing three times with 6 M $HClO_4$; (*c*) 0.2 ng of selenium(IV) + 1,2-diamino-4-chloro-5-fluorobenzene + washing three times with 9 M HCl; and (*d*) 0.2 ng of selenium as standard 5-chloro-6-fluoropiazselenol (weighed)

Procedure

An experiment to provide suitable biological material for total selenium determination was carried out using *Lolium perenne* seedlings. Selenium(VI) as sodium selenate was added to nutrient solutions in which the seedlings were grown hydroponically. The seedlings were germinated, allowed to establish themselves on exposure of 1 week to pure nutrient solution, followed by immersion in contaminated solutions for 3 weeks. The procedure has been discussed in detail elsewhere.[18,20]

Plant material was wet-digested in concentrated AnalaR nitric acid and an aliquot of the digest heated in an oven at 150 °C for 60–75 min in a PTFE vessel before the determination of selenium. Nickel nitrate was used as a matrix modifier in the GFAAS technique.[20]

Table 2. Melting-points and gas chromatographic properties of the piazselenols

Name	Piazselenol structural formula	Melting-point/°C		Retention time/min	Relative sensitivity		Sensitivity from literature		
		Found	Reported		At 200 °C column temperature	At constant retention time (5 min)	Reference 14	Reference 17	Reference 21
Unsubstituted*	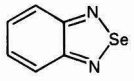	74	73–74	1.0	1	1	1	1	1
5-Fluoro-	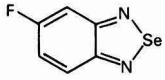	104–106	104	1.6	1.75	1.15	—	3.6	—
5-Trifluoro-methyl-	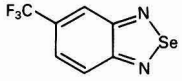	90–91	91	2.0	4.5	13.3	—	23.6	—
5-Chloro-*	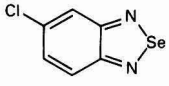	117–118	118–119	2.25	5.25	3.4	17	7.4	8.2
5-Nitro-*	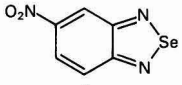	222–223	222–224	7.45	9.4	11.3	128	27.6	38.8
4,6-Dibromo-*		215–217	217–218	11.3	23.5	53.4	363	—	—
4-Bromo-6-fluoro-*	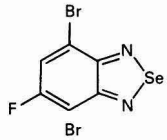	155–156	—	3.5	23.7	18.0	—	—	—
4-Bromo-6-tri-fluoromethyl-*	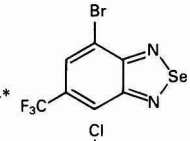	160–161	—	2.65	83.0	57.5	—	—	—
4-Chloro-6-tri-fluoromethyl-	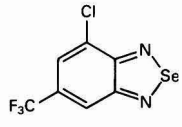	167–168	—	1.6	89.5	40.7	—	—	—
5-Chloro-6-fluoro-		130–131	—	2.0	15.2	9.7	—	—	—
4,5,6,7-Tetra-chloro-	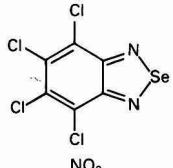	198–200	—	32.0	11.3	41.2	—	—	—
4,6-Dinitro-	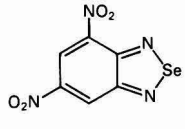	210–212	211–213	90.0	6.5	15.3	—	—	—

* See reference 3.

Results and Discussion

Clean-up Methods

Three methods for removing excess of reagent have been proposed.[17] In the present work, only two methods of clean-up or complex purification were examined. Both of these involved using separate aliquots (3 ml) of mineral acids (6 M $HClO_4$ or 9 M HCl)[18] to wash the toluene layer, a total of three times.

Fig. 1 gives the electron-capture detector responses showing peaks in the chromatograms of 5-chloro-6-fluoropiazselenol and the effect of clean-up. Fig. 1(*a*) shows the formation of the complex (containing 0.2 ng of selenium) obtained directly from the organic layer containing piazselenol without clean-up, while Fig. 1(*b*) depicts the result using perchloric acid as a washing agent. Note that some degradation of the complex occurs, especially when compared with the peak-height response obtained from the injection of a pure sample of the piazselenol, *viz.*, 0.2 ng (by mass) of the purified complex [Fig. 1(*d*)]. The effect is even more noticeable when hydrochloric acid is used instead of perchloric acid, see Fig. 1(*c*). Clearly the latter result [Fig. 1(*c*)] is unacceptable and was not used as a clean-up method, both in terms of the extra peaks created and the loss of selenium response.

Al-Attar and Nickless[3] recommended perchloric acid for the clean-up method for two new reagents for the determination of selenium. Perchloric acid, in spite of the greater danger, was used throughout the remainder of this work.

Retention Times

Table 2 lists the retention times for 12 piazselenols obtained under the same conditions; six of these have been reported elsewhere.[3] The other six piazselenols have varied retention times; four have retention times of less than 3 min, but unfortunately the last two piazselenols have very long retention times, even though they were measured at an isothermal column temperature of 200 °C.

Relative Sensitivities of Piazselenols

The relative sensitivities of the 12 piazselenols in comparison to the unsubstituted piazselenol were determined under the same experimental conditions by using two methods: (*i*) at an isothermal column temperature of 200 °C and (*ii*) at a constant retention time of 5 min. Table 2 lists the relative sensitivities for the 12 piazselenols when determined with the two methods and lists the retention times recorded at a column temperature of 200 °C. For the mono-substituted piazselenols for which data have been published[14] the most sensitive reagent was 5-nitropiazselenol [using method (*i*)]. However, when method (*ii*) was employed the most sensitive reagent was 5-trifluoromethylpiazselenol. Thus both methods confirmed the sensitivities reported in the literature[14,17,21] and listed in Table 2. For the di-substituted piazselenols the most sensitive reagent was 4-chloro-6-trifluoromethylpiazselenol when using method (*i*), however, when method (*ii*) (constant retention time) was employed the most sensitive was 4-bromo-6-trifluoromethylpiazselenol.

Fig. 2 illustrates the calibration results for 4-chloro-6-trifluoromethylpiazselenol at a constant column temperature of 200 °C.

Statistical Estimation of Detection Limits of Selenium by GLC-ECD

The statistical methods for assessing and comparing limits of detection are of importance. Limits of detection using the Liteanu and Rica[22] and Working - Hotelling[23] methods have been discussed elsewhere.[3,18] In general, the limit of detection of an analyte may be described as that concentration which gives an instrument signal significantly different from the blank or background signal.[24] Hunter[23] has commented in detail on the calibration and straight line graphs and on the calculations for the Working - Hotelling bounds for the true fitted line.

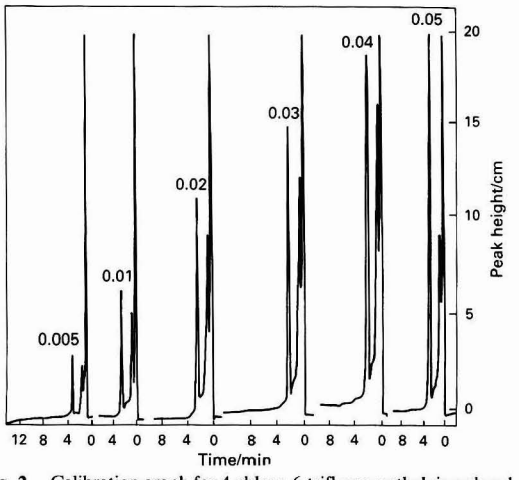

Fig. 2. Calibration graph for 4-chloro-6-trifluoromethylpiazselenol. Column temperature, 200 °C. The numbers above each peak represent the amount of selenium in ng

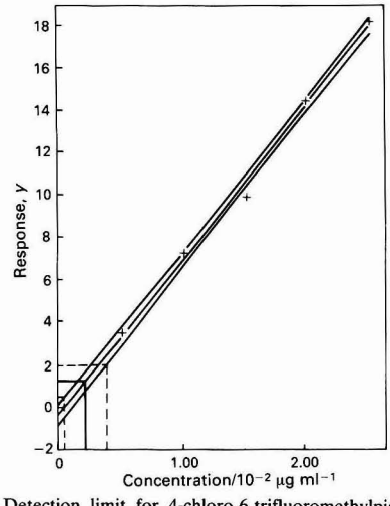

Fig. 3. Detection limit for 4-chloro-6-trifluoromethylpiazselenol. $y = -0.320 + 0.000728c$ (95.0% confidence limits); detection limit, 0.00221 μg ml^{-1}

The Working - Hotelling and Liteanu and Rica methods of estimating the detection limit were used for the piazselenols in the calibration data. In the present work, the detection limit for 4-chloro-6-trifluoromethylpiazselenol is shown in Fig. 3 as calculated using the Liteanu and Rica method.

Determination of Total Selenium in Standard Reference Materials

Two Standard Reference Materials (SRMs) from the National Institute of Standards and Technology (NIST) were examined, namely SRM 1577 Bovine Liver and SRM 1571 Orchard Leaves. Three methods of digestion were carried out with the SRMs and the results of all of the digestion procedures were in good agreement[13,25]: (*i*) nitric - perchloric - sulphuric acids, (*ii*) nitric acid - magnesium nitrate and (*iii*) nitric acid - bomb

Table 3. Analysis of standard reference materials for total selenium

Sample	No. of samples	Mass taken/g	Certified value/μg g^{-1}	Experimental value/μg g^{-1} 1,2-Diamino-3-chloro-5-trifluoromethylbenzene	1,2-Diamino-4-chloro-5-fluorobenzene	GFAAS
SRM 1577 Bovine Liver	5	0.25	1.1 ± 0.1	1.03 ± 0.10	1.20 ± 0.07	1.05 ± 0.08
SRM 1571 Orchard Leaves	5	0.50	0.08 ± 0.01	0.072 ± 0.013	0.083 ± 0.01	0.075 ± 0.008

Table 4. Total selenium in plant samples using 3-bromo-5-trifluoromethyl-1,2-diaminobenzene with GLC-ECD and GFAAS

Sample trial No.	Selenium/μg g^{-1} Root GLC-ECD	Root GFAAS	Shoot GLC-ECD	Shoot GFAAS
1	5.20	3.86	1.35	1.30
2	17.85	15.50	28.24	26.33
3	4.32	4.10	1.34	1.40
4	4.73	4.75	1.64	1.62
5	18.36	15.92	28.18	26.11
6	22.40	19.36	29.06	27.55
7	4.48	3.88	1.45	1.51
8	17.91	16.90	30.14	31.64
9	75.22	72.30	369.50	355.60
10	2.93	2.75	4.97	5.32
11	5.15	5.50	6.10	5.93
12	1.48	1.66	2.15	1.78
13	3.10	2.86	3.76	3.60
14	2.95	2.77	2.67	2.70
15	5.27	5.47	3.68	2.44
16	5.40	4.83	4.15	3.16
17	7.05	5.65	4.70	3.46
18	5.30	4.48	3.84	3.75
19	6.11	5.56	3.95	2.76
20	6.25	4.60	4.10	3.62
Mean	11.073	10.135	26.7485	25.579
t_{root} = 0.18118			t_{shoot} = 0.04513	

digestion. Table 3 lists a comparison of total selenium level in the SRMs using two reagents with GLC-ECD and GFAAS.

Digestion of Plant Samples

Kumpulainen *et al.*[26] studied a number of methods of digestion for selenium. They reported that in the digestion of selenium nutritional supplements, the use of perchloric acid or sulphuric acid is not necessary and recommended boiling samples overnight in concentrated nitric acid. Pettersson *et al.*[25] reported four digestion methods for the determination of selenium in Bovine Liver and confirmed that all of the procedures of digestion used gave concordant results.

In the present work, the digestion of plant samples was carried out by using nitric acid - bomb digestion (in a closed system), with a PTFE vessel contained within a stainless-steel sheath. In this instance, a portion of the sample (0.1–1.0 g depending on the selenium content) was placed in a PTFE vessel and 5 ml of concentrated nitric acid were added. The whole vessel was placed in a pre-heated electric oven at 150 °C for 60–75 min.

Determination of the selenium content of the acid-digested plant samples was carried out by GFAAS (adding nickel nitrate as a matrix modifier), and by GLC-ECD with 3-bromo-5-trifluoromethyl-1,2-diaminobenzene as the reagent.

When using GLC-ECD, an aliquot of the wet acid digestion mixture was reduced to selenium(IV) by adding 5 ml of 10 M HCl and heating at 100 °C in a water-bath for 15 min. Table 4 lists the results of the selenium content in 20 plant shoot samples and 20 root samples determined both by GLC-ECD and GFAAS.

Comparison of the Results of Two Different Techniques for Selenium Determination in Plant Samples

An accepted manner in which the results of an analytical method may be tested is by comparing them with those obtained when using a second technique,[24] preferably based on a completely different principle. In this instance, from Table 4, 20 root samples and 20 shoot samples were taken for calculation. The same number of determinations were carried out with both techniques (GLC-ECD and GFAAS).

The calculated values, t_{root} = 0.18118 and t_{shoot} = 0.04513 are substantially less than the tabulated value which is 2.5758 (at the 99% confidence level).[22,24] Although the determinations of total selenium in plant samples (Table 4) were carried out using different methods and different matrices, there is no significant difference between the two sets of individual results in each column.[22,24] Thus, the GLC-ECD method appears to be a very suitable method for the determination of the selenium content of material such as plant tissue and biological SRMs.

Conclusion

The synthesis and characterisation of four substituted 1,2-diaminobenzenes for the preparation of piazselenols has been described. Two of these compounds (fluorinated di-substituted piazselenols) were very sensitive and had short retention times. They were used for the gas chromatographic determination of selenium(IV) and the detection limits were found by using statistical methods.

A comparison of the results obtained using the two methods, GLC-ECD and GFAAS, for the determination of selenium in a number of biological samples showed no statistical difference at the 99% confidence level.

The authors acknowledge an award from the King Faisal Ministry of Higher Education, Riyadh, Saudi Arabia, to one of them (A. F. A-A.) during the tenure of which this research work was carried out.

References

1. Burk, R. F., *in* Prasad, A. S., and Oberleas, D., *Editors*, "Trace Elements in Human Health and Disease." Volume II, Academic Press, New York, 1976, pp. 105–133.
2. Robberecht, H. J., and Deelstra, H. A., *Clin. Chim. Acta*, 1984, **136**, 107.
3. Al-Attar, A. F., and Nickless, G., *J. Chromatogr.*, 1988, **440**, 333.
4. Lakin, H. W., *in* Kothny, E. I., *Editor*, "Trace Elements in the Environment," American Chemical Society, Washington, DC, 1973, pp. 96–111.
5. Eckerlin, R. H., Hoult, D. W., and Carnrick, G. R., *At. Spectrosc.*, 1987, **8**, 64.
6. Tsalev, D. L., "Atomic Absorption Spectrometry in Occupational and Environmental Health Practice," Volume II, CRC Press, Boca Raton, FL, 1984.

7. Bem, E. M., *Environ. Health Perspect.*, 1981, **37**, 183.
8. Shamberger, R. J., "Biochemistry of Selenium," Plenum Press, New York, 1983.
9. Robberecht, H. J., and Van Grieken, R., *Talanta*, 1982, **29**, 823.
10. Robberecht, H. J., and Deelstra, H. A., *Talanta*, 1984, **31**, 497.
11. Dilli, S., and Sutikno, I., *J. Chromatogr.*, 1984, **300**, 265.
12. Adeloju, S. B., Bond, A. M., Briggs, M. H., and Hughes, H. C., *Anal. Chem.*, 1983, **55**, 2076.
13. Siu, K. W. M., and Berman, S. S., *Talanta*, 1984, **31**, 1010.
14. Shimoishi, Y., *J. Chromatogr.*, 1977, **136**, 85.
15. Verlinden, M., Deelstra, H., and Adriaenssens, E., *Talanta*, 1981, **28**, 637.
16. Nakashima, S., and Toei, K., *Talanta*, 1968, **15**, 1475.
17. Dilli, S., and Sutikno, I., *J. Chromatogr.*, 1984, **298**, 21.
18. Al-Attar, A. F., *PhD Thesis*, University of Bristol, 1987.
19. Elvidge, J. A., Newbold, G. T., Percival, A., and Senciall, I. R., *J. Chem. Soc.*, 1965, 5119.
20. Al-Attar, A. F., Martin, M. H., and Nickless, G., *Chemosphere*, 1988, **17**, 845.
21. Bycroft, B. M., and Clegg, D. E., *J. Assoc. Off. Anal. Chem.*, 1978, **61**, 923.
22. Liteanu, C., and Rica, I., "Statistical Theory and Methodology of Trace Analysis," Halsted Press, Wiley, Chichester, 1980.
23. Hunter, J. S., *J. Assoc. Off. Anal. Chem.*, 1981, **64**, 574.
24. Miller, J. C., and Miller, J. N., "Statistics for Analytical Chemistry," Halsted Press, Wiley, Chichester, 1984.
25. Pettersson, J., Hansson, L., and Olin, A., *Talanta*, 1986, **33**, 249.
26. Kumpulainen, J., Raittila, A., Lehto, J., and Koivistoinen, P., *J. Assoc. Off. Anal. Chem.*, 1983, **66**, 1129.

Paper 9/05229A
Received December 8th, 1989
Accepted July 9th, 1990

Electrocatalytic Detection of Streptomycin and Related Antibiotics at Ruthenium Dioxide Modified Graphite - Epoxy Composite Electrodes

Donal Leech* and Joseph Wang†
Department of Chemistry, New Mexico State University, Las Cruces, NM 88003, USA

Malcolm R. Smyth
School of Chemical Science, Dublin City University, Dublin 9, Ireland

The application of ruthenium dioxide (RuO_2) modified electrodes to the electrocatalytic detection of the saccharide-related antibiotics streptomycin, novobiocin and neomycin, at low fixed potentials, was investigated. The RuO_2-modified graphite - epoxy composite electrodes give extremely stable and reproducible catalytic oxidation currents for these antibiotics at potentials as low as +0.2 V (*versus* Ag - AgCl). Rapid quantification at the micromolar level is therefore possible. Standard calibration graphs for streptomycin and neomycin yielded slopes of 4.43 and 0.08 nA μM^{-1} over the linear ranges of 1.5×10^{-6}–2.5×10^{-4} and 1×10^{-5}–2×10^{-3} M, respectively. Owing to its catalytic oxidation by the Ru^{III} - Ru^{IV} couple, rather than the Ru^{IV} - Ru^{VI} transition (which catalyses the oxidation of streptomycin and neomycin), novobiocin could be detected at a lower (+0.2 V) potential, with a sensitivity of 1.31 nA μM^{-1}. Detection limits of 1.5, 6.0 and 10 μM were obtained for streptomycin, novobiocin and neomycin, respectively. These catalytic surfaces can be renewed (by polishing), with a surface-to-surface reproducibility of 6.5% for the detection of 5×10^{-5} M streptomycin. The analytical application of RuO_2-modified carbon paste electrodes to the analysis of these antibiotics by flow injection was investigated, with a view to liquid chromatographic separation with electrochemical detection applications.

Keywords: *Ruthenium dioxide modified electrode; graphite - epoxy composite electrode; streptomycin; neomycin; novobiocin*

Streptomycin is a trisaccharide derivative that is important in tuberculosis therapy and the treatment of other infections such as tularemia and plague. The electrochemical reduction of streptomycin, involving the aliphatic aldehyde group, has been exploited for polarographic measurements of the drug using various mercury electrodes.[1–4] With d.c. polarography, millimolar concentrations of streptomycin can be quantified.[1,2] Differential-pulse polarography permits detection of micromolar levels,[3] whereas adsorptive stripping voltammetry of the drug offers detection limits in the nanomolar range.[4] The related saccharide antibiotics neomycin and novobiocin have also been determined using polarographic techniques.[4,5] Methods based on solid electrodes may be more desirable for sensing and flow [flow injection (FI)] applications. In particular, constant-potential amperometric monitoring of these antibiotics offers a more attractive and simpler approach to various flow or batch quantifications. Unfortunately, the anodic oxidation of saccharide antibiotics suffers from high overvoltages and poor reproducibility.

Recently, carbon paste electrodes modified with a ruthenium dioxide (RuO_2) catalyst have been shown to be effective for the electrocatalytic oxidation of hydroxylated compounds such as alcohols[6] and carbohydrates,[7] allowing their quantification via fixed-potential amperometry. Other recent studies in this and other laboratories have demonstrated the improved stability and reproducibility that composite graphite - epoxy electrodes containing electrocatalysts can offer over their carbon paste counterparts. Graphite - epoxy electrodes modified with RuO_2 have been utilised as glucose sensors.[8] These electrodes showed similar analytical attributes for the detection of glucose as their carbon paste counterparts, while offering benefits of increased mechanical stability, versatility and renewability. Polishable graphite - epoxy electrodes modified with other metal-containing catalysts[9–11] and biological entities[12] have been used successfully.

The purpose of this work was to investigate the application of RuO_2-modified electrodes to electrocatalytic detection of various saccharide antibiotics. The surface modifier greatly lowers the overvoltage for the oxidation of these antibiotics, hence allowing their quantification at low, fixed potentials. A highly stable and renewable electrocatalytic response is observed by incorporating the RuO_2 within the graphite - epoxy matrix. Preliminary FI experiments utilising RuO_2-modified carbon paste electrodes (RuO_2-CPEs) were also conducted in order to investigate the possible amperometric flow detection of saccharide antibiotics.

Experimental

Apparatus

Cyclic voltammetric and batch amperometric experiments were performed with an EG & G Princeton Applied Research Model 264A voltammetric analyser in conjunction with a Houston *x* - *y* recorder or a Recorder Company 4500 Microscribe strip-chart recorder, respectively. A Bioanalytical Systems (BAS) Model VC-2 electrochemical cell (10 ml) was employed in these experiments with the working electrode, reference electrode (Ag - AgCl, Model RE-1, BAS) and platinum wire auxiliary electrode inserted into the cell through holes in its Teflon cover. Mass transport in the batch system was achieved with an IKAMAG RE-G magnetic stirrer and a 1 cm long magnetic flea. A stirring rate of 400 rev min^{-1} was used in all studies.

The FI system consisted of a carrier reservoir, a Rainin Model 5041 sample injection valve (20-μl loop), interconnecting Teflon tubing, a thin-layer electrochemical detector (Model TL-4, BAS), an Ag - AgCl reference electrode (Model RE-1) and a stainless-steel auxiliary electrode. A gravity feed of the carrier with a flow-rate of 1 ml min^{-1} was used throughout this study.

* Permanent address: School of Chemical Science, Dublin City University, Dublin 9, Ireland.
† To whom correspondence should be addressed.

Reagents

All solutions were prepared from doubly distilled, de-ionised water. Standard solutions of streptomycin sulphate, neomycin sulphate and novobiocin sodium salt (Sigma), were prepared daily in the 0.5 M NaOH (Baker) electrolyte and carrier solutions.

Procedures

The graphite - epoxy electrodes were prepared by mixing equal amounts of the epoxy-bonded graphite (Dylon) resin and accelerator components. Ruthenium dioxide (Aldrich) modified graphite - epoxy electrodes were prepared by the subsequent addition and thorough hand-mixing of the required amount of RuO_2 (usually an 80:20% m/m ratio of graphite - epoxy : RuO_2) to the graphite paste. Portions of the resulting paste were then packed into the end of a glass tube (3 mm i.d.) and allowed to cure at room temperature for 48–72 h. The hardened electrode surface was then polished with wet and dry emery (1200 grade), rinsed with de-ionised water, polished with a 0.05-μm alumina slurry, rinsed with water again and finally ultrasonicated for 3 min to remove residual alumina.

Batch measurements were performed by the addition of volumes of concentrated (1×10^{-2}– 1×10^{-4} M) solutions of the antibiotics to the voltammetric cell to give the final micromolar concentrations in the cell.

The RuO_2-CPEs for FI were prepared by adding weighed amounts of RuO_2 and graphite powder (Acheson 38, Fisher) to 10 ml of diethyl ether and sonicating the resulting slurry until the diethyl ether had evaporated. The desired amount of mineral oil (Aldrich) was then added and thoroughly hand-mixed with the RuO_2-coated graphite. Portions of the resulting paste (usually a 40:40:20% m/m ratio of graphite : oil : RuO_2) were then packed into the cavity of the flow detector and the surface was smoothed on a weigh paper. The glassy carbon electrodes for cyclic voltammetry (BAS, 3 mm i.d.) were polished with a 0.05-μm alumina slurry, rinsed with de-ionised water and ultrasonicated for 3 min prior to use.

Results and Discussion

Cyclic Voltammetry

Preliminary experiments to investigate the catalytic activity of the RuO_2-graphite - epoxy electrodes towards the antibiotics were performed by cyclic voltammetry. Fig. 1(*a*)–(*c*) shows typical cyclic voltammetric responses obtained at the RuO_2-graphite - epoxy electrodes in 0.5 M NaOH, both with and without added analyte (solid and broken lines, respectively). The blank signal at the modified electrode shows two transitions: at 0.0 and +0.45 V, which have been identified previously as the RuO_2 - Ru_2O_3 and RuO_4^{2-} - RuO_2 transitions, respectively, in base.[13,14] This signal is identical with the blank signals obtained at RuO_2-CPEs,[6,7] confirming the retention of the ruthenium redox characteristics in the rigid graphite - epoxy matrix. As was observed at the RuO_2-CPE, for the electrocatalytic oxidation of alcohols[6] and carbohydrates,[7] the RuO_2-graphite - epoxy electrodes exhibit classic electrocatalytic behaviour[15] for the oxidation of the saccharide antibiotics with an increase in anodic and a decrease in cathodic peak currents. The oxidation of novobiocin appears to be catalysed by both of the ruthenium redox couples, with an increase in the anodic peak current at the RuO_2 - Ru_2O_3 transition at 0.0 V and the RuO_4^{2-} - RuO_2 transition at +0.45 V. In contrast [and as shown in Fig. 1(*d*)], the unmodified graphite - epoxy (B) and glassy carbon (A) electrodes do not respond to a solution containing 5 mM novobiocin. No transitions were evident in the voltammograms obtained for the three drugs at the unmodified graphite - epoxy electrodes. Broad, irreversible oxidation peaks at

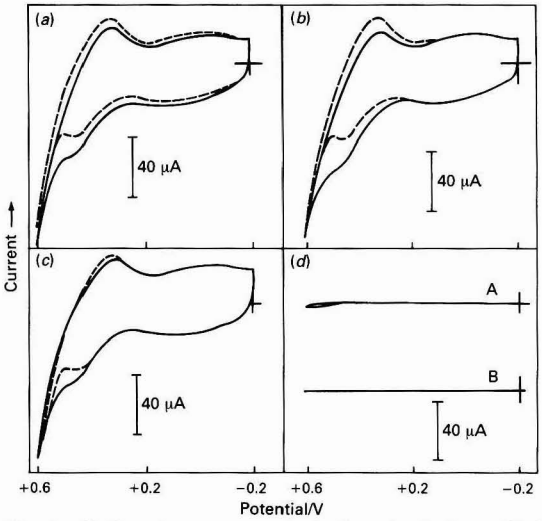

Fig. 1. Cyclic voltammograms obtained at the RuO_2-modified graphite - epoxy electrode in blank 0.5 M NaOH electrolyte (broken lines) and on the addition of: (*a*) 5 mM novobiocin; (*b*) 5 mM streptomycin; and (*c*) 20 mM neomycin (solid lines). Also shown (*d*) is the response for 5 mM novobiocin at A, a bare glassy carbon electrode, and B, an unmodified graphite - epoxy electrode. Scan rate, 20 mV s^{-1}

potentials of +0.75 and +0.80 V were observed for streptomycin and novobiocin, respectively, at the glassy carbon electrode. Surface poisoning of the glassy carbon electrode resulted in a gradual decrease in these oxidation currents. The peaks obtained at the RuO_2-modified electrodes, however, showed extremely good stability, with no apparent decrease in peak currents after continuous cycling for more than 60 min.

The presence of high concentrations of NaOH was required for the electrocatalytic oxidation of these antibiotics, with no oxidation apparent at low (<0.05 M) NaOH concentrations. This has been observed also for carbohydrate oxidation at RuO_2-CPEs,[7] Au electrodes[16,17] and Cu electrodes,[18,19] and for oxidation of alcohols at the RuO_2-CPE.[6] High OH^- concentrations are required to maintain the electrode oxide layer. Hydroxyl ions are also involved in the electrocatalytic oxidation mechanism at the Au[19,20] and RuO_2-modified[15] electrodes. An NaOH concentration of 0.5 M was utilised throughout this study.

Constant-potential Amperometry in Stirred Solutions

Batch fixed-potential operation was utilised to investigate further the analytical use of the RuO_2-graphite - epoxy electrodes. Fig. 2 shows hydrodynamic voltammetric profiles for batch additions of streptomycin (*a*), novobiocin (*b*) and neomycin (*c*) at both the modified (A) and unmodified (B) electrodes. The unmodified electrode does not permit convenient quantification of these analytes over the potential window studied. In contrast (and in agreement with cyclic voltammetric data), distinctly peak-shaped hydrodynamic voltammograms, with a maximum response in the vicinity of +0.45 V, are observed at the RuO_2-modified electrodes. Similar responses were obtained at RuO_2-CPEs for the catalytic oxidation of carbohydrates[7] and alcohols.[6] The hydrodynamic voltammogram obtained for the oxidation of novobiocin shows a catalytic current even at a potential as low as 0.0 V. This confirms the result given by cyclic voltammetry and allows convenient monitoring of novobiocin at lower potentials, hence minimising interferences and background currents associated with the RuO_2-graphite - epoxy elec-

trodes. A potential of +0.35 V was selected for detection of both streptomycin and neomycin. A potential of +0.2 V was selected for the determination of the analytical parameters for novobiocin in the batch cell. Subsequent experiments on novobiocin were carried out at a fixed potential of 0.0 V in order to minimise potential interferences from carbohydrates and alcohols, which do not give catalytic currents at this low monitoring potential.

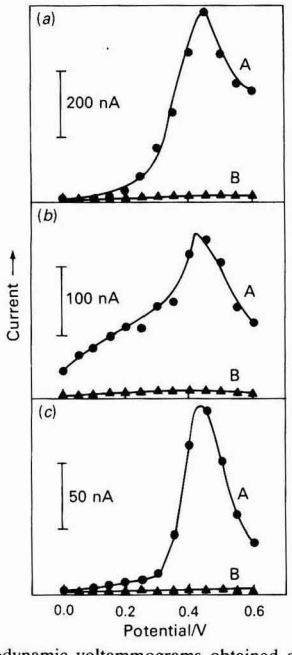

Fig. 2. Hydrodynamic voltammograms obtained at A, modified, and B, unmodified graphite - epoxy electrodes for the solutions of: (*a*) 5×10^{-5} M streptomycin; (*b*) 5×10^{-5} M novobiocin; and (*c*) 5×10^{-4} M neomycin. Electrolyte, 0.5 M NaOH; and stirring rate, 400 rev min^{-1}

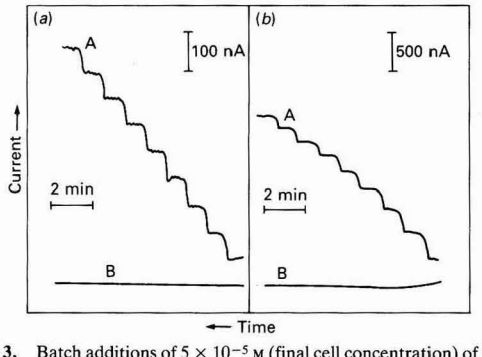

Fig. 3. Batch additions of 5×10^{-5} M (final cell concentration) of (*a*) novobiocin and (*b*) streptomycin at A, modified and B, unmodified graphite - epoxy electrodes with constant-potential detection at (*a*) +0.2 and (*b*) +0.35 V. Other conditions as in Fig. 2

Fig. 3 shows the batch amperometric detection of 5×10^{-5} M (final cell concentration) novobiocin (*a*) and streptomycin (*b*) at both the modified (A) and unmodified (B) electrodes. Excellent response times and signals are obtained for both of these drugs at the monitoring potentials used (see figure caption). Table 1 lists the analytical parameters obtained at the 20% RuO_2-modified graphite - epoxy electrodes for the three antibiotics. Good sensitivities with detection limits [signal to noise (S/N) ratio = 3] of 6×10^{-6} and 1.5×10^{-6} M were obtained for novobiocin and streptomycin (at monitoring potentials of +0.2 and +0.35 V), respectively. Neomycin did not exhibit large catalytic currents, however, and gave a detection limit (S/N ratio = 3) of only 1×10^{-5} M. These detection limits are higher than those observed for adsorptive stripping voltammetric measurements of these antibiotics at mercury electrodes.[4] However, as previously mentioned, methods based on mercury may be undesirable for many practical applications, including flow analysis. The application of RuO_2-modified electrodes to FI detection of the antibiotics studied in the batch system will be discussed later. The mechanism involved in catalytic RuO_2-detection is believed to be due to the oxidation of the C–OH moiety to aldehyde and carboxyl groups.[6,7] Steric hindrance and the presence of other functional groups also affect the sensitivity.[7] A direct correlation of response to hydroxy group content, for the drugs studied, is not apparent. Steric hindrance of the hydroxy groups on the more bulky neomycin molecule could explain the reduced response obtained for this compound compared with the response obtained for the similarly structured streptomycin.

The stability and precision of the RuO_2-graphite - epoxy electrodes towards the oxidation of the saccharide antibiotics are demonstrated in Fig. 4. Fig. 4(*a*) represents the precision of the electrode at the same electrode surface for the oxidation of 5×10^{-5} M novobiocin with the electrode being removed and rinsed with de-ionised water between injections. From the 20 repetitive injections made a mean current of 40.1 nA with a relative standard deviation of 3.7% was established. Fig. 4(*b*) shows the surface-to-surface precision to streptomycin detection (5×10^{-5} M). Between measurements the electrode was removed from the cell, polished for 30 s with a 0.5-μm alumina slurry and rinsed with de-ionised water. For a series of 20 consecutive measurements at different surfaces, a mean current of 486 nA with a relative standard deviation of 6.5% was calculated. These data demonstrate the very good stability and reproducibility of the polishable, graphite - epoxy modified electrode. The success of the graphite - epoxy electrode fabrication technique also compares favourably with other techniques for the incorporation of modifiers in polishable, robust electrodes.[21–24] All of the RuO_2-modified graphite - epoxy electrodes prepared functioned in a reproducible (±10%) fashion.

Flow Injection

The practical application of the RuO_2-modified electrodes to antibiotic monitoring in complex biological matrices is hampered by the general catalytic activity of these electrodes towards hydroxylated compounds such as alcohols,[6] carbohydrates[7] and other potential interferents. The application of the

Table 1. Analytical parameters calculated for the antibiotics from batch additions at fixed potentials. Background electrolyte, 0.5 M NaOH; stirring rate, 400 rev min^{-1}

	Streptomycin*	Neomycin*	Novobiocin†
Linear range/M	1.5×10^{-6}–2.5×10^{-4}	1×10^{-5}–2×10^{-3}	6×10^{-6}–4×10^{-4}
Sensitivity/nA μM^{-1}	4.43	0.08	1.31
Correlation coefficient	0.996	0.998	0.999
Limit of detection (S/N ratio = 3)/M	1.5×10^{-6}	1×10^{-5}	6×10^{-6}

* Fixed-potential detection at +0.35 V.
† Fixed-potential detection at +0.2 V.

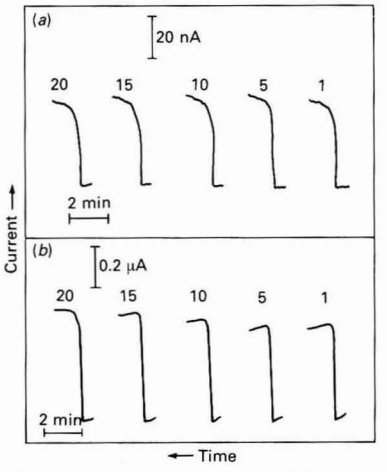

Fig. 4. (*a*) Same-surface precision for repeated batch additions of 5 × 10^{-5} M novobiocin, with constant-potential detection at 0.0 V; and (*b*) surface-to-surface precision for repeated batch additions of 5 × 10^{-5} M streptomycin, with constant-potential detection at +0.35 V, at the RuO_2-graphite - epoxy electrode. Other conditions as in Fig. 2

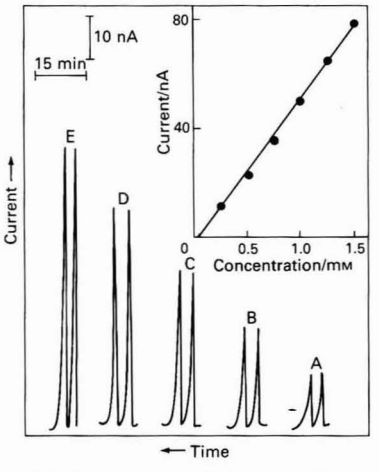

Fig. 5. Flow injection response at the RuO_2-modified carbon paste electrode to injections of: A, 0.25; B, 0.5; C, 0.75; D, 1.0; and E, 1.25 mM novobiocin. Constant-potential operation at 0.0 V. Flow-rate, 1 ml min^{-1}; and electrolyte, 0.5 M NaOH. Inset shows the current - concentration calibration graph obtained for novobiocin up to a concentration of 1.5 mM

RuO_2-modified electrodes to constant-potential detection of the saccharide antibiotics in flowing streams, with a view to liquid chromatographic separation with electrochemical detection (LC-EC) applications, was therefore investigated. For these preliminary experiments, RuO_2-CPEs were utilised.

The short-term stability of the RuO_2-CPE in the flow system was investigated. A series of 60 replicate injections of 1 × 10^{-4} M streptomycin over a 110-min period (not shown) yielded a mean current of 62.5 nA and a relative standard deviation of 3.1%, demonstrating the stability of these electrodes in flowing streams.

The current - concentration profile of novobiocin at the RuO_2-CPE is shown in Fig. 5. Excellent linearity is observed over the 0–1.5 mM range, with a slope of 52 nA mM^{-1} (correlation coefficient, 0.998). Detection limits (S/N ratio = 3) of 8 × 10^{-6} and 6 × 10^{-5} M were calculated for streptomycin and novobiocin, respectively. The above results indicate that the RuO_2-modified flow detectors could be used for the LC-EC determination of saccharide antibiotics.

Conclusion

The RuO_2-modified graphite - epoxy electrodes have been shown to be robust, polishable and stable detectors for the saccharide antibiotics streptomycin, novobiocin and neomycin. Favourable analytical parameters were obtained, at low constant-potential detection, demonstrating the application of these polishable modified electrodes to the batch amperometric determination of saccharide antibiotics. Interferences, however, present a problem in complex matrices. The utility of RuO_2-modified electrodes in FI was therefore investigated and future applications of these electrodes for the LC-EC separation and detection of carbohydrates and saccharide antibiotics are envisaged. Flow injection operation should be extremely useful for rapid assays of simple samples (*e.g.*, pharmaceutical formulations).

This work was supported by a grant to J. W. from the National Institutes of Health (No. GM 30913-06), D. L. gratefully acknowledges a Department of Science and Technology (Ireland) scholarship.

References

1. Levy, G. B., Schwed, P., and Sackett, J. W., *J. Am. Chem. Soc.*, 1946, **68**, 528.
2. Doan, L., and Riedel, B. E., *Can. Pharm. J. Sci.*, 1963, **96**, 109.
3. Siegerman, H., *in* Bard, A. J., *Editor*, "Electroanalytical Chemistry," Volume 11, Marcel Dekker, New York, 1979, p. 291.
4. Wang, J., and Mahmoud, J. S., *Anal. Chim. Acta*, 1986, **186**, 31.
5. Siegerman, H. D., Flato, J. B., and O'Dom, G. W., *in* Heden, C.-G., and Illeni, T., *Editors*, "Automation in Microbiology and Immunology," Wiley, New York, 1975, p. 306.
6. Leech, D., Wang, J., and Smyth, M. R., *Electroanalysis*, in the press.
7. Wang, J., and Taha, Z., *Anal. Chem.*, 1990, **62**, 1413.
8. Leech, D., Wang, J., and Smyth, M. R., in preparation.
9. Wang, J., Golden, T., Varughese, K., and El-Rayes, I., *Anal. Chem.*, 1989, **61**, 508.
10. Wring, S. A., Hart, J. P., and Birch, B. J., *Analyst*, 1989, **114**, 1563.
11. Wring, S. A., Hart, J. P., and Birch, B. J., *Analyst*, 1989, **114**, 1571.
12. Wang, J., and Varughese, K., *Anal. Chem.*, 1990, **62**, 318.
13. Burke, L. D., and Whelan, D., *J. Electroanal. Chem.*, 1979, **103**, 179.
14. Burke, L. D., and Murphy, O. J., *J. Electroanal. Chem.*, 1980, **109**, 199.
15. Burke, L. D., and Murphy, O. J., *J. Electroanal. Chem.*, 1979, **101**, 351.
16. Neuberger, G. G., and Johnson, D. C., *Anal. Chem.*, 1987, **59**, 203.
17. Neuberger, G. G., and Johnson, D. C., *Anal. Chem.*, 1987, **59**, 150.
18. Prahbu, S. V., and Baldwin, R. P., *Anal. Chem.*, 1989, **61**, 852.
19. Prahbu, S. V., and Baldwin, R. P., *Anal. Chem.*, 1989, **61**, 2258.
20. Larew, L. A., and Johnson, D. C., *J. Electroanal. Chem.*, 1989, **262**, 167.
21. Cox, J. A., and Kulkarni, K. R., *Talanta*, 1986, **33**, 911.
22. Shaw, B. R., and Creasy, K. E., *J. Electroanal. Chem.*, 1988, **243**, 209.
23. Shaw, B. R., and Creasy, K. E., *Anal. Chem.*, 1988, **60**, 1241.
24. Park, J., and Shaw, B. R., *Anal. Chem.*, 1989, **61**, 848.

Paper 0/02405H
Received May 30th, 1990
Accepted July 23rd, 1990

Mercurated Polystyrene as a Sensor for Anionic Surfactants in Ion-selective Polymeric Membrane Electrodes

Walenty Szczepaniak
Faculty of Chemistry, A. Mickiewicz University, 60–780 Poznań, ul.Grunwaldzka 6, Poland

Mercurated polystyrene (R–Hg–Ac) was employed as a sensor in a membrane electrode sensitive to anionic surfactants. A Nernstian dependence over the concentration range of sodium dodecyl sulphate of from 1×10^{-3} to 1×10^{-7} M and a high selectivity for anionic surfactants relative to inorganic anions were found for the electrode. Moreover, the electrode shows interesting properties towards hydroxyl ions. The electrode may find application in the analysis of surfactants, as an indicator electrode in the potentiometric titration of both cationic and anionic surfactants and in the physico-chemical studies of surfactant solutions.

Keywords: *Anionic surfactant; ion-selective electrode; mercurated polystyrene*

Synthetic surface-active agents (surfactants) are produced in large amounts and are used extensively in industry and household cleaning products, and also in chemistry and biochemistry research laboratories. Such wide application of surfactants may result in the pollution of surface waters. Hence, industry, environmental protection services and research laboratories have shown considerable interest in developing rapid methods for the determination of trace amounts of surfactants.

Anionic surfactants comprise about 70% of all the surfactants manufactured, hence they are often the subject of environmental monitoring. Many methods for the determination of anionic surfactants have been reported, of which the most important are titrimetric,[1–5] spectrophotometric,[6–10] spectrofluorimetric,[11,12] chromatographic[13–17] and electrochemical methods incorporating ion-selective electrodes sensitive to this group of compounds.[18–36]

In ion-selective electrodes sensitive to ionic surfactants, an ion associate of the type B^+A^- is used as the electroactive substance in which the anion A^- is an anionic surfactant and the cation B^+ is usually a cationic surfactant. Hence, such electrodes are sensitive to both cationic and anionic surfactants.

This paper describes the application of mercurated polystyrene as a sensor in an ion-selective polymeric membrane electrode sensitive to anionic surfactants. The mercurated polystyrene has the following formula:

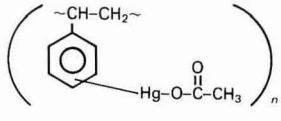

In previous papers,[37–39] the application of a mercurated styrene - divinylbenzene copolymer as an anion exchanger was proposed. In addition, the synthesis and extraction properties of mercurated polystyrene were studied. A solution of mercurated polystyrene [(R–Hg–Ac); mean relative molecular mass, 10000] in nitrobenzene exhibits anion-exchange properties in accordance with the reaction

$$(\text{R–Hg–Ac})_0 + (\text{X}^-)_{aq} \rightleftharpoons (\text{R–Hg–X})_0 + (\text{Ac}^-)_{aq}$$

In this way Cl^-, Br^-, I^-, SCN^-, CN^- and anionic surfactants were extracted.

In the present paper mercurated polystyrene was employed as a liquid polymeric anion exchanger and used as the active substance in a membrane electrode sensitive to anionic surfactants.

Experimental

Reagents

Surfactant solutions

Two anionic surfactants were used for testing the electrodes; sodium dodecyl sulphate (SDS) (Fluka, Buchs, Switzerland) and sodium *p*-dodecylbenzenesulphonate (SDBS) (Fluka). The surfactants were dried at 50 °C under reduced pressure to a constant mass. Weighed portions of SDS and SDBS were dissolved in distilled water to obtain basic solutions of concentrations of 1×10^{-3} M. The working solutions were prepared prior to use by dilution of the basic solutions.

Other reagents

The reagents used in this work were obtained from the following suppliers: 2-nitrophenyl octyl ether (NPOE) (Fluka), didecyl phthalate (DDP) (Fluka), dibutyl phthalate (DBP) (Fluka), tributyl phosphate (TBP) (Fluka), tri(2-ethylhexyl) phosphate (TEHP) (Koch-Light, Colnbrook, Buckinghamshire, UK), poly(vinyl chloride) (PVC) of high relative molecular mass (M_r) (Aldrich, Beerse, Belgium) and three polystyrene (PS) standards (Technical University, Szczecin, Poland) ($M_r = 2800$, $M_r/M_n = 1.20$; $M_r = 5800$, $M_r/M_n = 1.06$; $M_r = 9800$, $M_r/M_n = 1.08$). Analytical-reagent grade chemicals were used in all other instances and re-distilled water was used for preparing all aqueous solutions.

Electrode Preparation

An electrode with a polymeric membrane and a metallic contact of the coated-wire type was used. The active membrane component was mercurated polystyrene.

Three polystyrenes of different relative molecular masses, *viz.*, 2800, 5800 and 9800 g mol^{-1}, were employed. Mercuration was performed as described previously.[37,38] The content of Hg in the mercurated polystyrenes, as determined by atomic absorption spectrometry, was 0.3840, 0.3814 and 0.3832 g per gram of polymer, respectively. This implies that as a result of mercuration, half of the benzene rings in polystyrene contained the $-Hg-O-CO-CH_3$ substituent.

The coating mixture was prepared as a ternary cocktail consisting of matrix, sensor and plasticiser. Poly(vinyl chloride) or PS was used as the matrix support, R–Hg–Ac as the sensor and DDP, DBP, TBP, TEHP or NPOE as the solvent mediator.

The membrane coating solution was prepared as follows: to 2 ml of a 1% solution of R–Hg–Ac in dioxane, 0.5 ml of plasticiser and 2 ml of 10% PVC in tetrahydrofuran or 2 ml of 10% PS in dioxane were added. Prior to coating, the platinum wire was washed with concentrated H_2SO_4 and water and

Table 1. Composition of the different membranes and some electrode characteristics measured as a response to SDS

	Composition of the membrane				
No.	Matrix	Sensor	Solvent mediator	Slope at 25 °C/ mV decade^{-1}	Linear range/M
I	PVC	R–Hg–Ac (M_r 2800)	NPOE	58	1×10^{-3}–5×10^{-7}
II	PVC	R–Hg–Ac (M_r 5800)	NPOE	58	1×10^{-3}–5×10^{-7}
III	PVC	R–Hg–Ac (M_r 9800)	NPOE	58	1×10^{-3}–5×10^{-7}
IV	PVC	R–Hg–Ac (M_r 2800)	DBP	59	1×10^{-3}–1×10^{-7}
V	PVC	R–Hg–Ac (M_r 5800)	DBP	59	1×10^{-3}–1×10^{-7}
VI	PVC	R–Hg–Ac (M_r 9800)	DBP	59	1×10^{-3}–1×10^{-7}
VII	PVC	R–Hg–Ac (M_r 9800)	TBP	7	—
VIII	PVC	R–Hg–Ac (M_r 9800)	TEHP	21	1×10^{-3}–1×10^{-5}
IX	PVC	R–Hg–Ac (M_r 9800)	DDP	46	1×10^{-3}–1×10^{-6}
X	PVC	R–Hg–Ac (M_r 9800)	DDP - NPOE (1 + 1)	58	1×10^{-3}–1×10^{-6}
XI	PS	R–Hg–Ac (M_r 9800)	NPOE	41	1×10^{-3}–1×10^{-5}
XII	PS	R–Hg–Ac (M_r 9800)	DBP	36	1×10^{-3}–1×10^{-5}

dried with acetone. It was then rinsed with chloroform and allowed to dry. A piece of the platinum wire, 2 mm in diameter, was coated to a height of 0.5 cm by three successive immersions in the membrane solution. The electrode was left for 24 h in ambient air so that the solvents would evaporate. The surface of the coated part of the wire was further coated with unmodified PVC and shielded with a glass tube. Prior to use, the electrode was conditioned for 24 h in 1×10^{-4} M SDS or SDBS solution.

Apparatus

The measuring cell was

$$\mathrm{Pt} \left| \begin{matrix} \text{Membrane} \\ \end{matrix} \right| \begin{matrix} \text{Test} \\ \text{solution} \end{matrix} \Vert \begin{matrix} 1\ \text{M} \\ NH_4NO_3 \end{matrix} \left| \begin{matrix} 1\ \text{M} \\ KCl \end{matrix} \right| \mathrm{AgCl\text{-}Ag}$$

The e.m.f. was measured (±0.1 mV) with an N-512 pH meter (ELPO, Wrocław, Poland) connected to a V-544 digital voltmeter (Meratronik, Wrocław, Poland) and a G_1B_1 recorder (Carl Zeiss, Jena, GDR). Measurements were made in a 50-ml water-jacketed vessel at 25 ± 0.1 °C. The solution under study was stirred with a magnetic stirrer.

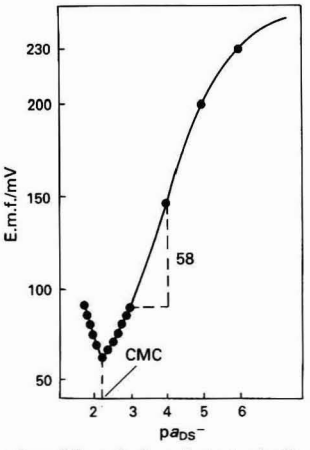

Fig. 1. Calibration of the anionic surfactant-selective electrode Pt/X in aqueous solutions of SDS

Results and Discussion

A membrane electrode sensitive to anions has been described. The electroactive substance of the electrode is a metallo-organic polymer. To date, this type of compound has not been used either in electrodes sensitive to anionic surfactants or in electrodes sensitive to other anions. Only dialkyltin chlorides (R_2SnCl_2) and their complexes have been employed in anion-selective electrodes.[40,41]

Electrodes with membranes of different composition (see Table 1) were tested. Both the sensor and the matrix and also the solvent mediator were changed. No significant differences between the three mercurated polystyrenes of various relative molecular masses were found. Both PVC and PS were tested as the matrix membrane, and PVC was found to be superior. In addition, it was shown that the matrix membranes based on PS were mechanically unstable. The best properties were found for electrodes with NPOE, DBP or a 1 + 1 mixture of NPOE - DDP as plasticiser. Hence, of the 12 electrodes shown in Table 1, the electrode with a membrane made of PVC - NPOE - R–Hg–Ac (M_r = 9800) (electrode Pt/III), the electrode with a membrane containing PVC - DBP - R–Hg–Ac (M_r = 9800) (electrode Pt/VI) and the PVC - NPOE - DDP - R–Hg–Ac (M_r = 9800) membrane-based electrode (electrode Pt/X) were used for further studies.

Calibration of the Electrode

Standard solutions of SDS were used for electrode calibrations. A typical calibration graph for SDS using the Pt/X electrode is presented in Fig. 1.

Studies on the calibration of electrodes gave the following results: (1) below the critical micellar concentration (CMC) the electrode system exhibited a Nernstian or near-Nernstian response giving a slope of 58 mV for the Pt/III and Pt/X electrodes and 59 mV for the Pt/VI electrode per decade change in DS^- activity (a_{DS^-}); (2) at a point corresponding to the CMC the calibration graph deviates from linearity, and at greater activities the potential increases; (3) the values of the CMC for SDS and SDBS, determined from the calibration graphs, are 8.2×10^{-3} and 1.2×10^{-3}, respectively. The former is fairly close to the literature value,[42] whereas the latter agrees well with the literature value;[42] (4) a broad range of linear Nernstian dependence was observed for the electrodes: for the Pt/III electrode, the range is from 1×10^{-3} to 5×10^{-7} M, for the Pt/VI electrode from 1×10^{-3} to 1×10^{-7} M and for the Pt/X electrode from 1×10^{-3} to 1×10^{-6} M. The lower limit for the Pt/III and Pt/VI electrodes is much lower than that reported for electrodes sensitive to SDS and based on ion pairs; (5) the time required for the potential to reach a stable value ranges from 30 s for a 1×10^{-3} M SDS solution to 3 min for a 1×10^{-7} M SDS solution.

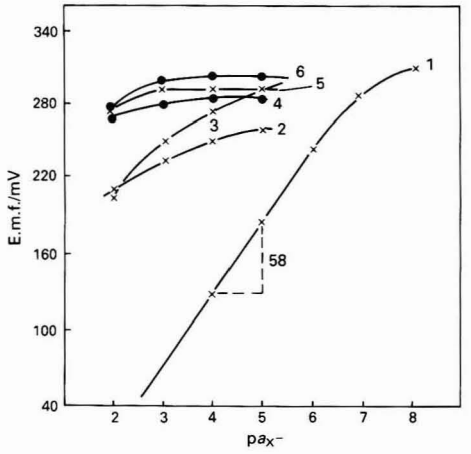

Fig. 2. Calibration of the anionic surfactant-selective electrode Pt/III in aqueous solutions of: 1, SDS; 2, NaCl; 3, $NaClO_4$; 4, Na_2SO_4; 5, NaBr; and 6, $NaNO_3$

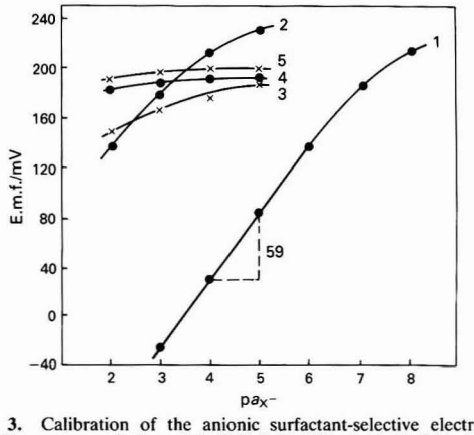

Fig. 3. Calibration of the anionic surfactant-selective electrode Pt/VI in aqueous solutions of: 1, SDS; 2, $NaClO_4$; 3, NaCl; 4, Na_2SO_4; and 5, $NaNO_3$

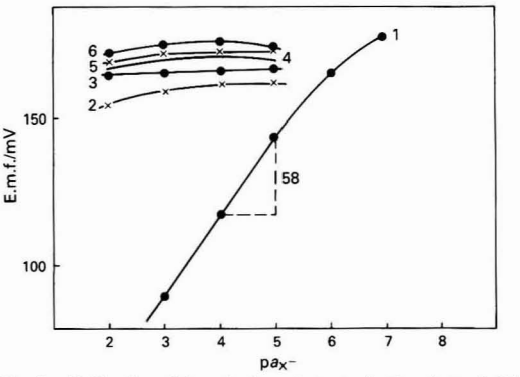

Fig. 4. Calibration of the anionic surfactant-selective electrode Pt/X in aqueous solutions of: 1, SDS; 2, $NaClO_4$; 3, NaCl; 4, Na_2SO_4; 5, $NaNO_3$; and 6, NaH_2PO_4

Table 2. Potentiometric selectivity coefficients (k_{DS^-/X^-}) for the Pt/III, Pt/VI and Pt/X electrodes

Anion X^{n-}	Selectivity coefficient Pt/III	Pt/VI	Pt/X
NO_3^-	2×10^{-5}	$<1 \times 10^{-5}$	$<1 \times 10^{-5}$
Cl^-	2×10^{-4}	1×10^{-4}	$<1 \times 10^{-5}$
ClO_4^-	9×10^{-4}	2.5×10^{-4}	4×10^{-4}
$H_2PO_4^-$	2×10^{-5}	$<1 \times 10^{-5}$	$<1 \times 10^{-5}$
SO_4^{2-}	2×10^{-5}	$<1 \times 10^{-5}$	$<1 \times 10^{-5}$
BO_2^-	3×10^{-5}	$<1 \times 10^{-5}$	$<1 \times 10^{-5}$
Br^-	4×10^{-5}	2×10^{-5}	$<1 \times 10^{-5}$

Interfering Substances

Inorganic salts

The effect of simple sodium salts such as $NaNO_3$, NaCl, $NaClO_4$, NaBr, Na_2SO_4, NaH_2PO_4 and $NaBO_2$ on the potential of the electrodes was tested. Calibration graphs of the anions tested and of SDS for the Pt/III, Pt/VI and Pt/X electrodes are presented in Figs. 2–4. As can be seen, the Pt/III and Pt/VI electrodes respond well to ClO_4^- and Cl^- anions, whereas they are not sensitive to other anions. The Pt/X electrode, within the limits of measurement error, is not sensitive for $NaClO_4$ over the concentration range 1×10^{-3}–1×10^{-5} M, and for other anions over the concentration range 1×10^{-2}–1×10^{-5} M.

Table 2 shows the potentiometric selectivity coefficients calculated using the separate solution method.[43] The results demonstrate the high selectivity of the electrodes in separate solutions to SDS. Moreover, it also follows that these electrodes either do not respond (as shown by a change in potential) to the change in activity of the anions tested or exhibit very poor sensitivity. On the other hand, in mixed solutions, consisting of an inorganic salt and an anionic surfactant, a very pronounced effect is observed, *i.e.*, at a constant concentration of SDS and an increasing concentration of inorganic salt, an increase in the electrode potential occurs. This effect is the opposite to that expected. Results of these experiments are given in Fig. 5, from which it follows that: (1) as the concentration of NaX salts in solutions of SDS and SDBS of a constant concentration increases, the potential increases also, which implies that no anionic potential forming effect of the anion X^- is observed; (2) an increase in the electrode potential following an increase in the NaX salt concentration testifies to the decrease in the activity of the anion to which the electrode is sensitive, *i.e.*, the DS^- or DBS^- anion, in the solution. These data demonstrate the known effect of a common ion to depress the CMC of anionic surfactants by mass action; (3) the type of anion affects the degree of association of the anionic surfactant, which is evidenced by the changes in ΔE shown in Fig. 5, at the same concentration of the surfactant and at the same concentration of different NaX salts; (4) the higher the dilution of the surfactant, the smaller the changes in ΔE and, further, the smaller the changes in the activity of the anionic surfactants; this follows from the equilibria of the association reactions.

Acids and bases

An unconditioned electrode, *i.e.*, with a liquid anion exchanger in the acetate form (R–Hg–Ac), and an electrode when no surfactants are present in the solution, shows: (1) sensitivity to OH^- ions (the anionic function, *i.e.*, a decrease in the potential) over the pH range 7.6–9.6, with a slope of 55 mV decade^{-1}; (2) for $9.6 < pH < 12.6$ an increase in electrode potential is observed (the cationic function); in this range the potential change is characteristic for univalent cations, with a slope of 55 mV decade^{-1}. The situations described above are illustrated in Fig. 6, curve 1. Similar dependencies on pH for pH >7 were found for the electrode conditioned in SDS when the changes in electrode potential with pH were measured at a

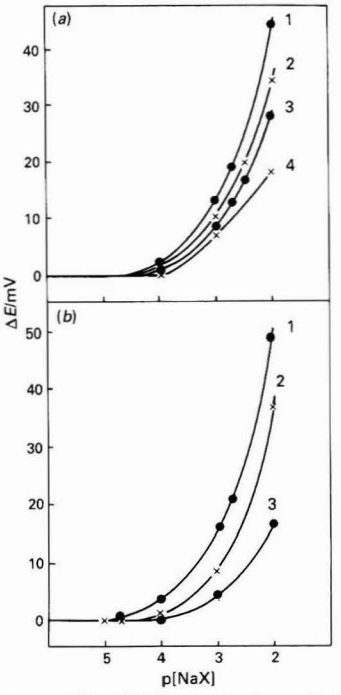

Fig. 5. Response of the Pt/X electrode to inorganic salts in a fixed background of (*a*) SDS: 1, 1×10^{-3} M SDS - $NaClO_4$; 2, 1×10^{-3} M SDS - NaCl; 3, 1×10^{-4} M SDS - $NaClO_4$; 4, 1×10^{-4} M SDS - NaCl; and (*b*) SDBS: 1, 1×10^{-3} M SDBS - $NaClO_4$; 2, 1×10^{-3} M SDBS - CH_3COONa; and 3, 1×10^{-4} M SDBS - CH_3COONa

constant SDS concentration of 1×10^{-4} M. The only difference was that the slope of the graph for the anionic function of the electrode was 17 mV decade^{-1}, whereas for the cationic function it was 30 mV decade^{-1}.

Over the pH range 5.2–7, a plateau occurs, and at pH <5 a sharp increase in potential is observed, which is connected with SDS association and, at the same time, with a decrease in its activity. This is shown by curve 2 in Fig. 6. The electrode containing the mercurated polystyrene was found to exhibit interesting electrochemical properties in the acid - base system. It is difficult to explain the unusual dependence of potential on hydroxyl ion activity. If it is assumed that the ion-exchange reaction between the electrode membrane and the aqueous solution is responsible for the e.m.f., then the following mechanisms can be used to explain the response of the electrode to the change in the activity of OH^- ions and DS^- anions:

pOH^- response mechanism:

$$[R\text{–}Hg\text{–}Ac]^0_{(mem)} \overset{H_2O}{\rightleftharpoons} [R\text{–}Hg]^+_{(mem)} +$$

$$Ac^-_{(aq)} \overset{pH<9,\ OH^-_{(aq)}}{\rightleftharpoons} [R\text{–}Hg\text{–}OH]^0_{(mem)}$$

$$\overset{pH>9,\ OH^-_{(aq)}}{\rightleftharpoons} [R\text{–}Hg(OH)_2]^-_{(mem)}$$

$$\overset{Na^+_{(aq)}}{\rightleftharpoons} \{[R\text{–}Hg\text{–}(OH)_2]^-Na^+\}^0_{(mem)}$$

Anion response mechanism:

$$[R\text{–}Hg\text{–}Ac]^0_{(mem)} \overset{H_2O}{\rightleftharpoons} [R\text{–}Hg]^+_{(mem)} +$$

$$Ac^-_{(aq)} \overset{DS^-_{(aq)}}{\rightleftharpoons} [R\text{–}Hg\text{–}DS]^0_{(mem)}$$

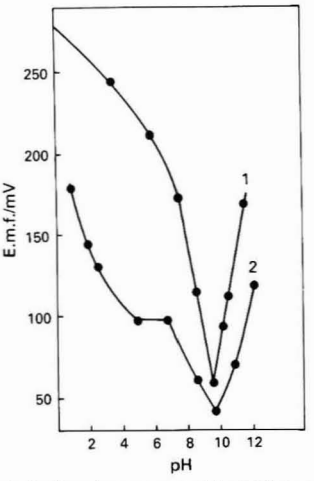

Fig. 6. Effect of pH on the response of the Pt/X electrode: 1, without surfactant; and 2, in the presence of 1×10^{-4} M SDS

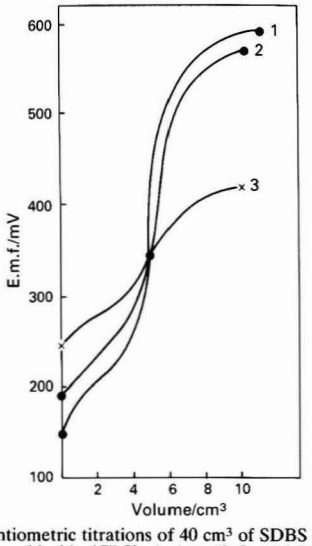

Fig. 7. Potentiometric titrations of 40 cm^3 of SDBS with the aid of cetylpyridinium chloride (CPC): 1, 1×10^{-3} M SDBS - 1×10^{-2} M CPC; 2, 1×10^{-4} M SDBS - 1×10^{-3} M CPC; and 3, 1×10^{-5} M SDBS - 1×10^{-4} M CPC in the presence of the anionic surfactant-selective electrode Pt/X

The electrode potential is reversible and the shape of the potential - pH graph is the same, regardless of whether one goes from a neutral to a highly alkaline solution or from a highly alkaline to a neutral solution. In both instances inflection of the calibration graph was observed at about pH 9.6.

The electrodes do not respond, *i.e.*, show a potential change, to changes in the activity of cationic surfactants such as cetylpyridinium chloride, cetyltrimethylammonium chloride and benzylcetyldimethylammonium bromide over the range 1×10^{-3}–1×10^{-6} M.

Titration

The electrodes containing mercurated polystyrene as a sensor may be used as indicator electrodes in the potentiometric titration of anionic surfactants by cationic surfactants, and *vice versa*. Titration curves for SDBS are presented in Fig. 7. Owing to the wide range over which the calibration graph was

rectilinear and the low value of the detection limit, well defined ionic curves were obtained for surfactant solutions at concentrations of 5×10^{-6} M.

Conclusions

An electrode that employs mercurated polystyrene as the sensor has been developed. The electrode was tested against anionic surfactants and a high selectivity for SDS and SDBS relative to inorganic anions was found. Moreover, the electrode shows interesting properties towards hydroxyl ions. On the basis of the data obtained, the electrode might be used to determine anionic surfactants: it might also act as an indicator electrode in potentiometric titrations for low concentrations of these substances. The electrode might also be employed in physico-chemical studies of surfactant solutions, for example, to determine the CMC, and in studies on the influence of different substances, *i.e.*, inorganic salts, on the process of surfactant association and the determination of their activity in solutions.

It might also be possible to apply the electrode to the analysis of other groups of compounds, including sulphonamides, thiols and complex-forming substances that react with the R–Hg^+ cation. This possibility is of particular interest, as it has been shown that the electrode is not sensitive to many inorganic anions.

This work was supported by project CPBP.01.17.04.07.

References

1. Jones, J. H., *J. Assoc. Off. Agric. Chem.*, 1944, **27**, 462.
2. Herring, D. E., *Lab. Pract.*, 1962, **11**, 113.
3. Reid, W. W., Longman, G. F., and Heinerth, E., *Tenside*, 1967, **4**, 292.
4. Kupfer, W., Janis, J., and Loh, L., *Tenside*, 1969, **6**, 15.
5. Geppert, G., and Liebscher, G., *Z. Chem.*, 1978, **18**, 188.
6. Taguchi, S., and Goto, K., *Talanta*, 1980, **27**, 289.
7. Uchigama, M., *Water Res.*, 1977, **11**, 205.
8. Hellman, H., *Fresenius Z. Anal. Chem.*, 1978, **293**, 359.
9. Canete, F., Rios, A., Luque de Castro, M. D., and Valcarcel, M., *Anal. Chem.*, 1988, **60**, 2354.
10. del Valle, M., Alonso, J., Bartrolí, J., and Martí, I., *Analyst*, 1988, **113**, 1677.
11. Rubio-Barroso, S., Rodriquez-Gamonal, V., and Polo-Diez, L. M., *Anal. Chim. Acta*, 1988, **206**, 351.
12. Rubio-Barroso, S., Gomez-Rodriquez, M., and Polo-Diez, L. M., *Microchem. J.*, 1988, **37**, 93.
13. Mathijs, E., and De Henau, H., *Tenside*, 1987, **24**, 193.
14. Nakae, A., Tsuji, K., and Yamanaka, M., *Anal. Chem.*, 1980, **52**, 2275.
15. Saito, T., Higashi, K., and Hagiwara, G., *Fresenius Z. Anal. Chem.*, 1982, **313**, 21.
16. McEvoy, I., and Giger, W., *Naturwissenschaften*, 1985, **72**, 429.
17. Abidi, S. I., *J. Chromatogr.*, 1980, **200**, 216.
18. Gavach, C., and Bertrand, C., *Anal. Chim. Acta*, 1971, **55**, 385.
19. Birch, B. J., and Clarke, D. E., *Anal. Chim. Acta*, 1972, **61**, 159.
20. Birch, B. J., and Clarke, D. E., *Anal. Chim. Acta*, 1973, **67**, 387.
21. Kabagashi, T., Katacka, M., and Kambara, T., *Talanta*, 1980, **27**, 253.
22. Ciocan, N., and Anghel, D. F., *Fresenius Z. Anal. Chem.*, 1978, **290**, 237.
23. Cutler, S., Meares, P., and Hall, D. G., *J. Electroanal. Chem.*, 1977, **85**, 145.
24. Coetze, C., and Freiser, H., *Anal. Chem.*, 1968, **40**, 2071.
25. Ciocan, N., and Anghel, D. F., *Anal. Lett.*, 1976, **9**, 705.
26. Anghel, D. F., and Ciocan, N., *Colloid Polym. Sci.*, 1976, **254**, 114.
27. Satake, J., Noda, S., and Maeda, T., *Bull. Chem. Soc. Jpn.*, 1983, **56**, 2581.
28. Ishibashi, N., Kobara, H., and Horinouchi, K., *Talanta*, 1973, **20**, 867.
29. Hoke, S. H., Collins, A. G., and Reynolds, C. A., *Anal. Chem.*, 1979, **51**, 859.
30. Dowle, C. J., Cooksey, B. G., Ottaway, J. M., and Campbell, W. C., *Analyst*, 1987, **112**, 129.
31. Dowle, C. J., Cooksey, B. G., Ottaway, J. M., and Campbell, W. C., *Analyst*, 1988, **113**, 117.
32. Birch, B. J., and Clarke, D. E., *Anal. Chim. Acta*, 1974, **69**, 473.
33. Ciocan, N., and Anghel, D. F., *Tenside*, 1976, **13**, 188.
34. Dilley, G. C., *Analyst*, 1980, **105**, 713.
35. Vytras, K., Dajkova, M., and Mach, V., *Anal. Chim. Acta*, 1982, **127**, 165.
36. Cutler, S., Meares, P., and Hall, D. G., *J. Chem. Soc., Faraday Trans. 1*, 1978, **74**, 1758.
37. Szczepaniak, W., *Chem. Anal. (Warsaw)*, 1968, **14**, 479.
38. Szczepaniak, W., *Chem. Anal. (Warsaw)*, 1971, **16**, 853.
39. Szczepaniak, W., unpublished results.
40. Chamiotakis, N. A., Park, S. B., and Meyerhoff, M. E., *Anal. Chem.*, 1989, **61**, 566.
41. Ma, S. C., Chamiotakis, N. A., and Meyerhoff, M. E., *Anal. Chem.*, 1988, **60**, 2293.
42. Lindman, B., and Wennerström, H., *Top. Curr. Chem.*, 1980, **87**, 3.
43. Recommendations for Nomenclature of Ion-selective Electrodes, *Pure Appl. Chem.*, 1975, **43**, 10.

Paper 0/00015I
Received January 2nd, 1990
Accepted June 26th, 1990

Study of Protolytic Equilibria of Flurazepam

Lidija B. Pfendt and Tomislav J. Janjić
Faculty of Chemistry, University of Belgrade, P.O. Box 550, 11001 Belgrade, Yugoslavia
Gordana V. Popović
Faculty of Pharmacy, University of Belgrade, 11001 Belgrade, Yugoslavia

Protolytic equilibria of flurazepam, a diprotic base which is sparingly soluble in water, were investigated. The investigations were carried out in the pH range 0–12, at constant ionic strength (0.1 M NaCl) and 25 ± 0.1 °C, by the application of spectrophotometric, pH-metric and solubility methods. The acidity, hydrolysis and equilibrium constants in the heterogeneous system were determined. In addition, a method, based on the application of a formation function to the hydrolytic process, is proposed. Finally, buffer characteristics of flurazepam in the homogeneous and heterogeneous systems were studied.

Keywords: *Flurazepam; protolytic equilibria; hydrolysis; heterogeneous equilibria; two-phase buffer*

Flurazepam [7-chloro-1-(2-diethylaminoethyl)-5-(2′-fluorophenyl)-1,3-dihydro-2*H*-1,4-benzodiazepin-2-one] belongs to the class of benzodiazepine derivatives. In addition to the pharmacological activity characteristic of this class of drugs, flurazepam shows a unique hypnotic action.

Chemically flurazepam behaves as a diprotic base[1] and is sparingly soluble in water. In acidic solution it undergoes reversible hydrolysis, the mechanism of which has been studied in detail.[2,3] However, no data are reported in the literature on the investigation of the equilibria of flurazepam in heterogeneous systems, and the data on acidity constants, particularly for pK_{a_2}, are not consistent. On the basis of polarographic investigations only the approximate values for the acidity constants of flurazepam have been determined, pK_{a_1} values ranging between 1 and 2 and pK_{a_2} values between 8 and 10.[4] Rudy and Senkowski[1] reported the unpublished data obtained by Toome and Raymond for the pK_a values of flurazepam (1.90 and 8.16), determined spectrophotometrically, whereas the value for pK_{a_2}, determined by titration, in a propan-2-ol - water mixture (1 + 1), after suitable corrections was found to be 7.9. However, in the opinion of Groves and Smyth[5] the pK_{a_2} value for flurazepam cannot be precisely determined spectrophotometrically because of the slight difference in the spectra of the non-protonated and monoprotonated base. Therefore, these workers have only determined spectrophotometrically, by the application of the acidity function, H_o, the value of pK_{a_1} (1.42).

The aforementioned data show that the acidity constants for flurazepam, determined by different workers, differ from one another both in value and precision, and also indicate that the heterogeneous equilibria of flurazepam have not been investigated to date. As shown in a previous paper,[6] the investigation of heterogeneous equilibria can afford useful information on acid - base equilibria in homogeneous systems. Hence, the aim of the present work is to extend the investigation to flurazepam and also to perform a quantitative study of other protolytic equilibria to which flurazepam is subjected. These investigations include the determination of its acidity, hydrolysis and equilibrium constants in heterogeneous systems and also the buffer characteristics of monophase and two-phase buffer systems consisting of the solid flurazepam, which is sparingly soluble, and its saturated solution. As has been reported previously[6] these investigations are of wide-ranging interest.

Experimental

Apparatus

Measurements and the interpretation of the pH values measured were carried out as described in a previous paper,[6] where the following relationships are valid: $[H_3O^+] = 10^{-pc_H} = 10^{-(pH_{GE} - 0.04)}$ and $pK_w^c = 13.81 \pm 0.01$ for ionic strength, $I = 0.1$ M (NaCl) at 25 ± 0.1 °C; pH_{GE} is the pH as determined with a pH meter, $pk_w^c = pc_h + pc_{OH}$, $pc_H = -\log[H_3O^+]$ and $pc_{OH} = -\log[OH^-]$. Spectrophotometric measurements were performed on a Beckman DU-50 spectrophotometer in 1-cm silica cells.

Reagents

All investigations were carried out with flurazepam monohydrochloride (Fz.HCl) produced by Hoffmann La Roche (Basle, Switzerland). A stock solution of the drug was prepared by weighing accurately the dry substance and dissolving it in water or 0.1 M NaCl. A freshly prepared solution was always used and all operations with the drug were carried out in the absence of light. Other reagents were of analytical-reagent grade. Standardisation of HCl and NaOH solutions was performed potentiometrically.

Methods

Determination of acidity constants

Optimum wavelengths for the determination of K_{a_1} were selected on the basis of the spectra of flurazepam solutions in the pc_H range 1–6, recorded in the 200–400 nm range, at fast scan (scan speed 750 nm min^{-1}). The solutions used for the recording of spectra and absorbance measurements at selected wavelengths were prepared immediately before measuring in order to prevent possible hydrolysis. For the determination of K_{a_1}, stock solutions of Fz.HCl (3.24×10^{-4} M) and HCl (8.42×10^{-3}–8.42×10^{-2} M) were prepared with the addition of NaCl to give $I = 0.1$ M. Aliquots of 0.2 and 0.5 ml of Fz.HCl solution were then rapidly mixed and shaken in cells with 3 ml of HCl, and the absorbances of these solutions were measured at 230 and 282 nm, respectively, against a corresponding blank.

The acid constant, K_{a_2} was determined from the data obtained by pH-metric titration. Aliquots of 20 and 25 ml of Fz.HCl solution (8.0×10^{-4} M in 0.1 M NaCl) were titrated with 0.01-ml increments of NaOH solution (0.079 M). From these data the formation function, $\bar{n}_H$, namely the mean number of protons bound to the base (Fz) was calculated by means of the following equation:

$$\bar{n}_H = \frac{c_{Fz.HCl} - [H_3O^+] + [OH^-] - c_{NaOH}}{c_{Fz.HCl}} \quad .. \quad (1)$$

In equation (1) and in all other instances c denotes the stoicheiometric concentrations, whereas square brackets denote equilibrium concentrations.

Determination of the hydrolysis constant

The hydrolysis constant, K_{h1}, was determined from the data of "slow" pH-metric titrations. These were carried out in two ways. For direct titration, to a series of solutions ($V = 20$ ml) of the same stoicheiometric Fz.HCl concentration (5.0×10^{-3} M in 0.1 M NaCl) various volumes (0.15–0.70 ml) of 0.2105 M HCl were added. For back-titration a solution of Fz.HCl (5.0×10^{-3} M) in 8.42×10^{-3} M HCl with the addition of NaCl to give $I = 0.1$ M, was prepared. This solution was left to stand for 6 h. Then to a series of this solution ($V = 20$ ml) various volumes (0.15–0.65 ml) of 0.1895 M NaOH were added. Both series of solutions were thermostated for 4 h. The equilibration was followed pH-metrically. From the pH_{GE} values measured at the equilibrium state, the formation function, $\bar{n}'$, in this instance was calculated according to the equation:

$$\bar{n}' = \frac{c_{Fz.HCl} + c_{HCl} + [OH^-] - [H_3O^+] - c_{NaOH}}{c_{Fz.HCl}} \quad (2)$$

In direct titration $c_{NaOH} = 0$.

Heterogeneous system

Saturated solutions for the determination of equilibrium constants in the heterogeneous system were obtained by partial precipitation of the free base from 20 ml of Fz.HCl solution (1.0×10^{-2} M in 0.1 M NaCl) by the addition of different aliquots of 0.3979 M NaOH. The samples were then thermostated for 4 h with occasional shaking until the equilibrium was established. From the pH_{GE} values measured at the equilibrium state, the concentration of protons bound to the base in the solution was calculated:

$$[H^+]_b = c_{Fz.HCl} - c_{NaOH} - [H_3O^+] + [OH^-] \quad . . \quad (3)$$

For the determination of the solubility of flurazepam the precipitate was separated by centrifugation. The aliquots of the solutions were then diluted, made alkaline (pH = 11) and the actual concentration of the base was determined spectrophotometrically at 230 nm, the validity of Beer's Law having been verified previously.

The buffer curve of a two-phase buffer was determined by titrating an Fz.HCl solution (20 ml; 1.0×10^{-2} M in 0.1 M NaCl) with a standard NaOH solution (0.3979 M) with vigorous stirring.

In the processing of experimental data, corrections were made for volume changes; the data were processed by means of suitable programs with a Texas Instrument TI-66 programmable calculator.

Results and Discussion

All equilibrium constants determined in this paper relate to an ionic strength of 0.1 M and accordingly are defined as concentration, *i.e.*, stoicheiometric constants.

Determination of the pK_a Values of Flurazepam

In the pH range 0–14 flurazepam undergoes a "simple" acid - base equilibrium as shown in Scheme 1.

The acidity constants of these processes are defined as:

$$K_{a_1} = \frac{[BH^+][H_3O^+]}{[BH_2^{2+}]} \quad . . \quad . . \quad . . \quad (4)$$

$$K_{a_2} = \frac{[B][H_3O^+]}{[BH^+]} \quad . . \quad . . \quad . . \quad (5)$$

Because the corresponding protolytic processes are "separated" (pK_a values of flurazepam differ by more than 4 pK units), both constants can be determined independently, as for monoprotic bases.

For the determination of pK_{a_1} the spectrophotometric method[7] was employed, according to which, from the absorbances of a flurazepam solution measured at different pc_H values, the following linear dependence was calculated:

$$A = A_{BH_2^{2+}} \pm K_{a_1} \frac{|A_{BH^+} - A|}{[H_3O^+]} \quad . . \quad . . \quad (6)$$

where $A_{BH_2^{2+}}$, A_{BH^+} and A are the absorbances of solutions containing BH_2^{2+}, BH^+ and their mixtures, respectively, at given wavelengths. Equation (6) shows that for the determination of pK_{a_1} it is not necessary to know the absorbance of the pure BH_2^{2+} species, and that the determination of pK_{a_1} is possible under the conditions applied ($I = 0.1$ M). The linear dependence expressed by equation (6) obtained on the basis of experimental data for two optimum wavelengths, is shown in Fig. 1. The slope of the straight lines obtained corresponds to the acidity constant $+K_{a_1}$ for $(A_{BH^+} - A) > 0$, and to $-K_{a_1}$ for $(A_{BH^+} - A) < 0$, respectively, whereas the intercept on the ordinate corresponds to the absorbance of the pure BH_2^{2+} species. Both magnitudes were calculated by regression analysis. The mean value obtained for pK_{a_1} is 1.53. Fig. 2 shows absorption spectra of the acidic flurazepam solutions recorded at fast scan, on the basis of which optimum wavelengths for the determination of K_{a_1} were selected. As can be seen in Fig. 2, the spectra of pure BH^+ and BH_2^{2+} species and of their mixtures intersect at three isosbestic points at the wavelengths 238, 248 and 262 nm, respectively. The

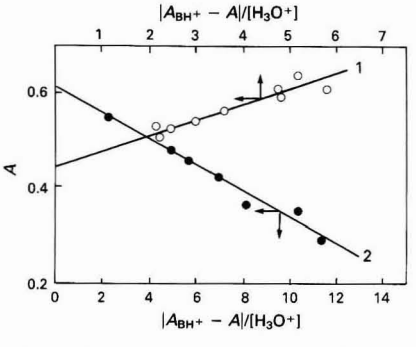

Fig. 1. Spectrophotometric determination of K_{a_1} according to equation (6): 1, $\lambda = 230$ nm, $c_{tot} = 2.025 \times 10^{-5}$ M; 2, $\lambda = 282$ nm, $c_{tot} = 4.63 \times 10^{-5}$ M

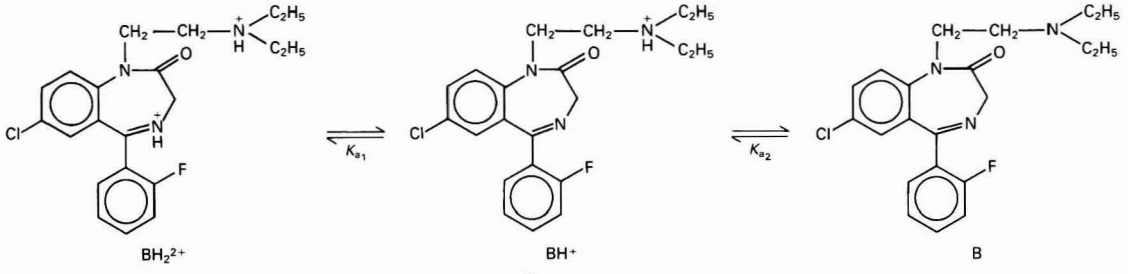

Scheme 1

appearance of these isosbestic points shows that the "simple" protolytic reactions, under working conditions, are not complicated by secondary processes. In addition, the absorption spectrum of the pure molecular base is also shown in Fig. 2. The slight difference observed in the spectra of pure BH^+ and B species indicates that spectrophotometry is not applicable to a reliable determination of K_{a_2}.

For the determination of pK_{a_2} the pH-metric titration method was employed; it is based on the determination of $\bar{n}_H$ which, in the situation concerned, *i.e.*, in the pH range in which BH^+ and B species are in equilibrium, can be given by the equation:

$$\bar{n}_H = \frac{[BH^+]}{[BH^+] + [B]} \quad \ldots \quad \ldots \quad \ldots \quad (7)$$

From the linear dependence which relates $\bar{n}_H$ [equation (7)] with K_{a_2} [equation (5)] *i.e.*,

$$\frac{1 - \bar{n}_H}{\bar{n}_H} = \frac{K_{a_2}}{[H_3O^+]} \quad \ldots \quad \ldots \quad \ldots \quad (8)$$

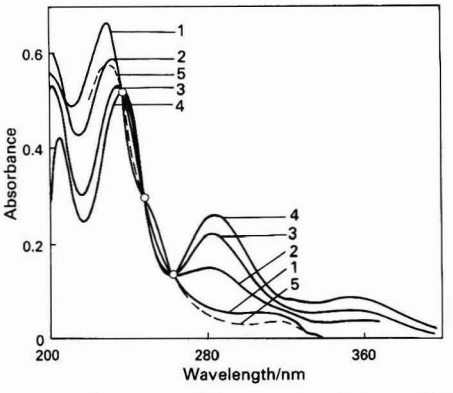

Fig. 2. Absorption spectra of flurazepam in solutions of different pc_H. Scan speed, 750 nm min^{-1}; path length, 1 cm; pc_H: 1, 5.81 (BH^+); 2, 1.80; 3, 1.10; 4, 1 M HCl (BH_2^{2+}); and 5, 0.1 M NaOH (B); $c_{tot} = 2.025 \times 10^{-5}$ M

K_{a_2} was calculated by regression analysis. Fig. 3 shows the corresponding linear dependence calculated as described under Experimental.

Determination of Hydrolysis Constants

On the basis of the kinetic studies of the hydrolysis of flurazepam[2,3] it was assumed that in acidic solution flurazepam undergoes a reversible ring-opening reaction at its azomethine group. One of the main objectives of the present paper is the quantitative study of the corresponding equilibria at various pH values, therefore, a method based on the application of a formation function to the hydrolytic process is proposed.

Taking into account "simple" protolytic and hydrolytic reactions occurring simultaneously in an acidic flurazepam solution the processes shown in Scheme 2 are possible when the equilibration is completed.

The equilibrium constants for the corresponding hydrolytic processes are given by the expressions:

$$K_{h_1} = \frac{[B'H_2^{2+}]}{[BH^+][H_3O^+]} \quad \ldots \quad \ldots \quad \ldots \quad (9)$$

$$K_{h_2} = \frac{[B'H_2^{2+}]}{[BH_2^{2+}]} \quad \ldots \quad \ldots \quad \ldots \quad (10)$$

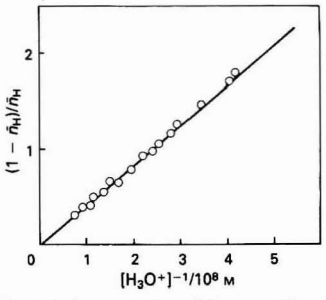

Fig. 3. pH-metric determination of K_{a_2} according to equation (8)

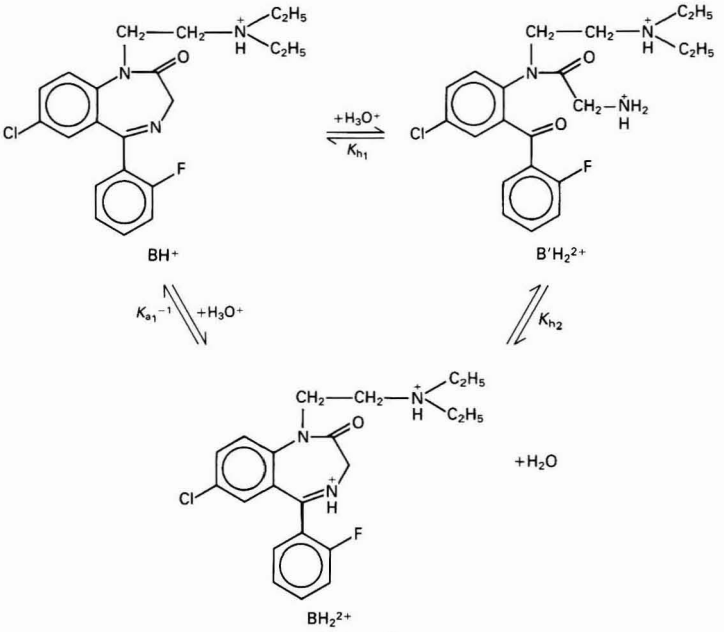

Scheme 2

The acidity constant, K_{a_1}, as described above, could be determined regardless of other processes as the "simple" protolytic reaction takes place instantly relative to the hydrolytic reaction. As the hydrolysis is a pH dependent process, the determination of K_{h_1} can also be performed pH-metrically but only after the equilibration is completed (by slow pH-metric titration as described in Experimental).

In the situation observed the formation function, $\bar{n}'$, can be defined as:

$$\bar{n}' = \frac{2[B'H_2^{2+}] + 2[BH_2^{2+}] + [BH^+]}{[B'H_2^{2+}] + [BH_2^{2+}] + [BH^+] + [B]} \quad .. \quad (11)$$

Considering that in acidic solution $[B] \rightarrow 0$, the combination of equations (4), (9) and (11), after appropriate transformations, gives:

$$\frac{\bar{n}' - 1}{2 - \bar{n}'} = \left(K_{h_1} + \frac{1}{K_{a_1}}\right)[H_3O^+] \quad .. \quad .. \quad (12)$$

From the slope of the linear dependence (Fig. 4) the constant K_{h_1} was calculated by regression analysis. For the determination of K_{h_2} the following relationship was used:

$$K_{h_2} = K_{h_1} \times K_{a_1} \quad .. \quad .. \quad .. \quad (13)$$

The assumed hydrolytic processes were confirmed spectrophotometrically by analysing the spectra shown in Fig. 5. The absorption spectra of acidic flurazepam solutions recorded after the establishment of the equilibrium for some selected

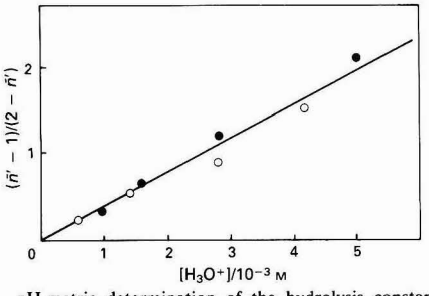

Fig. 4. pH-metric determination of the hydrolysis constant K_{h_1} according to equation (12): ○, direct titration; and ●, back-titration

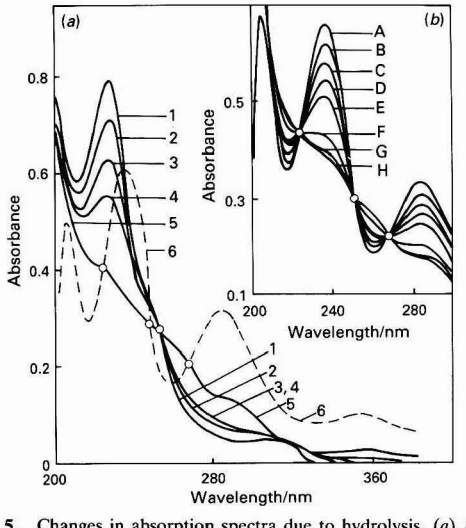

Fig. 5. Changes in absorption spectra due to hydrolysis. (*a*) As a function of pc_H; pc_H: 1, 5.81 (BH^+); 2, 2.92; 3, 2.56; 4, 2.34; 5, 0.3–1.17; and 6, pure BH_2^{2+} (recording at fast scan); $c_{tot} = 2.4 \times 10^{-5}$ M. (*b*) As a function of time in 1 M HCl: A, 0; B,15; C, 30; D, 45; E, 60; F, 120; G, 180; and H, 240 min after the initiation of the reaction

pc_H values are presented in Fig. 5(*a*). The fact that the spectrum of the solution containing the pure BH^+ species ($pc_H = 5.81$) and the spectra of solutions of lower pc_H values (down to 2.34) pass through the isosbestic point at a wavelength of 254 nm, points to the existence of only one pc_H dependent equilibrium. As these spectra differ from those recorded at fast scan (Fig. 2), this equilibrium can be ascribed only to the presence of the BH^+ and $B'H_2^{2+}$ species. At lower pc_H values down to a pc_H of about 1.2, changes in the absorption spectra are observed. In the pc_H interval from 1.2 to 0 the spectra are superimposable and at the same time they intersect at three isosbestic points at 224, 250 and 268 nm, respectively, with the spectrum of the pure BH_2^{2+} species being obtained while recording at fast scan; the latter findings can be ascribed to the existence of a new equilibrium. As the same isosbestic points appear also in spectra showing changes in the absorbance of BH_2^{2+} species with time at a definite pc_H value (1 M HCl), until the final state is reached, which is in both instances identical [Fig. 5(*b*)] but pc_H independent, the last equilibrium can be ascribed only to BH_2^{2+} and $B'H_2^{2+}$ species. From the absorbances measured at the wavelength of the most suitable isosbestic point at 224 nm [Fig. 5(*a*)] at which the molar absorption coefficients for BH_2^{2+} and $B'H_2^{2+}$ species are identical, the hydrolysis constant K_{h_1} was calculated[7] according to the equation:

$$\text{Log } K_{h_1} = pc_H + \log \frac{A_{BH^+} - A}{A - A_{B'H_2^{2+}}} \quad .. \quad (14)$$

where $A_{B'H_2^{2+}}$ and A_{BH^+} correspond to the absorbances of pure $B'H_2^{2+}$ and BH^+ species, respectively, whereas A is the absorbance of their mixtures in the pc_H interval from 2.34 to 2.96. The value of −2.47 obtained for pK_{h_1} is in agreement with the value obtained by the independent pH-metric procedure and this can be considered as confirmation of the hydrolytic processes that have previously been assumed.

A survey of constants determined in the homogeneous system of flurazepam is given in Table 1. On the basis of these constants, by the usual procedure,[8] the distribution of all equilibrium species in the homogeneous system as a function of the pc_H value was calculated. The corresponding distribution diagram is given in Fig. 6 which shows that in the pc_H range from 0 to 5 the hydrolysis of the azomethine group is not complete, although the equilibrium is almost entirely shifted towards the opening of the benzodiazepine ring.

Table 1. Concentration equilibrium constants in the homogeneous and heterogeneous system of flurazepam. $I = 0.1$ M (NaCl) and $T = 25$ °C

Equilibrium constant	Method employed	Found	Calculated
pK_{a_1}	Spectrophotometric [equation (6)]	1.53 ± 0.05	
pK_{a_2}	pH-metric [equation (8)]	8.37 ± 0.01	8.41 [equation (22)]
pK_{h_1}	pH-metric [equation (12)]	−2.56 ± 0.02	
	Spectrophotometric [equation (14)]	−2.47	
pK_{h_2}			−1.03 [equation (13)]
pK_{s_1}	Solubility [equation (20)]	3.15 ± 0.05	
	Solubility [equation (21)]	3.13 ± 0.01	
pK_{s_2}	Proton bound [equation (19)]	−5.27 ± 0.01	
	Solubility [equation (20)]	−5.27 ± 0.01	
pK_{s_3}			−6.80 [equation (23)]
pK'_{s_3}			−7.83 [equation (24)]

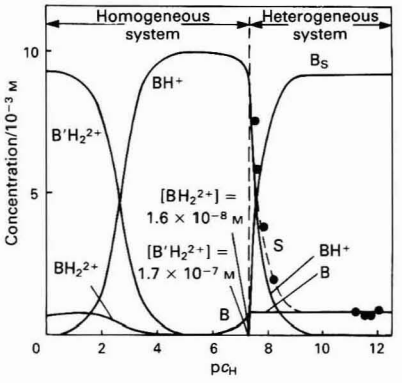

Fig. 6. Distribution diagram (solid line) and solubility curve (broken line) in equilibrium as a function of pc_H: ●, experimental data; $c_{tot} = c_{tot}^{app} = 1.0 \times 10^{-2}$ M; $pc_H = pH_{GE} - 0.04$

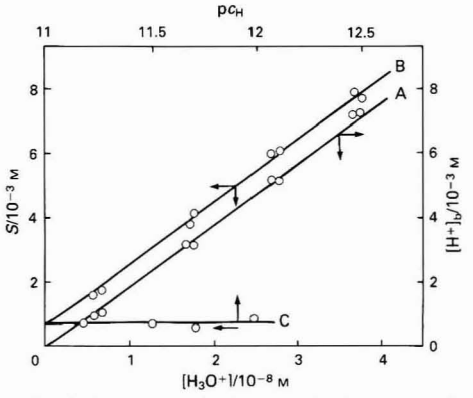

Fig. 7. Graphs for the determination of equilibrium constants in the heterogeneous system obtained according to A, equation (19); B, equation (20); and C, equation (21)

Heterogeneous System

In a saturated solution of a base, B, the following equilibria between the solid phase, B_s, and the solution may be assumed:

$$B_s \rightleftharpoons B \qquad K_{s_1} = [B] \quad .. \quad (15)$$

$$B_s + H_3O^+ \rightleftharpoons BH^+ + H_2O \qquad K_{s_2} = \frac{[BH^+]}{[H_3O^+]} \quad .. \quad (16)$$

$$B_s + 2H_3O^+ \rightleftharpoons BH_2^{2+} + 2H_2O \qquad K_{s_3} = \frac{[BH_2^{2+}]}{[H_3O^+]^2} \quad .. \quad (17)$$

$$B_s + 2H_3O^+ \rightleftharpoons B'H_2^{2+} + H_2O \qquad K'_{s_3} = \frac{[B'H_2^{2+}]}{[H_3O^+]^2} \quad .. \quad (18)$$

Because B is a relatively strong base ($pK_{a_2} = 8.37$) a small increase in the H_3O^+ ion concentration results in the formation of BH^+ species and the dissolution of the precipitate. In addition, $pK_{a_2} \gg [pK_{a_1}$ and $(-pK_{h_1})]$ *i.e.*, the concentrations of BH_2^{2+} and $B'H_2^{2+}$ species in equilibrium with the solid phase are virtually negligible and the heterogeneous system may be considered as a system containing a sparingly soluble monoprotic base. Therefore, for the determination of equilibrium constants in the corresponding heterogeneous system the methods described in a previous paper[6] were employed, namely the method of protons bound to the base in the solution and the solubility method. These methods yield the parameters $[H^+]_b$, the concentration of protons bound to the base in the saturated solution and S, the stoicheiometric solubility, respectively. The relationship between the magnitude of these two parameters and the corresponding equilibrium constants is given by the following expressions:

$$[H^+]_b = [BH^+] = K_{s_2}[H_3O^+] \quad .. \quad (19)$$

$$S = [BH^+] + [B] = K_{s_2}[H_3O^+] + K_{s_1} \quad .. \quad (20)$$

$$S = [B] = K_{s_1} \quad .. \quad (21)$$

Equations (19) and (20) are valid when the pH is $<(pK_{a_2} + 2)$ whereas equation (21) is valid when the pH is $>(pK_{a_2} + 2)$.

The results of the determination of the equilibrium constants by the methods given are shown graphically in Fig. 7. On the basis of the values obtained and the constants determined in the homogeneous system it was possible to calculate the values of the constants K_{a_2}, K_{s_3} and K'_{s_3} by means of the following dependencies:

$$pK_{a_2} = pK_{s_1} - pK_{s_2} \quad .. \quad .. \quad .. \quad (22)$$

$$pK_{s_3} = pK_{s_2} - pK_{a_1} \quad .. \quad .. \quad .. \quad (23)$$

$$pK'_{s_3} = pK_{s_2} + pK_{h_1} \quad .. \quad .. \quad .. \quad (24)$$

The equilibrium constants determined or calculated in the heterogeneous system together with constants determined in the homogeneous system are presented in Table 1. In addition, Table 1 shows that there is good agreement between the constants determined by different methods and it is worth emphasising the agreement between the acidity constant K_{a_2} determined pH-metrically and that calculated on the basis of the equilibrium constants determined in the heterogeneous system.

The distribution of the equilibrium species and the solubility as a function of pc_H, calculated on the basis of the corresponding equilibrium constants in the heterogeneous system, are shown in Fig. 6.

Buffer Capacity

The saturated solution of flurazepam represents a two-phase buffer system in which the solid phase is a sparingly soluble base and the saturated solution is the buffered phase. The dependence of the buffer capacity of this buffer on the pH (pc_H at constant I) is given by the relationship which is valid for buffer types containing a sparingly soluble monoprotic base[6]:

$$\beta_B = \frac{dc_b}{dpH} = \frac{dc_b}{dpc_H} = 2.3\,K_{s_2}[H_3O^+] = 2.3\,K_{s_2}\,10^{-pc_H} \quad (25)$$

where $c_b = [B] + [B_s] = c_{tot}^{app} - [BH^+]$ and c_{tot}^{app} is the stoicheiometric concentration of flurazepam which would exist in the solution if the total amount of flurazepam was dissolved. The exponential increase of the buffer capacity with decreasing pc_H is limited by the transition of the heterogeneous to the homogeneous system, which is followed by an abrupt decrease of the buffer capacity and the disappearance of the solid phase. Because $[B]_s \rightarrow 0$ at the transition point of the heterogeneous to the homogeneous system the following mass balance equation is valid:

$$c_{tot}^{app} = [BH^+] + [B] \quad .. \quad .. \quad .. \quad (26)$$

By introducing the relevant equilibrium constants [equations (15), (16) and (22)] into equation (26), an expression for pc_H at the transition point of the heterogeneous to the homogeneous system can be obtained:

$$pc_H = pK_{a_2} - pK_{s_1} - \log(c_{tot}^{app} - K_{s_1}) \quad .. \quad (27)$$

The equation given shows that the pc_H value at which the transition occurs can be changed by altering the total concentration of flurazepam. When $([BH^+] + [B]) \rightarrow c_{tot}^{app}$ the transition of the heterogeneous to the homogeneous system takes place, and this virtually corresponds to the applicability

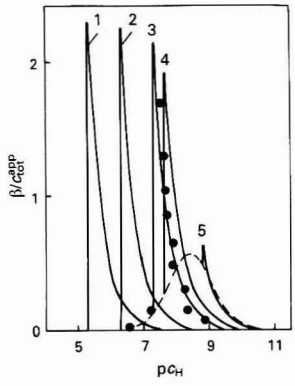

Fig. 8. Theoretical buffer curves of the two-phase (solid line) and mono-phase buffer BH^+ - B (broken line) as a function of pc_H for various flurazepam concentrations. c_{tot}^{app}: 1, 1.0; 2, 1.0×10^{-1}; 3, 1.0×10^{-2}; 4, 5.0×10^{-3}; and 5, 1.0×10^{-3} M; ●, experimental data for $c_{tot}^{app} = 1.0 \times 10^{-2}$ M

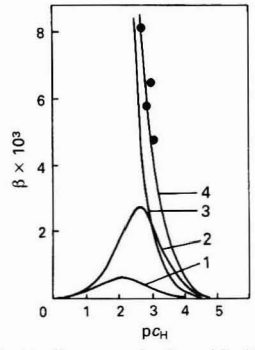

Fig. 9. Theoretical buffer curves for the acidic flurazepam solution: 1, $\beta_{BH_2^{2+}}$; 2, $\beta_{B'H_2^{2+}}$; 3, $\beta_{H_3O^+}$; and 4, β_{tot}; ●, experimental data; $c_{tot} = 5.0 \times 10^{-3}$ M

limit of the two-phase buffer. The theoretical curves showing the dependence of the buffer capacity on pc_H for different total flurazepam concentrations are shown in Fig. 8. The calculated result was experimentally confirmed for $c_{tot}^{app} = 1.0 \times 10^{-2}$ M. When c_{tot}^{app} changes, the maximum buffer capacity that can be achieved at the pc_H of the transition point is also changed:

$$\beta_{B\ max.} = 2.3\,(c_{tot}^{app} - K_{s_1}) \quad .. \quad .. \quad (28)$$

The buffer action of BH_2^{2+} - BH^+ and $B'H_2^{2+}$ - BH^+ pairs is shifted towards the strongly acidic region and is masked by the buffer action of H_3O^+ ions. Fig. 9 shows the contribution of the buffer capacity of the acid - base pairs BH_2^{2+} - BH^+ and $B'H_2^{2+}$ - BH^+ and the H_3O^+ ions to the total buffer capacity of the acidic flurazepam solution. The buffer curves were calculated on the basis of the concentrations of the corresponding species in the equilibrium state by the usual procedure for a mono-phase buffer.[9]

The authors are grateful to the Serbian Republic Research Fund for financial support, to Lea Cvitković and Pharmaceutical Industries "Krka" (Novo Mesto, Yugoslavia) for the generous gift of the flurazepam sample and to Dj. Bošković for illustration.

References

1. Rudy, B. C., and Senkowski, B. Z., *Anal. Profiles Drug Subst.*, 1974, **3**, 307.
2. Smyth, W. F., and Groves, J. A., *Anal. Chim. Acta*, 1982, **134**, 227.
3. De Silva, A. F., Puglisi, C. V., Brooks, M. A., and Hackman, M. R., *J. Chromatogr.*, 1974, **99**, 461.
4. Groves, J. A., and Smyth, W. F., *Analyst*, 1981, **106**, 890.
5. Groves, J. A., and Smyth, W. F., *Spectrochim. Acta, Part A*, 1979, **35**, 603.
6. Pfendt, L. B., Sladić, D. M., Janjić, T. J., and Popović, G. V., *Analyst*, 1990, **115**, 383.
7. Albert, A., and Serjeant, E. P., "The Determination of Ionization Constants," Second Edition, Chapman and Hall, London, 1971, p. 44.
8. Šucha, L., Kotrlý, St., "Solution Equilibria in Analytical Chemistry," van Nostrand Reinhold, London, 1972, p. 65.
9. Perrin, D. D., and Dempsey, B., "Buffers for pH and Metal Ion Control," Chapman and Hall, London, 1974, p. 10.

Paper 0/01975E
Received May 3rd, 1990
Accepted June 26th, 1990

Determination of Low Chemical Oxygen Demand Values in Water by the Dichromate Semi-micro Method

Josef Hejzlar and Jiří Kopáček
Section of Hydrobiology, Institute of Landscape Ecology, Czechoslovak Academy of Sciences, Na sádkách 7, 370 05 České Budějovice, Czechoslovakia

A semi-micro modification of the dichromate method for the determination of low concentrations (1–35 mg l^{-1}) of the chemical oxygen demand is described. It is based on the experimentally established dependencies of the oxidation efficiency on the concentrations of H_2SO_4, $K_2Cr_2O_7$ and Ag_2SO_4, and on the temperature and time of heating. The procedure involves increasing the concentration of H_2SO_4 and heating in closed test-tubes in a heating block at 170 °C for 40 min and the spectrophotometric determination of dichromate at 455 nm. The interfering effect of chloride, up to a concentration of 100 mg l^{-1}, is masked by using a combination of $HgSO_4$ and $KCr(SO_4)_2$. The modification has been tested on 30 samples of ground, tap, precipitation and surface waters and on 16 chemical compounds, and gives results comparable to those from a standard reflux method.

Keywords: *Chemical oxygen demand; sealed test-tube digestion; chloride suppression; chromium(III) addition*

For nearly 40 years,[1,2] the dichromate open reflux method for the determination of the chemical oxygen demand (COD) has been and is still used in water analysis[3] although it has several shortcomings: it requires large amounts of reagents and sample, it is space demanding, tedious, time consuming, and, in particular, its sensitivity (about 5 mg l^{-1} when using 0.0417 M $K_2Cr_2O_7$),[3] is too low for application to waters with low organic matter contents such as drinking, ground and non-polluted surface waters.

To reduce the consumption of chemicals and save space, alternative methods of COD determination on a semi-micro scale, with a comparable sensitivity, have been introduced within the past 20 years.[4–9] The digestion conditions are largely identical with those used in the original method; *i.e.*, 50% v/v (63.6% m/m) H_2SO_4 in the digestion mixture and heating at 150 °C for 2 h. The boiling under a reflux condenser, however, is usually replaced by heating in thermostated blocks, and the quantification is often based on the spectrophotometric determination of Cr^{3+} ions[4,5,7] or on the amperometric titration of the unconsumed dichromate.[8]

Efforts have been made to reduce the time of the original procedure[10–12]; however, for many compounds (*e.g.*, aliphatic acids)[12] shortening the digestion period leads to a decrease in oxidation efficiency, unless the concentration of H_2SO_4 and the temperature are increased. A solution to this problem, in many respects successful, has been offered by Wagner and Ruck,[13] who devised a rapid method applicable to the determination of COD at levels encountered in drinking waters, *i.e.*, in the range of about 1–10 mg l^{-1}. By increasing the concentration of H_2SO_4 to 83% m/m and the temperature to 170 °C, they were able to reduce the time of digestion to 45 min. Using perfectly purified reagents, they attained detection limits below 1 mg l^{-1}. The increased digestion temperature, however, brought about problems associated with the masking of chloride because at temperatures above 150 °C, $HgSO_4$ alone failed to mask chloride effectively. This problem was circumvented by removing chloride as HCl in vapour form prior to the digestion,[13,14] a procedure that is, however, tedious and time consuming.

This paper describes an approach to the determination of low COD values on a semi-micro scale, with digestion conditions optimised to attain comparable efficiency to that of the standard method,[3] and with a considerably reduced digestion time. The interfering effect of chloride is limited by the combined masking effects of $HgSO_4$ and Cr^{3+} ions.[15] This semi-micro method is compared with the open reflux method using samples of various waters and chemical compounds. In the open reflux method, which is used as a reference method, the digestion conditions of the standard method[3] were maintained, however, the manner in which the sample and reagent were dispensed, was modified, in order to achieve improved accuracy and ensure comparable precision, so that both methods could be compared.

Experimental

Chemicals

All chemicals used were of analytical-reagent grade, supplied by Lachema (Brno, Czechoslovakia). The digestion solutions and sulphuric acid reagents were prepared from 96 or 92% m/m sulphuric acid pre-treated by filtration and heated to boiling-point in an all-glass apparatus equipped with an air cooler. Sulphuric acid, 98.3% m/m, was obtained by distillation of the 96% m/m acid in an all-glass apparatus. All filtrations were carried out through a sintered glass funnel [type S1, 0.09–0.15-mm porosity (Jena Glass, Jena, GDR)]. Water for sample dilution and for the preparation of standard and reagent solutions was obtained from distilled water by re-distilling with the addition of $KMnO_4$ and H_2SO_4.

Reagents for the Semi-micro Method

Digestion solution (900 mg l^{-1} $K_2Cr_2O_7$, 7.2 g l^{-1} $KCr(SO_4)_2.12H_2O$ *and* 46 g l^{-1} $HgSO_4$ *in* 37.3% *m/v* H_2SO_4). Dissolve 0.900 ± 0.005 mg of $K_2Cr_2O_7$, 7.20 ± 0.01 g of $KCr(SO_4)_2.12H_2O$, 50 ± 1 ml of 96% m/m sulphuric acid and 46 ± 1 g of $HgSO_4$ in about 500 ml of water. After complete dissolution of all components, add 162 ± 1 ml of 96% m/m sulphuric acid, dilute with water to 1 l and filter.

Sulphuric acid reagent (10 g l^{-1} Ag_2SO_4 *in* H_2SO_4). Dissolve 10 ± 0.1 g of Ag_2SO_4 in 1 l of 96% m/m sulphuric acid; after dissolution, filter and heat to boiling-point in an all-glass apparatus.

Standard potassium hydrogen phthalate (*KHP*) *solution* (100 mg l^{-1} *COD*). Dissolve 85.1 ± 0.1 mg of KHP (previously dried at 120 °C for 2 h) in water and dilute with water to 1 l.

Calibration KHP solutions (5, 10, 15, 20, 25, 30 and 35 mg l^{-1} *COD*). Dilute 5, 10, 15, 20, 25, 30 and 35 ml of standard KHP solution to 100 ml with water.

KHP solution (4 g l^{-1}). Dissolve 200 ± 1 mg of KHP and 0.5 ± 0.05 ml of 96% m/m sulphuric acid (as a preservative) in 50 ml of water.

Reagents for the Open Reflux Method

Digestion solution (5.465 g l^{-1} $K_2Cr_2O_7$ *and* 89.1 g l^{-1} $HgSO_4$ in 33.2% *m/v* H_2SO_4). Add 5.465 ± 0.001 g of $K_2Cr_2O_7$, 50 ± 1 ml of 92% m/m sulphuric acid and 89.1 ± 0.1 g of $HgSO_4$ to about 500 ml of water. After dissolution of the components, add 148 ± 1 ml of 92% m/m sulphuric acid, dilute with water to 1 l and filter.

Sulphuric acid reagent (12.7 g l^{-1} Ag_2SO_4 *in* 92% *m/m* H_2SO_4). Dissolve 12.7 ± 0.1 g of Ag_2SO_4 in 1 l of 92% m/m sulphuric acid and filter.

Semi-micro Method

Mix 2 ml of sample and 1 ml of digestion solution in a 20 × 180 mm test-tube fitted with a ground-glass stopper (Sklo Union, Labora, Czechoslovakia), add carefully 5 ml of sulphuric acid reagent to form a layer on the bottom,[4] close the tube tightly with the stopper and mix the contents thoroughly but prevent their penetration to the ground glass joint. Immediately after mixing, place the tube in a thermostated block pre-heated to 170 ± 0.5 °C. (CAUTION: bumping may occur if mixing prior to the heating is omitted). After 40 ± 1 min remove the tube from the heating block, allow it to cool to 20–25 °C then add 7 ml of water and mix thoroughly. After cooling, read the absorbance at 455 nm in a 5-cm cell. At the same time determine at least two blanks by replacing the sample with re-distilled water. Calculate the COD value from the difference between the absorbances of the sample and the average value of the blanks according to the calibration graph prepared using the calibration KHP solutions.

For natural waters with suspended inorganic particles correction should be made to eliminate the error caused by the turbidity of the digestion mixture: follow the procedure described above for the sample and the blank but add 1 drop (0.05 ± 0.01 ml) of KHP solution (4 g l^{-1}) to the tubes before digestion in each instance, to reduce the dichromate in the digestion mixture. Measure the absorbances and subtract the difference between them from the absorbance of the sample obtained without dichromate reduction. Calculate the COD value using the corrected absorbance value.

Open Reflux Method

Follow the standard method,[3] but use 25 ml of sample, 5 ml of the digestion solution and 35 ml of the sulphuric acid reagent. This gives the same composition of the digestion mixture as the standard method[3] using 0.00833 M $K_2Cr_2O_7$.

Results and Discussion

Efficiency of Oxidation

Published data[1,2,12,16] indicate that the efficiency of oxidation depends appreciably on the concentrations of sulphuric acid, $K_2Cr_2O_7$ and Ag_2SO_4 in the digestion mixture and on the temperature and time of heating. The dependence of the efficiency of oxidation on these parameters was studied on the semi-micro scale; one parameter was varied at a time while keeping the others constant. Oxidation of nicotinic acid, which in the standard method using 0.0417 M $K_2Cr_2O_7$ proceeds only to 24.3% of the theoretical oxygen demand (TOD),[16] was chosen as the main criterion for the evaluation of the oxidation efficiency.

The influence of the concentration of Ag_2SO_4 in the reaction mixture is shown in Fig. 1 for nicotinic and acetic acids and for a sample of river water. While the organic

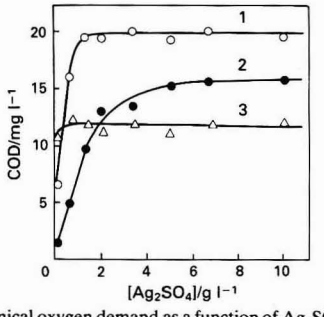

Fig. 1. Chemical oxygen demand as a function of Ag_2SO_4 concentration in the digestion mixture. 1, Acetic acid (TOD = 20.0 mg l^{-1}); 2, nicotinic acid (TOD = 71.6 mg l^{-1}); and 3, river water

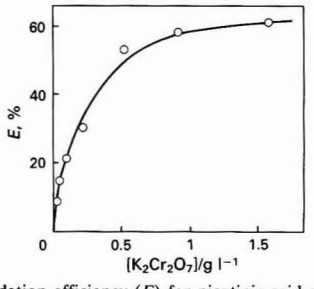

Fig. 2. Oxidation efficiency (E) for nicotinic acid as a function of $K_2Cr_2O_7$ concentration in the digestion mixture

Table 1. Comparison of the semi-micro (S) and open reflux (R) methods for various compounds (n = 2)

Sample	c*/ mg l^{-1}	TOD/ mg l^{-1}	c(S)/ mg l^{-1}	c(R)/ mg l^{-1}	S/R × 100, %
Glucose	18.6	19.8	19.2	18.8	102
Starch	16.0	19.0	18.6	17.9	104
Glycine	31.5	20.1	15.2	19.3	79
Aspartic acid	28.6	20.6	20.3	20.3	100
Tryptophan	11.6	20.9	21.9	21.1	104
Cysteine	16.7	19.9	16.3	14.1	116
Bovine serum albumin	14.4	—	17.9	16.6	108
Acetic acid	18.8	20.0	19.5	19.8	98
Sodium dodecyl sulphate	6.16	12.3	11.4	10.6	108
Humic acid (Fluka)	14.9	—	19.3	19.5	99
Humic acid (Roth)	15.3	—	16.7	16.7	100
Humic acid (peat-bog)	15.0	—	14.8	15.0	99
Pyridine	202	450	5.7	3.8	150
Nicotinic acid	50.1	71.6	15.7	10.4	151
Methylamine	75.8	122	12.2	16.0	76
Ethylamine	17.4	36.9	16.7	14.9	112

* c = mass concentration.

substances in the water were oxidised almost quantitatively even in the absence of Ag_2SO_4, its presence was requisite for the complete oxidation of acetic and nicotinic acids in concentrations of 1.3 and 6.5 g l^{-1}, respectively. Based on this result, an Ag_2SO_4 concentration of 6.77 g l^{-1} in the digestion mixture, *i.e.*, 10 g l^{-1} in the sulphuric acid reagent, was chosen.

The effect of the concentration of $K_2Cr_2O_7$ on the efficiency of nicotinic acid oxidation is shown in Fig. 2. The efficiency drops rapidly if the concentration of $K_2Cr_2O_7$ in the digestion mixture is reduced below 500 mg l^{-1}. On the other hand, the concentration of $K_2Cr_2O_7$ must not be too high if a reasonable sensitivity is to be achieved. In the method devised, a $K_2Cr_2O_7$ concentration of 120 mg l^{-1}, corresponding to COD values of up to approximately 70 mg l^{-1}, was chosen; the efficiency of oxidation of nicotinic acid is then about 22%. On depletion of $K_2Cr_2O_7$ to 60 mg l^{-1} the efficiency decreases by approximately one-third, *i.e.*, to 15%, which is comparable to the efficiency of oxidation of nicotinic acid in the standard method using 0.00833 M $K_2Cr_2O_7$ (see Table 1). Although the calibration graph for KHP is linear up to a COD of at least 60 mg l^{-1}, the efficiency for substances that are difficult to oxidise is poorer, restricting the upper limit of the method to a COD of 35 mg l^{-1}. This corresponds to a depletion of approximately half of the dichromate in the reaction mixture. Therefore, the semi-micro method could be modified for a COD of up to 100 mg l^{-1} by merely increasing the concentration of $K_2Cr_2O_7$ in the digestion solution approximately 2.5-fold while reducing the optical path length in the spectrophotometric determination of the remaining dichromate from 5 to 2 cm. In this modification the efficiency of oxidation would be improved (about 40% of nicotinic acid could be oxidised), the sensitivity, however, would apparently decrease.

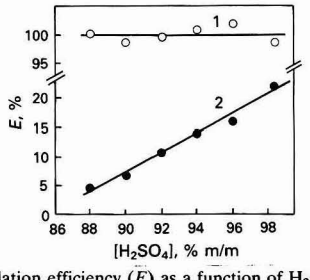

Fig. 3. Oxidation efficiency (E) as a function of H_2SO_4 concentration in the digestion mixture. 1, Acetic acid (TOD = 20.0 mg l^{-1}); and 2, nicotinic acid (TOD = 71.6 mg l^{-1})

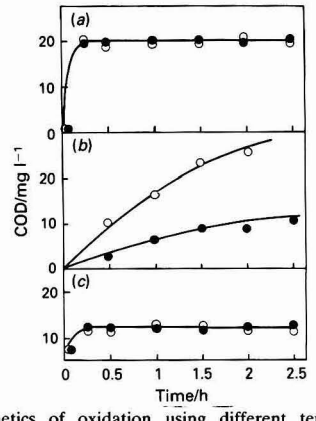

Fig. 4. Kinetics of oxidation using different temperatures of digestion for: (*a*) acetic acid (TOD = 20.0 mg l^{-1}); (*b*) nicotinic acid (TOD = 50.1 mg l^{-1}); and (*c*) river water. ●, 150; and ○, 170 °C

The efficiency of oxidation is also affected by the concentration of sulphuric acid in the digestion mixture. Fig. 3 shows the results of experiments with sulphuric acid reagents prepared from H_2SO_4 at concentrations in the range 88–98.3% m/m, which corresponds to H_2SO_4 concentrations in the digestion mixture in the range 67.9–75.9% m/m. As the concentration of H_2SO_4 is lowered, the efficiency of nicotinic acid oxidation decreases from 27% for 98.3% m/m H_2SO_4 to approximately 5% for 88% m/m H_2SO_4. The oxidation of acetic acid, on the other hand, is complete using any of the H_2SO_4 concentrations indicated.

Fig. 4 shows the rate of oxidation of nicotinic and acetic acids and of organic substances in river water at 150 and 170 °C. Increasing the temperature from 150 to 170 °C causes a higher efficiency of oxidation, particularly for nicotinic acid. To attain the same degree of oxidation as is achieved on heating at 170 °C for 30 min, heating at 150 °C requires a period of more than 2 h. Acetic acid and organic substances in river water were completely oxidised within 15 min at both 150 and 170 °C.

The increased oxidising ability of the reaction mixture at 170 °C is, of course, accompanied by a faster spontaneous decomposition of dichromate. Fig. 5 shows that the amount of dichromate decomposed in 40 min of heating at 170 °C is about 10 mg l^{-1}, which is approximately the same as that decomposed at 150 °C after 3 h of heating.

Interferences

Similarly as with the open reflux method, all inorganic substances capable of oxidation, such as Fe^{2+}, S^{2-} or nitrite, interfere with the semi-micro method. Correction is performed in the same manner as for the standard method.[3]

Turbidity of the reaction mixture, caused by inorganic particulate substances present in some surface water samples, increases the absorbance, causing a negative error in the determination. The method for the elimination of this error is

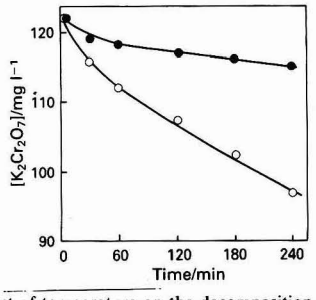

Fig. 5. Effect of temperature on the decomposition of $K_2Cr_2O_7$ in the digestion mixture in the absence of oxidisable organic matter. ●, 150; and ○, 170 °C

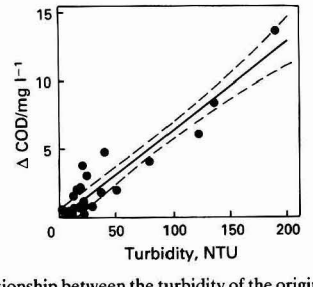

Fig. 6. Relationship between the turbidity of the original sample and the error of COD determination (Δ COD) caused by the turbidity of the digestion mixture (NTU = nephelometric turbidity unit). Linear regression: COD = 0.065 × turbidity −0.083 (n = 30, r = 0.95). Broken lines represent 99% confidence limits

described under Semi-micro Method. As an example, Fig. 6 shows the relationship between turbidity in the original water and the COD corresponding to the absorbance increment due to the presence of dispersions in samples taken from rivers in South Bohemia, Czechoslovakia.

Particular attention was given to the masking of chloride because this anion is common in both surface and ground waters and can cause considerable error, especially if the concentration of organic matter is low. In the proposed semi-micro method proposed, $HgSO_4$ and Cr^{3+} ions [as $KCr(SO_4)_2.12H_2O$] at respective concentrations of 6.22 and 0.1 g l^{-1} in the reaction mixture were used to mask chloride. This concentration of $HgSO_4$ allows for up to 600 mg l^{-1} of chloride in the sample. At higher concentrations, a turbidity caused by silver chloride appears in the system on dilution and cooling. If $HgSO_4$ is added in lower concentrations, the turbidity appears at lower chloride concentrations and the masking efficiency is poorer. Experiments in which the oxidation of chloride was examined at different concentrations of sulphuric acid and dichromate and at different temperatures and times of heating revealed that the dependencies of the oxidation of chloride on these parameters are basically the same as those for the oxidation of organic matter, *i.e.*, the oxidation efficiency improves if any of these parameters is increased. Fig. 7 shows the efficiency of oxidation of chloride as a function of COD at various concentrations of Cr^{3+} ions. Based on the relationship between the percentage of chloride oxidation and COD of the sample (Fig. 7), an equation can be derived to calculate the COD value caused by oxidation of chloride for the reaction conditions of the semi-micro method: COD of chloride = $0.23 \times c_{Cl^-} \times (0.022 - 0.00033 \times \text{COD})$ ($n = 5$, $r = 0.99$), where c_{Cl^-} and COD are, respectively the concentration of chloride and the COD in the sample, in mg l^{-1}. The effect of the oxidation of chloride can be disregarded in the semi-micro method up to a chloride concentration of about 100 mg l^{-1}, corresponding to a COD value not exceeding a maximum of 0.5 mg l^{-1} (about half of the detection limit). At higher chloride concentrations, the experimental COD value should be corrected.

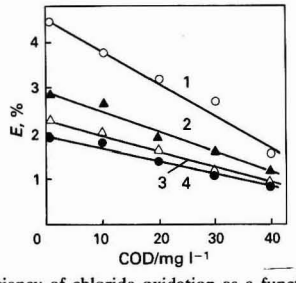

Fig. 7. Efficiency of chloride oxidation as a function of COD for different starting concentrations of Cr^{3+} ions in the digestion mixture: 1, 0; 2, 50; 3, 100; and 4, 250 mg l^{-1}. Determined for 600 mg l^{-1} of chloride and different concentrations of KHP

Comparison of the Semi-micro and Open Reflux Methods

The comparison was performed on two sets of samples: (*i*) 30 samples of water of various types (Table 2), and (*ii*) 16 chemical compounds (Table 1). The tables demonstrate that the results of the semi-micro and the open reflux methods are comparable. For sample set (*i*), the ratio of the means obtained by the two methods was 101%, with a standard

Table 2. Comparison of the semi-micro (S) and open reflux (R) methods for waters ($n = 5$)

		COD/mg l^{-1}				
		S		R		
Sample		Mean	SD	Mean	SD	S/R × 100, %
Ground water . .	1*	0.74	0.36	1.16	0.61	64
	2*	2.68	0.33	2.66	0.71	101
	3*	5.38	0.45	5.30	0.22	102
	4*	6.02	0.18	6.24	0.00	96
	5*	6.90	0.30	6.84	0.36	101
Tap water . .	1*	6.94	0.22	7.30	0.26	95
	2*	7.70	0.38	7.42	0.18	104
	3*	7.84	0.26	7.45	0.30	105
	4*	8.18	0.25	8.20	0.34	100
	5*	9.76	0.23	10.38	0.88	94
Precipitation . .	1*	3.26	0.48	2.72	0.36	120
	2*	3.44	0.17	3.10	0.42	111
	3*	4.24	0.38	3.06	0.71	139
	4*	5.18	0.31	5.20	0.34	100
	5*	10.20	0.54	10.16	0.41	100
River water . .	1*	14.14	0.49	14.22	0.30	99
	2*	14.28	0.30	14.40	0.35	99
	3*	18.10	0.26	18.08	0.39	100
	4*	19.36	0.26	19.40	0.81	100
	5*	33.60	0.29	34.02	0.18	99
Reservoir . .	1*	10.76	0.25	10.72	0.30	100
	2*	14.70	0.44	14.98	0.30	98
	3*	18.06	0.55	18.30	0.37	99
	4*	18.82	0.46	18.02	0.33	104
	5	24.76	0.26	23.84	0.22	104
Fish-pond . .	1*	11.54	0.36	11.24	0.17	103
	2*	16.78	0.29	16.42	0.30	102
	3*	20.64	0.26	22.30	0.63	93
	4	24.38	0.04	25.10	0.21	97
	5*	30.72	0.42	30.82	0.27	100
Mean		12.64	0.33	12.64	0.37	101

* Paired *t*-test showed no statistically significant difference at the 5% level.

Table 3. Recoveries of KHP added to samples with the semi-micro method ($n = 5$)

		COD/mg l^{-1}					
		Sample		KHP	Sample + KHP		Recovery,
Sample		Mean	SD	added	Mean	SD	%
Ground water . .	1	5.38	0.45	5.80	11.48	0.20	105
	2	6.90	0.30	5.80	12.56	0.41	98
Tap water . .	1	6.94	0.22	5.80	12.64	0.30	98
	2	8.18	0.25	5.80	14.02	0.35	101
River water . .	1	14.14	0.49	5.90	20.31	0.26	105
	2	26.46	0.35	5.80	31.98	0.18	95
Reservoir . .	1	14.70	0.25	5.90	20.61	0.05	100
	2	24.76	0.26	5.90	30.47	0.30	97
Fish-pond . .	1	11.54	0.35	5.90	17.51	0.36	101
	2	24.38	0.04	5.90	30.27	0.14	100
Mean							100

deviation (SD) of 5.7%. The agreement for the majority of chemical compounds was also good. A rather poorer efficiency of oxidation by the semi-micro method was observed only for glycine, for which the degrees of oxidation with the semi-micro method and the open reflux method were 76 and 96%, respectively, and for methylamine, for which the degrees of oxidation were 10 and 13%, respectively. Higher oxidation yields, on the other hand, were obtained with the semi-micro method for cysteine, pyridine, nicotinic acid and for volatile substances such as acetone or benzene. Their vapours in the open reflux method apparently leave the system via the reflux condenser. However, the oxidation was not complete in the semi-micro method either, probably because some of the vapours of the volatile substances pass into the gas phase and, perhaps, even leak through the ground glass joint.

Detection Limit, Precision and Accuracy

The detection limit of the semi-micro method was calculated as the mean bias of the blank plus twice the average SD using values obtained for sample set (*i*) (Table 2). The mean bias of the blank determination in the semi-micro method generally did not exceed 0.5 mg l^{-1}, the average SD was 0.33 mg l^{-1} and the COD detection limit was 1.16 mg l^{-1}. The modified open reflux method gave an average SD of 0.37 mg l^{-1} for the same set of samples, which leads to approximately the same detection limit.

The precision of the semi-micro method depends on the precision with which the sample and the reagents are dispensed, on the precision of the spectrophotometric measurement of dichromate and also on how strictly the time and temperature of heating are adhered to. For waters with suspended matter, the use of a representative sample must be ensured; if a coarse suspension is present, an appropriate homogenisation procedure[9] is necessary. Temperature variations within the heating block should not exceed ±0.5 °C and temperature gradients between different sites of the heating block must be eliminated to prevent dichromate from decomposing at different rates.

The accuracy of the semi-micro method for the determination of COD was tested by spiking ten samples of different types of water with KHP. The results are presented in Table 3. The yield with respect to KHP added was from 95 to 105%, with an average of 100%, which compares well with the standard method.[3]

References

1. Moore, W. A., Kroner, R. C., and Ruchhoft, C. C., *Anal. Chem.*, 1949, **21**, 953.
2. Moore, W. A., Ludzack, F. J., and Ruchhoft, C. C., *Anal. Chem.*, 1951, **23**, 1297.
3. American Public Health Association, American Water Works Association and Water Pollution Control Federation, "Standard Methods for the Examination of Water and Wastewater," Sixteenth Edition, American Public Health Association, Washington, DC, 1985, p. 532.
4. Jirka, A. M., and Carter, M. J., *Anal. Chem.*, 1975, **47**, 1397.
5. Himebaugh, R. R., and Smith, M. J., *Anal. Chem.*, 1979, **51**, 108.
6. De Casseres, K. E., *Water Pollut. Control, Maidstone, Engl.*, 1980, **79**, 143.
7. Messenger, A. L., *J. Water Pollut. Control Fed.*, 1981, **53**, 232.
8. Edwards, S. J., and Allen, M., *Analyst*, 1984, **109**, 671.
9. "Chemical Oxygen Demand (Dichromate Value) of Polluted and Waste Waters 1986," Second Edition, HM Stationery Office, London, 1986.
10. Jeris, J. S., *Water Wastes Eng.*, 1967, **4**, 89.
11. Leithe, W., *Vom Wasser*, 1970, **37**, 106.
12. Leithe, W., *Vom Wasser*, 1971, **38**, 119.
13. Wagner, R., and Ruck, W., *Z. Wasser Abwasser Forsch.*, 1984, **17**, 268.
14. Wagner, R., and Ruck, W., *Z. Wasser Abwasser Forsch.*, 1981, **14**, 145.
15. De Casseres, K. E., Best, D. G., and May, B. D., *Water Pollut. Control, Maidstone, Engl.*, 1984, **83**, 416.
16. Chudoba, J., and Zeis, K., *Acta Hydrochim. Hydrobiol.*, 1975, **3**, 275.

Paper 9/04306C
Received October 9th, 1989
Accepted July 2nd, 1990

Enrichment of Trace Metals in Water on Activated Carbon

P. Rama Devi and G. Rama Krishna Naidu*
Department of Chemistry, S.V. University College, Tirupati 517 502, India

Trace metals in water were pre-concentrated on activated carbon after chelation with potassium ethyl xanthate. Optimum conditions for the maximum recovery of metal ions were developed. The recoveries of Cd, Co, Cu, Hg and Zn, at concentrations ranging from 10 to 500 ng ml^{-1}, were >92, ≈85, >92, >93 and >92%, respectively. The method was used to determine these metals in water samples by instrumental neutron activation analysis and atomic absorption spectrometry.

Keywords: *Trace metal; pre-concentration; quantitative recovery; activated carbon; potassium ethyl xanthate*

Knowledge of the detrimental effects of trace and ultra-trace amounts of metals in the environment has greatly increased. In order to understand the impact of metals in the environment, accurate and reliable methods must be developed for their determination. Because of the extremely low concentrations of metals in water, a preliminary concentration step is usually necessary before the determination can be carried out. A survey of the literature on water analysis shows that enrichment of heavy metals on activated carbon offers good possibilities. A number of elements can be pre-concentrated by this technique, which is simple, fast and inexpensive. Van der Sloot[1] used activated carbon as a collector for colloidal trace elements in water, biological material and in rocks in combination with neutron activation analysis (NAA), atomic absorption spectrometry (AAS) and X-ray fluorescence. Matsueda and Morimoto[2] explained the adsorption behaviour of some metal ions on activated carbon treated with 8-hydroxyquinoline. An activated-carbon enrichment and AAS determination of trace amounts of metals has been reported by Liu.[3] Varderborght and Van Grieken[4] used a combination of multi-element chelation by 8-hydroxyquinoline with subsequent adsorption on activated carbon for the pre-concentration of trace metals from water samples.

In the present investigation, Cd, Co, Cu, Hg and Zn in water were enriched on activated carbon, after complexation with potassium ethyl xanthate, and determined by instrumental NAA (INAA) and flame AAS (FAAS). The pre-concentration procedure is simple, fast, sensitive, multi-elemental and inexpensive.

Experimental

Materials and Methods

All the chemicals used were of analytical-reagent grade.

Potassium ethyl xanthate was synthesised[5] and purified.[6] Activated carbon powder (analytical-reagent grade) was treated with 11 M hydrochloric acid and washed with doubly distilled water to remove any trace elements present.

Stock solutions of Cd, Co, Cu, Hg and Zn (1 mg ml^{-1}) were prepared by dissolving each metal in the minimum amount of 1 + 1 nitric acid separately and diluting the solution to 1 l with 1% v/v nitric acid. Multi-element standard solutions of Cd, Co, Cu, Hg and Zn (10 to 100 μg ml^{-1}) were prepared from the stock solutions.

A 0.4% solution of potassium ethyl xanthate was prepared in doubly distilled water.

Tracers used in the present study were ^{115}Cd, ^{60}Co, ^{65}Zn, ^{197}Hg and ^{64}Cu.

Water samples from different locations were collected in polyethylene bottles and acidified with 1.5 ml of 16 M nitric acid per litre of sample. The samples were filtered through 0.45-μm filter-discs and then analysed. The pre-concentration was carried out within 24 h of collection.

Neutron activation was carried out in the Apsara reactor at the Bhabha Atomic Research Centre, Bombay, in a neutron flux of 1 × 10^{12} n cm^{-2} s^{-1} for 6 h.

Analysis, in the example of the tracer method and NAA, was carried out by γ-ray spectrometry, with a Ge(Li) detector linked to a 4096-channel analyser. The FAAS studies were carried out with the use of a double-beam atomic absorption spectrometer (Perkin-Elmer, Model 2380). In the FAAS method, the carbon, containing the adsorbed metals, was treated with 1.5 ml of hot 16 M nitric acid (this ensures quantitative desorption of the metals) and the solution was evaporated to dryness under an infrared lamp. The metals were leached into 10 ml of 1.5 M nitric acid and then the sample was analysed for Co, Cu, Cd and Zn under the conditions cited in Table 1.

Procedure

To a 100-ml water sample, an aliquot of the tracer mixture, containing 10 μg each of Cd, Co, Cu, Hg and Zn, was added, and the pH was adjusted to 5 with 1 M nitric acid and 7 M ammonia solution, and 5 ml of 0.4% potassium ethyl xanthate solution were added. The mixture was stirred with 100 mg of activated carbon for 10 min by use of a mechanical stirrer. The suspension was filtered off, and the carbon was sealed into polyethylene strips and mounted for counting.

Preparation of standards

Standards were prepared by drying an aliquot of the tracer mixture, absorbed on a filter-paper, over calcium chloride in a desiccator, to prevent any loss of Hg by evaporation.

Results and Discussion

Optimum conditions for the quantitative recovery of metal ions were determined by studying the effect of pH, stirring time, concentration of potassium ethyl xanthate, concentration of metal ion, mass of activated carbon and sample volume.

Table 1. Conditions used for FAAS

Sample No.	Element	Lamp current/mA	Wavelength/nm	Slit/nm	Flame gases
1	Cd	4	228.8	0.7	A - Ac*
2	Co	30	240.7	0.2	A - Ac
3	Cu	30	324.8	0.7	A - Ac
4	Zn	15	213.8	0.2	A - Ac

* A - Ac = air - acetylene.

* To whom correspondence should be addressed.

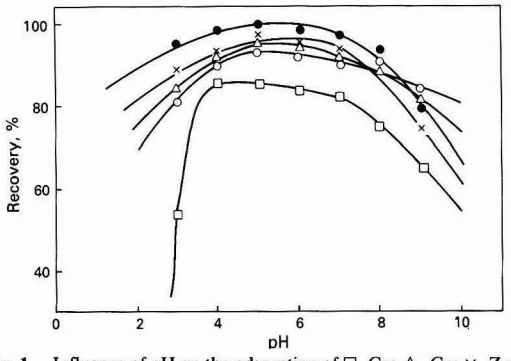

Fig. 1. Influence of pH on the adsorption of □, Co; △, Cu; ×, Zn; ○, Cd; and ●, Hg on activated carbon

pH

Zinc, Cd, Hg and Cu were recovered at levels >90% in the pH range 4–7, whereas the recovery of Co was ≈85%. The results are presented graphically in Fig. 1. The experiment was also carried out in the absence of potassium ethyl xanthate. Recovery of Cd, Co and Zn increases as the pH is raised, and reaches a maximum at pH 8 for Cu and Hg, where the recoveries are 90–100% in the pH range 4–8. The recovery of metal ions is not reproducible in the absence of xanthate; the adsorption could be due to their hydrolysed products.

Stirring Time

The recovery of Cd, Co, Cu, Hg and Zn is not quantitative when the metal ion solution with potassium ethyl xanthate is passed through a carbon-coated filter-disc. Hence, the recovery studies were carried out by stirring the solution with carbon. The recovery is quantitative for stirring times >5 min (up to 30 min).

Xanthate and Activated Carbon

Quantitative recovery of Cd, Co, Cu, Hg and Zn is observed for amounts of xanthate >10 mg (up to 40 mg). The recovery of Cu, Zn and Hg is >90% with 50 mg of carbon, whereas Co and Cd need a larger amount (70 mg).

Effect of Metal Ion

This study shows that metal ion concentrations of 10–500 ng ml^{-1} can give quantitative recovery values.

Sample Volume

The amount of metal studied, when present in volumes up to 500 ml, still gives a quantitative recovery, indicating that the recovery is independent of the mass : volume ratio.

Effect of Blank

Purified activated carbon was irradiated for 6 h in the Apsara reactor and then analysed for Cu, Cd, Co, Zn and Hg after a delay of 15 h. The blank contribution was negligible.

Conclusion

The pre-concentration method has been used for the analysis of "spiked" tap water samples by INAA and FAAS. For INAA, standards and samples, triply sealed in polyethylene strips, and then placed in a polyethylene bottle, were simultaneously subjected to irradiation in the Apsara reactor for 6 h, and the analysis was carried out after a delay of 15 h. The activity of the nuclides produced was measured by γ-ray spectrometry. For FAAS, the metals enriched on activated carbon were leached into 1.5 M nitric acid and then determined. The determination of Hg was not carried out owing to the non-availability of a cold-vapour atomisation system. The results presented in Table 2 show that the data obtained by INAA are comparable to those given by FAAS. The data pertaining to the analyses of authentic water samples are presented in Table 3. The γ-ray spectrum of a water sample enriched on activated carbon is presented in Fig. 2.

The advantage of INAA over FAAS is that the technique is non-destructive and multi-elemental. In FAAS, the metals must be leached into acid; this procedure results in a reduction in the enrichment factor. Analysis by FAAS is rapid and the equipment required is widely available.

Table 2. Recovery of Co, Cu, Zn, Cd and Hg from tap water

Sample No.	Element	Amount of metal ion taken/ ng ml^{-1}	Metal ion found, %* INAA	FAAS
1	Co	100	85.65	85.58
			85.60	85.52
			85.62	85.54
			(0.03)	(0.036)
2	Cu	100	95.54	95.56
			95.52	95.58
			95.50	95.54
			(0.021)	(0.021)
3	Zn	100	92.84	92.80
			92.78	92.83
			92.82	92.79
			(0.033)	(0.023)
4	Cd	100	94.50	94.52
			94.46	94.54
			94.48	94.47
			(0.021)	(0.038)
5	Hg	100	96.25	—
			96.72	—
			96.26	—
			(0.279)	—

* Coefficients of variation are given in parentheses.

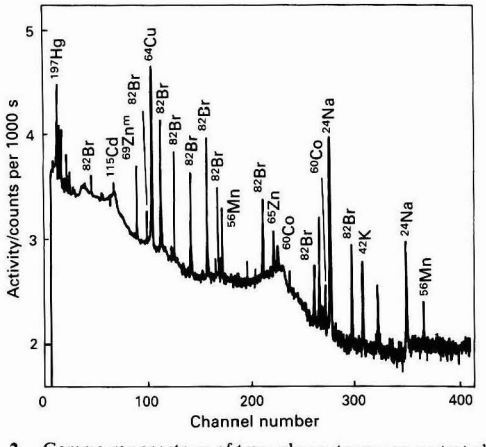

Fig. 2. Gamma-ray spectrum of trace elements pre-concentrated on activated carbon from a water sample measured after a delay of 15 h. Irradiation time, 6 h. Calibration: slope = 0.4946 keV per channel; intercept = 1.64 keV

Table 3. Determination of Co, Cu, Zn, Cd and Hg in water (concentrations in ng ml^{-1})*

Sample No.	Name of the sample	Co		Cu		Zn		Cd		Hg	
		INAA	FAAS	INAA	FAAS	INAA	FAAS	INAA	FAAS	INAA	FAAS
1	Renigunta	0.90	ND†	20.26	20.39	28.83	28.68	4.60	4.59	1.52	NA‡
		1.00	ND	20.35	20.27	28.75	28.81	4.62	4.71	1.45	NA
		0.89	ND	20.31	20.29	28.79	28.72	4.73	4.68	1.48	NA
		(6.54)		(0.223)	(0.317)	(0.138)	(0.232)	(1.505)	(1.340)	(2.388)	
2	Kalyani Dam	ND	ND	9.58	9.53	18.35	18.31	ND	ND	ND	NA
		ND	ND	9.59	9.61	18.38	18.32	ND	ND	ND	NA
		ND	ND	9.45	9.55	18.33	18.39	ND	ND	ND	NA
				(0.819)	(0.437)	(0.139)	(0.238)				
3	Papavinasam	ND	ND	16.45	16.54	32.76	32.79	ND	ND	ND	NA
		ND	ND	16.48	16.51	32.80	32.76	ND	ND	ND	NA
		ND	ND	16.52	16.46	32.78	32.71	ND	ND	ND	NA
				(0.215)	(0.246)	(0.061)	(0.124)				
	Blank	ND	ND	0.35	ND	0.53	ND	ND	ND	ND	NA
		ND	ND	0.29	ND	0.55	ND	ND	ND	ND	NA
		ND	ND	0.32	ND	0.58	ND	ND	ND	ND	NA
				(9.375)		(4.635)					

* Coefficients of variation are given in parentheses.
† ND: Not detected.
‡ NA: Not analysed.

The pre-concentration method developed is, therefore, simple and rapid compared with the method developed by Vanderborght and Van Grieken.[4] The concentration range covered in the present work can be enhanced by increasing the amount of activated carbon and the reagent concentration.

Hence, the proposed pre-concentration method can be used successfully for the determination of Cd, Hg, Co, Cu and Zn in water by INAA and also by FAAS.

The financial assistance rendered by the CSIR is gratefully acknowledged. Thanks are due also to the Analytical Chemistry Division, BARC, Bombay, for providing the facilities to carry out the research.

References

1. Van der Sloot, H. A., *Chem. Weekbl. Mag.*, 1979, **297**, 299.
2. Matsueda, T., and Morimoto, M., *Bunseki Kagaku*, 1978, **27**, 312.
3. Liu, X., *Huanjing Huaxue*, 1986, **5**, 53.
4. Vanderborght, B. M., and Van Grieken, R. E., *Anal. Chem.*, 1977, **49**, 311.
5. Vogel, A. I., "A Text-book of Practical Organic Chemistry Including Qualitative Organic Analysis," Third Edition, Longman, London, 1957, p. 499.
6. Ramachandra Rao, S., "Xanthates and Related Compounds," Marcel Dekker, New York, 1971, p. 15.

Paper 0/01292K
Received March 26th, 1990
Accepted July 9th, 1990

Extraction of Cobalt and Nickel Salicylates: Application to Steel and Industrial Wastewater Samples

Purnima L. Malvankar and Vijay M. Shinde*
Analytical Laboratory, Institute of Science, 15 Madam Cama Road, Bombay 400 032, India

Aliquat 336 was used as an extractant for cobalt and nickel salicylates. The proposed method was applied to the determination of cobalt and nickel in alloys and industrial wastewater. The results obtained with the proposed method agree well with certified values and are comparable to those given by atomic absorption spectrometry. The method has a high degree of accuracy and precision.

Keywords: *Solvent extraction; liquid ion exchanger; salicylate solution*

Cobalt and nickel are useful elements because of their strength and high resistance to corrosion in many media. Cobalt is widely used in high-speed tool steels, magnets and high-temperature alloys. Nickel is used in nickel-plating articles, nickel coating, etc. It is also used in pharmaceutical processing. Both cobalt and nickel are also used as catalysts in industrial processes.

In previous papers, high relative molecular mass amines such as trioctylamine,[1,2] tribenzylamine,[3] methyltrioctylammonium chloride (Aliquat 336),[4–6] di- and triethylamine[7] and di- and tributylamine[7] were used for extraction studies of cobalt and nickel. However, these methods have drawbacks such as a long shaking period,[1–3] prolonged time for phase separation[4] and multiple extraction[5]; moreover, the extraction is not quantitative.[3,6,7]

The present paper describes a method for the extraction of cobalt and nickel salicylates using Aliquat 336 as the extractant. The metal ions were stripped with ammonia solution and determined volumetrically[8] or spectrophotometrically.[9] Atomic absorption spectrometry (AAS) could also be used for the determination of the metal ions. The proposed method is fast, providing extraction in a single step, and has been applied to the determination of cobalt and nickel in alloys and nickel in industrial wastewater samples.

Experimental

Apparatus

A Bausch and Lomb Spectronic 20 spectrophotometer, a Control Dynamics digital pH meter with a combined glass electrode, a wrist-action flask shaker and a Varian Techtron AA6 atomic absorption spectrometer were used.

Chemicals and Reagents

Stock solutions of cobalt and nickel were prepared by dissolving 1.23 g of cobalt nitrate and 1.19 g of nickel sulphate in 250 ml of distilled water containing 1 ml of concentrated HNO_3 and 1 ml of concentrated H_2SO_4, respectively. The solutions were standardised by known methods[8] and test solutions of lower concentrations were prepared by suitable dilution.

A buffer solution of pH 4.7 was prepared using 0.01 M acetic acid and 0.01 M sodium acetate solution.

A 5% m/v solution of Aliquat 336 (Fluka, Buchs, Switzerland) in toluene was shaken with an equal volume of 2 M sodium salicylate solution for 45 min and used as the extractant.

General Extraction Procedure for Nickel(II) and Cobalt(II)

To 500 μg of nickel or cobalt in solution, sodium salicylate was added to give the desired concentration in a final volume of 25 ml. After adding 10 ml of buffer solution of pH 4.7 the solution was extracted with 10 ml of 5% Aliquat 336 dissolved in toluene. After phase separation the metal ions were stripped from the organic phase with two 5-ml portions of 1 M ammonia solution. The combined aqueous phase was shaken with 5 ml of toluene to remove any traces of dissolved Aliquat 336 and finally the metal ions were determined either volumetrically,[8] spectrophotometrically[9] or by AAS.

Results and Discussion

Extraction Conditions

The optimum extraction conditions for cobalt and nickel were established by varying the pH, sodium salicylate concentration, Aliquat 336 concentration and shaking time. The optimum extraction conditions are reported in Table 1. Milligram amounts of cobalt and nickel were determined volumetrically[8] whereas microgram amounts were determined either spectrophotometrically[9] or by AAS.

Effect of Various Diluents

Several solvents such as xylene, benzene, hexane, carbon tetrachloride, chloroform and toluene were tested. The results given in Table 2 show that quantitative extraction was feasible only with toluene and xylene. For further studies, toluene was used as the diluent.

Period of Extraction

The minimum shaking time was determined by varying the shaking time from 30 to 180 s. The optimum shaking time was 60 s. However, prolonged shaking had no adverse effect on the extraction of metal ions.

Effect of Stripping Agents

Various stripping agents (Table 3) at different concentrations were studied for the back-extraction of metal ions from the organic phase. Quantitative stripping of cobalt from the organic phase was possible with two 5-ml portions of HCl (1–4 M), H_2SO_4 (1–4 M), HNO_3 (1–4 M), water, NaOH (1–4 M) or ammonia solution (1–2 M), whereas the stripping of nickel from the organic phase was possible with two 5-ml portions of HCl (1–3 M), H_2SO_4 (1–3 M), HNO_3 (1–2 M), water or ammonia solution (1–2 M). Nickel was not back-extracted with NaOH (1–4 M).

* To whom correspondence should be addressed.

Table 1. Optimum extraction conditions for Co^{II} and Ni^{II}

Metal ion	[Salicylate]/M	Extractant	pH	Extraction time/s	Stripping agent
Co^{II} (500 μg) ..	0.18	3.5% Aliquat 336 in toluene	4.2–8.0	60	1 M ammonia solution
Ni^{II} (500 μg) ..	0.12	3.5% Aliquat 336 in toluene	4.2–8.0	60	1 M ammonia solution

Table 2. Effect of diluents on the extraction of Co^{II} and Ni^{II} with Aliquat 336. pH, 4.7; [salicylate], 0.18 M for Co^{II} and 0.12 M for Ni^{II}; [Aliquat 336], 3.5% for Co^{II} and Ni^{II}

Diluent	Relative permittivity	Extraction,%	
		Co^{II}	Ni^{II}
Xylene	2.30	99.9	99.7
Toluene	2.38	99.9	99.8
Benzene	2.28	98.5	97.0
Chloroform	4.80	77.6	72.0
Carbon tetrachloride ..	2.24	80.6	76.4
Hexane	1.89	97.0	94.1

Table 3. Effect of stripping solutions. Cobalt: pH, 4.7; [salicylate], 0.18 M; [Aliquat 336], 3.5% in toluene. Nickel: pH, 4.7; [salicylate], 0.12 M; [Aliquat 336], 3.5% in toluene

Solution	Recovery of cobalt,%	Solution	Recovery of nickel,%
HCl (1–4 M) (2 × 5 ml)	99.9	HCl (1–3 M) (2 × 5 ml)	99.9
H_2SO_4 (1–4 M) (2 × 5 ml)	99.9	H_2SO_4 (1–3 M) (2 × 5 ml)	99.9
HNO_3 (1–4 M) (2 × 5 ml)	99.9	HNO_3 (1–2 M) (2 × 5 ml)	99.9
Water (2 × 5 ml) ..	99.9	Water (2 × 5 ml) ..	99.9
Ammonia solution (1–2 M) (2 × 5 ml)	99.9	Ammonia solution (1–2 M) (2 × 5 ml)	99.9
NaOH (1–4 M) (2 × 5 ml)	99.9	NaOH (1–4 M) (2 × 5 ml)	0

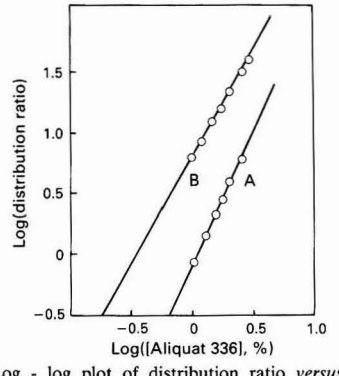

Fig. 1. Log - log plot of distribution ratio *versus* Aliquat 336 concentration: A, Ni^{II}; and B, Co^{II}

Nature of the Extracted Species

The logarithmic plot of distribution ratio *versus* salicylate concentration (at fixed pH and Aliquat 336 concentration) and the logarithmic plot of distribution ratio *versus* Aliquat 336 concentration (at fixed pH and sodium salicylate concentration) gave a slope nearly equal to 2 (Figs. 1 and 2), indicating a 1 : 2 ratio of metal to salicylate and the extractant in the extracted species. Hence the probable composition of the extracted species is $[(R_4N)_2{}^+M(HOC_6H_4COO)_2{}^{2-}]$, where M is either Co^{II} or Ni^{II}. Both cobalt and nickel form anionic complexes with salicylate and undergo anion exchange with an amine salt in the organic phase.

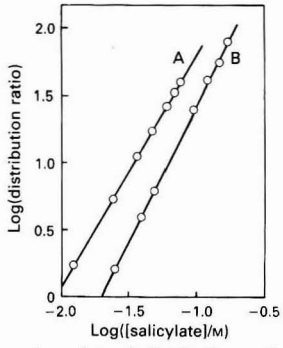

Fig. 2. Log - log plot of distribution ratio *versus* salicylate concentration: A, Ni^{II}; and B, Co^{II}

Table 4. Effect of foreign ions. Cobalt: pH, 4.7; [salicylate], 0.18 M; [Aliquat 336], 3.5% in toluene. Nickel: pH, 4.7; [salicylate], 0.12 M [Aliquat 336], 3.5% in toluene

Metal ion	Foreign ion tolerated*
Ni^{II}, 500 μg ..	Ba^{2+}(10); Al^{3+}(10); Pb^{2+}(10); Ca^{2+}(10); $WO_4{}^{2-}$(10); $MoO_4{}^{2-}$(10); $CrO_4{}^{2-}$(10); Mn^{2+}(10); $VO_3{}^-$(10); Pd^{2+}(10); As^{3+}(10); Ag^+(10); $OsO_6{}^{4-}$(5); Hg^{2+}(2.5); Au^{3+}(2.5); F^-(10); tartrate (10); SCN^-(10); $PO_4{}^{3-}$(10); Cl^-(10); I^-(10); Br^-(10); thiourea (10); $SO_4{}^{2-}$(10); $NO_3{}^-$(10); ascorbate (5); $NO_2{}^-$(5); CN^-(2.5)
Co^{II}, 500 μg ..	Ba^{2+}(10); Mg^{2+}(10); $CrO_4{}^{2-}$(10); $MoO_4{}^{2-}$(10); $WO_4{}^{2-}$(10); $VO_3{}^-$(10); Pb^{2+}(10); Ca^{2+}(10); Al^{3+}(5); Ag^+(5); Au^{3+}(5); Hg^{2+}(2.5); Bi^{3+}(0.500); $OsO_6{}^{4-}$(2.5); citrate(0.500); CN^-(0.500); $NO_2{}^-$(5); F^-(10); tartrate (10); SCN^-(10); $PO_4{}^{3-}$(10); Cl^-(10); I^-(10); Br^-(10); thiourea (10); $SO_4{}^{2-}$(10); $NO_3{}^-$(10)

* Values in parentheses (mg) are averages of triplicate analyses.

Effect of Foreign Ions

Various cations and anions were tested for interference in the extraction studies of cobalt and nickel. The tolerance limit was set at the amount required to cause an error of ±1% in the recovery of the metal ions. The results presented in Table 4 indicate that many cations and anions do not interfere; however, significant interferences are caused by Fe^{III}, Co^{II}, oxalate and citrate for Ni^{II}, and by Fe^{III}, Cu^{II} and oxalate for Co^{II}.

Determination of Cobalt or Nickel in a Synthetic Mixture Containing Aluminium, Iron, Copper, Zinc, Chromium and Manganese

Extraction of cobalt and nickel from 0.25 M sodium salicylate solution, adjusted to pH 8, with 10 ml of 5% Aliquat 336

Table 5. Determination of Co^{II} or Ni^{II} in synthetic mixtures

Synthetic mixture*	Amount of Co or Ni found†/μg	Recovery of Co or Ni,%	Error,%
$Co^{II}(500)$; $Al^{III}(500)$; $Fe^{III}(25)$; $Cu^{II}(500)$	499.5 Co	99.9 Co	0.1
$Co^{II}(500)$; $Cr^{VI}(500)$	499.7 Co	99.9 Co	0.1
$Co^{II}(500)$; $Zn^{II}(500)$	499.1 Co	99.8 Co	0.2
$Co^{II}(500)$; $Mn^{II}(500)$	499.6 Co	99.9 Co	0.1
$Ni^{II}(500)$; $Al^{III}(500)$; $Fe^{III}(25)$; $Cu^{II}(500)$	499.2 Ni	99.8 Ni	0.2
$Ni^{II}(500)$; $Cr^{VI}(500)$	499.9 Ni	99.9 Ni	0.1
$Ni^{II}(500)$; $Zn^{II}(500)$	499.4 Ni	99.8 Ni	0.2
$Ni^{II}(500)$; $Mn^{II}(500)$	499.2 Ni	99.8 Ni	0.2
$Ni^{II}(500)$; $Co^{II}(500)$	499.2 Ni	99.8 Ni	0.2
	499.5 Co	99.9 Co	0.1

* Values in parentheses are the amounts of each metal ion in micrograms.
† Average of six determinations.

Table 6. Analysis of alloys

Alloy	Composition,%	Certified value,%	Co or Ni found,*%	Standard deviation	Relative standard deviation,%
BCS-CRM† 387 Nimonic 901	Ni, 41.9; Fe, 36; Cr, 12.5; Mo, 5.8; Ti, 2.95; Al, 0.24; Co, 0.2; Cu, 0.3	41.9 Ni	41.8 Ni	0.11	0.26
BCS-CRM 383 Monel Alloy 400	Mn, 1.03; Cr, 0.02; Ni, 63.8; Al, 0.005; Co, 0.19; Cu, 32.93; Ti, 0.01; Fe, 1.70; Mg, 0.03	63.8 Ni	63.7 Ni	0.10	0.15
BCS-CRM 371 Commercial Nickel	Cu, 0.39; Mg, 0.60; Ni, 99.5	99.5 Ni	99.4 Ni	0.09	0.09
Cupronickel‡	Cu, 68.12; Ni, 30.35	30.35 Ni	30.29 Ni	0.10	0.12
BCS-CRM 483 High Speed Tool Steel	W, 10.8; Cr, 3.21; V, 0.54, Mo, 0.170; Co, 1.94; C, 0.67; Si, 0.11; S, 0.025; P, 0.019; Mn, 0.29	1.94 Co	1.87 Co	0.04	2.13
BCS-CRM 241/2 High Speed Tool Steel	W, 19.9; Cr, 5.35; V, 1.59; Mo, 0.53; Co, 5.70; C, 0.84; Si, 0.21; S, 0.025; P, 0.024; Mn, 0.27; Ni, 0.15; Cu, 0.08; Sn, 0.025	5.70 Co	5.65 Co	0.041	0.73
BCS-CRM 485 High Speed Tool Steel	W, 18.2; Cr, 4.15; V, 10.5; Mo, 0.67; Co, 5.06; C, 0.89; Si, 0.42; S, 0.043; P, 0.046; Mn, 0.50	5.06 Co	4.98 Co	0.054	1.08
BCS-CRM 484 High Speed Tool Steel	W, 22.4; Cr, 5.17; V, 0.94; Mo, 1.07; Co, 10.2; C, 0.85; Si, 0.20; S, 0.024; P, 0.030; Mn, 0.21	10.2 Co	10.1 Co	0.11	1.09

* Average of six determinations.
† BCS-CRM = British Chemical Standard, Certified Reference Material.
‡ Certified Reference Material obtained from IIT, Bombay, India.

Table 7. Analysis of industrial wastewater samples

Sample No.	Ni found* by proposed method, p.p.m.	Ni found† by AAS, p.p.m.
1	0.23	0.27
2	0.18	0.18

* Average of three determinations.
† Determined directly, before extraction, by AAS.

dissolved in toluene, facilitates their separation and determination in synthetic mixtures containing aluminium, iron and copper. Nickel and cobalt were stripped from the organic phase with 2 × 5 ml of 1 M ammonia solution and determined as described in the general extraction procedure. Results are reported in Table 5.

Cobalt and nickel were determined in the presence of zinc and manganese by extraction from 0.25 M sodium salicylate solution of pH 4.7. Zinc and manganese were co-extracted; however, cobalt and nickel were stripped selectively with water and determined as described above. The results are reported in Table 5.

Cobalt and nickel could be determined in the presence of chromium using the recommended procedure because chromium was not extracted into the Aliquat 336 solution.

Mutual Separation of Nickel and Cobalt

Results in Table 3 show that quantitative separation of cobalt and nickel is feasible. Cobalt and nickel were extracted from 0.25 M sodium salicylate solution, adjusted to pH 4.7, with 10 ml of 5% Aliquat 336 in toluene. Cobalt was stripped selectively from the organic phase with 1 M NaOH and determined volumetrically.[8] Finally, nickel was stripped from the Aliquat 336 solution with 1 M ammonia solution and determined volumetrically.[8] The results of this separation are given in Table 5.

Applications

Analysis of alloys

High Speed Tool Steel (2.0 g dissolved in 15 ml of 1 + 2 HNO_3 and 4 ml of 4 M HCl, finally diluted to 250 ml with distilled water), Cupronickel (0.05 g dissolved in 5 ml of concentrated HCl and diluted to 250 ml with distilled water), Nimonic 901, Monel Alloy 400 and Commercial Nickel (62, 33 and 20 mg, respectively, dissolved in concentrated HCl and diluted to 250 ml with distilled water) were analysed by using the recommended procedure. The recoveries of cobalt and nickel were ≥99.0%. The results are reported in Table 6.

Analysis of environmental samples

By use of the proposed method nickel was determined in industrial wastewater samples collected from the Maharashtra Pollution Control Board, Central Laboratory, New Bombay. The recovery of nickel was reproducible and accurate (Table 7).

References

1. McClellan, B. E., and Benson, V. M., *Anal. Chem.*, 1964, **36**, 1985.
2. Sato, T., *J. Inorg. Nucl. Chem.*, 1967, **29**, 547.
3. Mahlmann, H. A., Leddicott, G. W., and Moore, F. L., *Anal. Chem.*, 1954, **26**, 1939.
4. Goto, T., and Ozaki, T., *Mizu Shori Gijutsu*, 1979, **20**, 1139.
5. de Jong, G. J., and Brinkman, U. A. Th., *J. Radioanal. Chem.*, 1977, **35**, 223.
6. Sato, T., *J. Chem. Technol. Biotechnol.*, 1979, **29**, 39.
7. Gorlach, V. F., *Ukr. Khim. Zh.*, 1974, **40**, 760.
8. Vogel, A. I., "A Text-book of Quantitative Inorganic Analysis," Longman Green, London, 1961, pp. 358, 433, 435, 436 and 443.
9. Marczenko, Z., "Spectrophotometric Determination of Elements," Ellis Horwood, Chichester, 1976, pp. 216, 227, 311, 345 and 372.

Paper 0/01137A
Received March 14th, 1990
Accepted July 10th, 1990

Fluorogenic Reagents: 4-Aminosulphonyl-7-hydrazino-2,1,3-benzoxadiazole, 4-(*N,N*-Dimethylaminosulphonyl)-7-hydrazino-2,1,3-benzoxadiazole and 4-Hydrazino-7-nitro-2,1,3-benzoxadiazole Hydrazine for Aldehydes and Ketones

Sonoko Uzu, Susumu Kanda and Kazuhiro Imai*
Branch Hospital Pharmacy, University of Tokyo, 3-28-6 Mejirodai, Bunkyo-ku, Tokyo 112, Japan

Kenichiro Nakashima and Shuzo Akiyama
Faculty of Pharmaceutical Sciences, Nagasaki University, 1-14 Bunkyo-Machi, Nagasaki 852, Japan

Fluorogenic reagents for aldehydes and ketones, *viz.*, 4-aminosulphonyl-7-hydrazino-2,1,3-benzoxadiazole (ABD-H) and 4-(*N,N*-dimethylaminosulphonyl)-7-hydrazino-2,1,3-benzoxadiazole (DBD-H) and also purified 4-hydrazino-7-nitro-2,1,3-benzoxadiazole hydrazine (NBD-H.NH_2NH_2) were synthesised. These reagents are not fluorescent; however, their reaction products with aldehydes and ketones fluoresce at wavelengths from 548 to 580 nm with excitation from 450 to 470 nm. Both ABD-H and DBD-H exhibited similar reactivity and were more reactive than NBD-H.NH_2NH_2. The respective pseudo-first-order reaction rate constants for the production of the hydrazone of propionaldehyde with ABD-H, DBD-H and NBD-H.NH_2NH_2 were 8.9×10^{-2}, 7.2×10^{-2} and 4.2×10^{-2} min^{-1} (the reaction was carried out in 0.0025% trifluoroacetic acid in acetonitrile at room temperature, 22 °C). The detection limits using the manual method (*i.e.*, measurement of fluorescence intensity) for the hydrazones of aldehydes and ketones with ABD-H, DBD-H and NBD-H.NH_2NH_2 were in the μM range. The substrate blank fluorescence with ABD-H was half of that with DBD-H and NBD-H.NH_2NH_2. The reaction products were separated and analysed by reversed-phase high-performance liquid chromatography (HPLC) with spectrofluorimetric detection. The detection limits for propionaldehyde were 1040, 120 and 35.0 fmol with ABD-H, DBD-H and NBD-H.NH_2NH_2, respectively, and those for heptan-4-one were 2690, 560 and 673 fmol, respectively. Of the three reagents, DBD-H is recommended for the sensitive detection of ketones and NBD-H.NH_2NH_2 for the detection of aldehydes. The detection limits for aldehydes and ketones by HPLC were in the sub-pmol to pmol range.

Keywords: *Fluorogenic reagents for aldehydes and ketones; 4-aminosulphonyl-7-hydrazino-2,1,3-benzoxadiazole; 4-(N,N-dimethylaminosulphonyl)-7-hydrazino-2,1,3-benzoxadiazole; 4-hydrazino-7-nitro-2,1,3-benzoxadiazole hydrazine; high-performance liquid chromatography*

There are many biologically important compounds in nature that have a carbonyl moiety in their skeleton, such as sugars and oxo-steroids. The sensitive determination of these compounds has been performed usually by derivatisation with fluorogenic reagents such as dansylhydrazine (5-hydrazino-1-naphthalene-*N,N*-dimethylsulphonamide, DNS-H)[1,2] and 4-hydrazino-7-nitro-2,1,3-benzoxadiazole (NBD-H)[3] followed by the separation and detection of sugars,[4,5] oxo-steroids[6–10] and various aldehydes and ketones[3] by high-performance liquid chromatography (HPLC). The reagent DNS-H has been reported to afford a high fluorescent background, produced by the reagent itself. To remove the excess of reagent, high-performance gel-permeation chromatography has been adopted.[9,10] Recently anthracence-1- and 2-carboxylic acid hydrazides and *O*-(1-, 2- and 9-anthrylmethyl)hydroxylamines have been used as fluorogenic labelling reagents for carbonyl compounds.[11] However, these reagents also fluoresce themselves. The physico-chemical properties of NBD-H, including melting-point and elemental analysis, have not been described owing to the difficulty in obtaining the pure compound.[3]

In order to study the feasibility of using aryl hydrazines having a 2,1,3-benzoxadiazole skeleton, such as NBD-H, for the sensitive detection of aldehydes and ketones, two hydrazino-benzoxadiazoles namely, 4-aminosulphonyl-7-hydrazino-2,1,3-benzoxadiazole (ABD-H) and 4-(*N,N*-dimethylaminosulphonyl)-7-hydrazino-2,1,3-benzoxadiazole (DBD-H) and also purified 4-hydrazino-7-nitro-2,1,3-benzoxadiazole hydrazine (NBD-H.NH_2NH_2) have been synthesised and their reactivities towards aldehydes and ketones, physico-chemical properties, fluorescence characteristics and the liquid chromatographic detection of their hydrazones have been investigated.

* To whom correspondence should be addressed.

Experimental

Materials

Acetonitrile, methanol and water of HPLC grade, and acetone, trifluoroacetic acid (TFA) and *p*-hydroxybenzaldehyde were purchased from Wako Pure Chemicals (Tokyo, Japan). Propionaldehyde, butyraldehyde, heptan-4-one and 4′-ethylacetophenone and all of the other chemicals used were of analytical-reagent grade obtained from Tokyo Kasei Kogyo (Tokyo, Japan). The 4-(aminosulphonyl)-7-fluoro-2,1,3-benzoxadiazole (ABD-F[12]) and 4-fluoro-7-nitro-2,1,3-benzoxadiazole (NBD-F[13]) were from Wako Pure Chemicals, and 4-(*N,N*-dimethylaminosulphonyl)-7-fluoro-2,1,3-benzoxadiazole (DBD-F[14]) was from Tokyo Kasei Kogyo.

Apparatus

Proton nuclear magnetic resonance spectra were recorded on a JEOL Model JNM-FX-90Q spectrometer at 90 MHz using tetramethylsilane as an internal standard. Infrared (IR) spectra were obtained with a JASCO Model IRA 810 spectrophotometer using potassium bromide discs. Electron impact mass spectrometry (EI-MS) was performed with a JEOL JMS-DX-303 instrument. For manual measurements a Hitachi 650-60 fluorescence spectrophotometer with a 1-cm quartz cell was used. Ultraviolet (UV), visible and fluorescence wavelengths were obtained without spectral correction. Reaction temperatures were controlled by a Mini Thermo Unit L-1 (Taiyo Bussan, Tokyo, Japan).

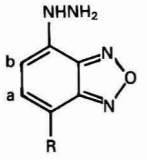

ABD-H; R = SO_2NH_2
DBD-H; R = $SO_2N(CH_3)_2$
NBD-H.NH_2NH_2; R = NO_2.NH_2NH_2

Fig. 1. Structures of ABD-H, DBD-H and NBD-H.NH_2NH_2

High-performance Liquid Chromatography

An L-6200 Intelligent Pump (Hitachi Seisakusho, Tokyo, Japan) equipped with a Rheodyne injector (Model 7125, Cotati, CA, USA) was used. The data were processed by a C-RIA Chromatopac (Shimadzu Seisakusho, Kyoto, Japan). A TSK-LS 80Tm (ODS) column [150 × 4.6 mm i.d., 5 μm (Tosoh, Tokyo, Japan)] was used at ambient temperature. A Hitachi F-1000 fluorescence spectrophotometer equipped with a 12-μl flow cell was used to monitor eluates from the column. All mobile phases were de-gassed by aspiration under sonication on a Bransonic 42 before use. The eluent flow-rate was 1.0 ml min^{-1}.

Synthesis of ABD-H, DBD-H and NBD-H.NH_2NH_2 (Fig. 1)

4-Aminosulphonyl-7-fluoro-2,1,3-benzoxadiazole (ABD-F) (24 mg, 0.11 mmol) was dissolved in 3 ml of acetonitrile. After the addition of 10 μl of 98% hydrazine hydrate, the mixture was heated at 50–55 °C for 20 min in the dark. After evaporation, the residue was recrystallised from methanol to give ABD-H [yellow - orange needles, yield 18 mg (71%)]: m.p. 184–185 °C (decomp.); δ_H[$(CD_3)_2SO$], 6.54 (1 H, d, J_{ab} = 8.1 Hz, H^a or H^b), 7.83 (1 H, d, J_{ab} = 8.1 Hz, H^a or H^b); IR (KBr), 1640, 1560, 3370 cm^{-1}; UV $\lambda_{max.}$ (in CH_3CN), 258 nm (ε = 4100 l mol^{-1} cm^{-1}); EI-MS, *m/z* 229 (M^+); calculated for $C_6H_7N_5O_3S$, C 31.44, H 3.08, N 30.55, S 13.99%; found, C 30.94, H 2.99, N 29.89, S 13.82%.

4-(*N,N*-Dimethylaminosulphonyl)-7-fluoro-2,1,3-benzoxadiazole (DBD-F) (80 mg, 0.33 mmol) was dissolved in 12 ml of acetonitrile. The same treatment (50–55 °C for 20 min) as described above for ABD-F with 40 μl of 98% hydrazine hydrate was performed and the crude product obtained was then recrystallised from methanol to give DBD-H [reddish brown crystals, yield 60 mg (71%)]: m.p. 138–139 °C (decomp.); δ_H ($CDCl_3$), 2.87 (6 H, s, Me), 6.67 (1 H, d, J_{ab} = 7.9 Hz, H^a or H^b), 7.93 (1 H, d, J_{ab} = 7.9 Hz, H^a or H^b); IR (KBr), 1575, 3330 cm^{-1}; UV $\lambda_{max.}$ (in CH_3CN), 246 nm (ε = 4300 l mol^{-1} cm^{-1}); EI-MS, *m/z* 257 (M^+); calculated for $C_8H_{11}N_5O_3S$, C 37.35, H 4.31, N 27.23, S 12.47%; found, C 37.15, H 4.23, N 27.11, S 12.55%.

To the NBD-F solution (50 mg, 0.27 mmol) in 10 ml of methanol were added 100 μl of 98% hydrazine hydrate in the dark. After heating at 50–53 °C for 20 min, the precipitate obtained was filtered and recrystallised from methanol to give NBD-H.NH_2NH_2 [yellow-brown crystals, yield 45 mg (73%)]: m.p. >300 °C; δ_H [$(CD_3)_2SO$], 5.79 (1 H, d, J_{ab} = 10.3 Hz, H^a or H^b), 7.01 (1 H, d, J_{ab} = 10.3 Hz, H^a or H^b); IR (KBr), 1610, 3370 cm^{-1}; UV $\lambda_{max.}$ (in CH_3CN), 225 nm (ε = 5200 l mol^{-1} cm^{-1}); EI-MS, *m/z* 195 (M^+); calculated for $C_6H_5N_5O_3.N_2H_4$, C 31.72, H 3.99, N 43.16%; found, C 31.66, H 3.85, N 42.71%.

Synthesis of the Hydrazones of Propionaldehyde and Acetone With ABD-H, DBD-H and NBD-H.NH_2NH_2

The ABD-H (17 mg, 0.074 mmol) in 10 ml of methanol was added to propionaldehyde (43 mg, 0.74 mmol) in 5 ml of methanol. The mixture was refluxed for 30 min. After evaporation of the reaction solvent, the residue obtained was recrystallised from diethyl ether - benzene to give the hydrazone of propionaldehyde with ABD-H [yellowish orange powder, yield 9 mg (45%)]: m.p. 178–180 °C; δ_H ($CDCl_3$), 6.98 (1 H, d, J_{ab} = 8.0 Hz, H^a or H^b), 8.00 (1 H, d, J_{ab} = 8.0 Hz, H^a or H^b), 7.35 (1H, t, =CH–), 2.4–2.6 (2 H, m, $-CH_2-$), 1.20 (3H, t, *J* = 7.1 Hz, Me), 5.12 (2H, s, $-NH_2$), 8.56 (1 H, s, NH); IR (KBr), 1580, 1615, 3250 cm^{-1}; fluorescence in CH_3CN - H_2O (1 + 1, v/v), $\lambda_{max.}$(excitation), 450 nm; $\lambda_{max.}$(emission), 570 nm; EI-MS, *m/z* 269 (M^+); calculated for $C_9H_{11}N_5O_3S$, C 40.14, H 4.12, N 26.01, S 11.91%; found, C 40.53, H 4.13, N 25.91, S 11.75%.

The ABD-H (20 mg, 0.087 mmol) in 10 ml of acetone was refluxed for 30 min. After cooling to room temperature, the mixture was evaporated. The residue obtained was recrystallised from acetone - benzene to give the hydrazone of acetone with ABD-H [yellowish orange powder, yield 8 mg (34%)]: m.p. 183–185 °C; δ_H ($CDCl_3$), 7.00 (1 H, d, J_{ab} = 7.9 Hz, H^a or H^b), 7.99 (1 H, d, J_{ab} = 7.9 Hz, H^a or H^b), 2.16 (3 H, s, Me), 2.07 (3 H, s, Me), 5.14 (2 H, s, NH_2), 8.23 (1 H, s, NH); IR (KBr), 1412, 1580, 3300 cm^{-1}, fluorescence in CH_3CN - H_2O (1 + 1, v/v), $\lambda_{max.}$ (excitation), 450 nm; $\lambda_{max.}$ (emission), 570 nm; EI-MS, *m/z* 269 (M^+); calculated for $C_9H_{11}N_5O_3S$, C 40.15, H 4.12, N 26.02, S 11.92%; found, C 40.49, H 4.09, N 25.97, S 11.86%.

The hydrazones of propionaldehyde and acetone with DBD-H and NBD-H.NH_2NH_2 were also obtained in the same manner as mentioned above (refluxed for 30 min) with the following amount of each substance: DBD-H, 0.078 mmol; propionaldehyde, 0.78 mmol; DBD-H, 0.078 mmol; acetone, 10 ml; NBD-H.NH_2NH_2, 0.15 mmol; propionaldehyde, 1.5 mmol; NBD-H.NH_2NH_2, 0.25 mmol; and acetone, 20 ml. The physico-chemical properties of each hydrazone were as follows.

Hydrazone of propionaldehyde with DBD-H: the residue obtained was recrystallised from benzene - hexane (orange powder, yield 38%): m.p. 167–168 °C (decomp.); δ_H ($CDCl_3$), 7.01 (1 H, d, J_{ab} = 7.9 Hz, H^a or H^b), 7.95 (1 H, d, J_{ab} = 7.9 Hz, H^a or H^b), 2.88 (6 H, s, NMe_2), 8.56 (1 H, s, NH), 1.20 (3 H, t, *J* = 7.2 Hz, Me), 2.3–2.6 (2 H, m, CH_2), 7.46 (1 H, t, *J* = 4.6 Hz, CH); IR (KBr), 1580, 1610, 3310 cm^{-1}; fluorescence in CH_3CN - H_2O (1 + 1, v/v), $\lambda_{max.}$ (excitation), 450 nm; $\lambda_{max.}$ (emission), 565 nm; EI-MS, *m/z* 297 (M^+); calculated for $C_{11}H_{15}N_5O_3S$, C 44.44, H 5.09, N 23.56, S 10.79%; found, C 44.70, H 4.98, N 23.49, S 10.91%.

Hydrazone of acetone with DBD-H: the residue obtained was recrystallised from benzene - hexane (yellowish brown powder, yield 38%): m.p. 140–143 °C (decomp.); δ_H ($CDCl_3$), 7.03 (1 H, d, J_{ab} = 8.1 Hz, H^a or H^b), 7.95 (1 H, d, J_{ab} = 8.1 Hz, H^a or H^b), 2.88 (6 H, s, NMe_2), 2.16 (3 H, s, CH_3), 2.06 (3 H, s, CH_3), 8.21 (1 H, s, NH); IR (KBr), 1570, 1615, 3300 cm^{-1}; fluorescence in CH_3CN - H_2O (1 + 1, v/v), $\lambda_{max.}$(excitation), 450 nm; $\lambda_{max.}$(emission), 570 nm; EI-MS, *m/z* 297 (M^+); calculated for $C_{11}H_{15}N_5O_3S$, C 44.44, H 5.09, N 23.56, S 10.79%; found, C 44.12, H 4.93, N 23.07, S 10.83%.

Hydrazone of propionaldehyde with NBD-H.NH_2NH_2: the residue obtained was recrystallised from benzene - hexane (reddish powder, yield 43%): m.p. 123–125 °C (decomp.); δ_H ($CDCl_3$), 7.05 (1 H, d, J_{ab} = 8.6 Hz, H^a or H^b), 8.53 (1 H, d, J_{ab} = 8.6 Hz, H^a or H^b), 1.23 (3 H, t, *J* = 7.5 Hz, Me), 2.3–2.7 (2 H, m, CH_2), 7.59 (1 H, t, *J* = 4.8 Hz, CH), 9.02 (1 H, s, NH); IR (KBr), 1590, 1620, 3380 cm^{-1}; fluorescence in CH_3CN - H_2O (1 + 1, v/v), $\lambda_{max.}$(excitation), 468 nm; $\lambda_{max.}$(emission), 548 nm; EI-MS, *m/z* 235 (M^+); calculated for $C_9H_9N_5O_3$, C 45.96, H 3.86, N 29.78%; found, C 45.91, H 3.89, N 29.24%.

Hydrazone of acetone with NBD-H.NH_2NH_2: the residue obtained was recrystallised from methanol (reddish powder, yield 66%): m.p. 181–182 °C (decomp.); δ_H ($CDCl_3$), 7.06 (1 H, d, J_{ab} = 8.6 Hz, H^a or H^b), 8.53 (1 H, d, J_{ab} = 8.6 Hz, H^a or

H[b]), 2.20 (3 H, s, Me), 2.11 (3 H, s, Me), 8.64 (1 H, s, NH); IR (KBr), 1580, 1620, 3330 cm^{-1}; fluorescence in CH_3CN - H_2O (1 + 1, v/v), $\lambda_{max.}$ (excitation), 468 nm; $\lambda_{max.}$ (emission), 550 nm; EI-MS, *m/z* 235 (M^+); calculated for $C_9H_9N_5O_3$, C 45.96, H 3.84, N 29.78%; found, C 46.14, H 3.90, N 29.45%.

Fluorescence Intensities and Wavelength Maxima of Hydrazones in the Buffer at Various pH Values and in Acetonitrile - Water Solution

The relative fluorescence intensities of 2.5 μM of the standard hydrazones of propionaldehyde and acetone with ABD-H, DBD-H and NBD-H.NH_2NH_2, dissolved in CH_3CN - Theorell - Stenhagen buffer (1 + 1, v/v) (for a solution pH in the range 2–12 and 0.1 M HCl for a solution with a pH of 1), were measured at the optimum wavelengths for each hydrazone at 540–570 nm (excitation at 450–470 nm). Theorell - Stenhagen buffer was prepared as follows: orthophosphoric acid (3%) was neutralised with 1 M NaOH (solution A). Citric acid (70 g l^{-1}) was also neutralised with 1 M NaOH (solution B). Solutions A and B (100 ml of each), 3.54 g of boric acid and 343 ml of 1 M NaOH were mixed and diluted to 1 l (solution C). The pH of solution C (100 ml) was adjusted to pH 12 with 0.1 M HCl and the solution diluted to 500 ml. The other buffer solutions (pH 2–11) were prepared in the same manner.

To examine the effect of organic solvent on the fluorescence intensity, an aqueous solution (5 μM) of each hydrazone containing CH_3CN in various ratios was measured at 540–570 nm (excitation at 450–470 nm).

Time Course of the Reaction of Aldehydes and Ketones With ABD-H, DBD-H and NBD-H.NH_2NH_2

A 20-μl volume of 500 μM ABD-H, DBD-H or NBD-H.NH_2NH_2, 10 μl of 13.9 μM propionaldehyde or acetone and 10 μl of 0.01% (or 0.02, 0.05 and 0.1%) TFA in acetonitrile were mixed in a 1.5-ml brown Eppendorf tube. The tube was capped and allowed to stand at room temperature. At fixed reaction time intervals, a portion of the reaction mixture was taken and subjected to HPLC analysis as described below. The reagent blank without propionaldehyde or acetone was treated similarly.

Measurement of Pseudo-first-order Reaction Rate Constants

The pseudo-first-order reaction rate constants were obtained under the following conditions: propionaldehyde, 3.48 μM; hydrazine, 250 μM; and 0.0025% TFA in acetonitrile at room temperature (22 °C). The calculation made was based on the peak heights of the standard hydrazones of propionaldehyde with ABD-H, DBD-H or NBD-H.NH_2NH_2.

Detection Limits of the Hydrazones in the Manual Method

Aldehydes or ketones (75 μl) (15–70 μM) in CH_3CN, 75 μl of 0.1% TFA (for aldehydes) or 1% TFA (for ketones), and 150 μl of 500 μM ABD-H, DBD-H or NBD-H.NH_2NH_2 were mixed and allowed to stand for 1 h (aldehydes) or 5 h (ketones). The fluorescence intensity was measured at each maximum wavelength. The reagent blank without carbonyl was treated in the same manner as the carbonyl samples. The detection limit was calculated as that concentration at which the fluorescence intensity of the sample was equal to three times the fluorescence intensity of the reagent blank.

High-performance Liquid Chromatography of Hydrazones

Aldehydes or ketones (10 μl) (2–3 μM), 20 μl of 500 μM, ABD-H, DBD-H or NBD-H.NH_2NH_2 and 10 μl of 0.1% TFA (for aldehydes) or 1% TFA (for ketones) were reacted in CH_3CN for 1 h (for aldehydes) or for 5 h (for ketones) at room temperature. The reaction mixture was then subjected to HPLC. Isocratic elution with CH_3CN - H_2O containing 0.05% TFA was adopted. The column eluate was monitored with fluorescence at the optimum wavelength for each hydrazone as indicated in Table 2.

Results and Discussion

According to the method used by Gubitz *et al.*,[3] NBD-H was synthesised from hydrazine with 4-chloro-7-nitro-2,1,3-benzoxadiazole (NBD-Cl), at room temperature in the dark for 1 h under a nitrogen atmosphere. The precipitate thus produced, presumably NBD-H, was washed with benzene and dried at room temperature but failed to recrystallise. However, pure NBD-H.NH_2NH_2, the hydrazine adduct, can be obtained by use of NBD-F which is about ten times more reactive than NBD-Cl.[13] The solid NBD-H.NH_2NH_2 should be kept in the dark as it turns brown when exposed to light. On the other hand, pure ABD-H and DBD-H, without the addition of hydrazine, were obtained with ABD-F[12] and DBD-F[14] as starting materials as described under Experimental. Both the reagents were light stable. The ABD-H and DBD-H were soluble in methanol and acetonitrile at a concentration of more than 5 mM, but NBD-H.NH_2NH_2 was soluble in methanol only at concentrations of less than 1 mM. Thus, for NBD-H.NH_2NH_2 at a concentration of 2.5 mM, 0.025% TFA was added to the reaction medium to achieve complete dissolution.

Effect of pH and Organic Solvent Concentration on the Fluorescence Intensities of Hydrazones of Propionaldehyde and Acetone With ABD-H, DBD-H and NBD-H.NH_2NH_2

The standard samples of each hydrazone of propionaldehyde and acetone with ABD-H, DBD-H and NBD-H.NH_2NH_2 were dissolved in CH_3CN - Theorell - Stenhagen buffers (pH 2–12) or 0.1 M hydrochloric acid (pH 1) and the fluorescence intensities were measured at the appropriate maximum wavelengths (548–570 nm) for each hydrazone with excitation at 450–470 nm. As shown in Fig. 2(*a*) and (*b*), almost constant fluorescence intensities were obtained for the hydrazone with ABD-H and DBD-H in the pH range 2–9. The intensities with DBD-H were about three times those found with ABD-H and gradually decreased outside this pH range. The intensities of the hydrazones with NBD-H.NH_2NH_2, however, were different from those of ABD-H and DBD-H. The maximum intensities were obtained at pH 2–3 and the lowest from pH 6 to 12. At pH 2, the intensities of the hydrazones with NBD-H.NH_2NH_2 were about seven times higher than those with DBD-H and about 12 times those observed with ABD-H, while at pH 7–12, the intensities were less than those with ABD-H and DBD-H. The greater electronegativity (discussed below) at the *para* position to the hydrazine moiety would enhance the fluorescence intensity of the hydrazone below pH 6. The same trend in fluorescence intensity was observed for the NBD-amines (the reaction products of amines with NBD-F), DBD-amines (the reaction products of amines with DBD-F) and ABD-amines (the reaction products of amines with ABD-F) (data not shown). Considering these results, the fluorescence intensity of the hydrazone with 7-hydrazino-2,1,3-benzoxadiazole-4-sulphonate (SBD-H) would be lower than that of the hydrazone with ABD-H. Thus, the preparation of SBD-H from ammonium 7-fluoro-2,1,3-benzoxadiazole-4-sulphonate (SBD-F)[15] was not carried out.

As to the effect of organic solvent composition on the fluorescence intensities, the larger ratio of organic solvent (acetonitrile) to water gave the higher intensities for the six hydrazones as shown in Fig. 3(*a*) and (*b*). This trend was also mentioned, but without data, for the hydrazone with NBD-H by Gubitz *et al.*[3]

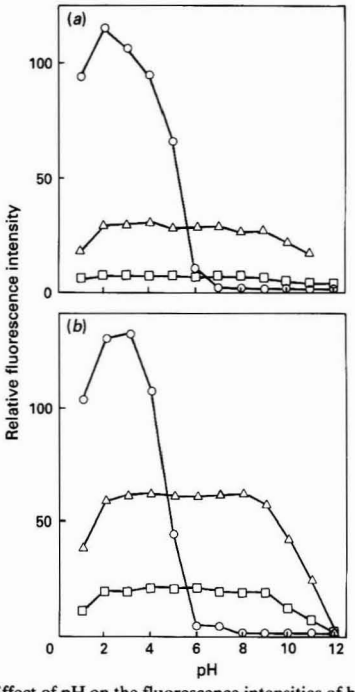

Fig. 2. Effect of pH on the fluorescence intensities of hydrazones of propionaldehyde and acetone with ABD-H, DBD-H and NBD-H.NH_2NH_2. The hydrazones of (*a*) propionaldehyde and (*b*) acetone were dissolved in CH_3CN - Theorell - Stenhagen buffer (pH 2–12) or 0.1 M HCl (1 + 1, v/v) at a concentration of 5 μM for each hydrazone. The fluorescence intensities were measured at 570 nm ($\lambda_{ex.}$ = 450 nm), 565 nm ($\lambda_{ex.}$ = 450 nm) and 550 nm ($\lambda_{ex.}$ = 470 nm) for the hydrazones with □, ABD-H; △, DBD-H; and ○, NBD-H.NH_2NH_2, respectively

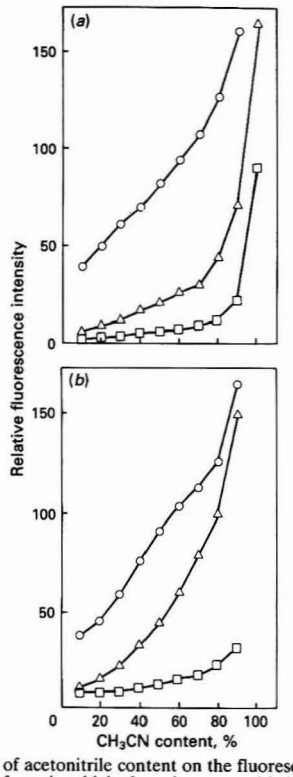

Fig. 3. Effect of acetonitrile content on the fluorescence intensities of hydrazones of propionaldehyde and acetone with ABD-H, DBD-H and NBD-H.NH_2NH_2. The hydrazones of (*a*) propionaldehyde or (*b*) acetone were dissolved at a concentration of 1 μM in solutions of various ratios of CH_3CN to H_2O containing 0.05% TFA. The fluorescence intensities were measured at 570 nm ($\lambda_{ex.}$ = 450 nm), 565 nm ($\lambda_{ex.}$ = 450 nm) and 550 nm ($\lambda_{ex.}$ = 470 nm) for the hydrazones with □, ABD-H; △, DBD-H; and ○, NBD-H.NH_2NH_2, respectively

Comparison of the Reactivities of ABD-H, DBD-H and NBD-H.NH_2NH_2 Towards Aldehydes and Ketones

As the reactivity of 4-fluorobenzofurazan towards nucleophiles (*e.g.*, thiols and amines) was dependent on the electron withdrawing effect of the substituent at the 7 position of 4-fluorobenzofurazan, the order was NBD-F, DBD-F and ABD-F (electron withdrawing activity, NO_2>$SO_2N(CH_3)_2$>SO_2NH_2).[14,16] Thus the order of reactivity of ABD-H, DBD-H and NBD-H.NH_2NH_2 towards aldehydes and ketones would be in this order because the reaction of hydrazines with aldehydes and ketones proceeds via nucleophilic attack of the carbonyl group.

In a preliminary experiment, the reactivity of acetone with NBD-H.NH_2NH_2 was tested in methanol - water (3 + 1, v/v) as suggested by Gubitz *et al.*,[3] *i.e.*, 1.6–5 mM acetone, 8–25 mM NBD-H in methanol at 50 °C for 30 min. However, NBD-H.NH_2NH_2 was not soluble in methanol at a concentration greater than 1 mM and no derivatisation of acetone occurred under these conditions in methanol - water. Then, hydrochloric acid (0.025 or 0.25 M) was added to the latter reaction mixture. The yields were 48.3 and 58.5%, respectively, for a 30-min reaction. To test the negative effect of water further, the reaction was performed with 0.025% TFA in acetonitrile. Under these conditions, the reaction proceeded and was complete in 30 min. The effect of the concentration of TFA was further investigated. The reaction yields decreased with decreasing concentration from 0.025 to 0.0025%. When the concentration was increased further, more by-product peaks were observed on the liquid chromatogram as described below.

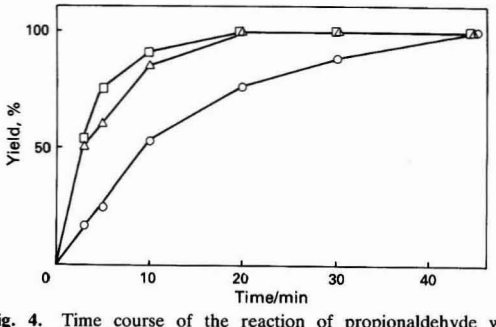

Fig. 4. Time course of the reaction of propionaldehyde with ABD-H, DBD-H and NBD-H.NH_2NH_2. Propionaldehyde (3.48 μM) was reacted with 250 μM ABD-H, DBD-H or NBD-H.NH_2NH_2 in CH_3CN containing 0.25% TFA at room temperature for various periods of time. The reaction mixtures were subjected to HPLC analysis and each hydrazone with □, ABD-H; △, DBD-H; and ○, NBD-H.NH_2NH_2 was detected at 570 nm ($\lambda_{ex.}$ = 450 nm), 565 nm ($\lambda_{ex.}$ = 450 nm) and 550 nm ($\lambda_{ex.}$ = 470 nm), respectively

When the reaction mixture in 0.025% TFA in acetonitrile was stored in a refrigerator for 1 week, no degradation of the hydrazone of propionaldehyde with ABD-H, DBD-H or NBD-H.NH_2NH_2 was observed. However, several peaks at the front of the chromatograms became larger and interfered with the detection of the relatively early eluting hydrazones such as that of acetone, especially for the reaction with NBD-H.NH_2NH_2.

As shown in Fig. 4, the reactivities of propionaldehyde with ABD-H and DBD-H were higher than that with NBD-H.NH_2NH_2 under the same reaction conditions (0.025% TFA). The reactivities of acetone with these reagents were lower than those of propionaldehyde as shown in Fig. 5 (curve A). Thus, 0.25% TFA was necessary for the reaction.

The pseudo-first-order rate constants at room temperature for the production of the hydrazone of propionaldehyde with ABD-H, DBD-H and NBD-H.NH_2NH_2 were 8.9×10^{-2}, 7.2×10^{-2} and 4.2×10^{-2} min^{-1}, respectively.

Selectivity of the Reaction and the Detection Limits in the Manual Method

Table 1 shows the detection limits for aldehydes and ketones in the manual method. Aldehydes were detected at similar sensitivity with the three reagents except *p*-hydroxybenzaldehyde. For ketones, the detection limits for hydrazones with ABD-H and DBD-H were half those obtained for NBD-H.NH_2NH_2. The values for blank fluorescence intensities without substrates for ABD-H were half those found with DBD-H and NBD-H.NH_2NH_2. The hydrazones of ketones with DBD-H fluoresced about twice as much as those with ABD-H and NBD-H.NH_2NH_2. Thus, ABD-H gave the lowest detection limits and should be suitable for detecting aldehydes and ketones in the manual method. Alanine and proline as representatives of amino acids which are abundant in the environment were not detected with all three of the reagents at a concentration of 100 μM.

High-performance Liquid Chromatographic Separation and Detection of Hydrazones of Aldehydes and Ketones With ABD-H, DBD-H and NBD-H.NH_2NH_2

As indicated in Fig. 2, more sensitive detection could be achieved in less polar solvents. This means that separation of the hydrazones should be carried out in the normal-phase mode. However, the reversed-phase mode was adopted in this work as it is more popular and easy to use. The chromatograms of the hydrazones of propionaldehyde with ABD-H, DBD-H and NBD-H.NH_2NH_2 are shown in Fig. 6(*a*), (*b*) and (*c*), respectively. They were obtained after complete reaction under the following conditions: propionaldehyde, 1.7 μM; hydrazine, 250 μM; and 0.025% TFA in acetonitrile at room temperature for 30 min (ABD-H and DBD-H) or 60 min (NBD-H.NH_2NH_2). As can be seen rather large by-product peaks appeared at the front of the chromatograms in the reaction mixture with NBD-H.NH_2NH_2 as compared with ABD-H and DBD-H. However, as suggested by Fig. 2(*a*), the quantum fluorescence yield for the hydrazone of propionaldehyde with NBD-H.NH_2NH_2 was 12 and 3 times larger than those with ABD-H and DBD-H, respectively, and resulted in a larger peak height and lower detection limits, despite the appearance of the by-products of NBD-H.NH_2NH_2 (Table 2).

For heptan-4-one, the following conditions were employed and the chromatograms obtained are shown in Fig. 7: heptan-4-one, 0.90 μM; hydrazine, 250 μM; and 0.25% TFA in acetonitrile at room temperature for 5 h. As shown in Fig. 7, there were many more by-product peaks at the front of the chromatogram in the reaction mixture with NBD-H.NH_2NH_2

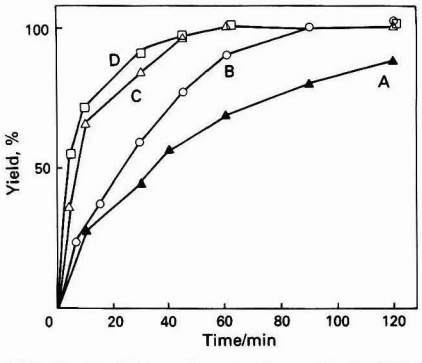

Fig. 5. Time course of the reaction of acetone with ABD-H, DBD-H and NBD-H.NH_2NH_2. Acetone (3.5 μM) was reacted with 250 μM ABD-H, DBD-H or NBD-H.NH_2NH_2 in CH_3CN containing A, 0.025% or B, C and D, 0.25% TFA at room temperature for various periods of time. The reaction mixtures were subjected to HPLC analysis and the hydrazones with D, ABD-H; A and C, DBD-H; and B, NBD-H.NH_2NH_2 were detected at 570 nm ($\lambda_{ex.}$ = 450 nm), 565 nm ($\lambda_{ex.}$ = 450 nm) and 550 nm ($\lambda_{ex.}$ = 470 nm), respectively

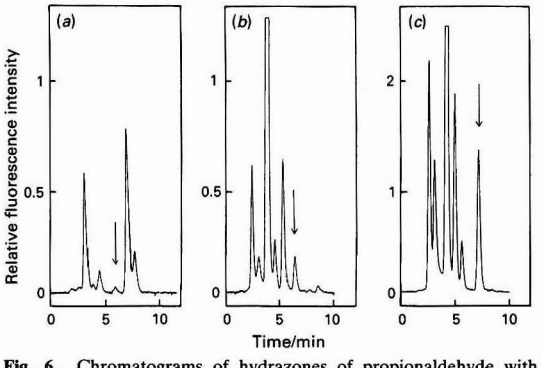

Fig. 6. Chromatograms of hydrazones of propionaldehyde with ABD-H, DBD-H and NBD-H.NH_2NH_2. Propionaldehyde (0.17 μM) was reacted with 250 μM ABD-H, DBD-H or NBD-H.NH_2NH_2 in CH_3CN containing 0.025% TFA for 1 h at room temperature. The reaction mixture containing 1.7 pmol of each hydrazone was injected on to the HPLC column with elution with CH_3CN - H_2O: (*a*) 35 + 65; (*b*) 46 + 54; and (*c*) 41 + 59 v/v, containing 0.05% TFA. The hydrazones (indicated by arrows) with (*a*) ABD-H; (*b*) DBD-H; and (*c*) NBD-H.NH_2NH_2 were detected at 570 nm ($\lambda_{ex.}$ = 450 nm), 565 nm ($\lambda_{ex.}$ = 450 nm) and 550 nm ($\lambda_{ex.}$ = 470 nm), respectively

Table 1. Detection limits and maximum wavelengths for various aldehydes and ketones with ABD-H, DBD-H or NBD-H.NH_2NH_2 in the manual method (for details see text)

	ABD-H		DBD-H		NBD-H.NH_2NH_2	
Carbonyl compound	$\lambda_{ex.}/\lambda_{em.}$/nm	LD*/μM	$\lambda_{ex.}/\lambda_{em.}$/nm	LD/μM	$\lambda_{ex.}/\lambda_{em.}$/nm	LD/μM
Propionaldehyde	450/550	6.7	450/545	7.5	468/535	6.3
Butyraldehyde	450/550	4.3	450/545	5.6	468/535	4.4
p-Hydroxybenzaldehyde	470/562	84.9	455/560	109	468/545	>200
Acetone	450/550	10.2	450/548	9.9	468/535	17.9
Heptan-4-one	450/558	18.8	450/550	17.1	468/535	56.4
4′-Ethylacetophenone	450/555	28.2	450/550	31.8	468/535	77

* LD = lower detection limit (signal to noise ratio = 3)

Table 2. Detection limits of hydrazones of aldehydes and ketones with ABD-H, DBD-H and NBD-H.NH_2NH_2 in HPLC. Each aldehyde or ketone and 250 μM ABD-H, DBD-H or NBD-H.NH_2NH_2 were reacted in CH_3CN containing 0.025% TFA (for aldehydes) or 0.25% TFA (for ketones) for 1 h (aldehydes) or 5 h (ketones) at room temperature. Then, each of the reaction mixtures was subjected to HPLC analysis with isocratic elution of CH_3CN - H_2O (41 + 59–71 + 29, v/v) containing 0.05% TFA and detected at 570 nm ($\lambda_{ex.}$ 450 nm), 565 nm ($\lambda_{ex.}$ 450 nm) and 550 nm ($\lambda_{ex.}$ 470 nm) for the hydrazone with ABD-H, DBD-H and NBD-H.NH_2NH_2, respectively

	ABD-H		DBD-H		NBD-H.NH_2NH_2	
Carbonyl compound	$\lambda_{ex.}/\lambda_{em.}$/nm	LD*/fmol	$\lambda_{ex.}/\lambda_{em.}$/nm	LD/fmol	$\lambda_{ex.}/\lambda_{em.}$/nm	LD/fmol
Propionaldehyde	450/570	1040	450/565	120	470/550	35
Butyraldehyde	450/570	1060	450/565	98	468/550	28
p-Hydroxybenzaldehyde	470/580	28800	455/570	9700	468/548	27000
Acetone	450/570	4960	450/570	905	468/560	710
Heptan-4-one	450/560	2690	450/570	560	468/552	673
4′-Ethylacetophenone	450/570	19400	450/570	3100	468/552	9600

* LD = lower detection limit (signal to noise ratio = 3)

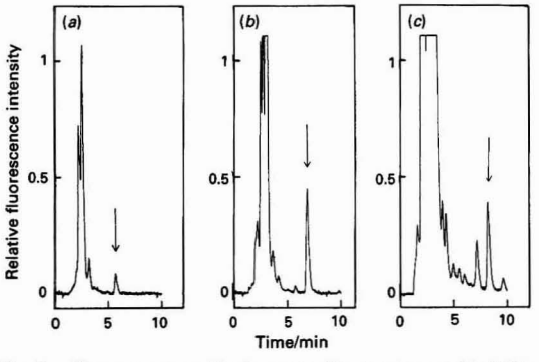

Fig. 7. Chromatograms of hydrazones of heptan-4-one with ABD-H, DBD-H and NBD-H.NH_2NH_2. Heptan-4-one (0.90 μM) was reacted with 250 μM ABD-H, DBD-H or NBD-H.NH_2NH_2 in CH_3CN containing 0.25% TFA at room temperature for 5 h. The reaction mixture containing 9.0 pmol of each hydrazone was injected on to the HPLC column with elution with CH_3CN - H_2O: (*a*) 61 + 39; (*b*) 71 + 29; and (*c*) 65 + 35, v/v containing 0.05% TFA. The hydrazones (indicated by arrows) with (*a*) ABD-H; (*b*) DBD-H and (*c*) NBD-H.NH_2NH_2 were detected at 570 nm ($\lambda_{ex.}$ = 450 nm), 465 nm ($\lambda_{ex.}$ = 450 nm) and 550 nm ($\lambda_{ex.}$ = 470 nm), respectively

as compared with ABD-H and DBD-H. It thus appears to be difficult to detect trace amounts of hydrazones of ketones with NBD-H.NH_2NH_2. Moreover, as shown in Fig. 2(*b*), the fluorescence quantum yields of the hydrazone of acetone with NBD-H.NH_2NH_2 were similar to those with DBD-H. Thus, the detection limits (signal to noise ratio of 3) for ketones with NBD-H.NH_2NH_2 were similar (Table 2). When 0.9 pmol of heptan-4-one was subjected to the method utilising DBD-H, the values obtained were 0.9 ± 0.026 pmol on triplicate runs.

In summary, the ABD-H, DBD-H and purified NBD-H.NH_2NH_2 themselves had negligible fluorescence and the hydrazones of aldehydes and ketones with ABD-H, DBD-H and NBD-H.NH_2NH_2 had long fluorescence wavelengths (excitation at 450–470 nm, emission at 548–580 nm). The reactivities of ABD-H and DBD-H were of the same order and were greater than that of NBD-H.NH_2NH_2. In the manual method, the values for the blank fluorescence intensities with ABD-H were half of those obtained with DBD-H and NBD-H.NH_2NH_2. Therefore, ABD-H is preferable for the manual method in the sensitive detection of aldehydes and ketones. However, some improvement to lower the blank fluorescence is recommended before practical application. For HPLC, the very large amounts of by-products (ascribed to blank fluorescence observed in the manual method) did not interfere as they were eluted relatively early. Thus, the contribution of the quantum efficiency of the hydrazone is important in lowering the detection limits. Therefore, NBD-H.NH_2NH_2 is preferable for the sensitive detection of aldehydes. For the sensitive detection of ketones, DBD-H is recommended as it gives fewer by-product peaks than NBD-H.NH_2NH_2.

The authors thank Dr. C. K. Lim of the Clinical Research Center for his kind review of the manuscript. Thanks are also due to the Tosoh Company for providing the TSK columns.

References

1. Graef, V., *Z. Klin. Chem. Klin. Biochem.*, 1970, **8**, 320.
2. Chayen, R., Dvir, R., Gould, S., and Harrel, A., *Anal. Biochem.*, 1971, **42**, 283.
3. Gubitz, G., Wintersteiger, R., and Frei, R. W., *J. Liq. Chromatogr.*, 1984, **7**, 839.
4. Avigad, G., *J. Chromatogr.*, 1977, **139**, 343.
5. Takeda, M., Maeda, M., and Tsuji, A., *J. Chromatogr.*, 1982, **244**, 347.
6. Kawasaki, T., Maeda, M., and Tsuji, A., *J. Chromatogr.*, 1981, **226**, 1.
7. Kawasaki, T., Maeda, M., and Tsuji, A., *J. Chromatogr.*, 1982, **232**, 1.
8. Winberger, R., Koziol, T., and Millington, G., *Chromatographia*, 1984, **19**, 452.
9. Imai, K., Higashidate, S., Tsukamoto, Y., Uzu, S., and Kanda, S., *Anal. Chim. Acta*, 1989, **225**, 421.
10. Imai, K., Higashidate, S., Nishitani, A., Tsukamoto, Y., Ishibashi, H., Shoda, J., and Osuga, T., *Anal. Chim. Acta*, 1989, **227**, 21.
11. Goto, J., Saisho, Y., and Nambara, T., *Anal. Sci.*, 1989, **5**, 399.
12. Toyo'oka, T., and Imai, K., *Anal. Chem.*, 1984, **56**, 2461.
13. Watanabe, Y., and Imai, K., *Anal. Chim. Acta*, 1981, **130**, 377.
14. Toyo'oka, T., Suzuki, T., Saito, Y., Uzu, S., and Imai, K., *Analyst*, 1989, **114**, 413.
15. Imai, K., Toyo'oka, T., and Watanabe, Y., *Anal. Biochem.*, 1983, **128**, 471.
16. Toyo'oka, T., Suzuki, T., Saito, Y., Uzu, S., and Imai, K., *Analyst*, 1989, **114**, 1233.

Paper 0/01388I
Received March 30th, 1990
Accepted July 6th, 1990

Indicators for Alkyllithium Assay. Nuclear Magnetic Resonance Evidence for the Dianion of Benzophenonetosylhydrazone

René Miranda, Abrahan Hernández and Enrique Angeles
Facultad de Estudios Superiores-Cuautitlán, Universidad Nacional Autónoma de México, Cuautitlán, Izcalli, Estado de México, Mexico

Armando Cabrera and Manuel Salmón
Instituto de Química, Universidad Nacional Autónoma de México, Circuito Exterior, Ciudad Universitaria, Coyoacán 04510, Mexico, D.F., Mexico

Pedro Joseph-Nathan
Departamento de Química, Centro de Investigación y de Estudios Avanzados, Instituto Politécnico Nacional, Apartado 14-740, Mexico, D.F., 07000 Mexico

Several benzenesulphonyl- and tosylhydrazones have been used for the routine quantitative determination of alkyllithium solutions. The structure of one of the chromophores was determined by nuclear magnetic resonance studies of the derived deuteriated molecule.

Keywords: *Indicator; alkyllithium assay; benzenesulphonylhydrazone; tosylhydrazone*

Alkyllithium compounds are very important reagents in many organic reactions and their accurate dosage is always desirable. Although commercial alkyllithium reagents[1] are carefully analysed at source, freshly purchased solutions easily deteriorate as a result of exposure to moisture and oxygen. It is therefore very important to know the concentration of alkyllithium reagents at the time of their use.

A convenient method for the determination of lithium alkyls by use of 4-biphenylmethanol, 4-biphenylacetic acid and 4-biphenylcarboxylic acid - triphenylmethane as indicators has been reported.[2] In addition, other methods, some involving more expensive commercial reagents,[3–8] and double titration methods,[9,10] have been reported.

Based on the formation of coloured dianions,[11] this paper

Table 1. Titration of alkyllithium solutions. M is the molar concentration for at least three replicate measurements and D is the deviation

Indicator	Compound number; R group	BuLi (Lot No. 1)		BuLi (Lot No. 2)		*tert*-BuLi		End-point
		M	D	M	D	M	D	
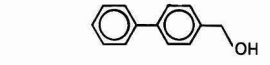	Literature[2] procedure	0.876		0.905		1.580		Orange
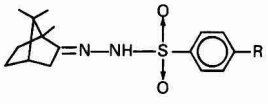	**1**; H	0.871	−0.005	0.961	+0.056	1.520	−0.060	Orange
	2; Me	0.865	+0.011	0.892	−0.013	1.495	−0.085	
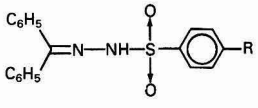	**3**; H	0.815	−0.061	0.944	+0.039	1.510	−0.070	Red - orange
	4; Me	0.865	−0.011	0.950	+0.045	1.580	0.000	
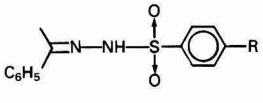	**5**; H	0.985	+0.109	1.013	+0.108	1.320	−0.260	Yellow
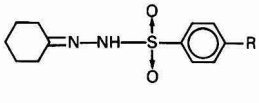	**6**; H	0.967	+0.091	1.190	+0.285	1.605	+0.025	Yellow
	7; Me	0.995	+0.119	1.250	+0.345	1.670	+0.090	
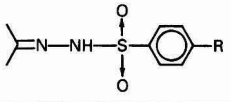	**8**; H	0.993	+0.116	1.160	+0.255	1.680	+0.100	Yellow
	9; Me	1.041	+0.164	1.260	+0.355	1.640	+0.060	

presents the use of a wide range of benzenesulphonyl- and tosylhydrazones (**1–9**) (Table 1) as an alternative method for the quantification of alkyllithium reagents. This method, in addition to providing comparable results to existing procedures, has its major advantages in being both convenient and simple, as all used substrates are easily prepared from materials that are readily available. In addition, some comments are made about the structure of the chromophore derived from benzophenonetosylhydrazone (**4**).

Experimental

Arylsulphonylhydrazones were prepared by previously reported methods[12] and stored without special precautions. All of the chemicals used were characterised by common spectroscopic methods. Proton nuclear magnetic resonance (^{1}H NMR) spectra were recorded on a Varian EM-390 spectrometer. The ^{13}C NMR spectra and HETCOR measurements were determined on a Varian Associates XL-300GS spectrometer. Mass spectra were obtained on a Hewlett-Packard 5985-B GS/MS spectrometer. All glassware, stirring bars and hypodermic needles were dried overnight at 100 °C prior to use and allowed to cool in a desiccator over anhydrous calcium chloride under vacuum before use. Analytical-reagent grade tetrahydrofuran (THF) was purchased from J. T. Baker and dried by distillation over sodium metal - benzophenone immediately prior to use. Alkyllithium solutions were obtained from previously opened containers purchased from Aldrich.

Procedure

Alkyllithium assay

An exactly weighed amount (100–200 mg) of the corresponding arylsulphonylhydrazone was placed in an oven-dried 50-ml Erlenmeyer flask containing a magnetic stirring bar. The flask was capped with a rubber septum and flushed with nitrogen before the introduction of *ca.* 10 ml of anhydrous THF. The alkyllithium solution was then added dropwise from a graduated syringe, until a sharp colour change (as indicated in Table 1) was observed. The amount of the alkyllithium solution consumed thus contained 1 equivalent of alkyllithium, relative to the weighed amount of arylsulphonylhydrazone.

[^{2}D]-Benzophenonetosylhydrazone (**4d**)

To a solution of 350 mg of benzophenonetosylhydrazone (**4**) in 10 ml of anhydrous THF were added 2 equivalents of butyllithium. The solution was immediately quenched with 1 ml of D_2O. The material recovered, after recrystallisation from ethanol, showed about 66% monodeuteriation, as measured by mass spectrometry: *m/z* 350 (M^+; 2.6%), 351 ($M^+ + 1$; 5.9), 352 ($M^+ + 2$; 1.9), 353 ($M^+ + 3$; 0.5).

Results and Discussion

The results obtained for the determination of several alkyllithium solutions using the common arylsulphonylhydrazones **1–9** are summarised in Table 1. It is obvious from these results that each reagent offers an alternative for the accurate quantification of alkyllithium concentrations. Nevertheless, compounds **1–4** are the reagents of choice as their colour changes at the equivalence point are the sharpest and they provide values in agreement with those found using published procedures.[2] In addition, compounds **5–9** can also be adapted for the routine standardisation of commercial alkyllithium solutions.

Colour at the End-point

Arylsulphonylhydrazones instantaneously develop, at the end-point of the titration, a chromophore which requires less than a 0.01 mmol excess of alkyllithium reagent. The appearance of colour is not affected in aged alkyllithium

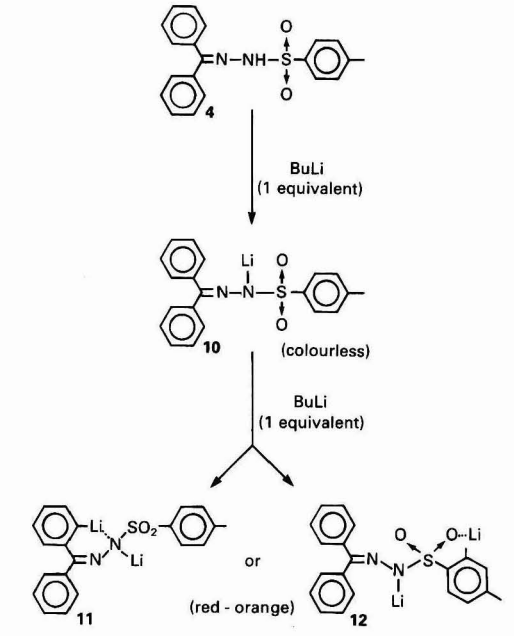

Scheme 1

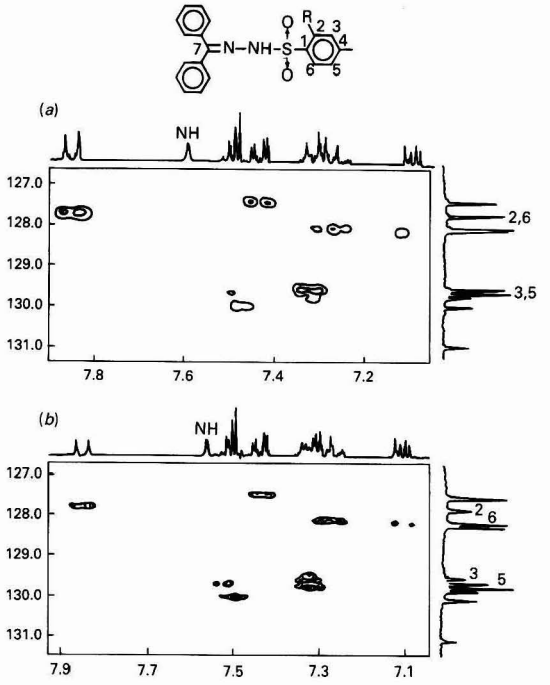

Fig. 1. Low-field region of the HETCOR spectra of (*a*) benzophenonetosylhydrazone (R = H); and (*b*) [^{2}D]-benzophenonetosylhydrazone (R = D). The values on the *x*- and *y*-axes are δ values in p.p.m.

Table 2. Carbon-13 NMR chemical shifts of benzophenonetosylhydrazone (**4**) and 2-[D]-benzophenonetosylhydrazone (**4d**) at 75.47 MHz in $CDCl_3$, δ in p.p.m. The two monosubstituted phenyl groups are non-equivalent and it was not possible to assign the signals individually, although *ipso* (*i*), *ortho* (*o*), *meta* (*m*) and *para* (*p*) carbons could be distinguished from their multiplicities in a coupled spectrum

Compound **4**		Compound **4d**	
C_7	154.25	C_7	154.25
C_4	144.14	C_4	144.14
C_i	136.39	C_i	136.39
C_1	135.49	C_1	135.49
		C_{1d}	135.40
C_i	131.08	C_i	131.08
C_p	130.08	C_p	130.08
C_p	129.85	C_p	129.85
C_m	129.76	C_m	129.76
$C_{3,5}$	129.66	C_5	129.66
		C_3	129.55
C_o	128.24	C_o	128.24
C_m	128.18	C_m	128.18
$C_{2,6}$	127.88	C_6	127.88
C_o	127.56	C_o	127.56
CH_3	21.61	CH_3	21.61

solutions containing large amounts of suspended oxides. As the reaction is performed under a nitrogen atmosphere in anhydrous THF, the suspended solids are dissolved leaving a bright, clear solution throughout the titration and therefore provide clearly visible and reproducible titration end-points.

Nature of Chromophores

It has been shown[13] that the formation of intensely coloured dianions in tosylhydrazones containing protons alpha to the carbon–nitrogen double bond lead to intermediates that decompose yielding alkenes.[14] When the diphenyltosylhydrazone, **4**, was used in the above procedure, the compound was recovered quantitatively. Nevertheless, compounds **3** and **4** show a red-orange chromophore at the end-point of the titration.

It was assumed that the dianions derived from compound **4** were formed by the abstraction of one *ortho* proton from a phenyl group or from the tosyl group, as the carbon–nitrogen double bond[15–17] and the sulphonyl group[16–18] have been recognised as powerful directors of orthometallation, thus affording both or one of two possible metallated derivatives **11** and **12** (Scheme 1). Therefore, structural evidence of the dianion seemed desirable.

In order to determine the structure of the species responsible for the chromophore, compound **4** was treated with two equivalents of BuLi and immediately quenched with D_2O. The material recovered, after recrystallisation from ethanol, showed about 66% of deuterium incorporation, as measured by mass spectrometry. The HETCOR NMR spectra of **4** and **4d** were used to establish the position of the deuterium atom as shown in Fig. 1. The ^{13}C NMR signals of both the labelled and unlabelled compounds are given in Table 2. The HETCOR experiment shows the AA′BB′ signals at 7.85 and 7.33 p.p.m., assigned to the aromatic tosyl protons, correlated with the C_2/C_6 and C_3/C_5 signals, respectively. The deuterium atom at C_2 is assigned from the decreased intensity of the signal at 127.88 p.p.m. and from the deuterium/hydrogen NMR isotope effects on ^{13}C chemical shift (DHIECS) values.[19,20] Thus, the $^2\Delta$ DHIECS at C_3 (114 p.p.b.) and at C_1 (88 p.p.b.) clearly confirm the position of the deuterium atom. These results substantiate structure **4d** (Scheme 1), showing that in this instance the aromatic protons of the tosyl group are more reactive than those *ortho* to the carbon–nitrogen double bond.

References

1. Stowell, J. C., "Carbanions in Organic Synthesis," Wiley, New York, 1979, p. 1.
2. Juaristi, E., Martínez-Richa, A., García-Rivera, A., and Cruz-Sánchez, S. J., *J. Org. Chem.*, 1983, **48**, 2603.
3. Kuyper, J., Keijzer, P. C., and Vrieze, K., *J. Organomet. Chem.*, 1976, **116**, 1.
4. Winkle, M. R., Lansinger, J. M., and Ronald, R. C., *J. Chem. Soc., Chem. Commun.*, 1980, 87.
5. Kofron, W. G., and Baclawski, L. M., *J. Org. Chem.*, 1976, **41**, 1879.
6. Watson, S. C., and Eastham, J. F., *J. Organomet. Chem.*, 1967, **9**, 165.
7. Bergbreiter, D. E., and Pendergrass, E., *J. Org. Chem.*, 1981, **46**, 219.
8. Lucette, D., and Jean-Christophe, P., *J. Org. Chem.*, 1979, **44**, 3404.
9. Gilman, H., and Haubein, A. H., *J. Am. Chem. Soc.*, 1944, **66**, 1515.
10. Gilman, H., and Cartledge, F. K., *J. Organomet. Chem.*, 1964, **2**, 447.
11. Lipton, M. F., Sorensen, C. M., Sadler, A. C., and Shapiro, R. H., *J. Organomet. Chem.*, 1980, **186**, 155.
12. Bamford, W. R., and Stevens, T. S., *J. Chem. Soc.*, 1952, 4735.
13. Shapiro, R. H., Lipton, M. F., Kolonko, K. J., Buswell, R. L., and Capuano, L. A., *Tetrahedron Lett.*, 1975, 1811.
14. Shapiro, R. H., *Org. React. NY*, 1976, **23**, 406.
15. Beak, P., and Snieckus, V., *Acc. Chem. Res.*, 1982, **15**, 306.
16. Snieckus, V., *Bull. Soc. Chim. Fr.*, 1988, 67.
17. Gschwend, H. W., and Rodríguez, H. R., *Org. React. NY*, 1979, **26**, 1.
18. Chamberlin, A. R., Stemke, J. E., and Bond, F. T., *J. Org. Chem.*, 1978, **43**, 147.
19. Morales-Ríos, M. S., and Joseph-Nathan, P., *Magn. Reson. Chem.*, 1989, **27**, 75.
20. Morales-Ríos, M. S., del Río, R. E., and Joseph-Nathan, P., *Magn. Reson. Chem.*, 1989, **27**, 1039.

Paper 0/02276D
Received May 22nd, 1990
Accepted July 18th, 1990

Transmittance Ratio Spectrometry as a Stray Radiant Energy Test Method for Optical-null Spectrophotometers

Paddy Fleming
Sligo Regional Technical College, Sligo, Ireland

A stray radiant energy (SRE) test method for optical-null double-beam spectrophotometers is described based on transmittance ratio measurements made on an absorbing species placed in a pair of matched cuvettes whose path-length ratio is maintained constant while the said path-length is gradually increased. A theoretical expression is derived which relates the coordinates of the minimum of the resulting characteristic transmittance ratio *versus* reference transmittance plot, to the relative SRE level, and to the sample cell to reference cell path-length ratio employed. The effect of sample absorption of the SRE on transmittance ratio measurements is also explored. The result obtained with a Perkin-Elmer 297 spectrophotometer is compared with that obtained by applying the SRE test method of Mielenz *et al.* to the same instrument.

Keywords: *Infrared spectrometry; optical-null spectrophotometer; stray radiant energy; path-length ratio; transmittance ratio*

Stray radiant energy (SRE), a universal problem in spectrometry, is radiation scattered by imperfections on the surface of the diffraction grating and then sensed by the detector to give spurious transmittance readings. An optical-null double-beam spectrophotometer uses a nulling comb in the reference beam to balance sample absorption automatically, and because of its poor linearity and zero transmittance (0% T) drift, due to electrical pick-up, it makes unreliable transmittance readings below 10% T. [American Society for Testing and Materials (ASTM) E 387–84.][1] Therefore, an SRE test procedure must be designed to give transmittance readings greater than 10% T. The ASTM Test Method E 387–84, which measures the apparent transmittance of a sharp cut-off filter while keeping the transmittance reading greater than 10% T by the stepwise attenuation of the reference beam using screens of varying mesh size, is currently recommended. The nulling comb attenuates the SRE in the reference beam relative to the SRE in the sample beam and therefore the analysis proposed by the author[2] for a ratio-recording instrument must be revised. Most optical-null spectrophotometers now in use deal with the mid-infrared region. Transmittance ratio spectrometry in the infrared (IR) region uses matched cells to measure the transmittance of a sample-beam solution relative to that of an identical reference-beam solution, the sample cell being a constant factor thicker than the reference cell.

Theoretical expressions are derived in this paper showing how the relative SRE level in an optical-null double-beam spectrophotometer is related to the observable coordinates of the minimum of the transmittance ratio *versus* the true reference transmittance plot, and to the relevant sample cell to reference cell thickness ratio. The proposed analysis is applied to transmittance ratio measurements made on a Perkin-Elmer Model 297 optical-null spectrophotometer. The ensuing experimental SRE value is compared with the corresponding experimental SRE value determined using the test method of Mielenz *et al.*[3] as modified by the author[4] to suit optical-null instruments. The leading and trailing edges of a CCl_4 band-stop absorption peak were used in this latter method. The method of Mielenz *et al.*[3] gradually increases differential absorbance by wavelength scanning through the leading and trailing absorbance edges of a cut-off solution which has been placed in both the sample and reference beams, whereas the method proposed herein is to be carried out at a fixed wavelength while differential absorbance is increased by gradually increasing the path lengths of the solution held in the sample and reference beams. The recorded differential absorbance for both methods will not increase indefinitely but will peak at a value determined by the SRE level present in the instrument and by the path-length ratio in use. The terms transmittance ratio and differential absorbance are used interchangeably in the text.

The presence of test materials which may not be transparent to SRE in a spectrophotometer means that the relative SRE levels may be underestimated. This effect can be minimised by using materials having simple absorption spectra.

Formulation of Experimental Quantities

If similar solutions are placed in the cells, the sample cell being α-times thicker than the reference cell, then the transmittance ratio of the sample solution relative to the reference solution (R_σ), as per the Beer-Lambert law, is given by;

$$R_\sigma = T_\sigma^\alpha / T_\sigma = T_\sigma^{\alpha-1} \quad \ldots \quad \ldots \quad \ldots \quad (1)$$

where T_σ is the absolute transmittance of the reference sample to radiation of wavenumber σ.

However, equation (1) ignores the inevitable presence of SRE which may be absorbed by a sample. The observed transmittance ratio R'_σ is given in terms of the ratio of the transmittances of the sample and the reference beams as follows

$$R'_\sigma = \frac{T_\sigma^\alpha + sm^{\alpha A_\sigma}}{T_\sigma + R'_\sigma sm^{A_\sigma}} \quad \ldots \quad \ldots \quad \ldots \quad (2)$$

where $0 < s \ll 1$ is the relative SRE level and $0 < m \leqslant 1$ is the SRE transmittance of the reference sample whose monochromatic absorbance, A_σ ($= \log_{10} T_\sigma$), is unity.

In equation (2) it is assumed that the SRE levels in the beams of an optical-null spectrophotometer are equal when a transparent substance is present in both beams and the beams are balanced at 100% T. However, the SRE in the reference beam is attenuated (relative to the SRE in the sample beam) by the nulling comb as it moves to balance the beams optically whenever the sample beam becomes more monochromatically absorbing than the reference beam, hence the presence of R'_σ in the denominator of equation (2). A typical optical nulling arrangement in a double-beam optical-null spectrophotometer is shown in Fig. 1.

Equation (2) is formulated so as to accommodate the progressive attenuation of the SRE in both beams as the thickness of the cells is increased. If m is the SRE transmittance of the reference beam when its monochromatic absorbance is unity, then m^{A_σ} is its SRE transmission when its

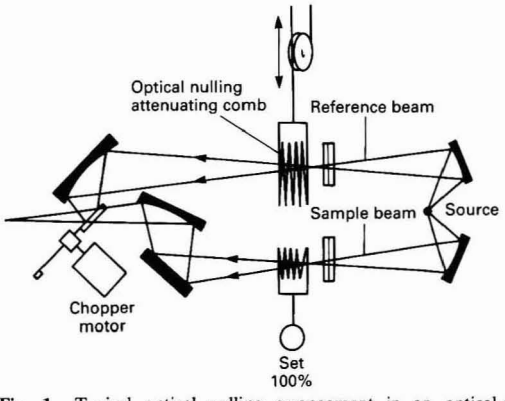

Fig. 1. Typical optical nulling arrangement in an optical-null double-beam spectrophotometer

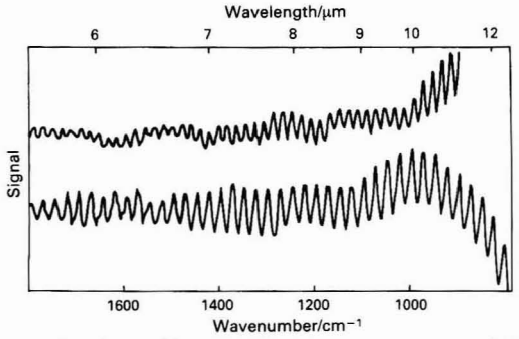

Fig. 2. Interference fringe patterns generated by the empty variable path-length cells. The reference cell, which was set to 250 μm (nominal), gave the upper trace and the sample cell, which was set to 200 μm (nominal), gave the lower trace

monochromatic absorbance is A_σ and $m^{\alpha A_\sigma}$ is the corresponding SRE transmittance of the sample beam.

$$sm^{A_\sigma}R'^2_\sigma + T_\sigma R'_\sigma - (T^2_\sigma + sm^{\alpha A_\sigma}) = 0 \quad .. \quad (3)$$

Equation (3) gives the following positive solution

$$R'_\sigma = \frac{\sqrt{T^2_\sigma + 4(T^2_\sigma + sm^{\alpha A_\sigma})sm^{A_\sigma}} - T_\sigma}{2sm^{A_\sigma}} \quad .. \quad (4)$$

Equation (4) follows equation (1) for large values of T_σ but SRE causes equation (4) to deviate from equation (1) as T_σ decreases so that equation (4) will have a minimum, R'_σ (min) = ρ at $T_\sigma = \tau$, where the first derivative of R'_σ with respect to T_σ is zero. This derivative method, when applied to equation (4) and assuming that the sample is transparent to SRE, *i.e.*, $m = 1$, yields (*cf.* Appendix)

$$s = \frac{(\alpha - 1)\tau^\alpha}{1 - (\alpha\tau^{\alpha-1})^2} \quad .. \quad .. \quad .. \quad (5)$$

If equation (5) is substituted into equation (4) then the following relationship ensues between the coordinates of the minimum of the transmittance ratio *versus* reference transmittance curve, *i.e.*, τ and ρ, and the thickness ratio, *i.e.*, α

$$\rho = \alpha\tau^{\alpha-1} \quad .. \quad .. \quad .. \quad .. \quad (6)$$

If equation (6) is substituted into equation (5) then

$$s = \frac{(\alpha - 1)(\rho/\alpha)^{\alpha/(\alpha-1)}}{1 - \rho^2} \quad .. \quad .. \quad .. \quad (7)$$

Both τ and ρ can be observed in this spectrophotometric method. However, the function defined in equation (4) is flat-bottomed (*cf.* Figs. 3 and 4). Therefore, the SRE estimate based on equation (7) is more reliable than that based on equation (5).

The method of Mielenz *et al.*,[3] as generalised by Fleming,[4] gives the relative SRE level as follows

$$s = \frac{(\alpha - 1)(\rho'/\alpha)^{\alpha/(\alpha-1)}}{n^\alpha - n\rho'^2} \quad .. \quad .. \quad (8)$$

where ρ′ stands for the transmittance ratio minima of the Mielenz peaks encountered in the differential scan through the leading and trailing absorption edges of the chosen band-stop peak and n is the SRE transmittance of unit thickness of reference sample. If $n = 1$ it can be seen that equations (7) and (8) have identical forms and this suggests that both SRE test methods are essentially identical.

Methods and Materials

Zero transmittance (0% T) is checked automatically under black-out conditions in ratio-recording spectrophotometers but it must be manually checked from time to time in optical-null recording spectrophotometers. Ratio-recording instruments utilise a live 0% T, yielding real information under black-out conditions, in contrast to optical-null instruments which have no energy in either beam at 0% T, where the recorder pen does not move. Full-scale transmittance is automatically set at all wavelengths in a double-beam ratio-recording instrument when a pair of matched samples is placed in the beams. It is usual to balance the beams of an optical-null double-beam instrument optically at 100% T with a pair of matched samples in its beams by manually adjusting the optical attenuator in the sample beam. The amplifier gain in optical-null IR instruments is optimised for the spectral region of interest.

Transmittance ratio measurements in the IR are made with a Perkin-Elmer 297 spectrophotometer on a given pure liquid sample having a broad isolated absorbance peak, *e.g.*, CCl_4 has such a peak at 1548 cm^{-1}. The CCl_4 is placed in a pair of mounted variable path-length matched cells. The path length of a cell is controlled by an accurately graduated micrometer which may be set at ever increasing thicknesses in the range $0.050 \leqslant b(\text{mm}) \leqslant 10$ with a precision of ±0.002 mm. This allows transmittance ratio determinations to be made at ever increasing cell thicknesses while keeping a fixed cell thickness ratio between the sample and reference cells. The graduations of the variable path-length cells were checked by measurements of the interference fringe patterns generated by placing each empty cell in turn in the sample beam and scanning slowly throughout the mid-IR region of an optical-null spectrophotometer (Fig. 2). The thickness of the reference cell was thus calculated to be 255 μm when the micrometer was set to read 250 μm. The thickness of the sample cell was likewise calculated to be 200 μm for a micrometer setting of 200 μm. The differential zero error of the sample and reference cells was established by measuring the differential absorbances of the CCl_4 peaks at 1548, 1253 and 1218 cm^{-1}, for reference micrometer settings in the range $100 \leqslant b(\mu\text{m}) \leqslant 450$, $\alpha_b = 2$ and by using the Perkin-Elmer 983 spectrophotometer, extrapolating to zero differential absorbance. This yields an average differential zero error of −3 μm. The zero error in the reference micrometer was not allowed for in this experiment. However, it had a diminishing effect on the chosen cell thickness ratio as the cell thicknesses were increased from an initial reference thickness of 100 μm.

The sample and reference beams are optically balanced at 100% T for equal thickness of sample in both cells. The sample

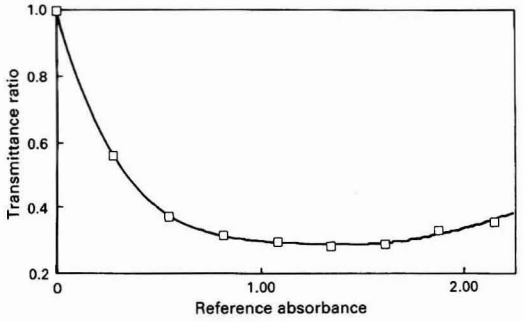

Fig. 3. Experimental transmittance ratio *versus* reference absorbance at the CCl_4 1548 cm^{-1} peak for a thickness ratio, α_b, of 2. The thickness range of the reference cell is $0.1 \leqslant b_r$ (mm) $\leqslant 0.8$

Table 1. Measurements and ensuing calculations on Fig. 3 together with the corresponding measurements and calculations arising from applying the generalised SRE test method of Mielenz *et al.*

Instrument type	Perkin-Elmer Model 297
Cell path-length ratio, α_b	2
SRE test method	Transmittance ratio spectrometry
CCl_4 peak wavenumber	1548 cm^{-1}
Slit-width	Slit programme 3
Transmittance ratio minimum, ρ	0.28
Relative SRE level based on equation (7) for $m = 1$, s	0.02 (2%)
SRE test method	Mielenz
CCl_4 leading-edge Mielenz peak wavenumber	1590 cm^{-1}
CCl_4 trailing-edge Mielenz peak wavenumber	1490 cm^{-1}
Leading-edge Mielenz peak average transmittance, ρ'	0.33
Trailing-edge Mielenz peak average transmittance, ρ'	0.38
Relative SRE level based on equation (8) and $n = 1$, s	0.04 (4%)
Relative SRE level based on specification, s	0.005 (0.5%)

cell thickness is then increased by the chosen cell thickness ratio, and its transmittance ratio relative to the reference cell can be determined. This process is repeated for increasing cell thicknesses until it is no longer possible to balance both beams optically at 100% T at 1548 cm^{-1}.

If the variable path-length cells are set wide enough then the 1548 cm^{-1} CCl_4 peak becomes a band-stop absorption peak with leading and trailing edges. The method of Mielenz *et al.*[3] is applied to this band-stop peak by scanning the differential spectrum of b (mm) CCl_4 in the reference beam and αb (mm) CCl_4 in the sample beam between 1750 and 1350 cm^{-1}, where $1 \leqslant b$ (mm) $\leqslant 1.5$ and $\alpha_b = 2$.

Experimental

The experimental transmittance ratio measurements made on the Perkin-Elmer 297 spectrophotometer are plotted in Fig. 3. The transmittance ratio minimum (ρ) is well established in the figure but the corresponding reference absorbance coordinate, $-\log \tau$, is uncertain because of the flat-bottomed shape of the experimental curve and, therefore, equation (7) is used instead of equation (5) for calculating the relative SRE level. Measurements and ensuing calculations on Fig. 3 together with the corresponding measurements and calculations arising from applying the generalised SRE test method of Mielenz *et al.*[3] are presented in Table 1.

Equation (4) is plotted in Fig. 4 for $s = 0.02$ (2%) and $m = 1$ and $m = 0.85$. Fig. 4 indicates that the absorption of SRE by

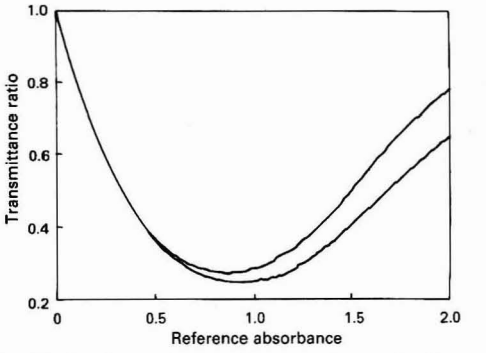

Fig. 4. Simulated transmittance ratio *versus* reference absorbance at the CCl_4 1548 cm^{-1} peak for SRE transmittances, m, of 1.0 and 0.85, a relative SRE level, s, of 0.02 and a thickness ratio, α_b, of 2

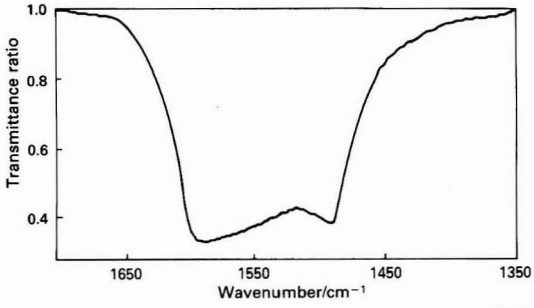

Fig. 5. Experimental Mielenz transmittance ratio spectrum of CCl_4 in a 3-mm sample cell *versus* CCl_4 in a 1.5-mm reference cell in the spectral range $1750 \geqslant \sigma$ (cm^{-1}) $\geqslant 1350$

the sample shifts the coordinates of the transmittance ratio minimum towards lower values and makes the transmittance-ratio curve more flat-bottomed. If Fig. 3 is compared with Fig. 4 then the premise that the sample is transparent to SRE, *i.e.*, $m = 1$, must be false. Therefore, calculations based on applying equation (7) underestimate the relative SRE level involved. However, the SRE transmittance of the sample is an elusive quantity and a remedy for this may lie in fitting equation (4) to the curve in Fig. 3 using realistic trial values for s and m, *i.e.*, by incrementally increasing the value for s from that calculated by applying equation (7) to Fig. 3 and simultaneously gradually decreasing m from unity until a reasonable agreement is achieved between the experimental curve and equation (4).

The differential absorbance spectrum of CCl_4 in a 3-mm sample cell plotted against CCl_4 in a 1.5-mm reference cell, in the spectral range $1750 \geqslant \sigma(cm^{-1}) \geqslant 1350$, is shown in Fig. 5.

If the absolute absorbance of 0.1 mm CCl_4 at 1548 cm^{-1} is 0.266 then the peak differential absorbance in the absence of SRE for the above Mielenz scan should have been 4. However, Mielenz SRE peaks are observed on the leading and trailing edges of the band-stop peak at 1590 and 1490 cm^{-1}, respectively. The transmittance ratio minima (ρ') of these peaks together with an estimate of SRE based on equation (8) for $n = 1$ are recorded in Table 1.

Conclusion

Optical-null spectrophotometry is now a curiousity in ultraviolet - visible spectrometry and is being displaced in the mid-IR by ratio-recording and Fourier transform instruments. However, there are many optical-null IR spectrophotometers in use and SRE affects quantitative measurements made by

such instruments. The transmittance ratio test method may be more useful for quantifying the relative SRE level in such instruments than the cut-off filter test method in use heretofore as it employs materials that are readily available and it gives transmittance scale readings greater than 10% T.

The experimental SRE levels reported in Table 1 are in the range $2 \leqslant \mathrm{SRE}(\%) \leqslant 4$. The generalised test method of Mielenz *et al.*[3] yields a 4% relative SRE level while the transmittance ratio method yields a level of 2%. These values are larger than the 0.5% specified by Perkin-Elmer but the instrument in question has been in use for nearly 20 years.

The proposed SRE test method has been refined to allow for the absorption of SRE. However, this refinement is not pursued here because the SRE transmittance of a given sample is unknown and it may vary from instrument to instrument.

Appendix

Equation (4) for $m = 1$ and $s > 0$ may be rewritten as

$$R'_\sigma = \sqrt{(T_\sigma/2s)^2 + T_\beta^\alpha/s + 1} - T_\sigma/2s \quad .. \quad \text{(A1)}$$

The first derivative of equation A1 with respect to T_σ is given by

$$\mathrm{d}R'_\sigma/\mathrm{d}T_\sigma = \frac{T_\sigma/2s^2 + \alpha T_\beta^{\alpha-1}/s}{2\sqrt{(T_\sigma/2s)^2 + T_\beta^\alpha/s + 1}} - 1/2s \quad .. \quad \text{(A2)}$$

But $\mathrm{d}R'_\sigma/\mathrm{d}T_\sigma = 0$ at $T_\sigma = \tau$ where $R'_\sigma(\mathrm{min}) = \rho$ and therefore

$$(\tau/2s)^2 + \tau^\alpha/s + 1 = (\tau/2s + \alpha\tau^{\alpha-1})^2 \quad .. \quad \text{(A3)}$$

Solving equation (A3) for s yields equation (5) in the main text

$$s = \frac{(\alpha-1)\tau^\alpha}{1-(\alpha\tau^{\alpha-1})^2} \quad .. \quad .. \quad .. \quad \text{(A4)}$$

Substituting $y = \tau^{\alpha-1}$ and using equation (A4) gives

$$\tau/s = \frac{1-(\alpha y)^2}{(\alpha-1)y} \text{ and } \tau^\alpha/s = \frac{1-(\alpha y)^2}{\alpha-1}$$

If equation (A4) is substituted into equation (A1) at $T_\sigma = \tau$ where $R'_\sigma(\mathrm{min}) = \rho$ then equation (6) can be obtained as follows

$$\begin{aligned}\rho &= \sqrt{\frac{[1-(\alpha y)^2]^2}{[2(\alpha-1)y]^2} + \frac{1-(\alpha y)^2}{\alpha-1} + 1} - \frac{1-(\alpha y)^2}{2(\alpha-1)y} \\ &= \frac{\sqrt{[1-(\alpha y)^2]^2 + 4(\alpha-1)(y^2-\alpha^2y^4) + 4(\alpha-1)^2y^2} - 1 + (\alpha y)^2}{2(\alpha-1)y} \\ &= \frac{\sqrt{(1-2\alpha y^2+\alpha^2y^2)^2} - 1 + (\alpha y)^2}{2(\alpha-1)y} \\ &= \alpha\tau^{\alpha-1} \end{aligned} \quad \text{(A5)}$$

References

1. ASTM Committee E-13, "Manual on Recommended Practical Spectrophotometry," ASTM E 387–84, American Society for Testing and Materials, Philadelphia, 1984, pp. 136–145.
2. Fleming, P., *Analyst*, 1990, **115**, 375.
3. Mielenz, K. D., Weidner, V. R., and Burke, R. W., *Appl. Opt.*, 1982, **21**, 3354.
4. Fleming, P., *Appl. Spectrosc.*, 1990, **44**, 522.

Paper 0/00137F
Received January 9th, 1990
Accepted July 3rd, 1990

Determination of Carbendazim in Benomyl Using Infrared Spectrophotometry

Gábor Meszlényi, Judit Körtvélyessy, Éva Juhász and Mária Lelkes
Research Institute for Organic Chemical Industry, P.O. Box 41, H-1428 Budapest, Hungary

Benomyl is a well known fungicide that will undergo decomposition to carbendazim in both aqueous and non-aqueous solutions. Infrared spectrophotometry was found to be the most suitable method for the determination of carbendazim in benomyl, as it avoids the need to use a solvent. The limit of detection of the method (for carbendazim in benomyl) is 2.0–2.5%, with a precision of 5–6% relative, at the 95% probability level.

Keywords: *Benomyl; carbendazim; fungicide; infrared spectrophotometry; ultraviolet spectrophotometry*

Benomyl [methyl 1-(butylcarbamoyl)-2-benzimidazolylcarbamate] (Fundazol 50 WP in Hungary) is a well known fungicide. The determination of residual amounts of benomyl in soil and plant material by ultraviolet (UV) spectrophotometry has been reported.[1,2] High-performance liquid chromatography (HPLC) methods have been described for the determination of benomyl in the form of its principal degradation product, carbendazim (methyl 2-benzimidazole carbamate).[3–5]

The decomposition of benomyl, shown in Fig. 1, is the reverse of the last step of its synthesis; the compound is cleaved to give butyl isocyanate and carbendazim.

Chiba and Veres[6] developed an HPLC method to determine benomyl and carbendazim separately; the latter compound was detected in the form of its propyl isocyanate adduct.

The aim of the present work was to re-examine the decomposition of benomyl[7] and to develop an infrared (IR) spectrophotometric method for the determination of the carbendazim content in benomyl.

Experimental

Apparatus

A Perkin-Elmer 783 IR spectrophotometer was used.

Reagents

The samples of benomyl and carbendazim were of technical grade and were obtained from Chinoin Works, Budapest, Hungary. The potassium bromide used for the preparation of the KBr disc and for IR spectrophotometry was from Fluka Chemie, Buchs, Switzerland.

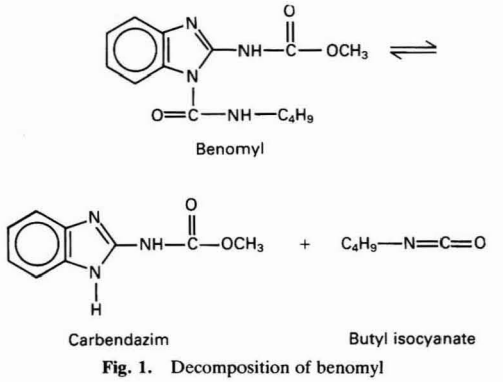

Fig. 1. Decomposition of benomyl

Procedure

Benomyl (5 mg) or carbendazim (5 mg) and potassium bromide (300 mg) were ground together (the accuracy of the weighing was 0.1 mg) and pressed into pellets. The IR spectra were recorded and then a series of carbendazim - benomyl mixtures containing different carbendazim concentrations (2–50%) were prepared (Fig. 5). Samples (5 mg) of the mixtures were used to obtain the calibration graph. The samples with an unknown carbendazim content were then analysed under the same conditions (see Table 1).

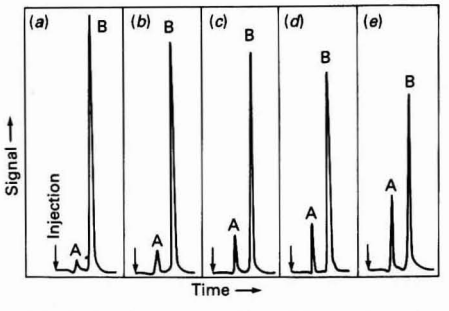

Fig. 2. Monitoring the decomposition of benomyl by chromatograms recorded at given periods of time: (*a*) 3; (*b*) 10; (*c*) 17; (*d*) 24; and (*e*) 67 min. Stationary phase, Alltech RP-18; mobile phase, acetonitrile - water (8 + 2); and wavelength of detection, 280 nm. A, Carbendazim; and B, benomyl

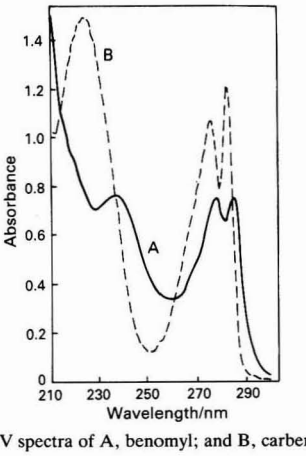

Fig. 3. UV spectra of A, benomyl; and B, carbendazim

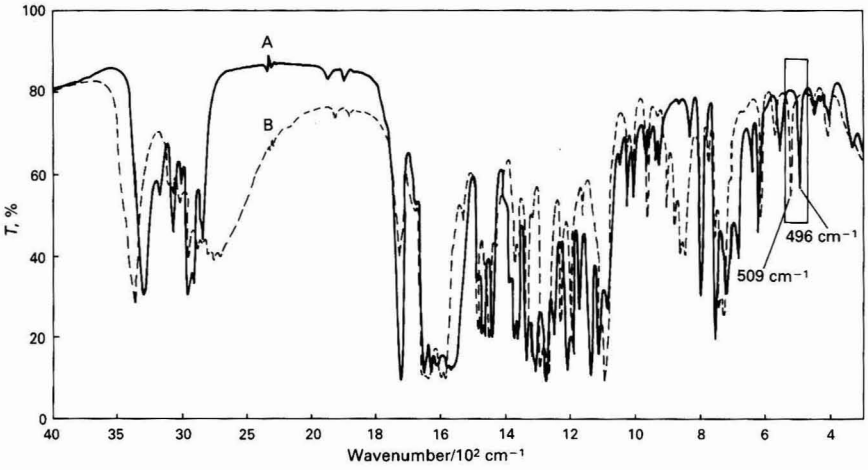

Fig. 4. IR spectra of A, benomyl; and B, carbendazim

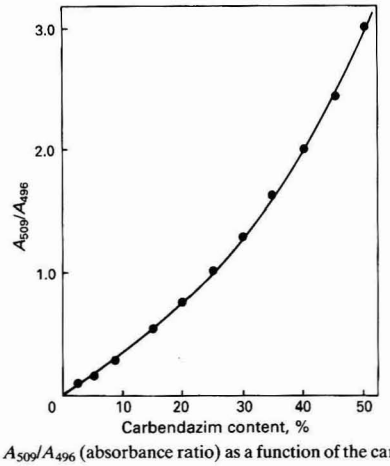

Fig. 5. A_{509}/A_{496} (absorbance ratio) as a function of the carbendazim content

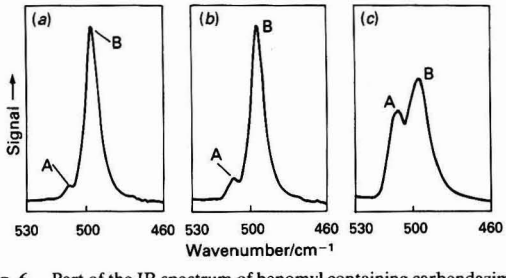

Fig. 6. Part of the IR spectrum of benomyl containing carbendazim. Carbendazim content: (*a*) 2.5, (*b*) 3.0; and (*c*) ≈20–25%. A, Carbendazim (509 cm^{-1}); B, benomyl (496 cm^{-1})

Results and Discussion

Fig. 2 illustrates the decomposition of benomyl by means of a typical series of HPLC traces. Although some evidence can be found in the literature[3–5] relating to this decomposition, the measurements made here were aimed at a more detailed examination of this feature of the compound.[7]

Based on our experiments[7] UV spectrophotometry was found to be unsatisfactory, because carbendazim can be detected only at 225 nm, and the presence of small amounts of carbendazim is shown at this wavelength only by an increase in the absorption minimum of benomyl (Fig. 3).

Table 1. Summary of IR measurements

No.	Carbendazim content, % m/m
1	35.0
2	20.0
3	9.0
4	9.0
5	3.5
6	6.0
7	5.8
8	3.5
9	3.0
10	2.0
11	2.0

The lack of success described above prompted us to consider the use of IR spectrophotometry. As can be seen in Fig. 4, the IR spectra of both benomyl and carbendazim are very similar; therefore, this technique appeared, at first sight, not to be very promising.

As a result of several experiments concerning the selection of the measuring wavenumbers, those at 509 cm^{-1} (characteristic of carbendazim) and 496 cm^{-1} (characteristic of benomyl) were found to be the most suitable. Using the method of absorbance ratios, there is no need to determine the thickness of the KBr pellet. The graph of A_{509}/A_{496} *versus* carbendazim content (X) is a hyperbola that approaches infinity at a value of $X = 100\%$ (Fig. 5).

In the concentration range $X = 0$–10%, the calibration graph is a straight line that can be described by the equation

$$Y = C\frac{X}{100 - X} = C(0.01X)[1 + 0.01X + (0.01X)^2 \ldots] \qquad (1)$$

where C is a constant.

Of course, equation (1) is only an approximate relationship; for a more precise determination or at higher carbendazim concentrations the whole hyperbolic curve must be considered.

The difference between the two peaks (13 cm^{-1}) might appear too small; however, a five-fold expansion of the abscissa (wavenumber scale) can provide good selectivity (Fig. 6). Further increase in the sensitivity can be achieved by employing a three-fold expansion of the ordinate.

The calibration graph was constructed using more than ten samples of benomyl - carbendazim mixtures. Experiments showed that the lowest measuring limit is for a carbendazim content of 2.0–2.5%. The accuracy of the method is ±5–6%, at a probability level of 95%. In view of the accuracy of quantitative IR measurements, this result appears to be good.

In our institute both the quality and amount of solvent used in the last step of the synthesis (Fig. 1) was modified for economic reasons. Incorrect choice of the solvent resulted in high carbendazim contents (Table 1, entries 1 and 2). The use of IR spectrophotometry to monitor the carbendazim content in the benomyl thus produced (Table 1) enabled the correct solvents for obtaining a pure product to be found (see entries 8–11 in Table 1).

Conclusion

The determination of the carbendazim content of benomyl cannot be effected satisfactorily by HPLC or UV spectrophotometry because of the occurrence of decomposition. No decomposition takes place in a KBr pellet, hence IR spectrophotometry is suitable for determining or checking the carbendazim content in benomyl. The proposed method is simple and does not require tedious sample preparation.

References

1. Pavoni, G., *Boll. Chim. Unione Ital. Lab. Prov. Parte Sci.*, 1979, **5**, 601.
2. El-Zeftawi, B. M. J., *Sci. Hortic. Amsterdam*, 1982, **17**, 241.
3. Kirkland, J., Holt, R., and Pease, H., *J. Agric. Food Chem.*, 1973, **21**, 368.
4. Mayer, W. J., and Greenberg, M. S., *J. Chromatogr.*, 1981, **208**, 295.
5. Burzi, F. F., Berri, A., and Zacchetti, M., *Riv. Soc. Ital. Sci. Aliment.*, 1981, **10**, 19.
6. Chiba, M., and Veres, D. F., *J. Assoc. Off. Anal. Chem.*, 1980, **63**, 1291.
7. Meszlényi, G., and Körtvélyessy, J., unpublished results.

Paper 0/01497D
Received April 4th, 1990
Accepted July 9th, 1990

Rapid Spectrophotometric Method for the Determination of Fluorene

Masaki Tachibana and Motohisa Furusawa
Faculty of Engineering, Yamanashi University, 4-3-11 Takeda, Kofu, Yamanashi 400, Japan

Fluorene reacts rapidly with the sodium salt of 1,2-naphthoquinone-4-sulphonic acid in an alkaline dimethyl sulphoxide medium containing sodium methoxide and methanol to give a coloured product. The time necessary for this reaction was 30 s with continuous and thorough stirring. The intensity of the colour was measured spectrophotometrically at 655 nm following dilution with methanol. The apparent molar absorptivity is approximately 8.7×10^3 l mol^{-1} cm^{-1}, and Beer's law is obeyed over the concentration range 1–16 μg ml^{-1} of fluorene. The colour was stable if the product was kept in a tightly stoppered flask for at least 1.5 h in the presence of small amounts of 2,6-di-*tert*-butyl-4-methylphenol.

Keywords: *Fluorene determination; 1,2-naphthoquinone-4-sulphonic acid sodium salt; spectrophotometry; alkaline dimethyl sulphoxide medium*

Fluorene, a three-ring aromatic hydrocarbon, is a common component of the hydrocarbon fractions of various fossil fuels[1–3] and is known to be an important component of environmental pollution.[4–7] For the analysis of industrial and environmental samples containing fluorene, chromatographic separation has been used extensively in combination with mass spectrometry,[3,5] fluorimetry[1,6,7] and ultraviolet spectrophotometry.[2,7] Various methods have been used not only because the samples are complex but also because the chemical properties of the constituent hydrocarbons are very similar. It is, therefore, important to develop a simple and selective method for the determination of fluorene based on its chemical reactions. However, although a number of reactions of fluorene: carboxylation[8]; acylation[9]; oxidation[10]; and so forth,[11,12] have been discussed in the literature, spectrophotometric methods for its determination have not been presented due to the lack of a simple and selective colour reaction.

In this work, the reaction conditions of fluorene with the sodium salt of 1,2-naphthoquinone-4-sulphonic acid (NQSS) were investigated for the spectrophotometric determination of fluorene. The colour development proceeded exclusively in an alkaline dimethyl sulphoxide (DMSO) medium which contained small amounts of sodium methoxide and methanol. This colour reaction has not been reported to date, although the reaction of fluorene with some other quinones in ammoniacal media has been studied for the determination of quinones.[13] The structure of the resulting product has not been elucidated but the method proposed in this paper was applicable to the quantitative determination of fluorene with several advantages, including rapidity, selectivity and simplicity.

Experimental

Reagents

Commerically available DMSO was cooled to a temperature below its freezing point (18.5 °C) until approximately 90% of it had been frozen. The remaining liquid was then removed, and the solid, which was hence more pure than the original, was collected and melted. This procedure was repeated three times for further purification. The DMSO thus obtained was stored in a tightly stoppered vessel because of its hygroscopic nature. Fluorene was purified by zone melting after the removal of concomitant anthracene using the Diels - Alder reaction with maleic anhydride. The NQSS was of guaranteed-reagent grade (Wako Pure Chemical Industries) and used without further purification. The quality of this reagent, even for the same grade, varied greatly from manufacturer to manufacturer. In preliminary experiments, the absorbance of the reaction product of fluorene (160 μg) with the reagent (10 mg) ranged from 0.2 to 0.8 according to the quality. The reagents 2,6-di-*tert*-butyl-4-methylphenol (butylated hydroxytoluene, BHT) and methanol of guaranteed-reagent grade were used (purchased from Kanto Chemical and Wako Pure Chemical Industries, respectively).

Solutions

DMSO solution of NQSS, 10 mg ml^{-1}. As the stock solution tends to decompose slowly, it is preferable to prepare the solution fresh, every one or two days.

Methanolic solution of sodium methoxide, saturated. Sodium methoxide, about 28% m/m in methanol (Nacalai Tesque), was used.

Methanolic solution of BHT, 10 mg ml^{-1}. The solution was stable for periods exceeding 1 month in a tightly stoppered vessel.

Apparatus

The absorbance and absorption spectra measurements were obtained using a Hitachi Model 200-20 spectrophotometer with 1.00-cm path length glass cells. Dried flasks and pipettes were used for the colour reaction.

Procedure

Transfer 5 ml of a sample DMSO solution containing less than 160 μg of fluorene into a 10-ml calibrated flask. Add 1.0 ml of the DMSO solution of NQSS and mix, then add 0.5 ml of the methanolic solution of sodium methoxide. Without delay stopper the flask with a tight-fitting glass plug, and stir the mixture thoroughly for exactly 30 s. Immediately dilute the mixture to the mark with the methanolic solution of BHT and mix well. Measure the absorbance of the resultant solution, at 655 nm, against the reagent blank.

Results and Discussion

Absorption Spectra

Fig. 1 shows the absorption spectra of the coloured solution and the reagent blank, which were measured against the reagent blank and distilled water, respectively. As is shown in Fig. 1, the solution obtained exhibits a maximum absorption in the vicinity of 655 nm. The wavelength, however, varied within the range 600–720 nm when the DMSO to methanol ratio in solution was changed by further dilution.

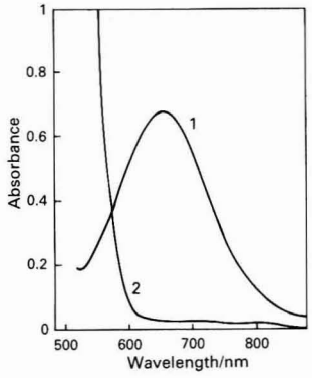

Fig. 1. Absorption spectra of: 1, the reaction product of fluorene (125 μg) with NQSS (10 mg); and 2, the reagent blank, measured against the blank and distilled water, respectively

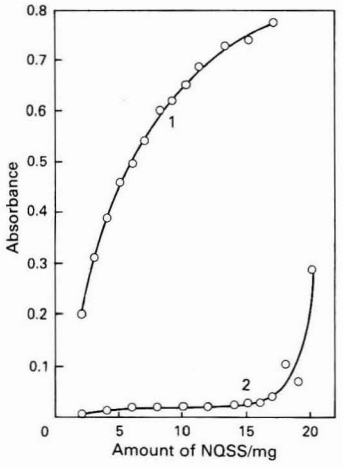

Fig. 2. Effect of the amount of NQSS. The absorbance of: 1, the reaction product of fluorene (125 μg); and 2, the reagent blank, measured at 655 nm against the corresponding reagent blank and distilled water, respectively

Effect of the Amount of NQSS

The reaction of fluorene (125 μg) was carried out using 1–17 mg of NQSS, and the absorbance of the resulting product was measured. At the same time, the effect of the reagent blank at levels up to 20 mg was also measured against distilled water. The results of these experiments are illustrated graphically in Fig. 2. The Figure (curve 1) indicates that the absorbance of the reaction product increases with an increase in the amount of NQSS used and does not become constant within the range studied. However, the variation in the absorbance is non-linear and gradually diminishes. On the other hand Fig. 2 (curve 2) shows that an increase in the amount of NQSS of more than approximately 16 mg causes the absorption signal of the reagent blank not only to rise steeply but also to be unstable. It is, therefore, recommended that 10 mg of NQSS, measured accurately, be used for the determination of fluorene.

Reaction Time and Temperature

The reaction was instantly complete in the proposed medium at room temperature. However, the absorbance of the product could not be measured instantly due to interference from the coloured by-product, which formed because decomposition of NQSS had taken place simultaneously in the medium. In order to avoid this interference, the mixture needed subsequent continuous and thorough stirring in a tightly stoppered flask. Fig. 3 shows the effect of stirring time on the absorbance of both the reaction product and the reagent blank. The result, obtained from additional experiments, in which 15 mg of NQSS were used instead of 10 mg is also shown in Fig. 3, for comparison. These results demonstrate that the absorbance of the blank can be quickly diminished by stirring the mixture, however, the absorbance of the product also decreases gradually. For the rapid determination of fluorene a 30-s reaction time was chosen.

An increase in reaction temperature produced a similar effect to that observed with an increase in stirring time. When the temperature ranged from 20 to 30 °C the absorbance of the reaction product obtained decreased by 6.5%, compared with that obtained at 20 °C. The difference between the absorbances is, however, not that large, and the variation in temperature appeared to be negligible under ordinary conditions. Therefore, the reactions were carried out at room temperature.

Effect of the Amount of Sodium Methoxide and Methanol

The presence of large amounts of methanol, being used to increase the solubility of sodium methoxide in DMSO,

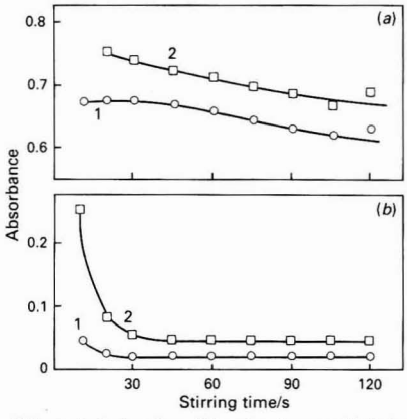

Fig. 3. Effect of stirring time. The absorbance of (*a*) the reaction product of fluorene (125 μg) with 1, 10 mg of NQSS and 2, 15 mg of NQSS; and (*b*) the corresponding reagent blanks measured against the blank and distilled water, respectively. The mixture was stirred continuously and thoroughly in a tightly stoppered flask

inhibited the reaction. Therefore, a saturated methanolic solution of sodium methoxide was used in order to minimise the amount of methanol in the reaction system. The effect of the amount of the saturated solution was studied over the range 0.1–2 ml for 6 ml of the fluorene - NQSS - DMSO mixture. In these experiments, the absorbance was almost constant for additions greater than 0.2 ml. Therefore, 0.5 ml of the saturated solution was used for the reaction.

Prevention of Colour Fading

The reaction product was unstable in the alkaline DMSO - methanol medium. Although the solution was allowed to stand in a tightly stoppered flask, the colour gradually faded as time elapsed, as shown in Fig. 4 (curve 2). However, this fading could be prevented by the addition of small amounts of BHT which is an effective anti-oxidant. Fig. 4 (curve 1) indicates that the colour is stable for at least 1.5 h in the presence of approximately 35 mg of BHT.

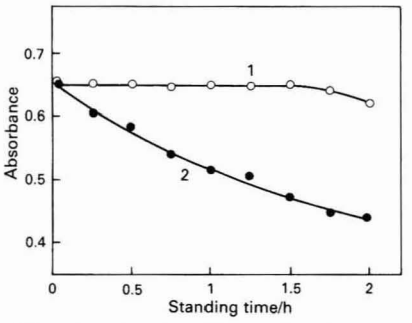

Fig. 4. Effect of standing time. The reaction mixture consisting of fluorene (125 μg), NQSS (10 mg), sodium methoxide, methanol and DMSO solution was diluted to the mark with 1, a 10 mg ml^{-1} methanolic solution of BHT or 2, methanol only

Calibration Graph

Beer's law was obeyed up to a concentration of 16 μg ml^{-1} of fluorene. The relative standard deviation was 1.3% on ten measurements carried out using 125 μg of fluorene. The reaction product possesses an apparent molar absorptivity of 8.7×10^3 l mol^{-1} cm^{-1} which was calculated on the basis of the resulting absorbance (0.657) at 655 nm in the final dilute solution (10 ml) obtained from 125 μg of fluorene and 10 mg of NQSS, even if further additions of NQSS result in an increase in the absorbance (see Fig. 2).

Effect of Foreign Compounds

The effect of 19 different aromatic compounds on the determination of fluorene (100 μg) was studied and the results are summarised in Table 1. Some aromatic carbonyl compounds and quinones have an appreciable effect on the colour development, but even in the presence of 10-fold amounts of these compounds the colour reaction of fluorene proceeds, albeit with a decrease in absorbance. Unlike such interfering compounds, analogous polycyclic aromatic hydrocarbons (except anthracene and 9,10-dihydroanthracene) and dibenzofuran do not interfere even in amounts 1000-fold greater than fluorene. Judging from the influence of anthraquinone given in Table 1, it can be presumed that the adverse effects of anthracene and 9,10-dihydroanthracene are attributable to that of anthraquinone produced by the oxidation of both hydrocarbons in the reaction mixture. Therefore, Table 1 indicates that the colour reaction is easily applicable to the selective determination of fluorene in the presence of other hydrocarbons.

Application to Practical Samples

The proposed method was applied directly to the determination of fluorene in commercially available phenanthrene and pyrene without pre-treatment. As the purification of such polycyclic aromatic hydrocarbons, mostly obtained from coal tar, is relatively difficult, the commercial chemicals usually contain a variety of small amounts of the analogues as impurities. Therefore, it is useful to determine fluorene as one of the impurities in these samples because the results may provide valuable information on the purity and the source. Fig. 5 shows the resulting absorption spectra obtained from phenanthrene (52 mg) and pyrene (105 mg) samples, which were of guaranteed-reagent grade, and the spectrum from a fluorene standard solution (120 μg). These three spectra are virtually identical over the wide wavelength range 550–850 nm, as shown in Fig. 5. Therefore, Fig. 5 indicates that the proposed spectrophotometric method is selective for the determination of fluorene in these analogous hydrocarbons.

Table 1. Effect of a variety of aromatic compounds

Compound added	Amount of added compound/mg	Absorbance at 655 nm	Difference
None*	—	0.520	—
Biphenyl	102	0.526	+0.006
Naphthalene	102	0.524	+0.004
Acenaphthene	102	0.520	0.000
Phenanthrene	105	0.521	+0.001
Anthracene	10.7	0.511	−0.009
	20.8	0.500	−0.020
9,10-Dihydroanthracene	0.12	0.508	−0.012
	0.35	0.500	−0.020
	1.2	0.494	−0.026
Fluoranthene	101	0.515	−0.005
Pyrene	101	0.514	−0.006
Dibenzofuran	102	0.516	−0.004
Dibenzothiophene	23.0	0.516	−0.004
Carbazole	0.33	0.513	−0.007
	1.1	0.493	−0.027
Acridine	2.0	0.521	+0.001
	5.0	0.503	−0.017
	10.8	0.494	−0.026
9-Fluorenone	0.34	0.515	−0.005
	1.1	0.490	−0.030
Anthrone	0.12	0.509	−0.011
	0.36	0.473	−0.047
	1.2	0.412	−0.108
Xanthene	0.31	0.509	−0.011
	1.0	0.501	−0.019
1,4-Naphthoquinone	0.010	0.509	−0.011
	0.031	0.491	−0.029
	0.10	0.469	−0.051
	0.31	0.410	−0.110
	1.0	0.400	−0.120
Acenaphthenequinone	1.1	0.514	−0.006
	2.2	0.504	−0.016
Anthraquinone	0.011	0.513	−0.007
	0.032	0.484	−0.036
	0.11	0.430	−0.090
	0.32	0.340	−0.180
	1.1	0.215	−0.305
9,10-Phenanthrenequinone	0.52	0.528	+0.008
	1.0	0.530	+0.010
	2.1	0.499	−0.021

* According to the procedure, 100 μg of fluorene were allowed to react.

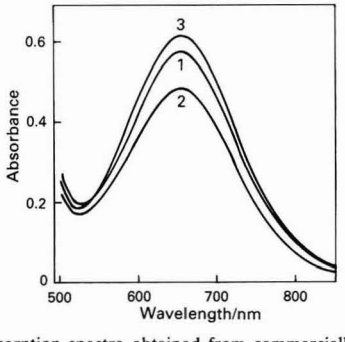

Fig. 5. Absorption spectra obtained from commercially available phenanthrene and pyrene. According to the determination procedure: 1, 52 mg of the phenanthrene; 2, 105 mg of the pyrene; and 3, fluorene standard solution (120 μg) were allowed to react

The concentrations of fluorene in commercial phenanthrene and pyrene samples were 0.21 and 0.086% m/m, respectively, according to calculation from the calibration graph. The net time required to determine fluorene in each sample was less than 5 min. In comparison with the chromatographic separa-

tion, the proposed determination procedure is selective, rapid and simple.

References

1. Bagheri, H., and Creaser, C. S., *Analyst*, 1988, **113**, 1175.
2. Davies, I. L., Bartle, K. D., Williams, P. T., and Andrews, G. E., *Anal. Chem.*, 1988, **60**, 204.
3. Wozniak, T. J., and Hites, R. A., *Anal. Chem.*, 1983, **55**, 1791.
4. Morselli, L., and Zappoli, S., *Sci. Total Environ.*, 1988, **73**, 257.
5. Bedding, N. D., McIntyre, A. E., Lester, J. N., and Perry, R., *J. Chromatogr. Sci.*, 1988, **26**, 597.
6. Draisci, R., Cecinato, A., Brancaleoni, E., and Ciccioli, P., *Chromatographia*, 1987, **23**, 803.
7. Lebo, J. A., and Smith, L. M., *J. Assoc. Off. Anal. Chem.*, 1986, **69**, 944.
8. Minabe, M., Isozumi, K., Kawai, K., and Yoshida, M., *Bull. Chem. Soc. Jpn.*, 1988, **61**, 2063.
9. Bokova, A. I., and Badiu, M., *Sint. Reakts. Sposobn. Org., Soedin.*, 1983, 38; *Chem. Abstr.*, 1984, **101**, 72396k.
10. Bhattacharjee, A. K., and Mahanti, M. K., *Oxid. Commun.*, 1984, **7**, 145.
11. Hashimoto, S., *Chem. Express*, 1988, **3**, 479.
12. Kajigaeshi, S., Kadowaki, T., Nishida, A., and Fujisaki, S., *Bull. Chem. Soc. Jpn.*, 1986, **59**, 97.
13. Zaki, M., Tarek, M., Fawzy, M. H., and Assey, M. M., *Mikrochim. Acta*, 1987, **3**, 321.

Paper 0/01383H
Received March 30th, 1990
Accepted July 24th, 1990

Spectrofluorimetric Determination of Sulphide in Natural and Wastewaters With 1,2-Naphthoquinone-4-sulphonate

A. Punta, F. J. Barragán,* M. Ternero and A. Guiraum
Department of Analytical Chemistry, University of Sevilla, 41012 Seville, Spain

A simple and sensitive spectrofluorimetric method for the determination of sulphide with 1,2-naphthoquinone-4-sulphonate (NS) has been developed. Sulphide in water samples (preserved as ZnS and then dissolved at pH 5.2 with ethylenediaminetetraacetic acid) gives a blue fluorescence (λ_{ex} 235 nm and λ_{em} 470 nm) after reaction with NS, which allows the quantitative determination of this species. The samples were stored in the dark by wrapping the storage flasks in aluminium foil. Sulphide can be determined in solutions with concentrations in the range 0.08–0.48 μg ml^{-1} with a coefficient of variation of 3.20% ($p = 0.10$; $n = 15$) for a concentration of 0.25 μg ml^{-1}. The proposed method is tolerant of many common cations and anions. A 280-fold excess of cyanide with respect to sulphide does not interfere with the analysis. A complementary procedure including a prior distillation step is described for samples with suspended materials or with a lower sulphide content. To test the utility of both procedures (direct and with distillation) various samples of natural waters, industrial wastewaters and municipal wastewaters were successfully analysed.

Keywords: *Sulphide determination; waters analysis; spectrofluorimetry; 1,2-naphthoquinone-4-sulphonate*

Hydrogen sulphide is evolved in waters during the anaerobic decomposition of sulphate or sulphur-containing compounds. The sulphide ion is also found in industrial effluents. The toxicity of the sulphide ion, caused by its great ability to co-ordinate with many metals involved in human metabolism, leads to the necessity for new sensitive and selective analytical methods for its determination. Thus, several spectrofluorimetric methods have been developed as alternatives to the Methylene Blue colorimetric method.[1] There are many instrumental methods described in the literature for the determination of sulphide at trace levels, including: spectrophotometry[2–5]; inductively coupled plasma atomic emission spectrometry[6]; gas chromatography[7,8]; ion chromatography[9,10]; potentiometry with selective electrodes[11,12]; rapid d.c. polarography[13]; normal pulse polarography[14]; and cathodic stripping voltammetry.[15,16]

The spectrofluorimetric methods currently available for the determination of sulphide are based generally on substitution reactions of sulphide ion with an organic reagent that initially forms a chelate with the cation. There are methods in which the cation forms a fluorescent chelate and the sulphide ion inhibits its fluorescence (quenching action)[17–20] and also methods in which the initial chelate is non-fluorescent and the substitution reaction releases the fluorescent organic reagent (fluorogen action).[21] The quenching of sulphide ion on tetra(acetoxymercurio)fluorescein has been used by Wronski,[17] on di(acetoxymercurio)fluorescein by Grünert *et al.*[18] and on the 3,4,5,6-tetrachlorofluorescein-mercury compound by Mori *et al.*[19] Vernon and Whitham[20] proposed a method for the determination of sulphide based on its reaction with an excess of copper, and addition, in excess, of 2-(*o*-hydroxyphenyl)benzoxazole (HPB), which forms a non-fluorescent complex with the remaining copper. The fluorescence intensity of free HPB is then measured. Bark and Rixon[21] have described a very sensitive method (detection limit 3×10^{-4} μg ml^{-1}) based on the liberation of 2,2′-pyridylbenzimidazole from its non-fluorescent mercury(II) complex by the sulphide ion.

Using the enzyme peroxidase, homovanillic acid is converted by hydrogen peroxide into a highly fluorescent product; sulphide can then be determined by its inhibitory action on this system.[22]

Only one method is based on the reducing action of sulphide in spite of its notable reducing character. In this method sulphide competes with thiamine when it is oxidised to the fluorophore thiochrome.[23]

Recently, the *o*-phthalaldehyde reaction with thiols (generated by alkylation of the sulphide ion), in the presence of the primary amine taurine to form a fluorophore, was applied to the determination of sulphide by Sano and Takitani.[24]

At present, none of the spectrofluorimetric determinations of sulphide uses a reaction involving both the reducing character of sulphide and the appearance of fluorescence. The proposed method implies the formation of a fluorescent product from the reduction of potassium 1,2-naphthoquinone-4-sulphonate (NS) by sulphide ion. This method is obviously simpler than those in the literature, indicating the formation of chelates and/or systems with multiple species. Furthermore, as it also involves fluorescence, better selectivity is attained and interferences commonly associated with other methods, such as those for cyanide, thiocyanate, thiosulphate, iodide and carbonate, are absent.

Experimental

Apparatus

Spectrofluorimeter. A Perkin-Elmer LS-5 spectrofluorimeter equipped with a Colora KS ultrathermostat and 1.00-cm cells, was used.

pH-meter. A Beckman 70 pH-meter with a combined saturated calomel - glass electrode was used for pH measurements.

Distillation apparatus. A standard distillation assembly (Büchi)[25] equipped with a 250-ml distillation flask was used. This flask was fitted with a dropping funnel and a gas inlet so that the inert gas (nitrogen) could be bubbled through the solution. The receiving vessel was a 100-ml calibrated flask.

Reagents

Sulphide standard solution. An approximately 100 mg l^{-1} solution was prepared by dissolving 0.75 g of sodium sulphide nonahydrate in 1 l of water. This was renewed and standardised every day using the iodimetric method. Solutions were used within 6 h.

Potassium 1,2-naphthoquinone-4-sulphonate solution. A 3.77×10^{-3} M solution was prepared by dissolving 0.104 g of

* To whom correspondence should be addressed: c/o Professor Garcia Gonzalez s/n. 41012-Seville, Spain.

the potassium salt in 100 ml of water and stored in an amber-coloured bottle. This NS solution must be prepared daily.

Acetic acid - potassium acetate buffer solution. A 0.1 M (total concentration) pH 5.2 solution was prepared by dissolving 6 ml of glacial acetic acid and 3.5 g of potassium hydroxide in 1 l of water.

Zinc acetate solution. An approximately 0.1 M solution was prepared by dissolving 22 g of zinc acetate dihydrate in 1 l of water. Dilute this stock solution as appropriate to produce a 0.01 M working solution.

Ethylenediaminetetraacetic acid solution (EDTA). An approximately 0.1 M solution was prepared by dissolving 40 g of the disodium dihydrate salt in 1 l of water.

Potassium chlorate solution. An approximately 0.1 M solution was prepared by dissolving 12.2 g of the salt in 1 l of water.

Phosphoric acid solution. Concentrated phosphoric acid solution (85%) (sp.gr. 1.71) was used.

Nitrogen-purifying solution. Mercury(II) chloride (5 g) was dissolved in 100 ml of 2% m/v potassium permanganate solution.

The reagents for the Methylene Blue reference method used for evaluating the performance of the proposed method were prepared as described in reference 1.

All reagents and solvents were of analytical-reagent grade. Distilled, de-ionised water was used throughout.

Procedure

Spectrofluorimetric determination of sulphide

To the sample solution, containing 2–12 μg of sulphide, in a 25-ml calibrated flask wrapped with aluminium foil to secure a convenient darkness, add 5 ml of pH 5.2 buffer solution and 0.8 ml of 3.77×10^{-3} M NS solution and dilute to the mark with water. After mixing, allow to stand for 30 min, prepare a blank solution without sulphide and measure the fluorescence intensities (25 ± 1 °C) of both solutions at 470 nm, using an excitation wavelength of 235 nm. Then calculate the difference in fluorescence intensities and plot a calibration graph.

Determination of sulphide in waters

Preserve the sample by placing 2 ml of 0.1 M zinc acetate solution into a 1000-ml flask, filling completely with the sample and stoppering. Total sulphide was determined spectrofluorimetrically either by a direct method, or by distilling as hydrogen sulphide from acidic media if the sample is not entirely free from suspended solids, or to concentrate the sulphide content into a smaller volume for greater analytical sensitivity.

(*a*) *Direct determination without distillation.* Depending on the sulphide ion content, transfer an accurate volume of sample (up to 15 ml), containing 2–12 μg of sulphide into a 25-ml calibrated flask wrapped in aluminium foil and then add 2.5 ml of 0.1 M chlorate solution. After mixing, add 5 ml of pH 5.2 buffer solution, 0.8 ml of 3.77×10^{-3} M NS solution and 0.5 ml of 0.1 M EDTA solution, and dilute to the mark with water. Similarly, prepare a blank solution without sulphide. Allow it to stand for 30 min and measure the fluorescence intensities (25 ± 1 °C) at 470 nm, using an excitation wavelength of 235 nm. Calculate the difference in fluorescence values and determine the concentration of sulphide in the sample from the calibration graph prepared using data obtained under identical conditions.

(*b*) *Determination with distillation.* Depending on the sulphide ion content, place up to 200 ml of the sample containing 8–48 μg of sulphide into a 250-ml distillation flask (for samples with sulphide concentrations lower than 0.04 μg ml^{-1}, place up to 400 ml into a 500-ml distillation flask). Introduce 1 ml of 0.01 M zinc acetate solution and 20 ml of distilled water into a 100-ml calibrated flask. Heat until boiling under a moderate flow of nitrogen (2 ml min^{-1}) which has passed through a wash bottle containing the nitrogen-purifying solution to remove sulphide and other reducing impurities. When the water begins to distil over into the receiver, add 5 ml of phosphoric acid solution to the distillation flask through the dropping funnel. After 15 min, when approximately 70 ml have distilled over, cease distillation. Remove the calibrated flask and inlet tube from the apparatus, wrap in aluminium foil and add 10 ml of 0.1 M chlorate solution. After mixing, add 10 ml of pH 5.2 buffer solution, 3.2 ml of 3.77×10^{-3} M NS solution and 2 ml of 0.1 M EDTA solution, dilute to the mark with water and proceed as described under (a) Direct determination without distillation. Prepare the calibration graph by using standard solutions of sulphide treated in the same manner.

Results and Discussion

Study of the NS - Sulphide System

When a solution of NS, which is yellow, is treated with a weakly acidic solution of sulphide, a colourless product is formed. The colour reaction has already been used for the indirect determination of sulphide in the spectrophotometric determination of unreacted NS with sulphanilic acid.[26]

The product of this reaction has fluorescence properties and the maximum wavelengths of the excitation and emission spectra at pH 5.2 are 235 and 475 nm, respectively. Ascorbic acid also produces a similar fluorescent product with NS, but its fluorescence intensity is about 10-fold lower, under similar conditions. On the other hand, NS itself shows some fluorescence when boiled for 30 min in aqueous solutions[27] (Fig. 1).

The addition of sulphide ion to a solution of the NS reagent induces fluorescence, which increases slightly over 25 min and then reaches a constant value at room temperature; the fluorescence remains constant for a further 120 min after which a decrease in the fluorescence is observed.

The measured fluorescence intensity diminished under normal light, as NS is susceptible to photochemical decomposition which increases the fluorescence of the blank. Hence, a decrease of the measured fluorescence of 5% from the initial value was observed for samples under ultraviolet or visible light. Throughout this work the samples were protected against light decomposition by wrapping them in aluminium foil to ensure good reproducibility and a consistent magnitude of measurements.

The effect of temperature was tested in the range 20–70 °C, under the conditions given in the procedure for the spectrofluorimetric determination of sulphide (see Table 1). The fluorescence intensity remained stable for measurements made at temperatures of up to 50 °C. At higher temperatures,

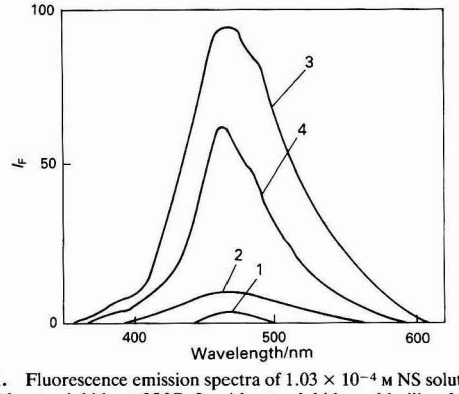

Fig. 1. Fluorescence emission spectra of 1.03×10^{-4} M NS solution. 1, Without sulphide at 25 °C; 2, without sulphide and boiling for 30 min; 3, with sulphide (1.07×10^{-5} M), at 25 °C; and 4, with ascorbic acid (1.07×10^{-5} M), at 25 °C

Table 1. Effect of temperature on the relative fluorescence intensity of the NS - sulphide system (amount of sulphide taken = 0.409 μg ml^{-1})

T/°C	Relative fluorescence intensity
20	57.1
25	55.5
30	55.5
35	55.2
40	54.9
45	56.2
50	54.5
55	53.0
60	52.0
65	52.3
70	52.5

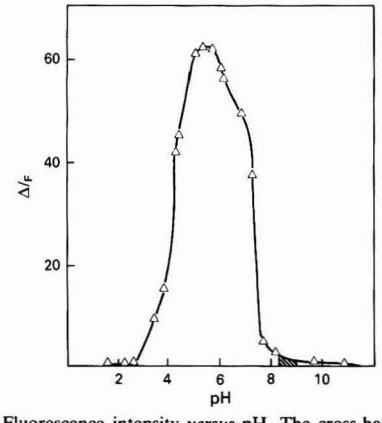

Fig. 2. Fluorescence intensity *versus* pH. The cross-hatched zone represents precipitation of NS in the sample

the relative decrease in fluorescence is due to the increase of fluorescence in the blank. Subsequent measurements were carried out at 25 ± 1 °C.

Spectrofluorimetric Determination of Sulphide

The optimisation of every variable influencing the reaction between sulphide and NS has been studied.

The reaction is dependent on pH. The fluorescence intensity *versus* pH graph (Fig. 2) shows a useful working pH range between 5.00 and 5.70. Acetate buffer (pH 5.2) was used in all subsequent fluorescence work.

The effect of the NS concentration on the intensity of the fluorescence was tested. A 5-fold molar excess of the reagent is necessary for maximum fluorescence.

The ionic strength of the solution does not affect the fluorescence of the NS - sulphide system.

The order of addition of the reagents was found not to be important. The sequence: sulphide; buffer solution; NS was adhered to during the preparation of all measured solutions.

A linear calibration graph was obtained over the concentration range 0.08–0.48 μg ml^{-1} of sulphide. The coefficient of variation (p = 0.10, n = 15) of the method is 3.02% for 0.25 μg ml^{-1} of sulphide and 3.53% for 0.12 μg ml^{-1} of sulphide.

In order to assess the possible analytical applications of the spectrofluorimetric method, the influence of some of the anions that often accompany sulphide was examined by adding different amounts of these anions to a 0.35 μg ml^{-1} sulphide ion solution. An error of 2% in the fluorescence readings was considered tolerable. The results obtained are shown in Table 2. The major interferences were caused by anions such as sulphite and nitrite. Other sulphur anions such as thiocyanate, thiosulphate and sulphate can be tolerated in greater amounts, which is of analytical interest. The relative amounts of thiosulphate, cyanide and iodide that can be tolerated are greater than those in the Methylene Blue method and most of the spectrofluorimetric methods (Table 5).

Other anions such as chlorate, iodate and periodate, that cause oxidation of sulphide also interfere. Therefore, if these oxidants are present in a sample it is unlikely that any sulphide will be present, hence, examination of these incompatible ions as interferents in these methods becomes unnecessary.

Next, the effect of foreign cations was studied. Cations which react with sulphide to form precipitates showed interferences. Other cations (calcium, magnesium, sodium, potassium and ammonium) which do not form insoluble sulphides can be tolerated to a greater excess.

Zinc acetate is normally used to preserve sulphide in water samples[9,28] and as a reagent to collect hydrogen sulphide in distillation procedures. A preliminary interference study was carried out in the presence of zinc acetate in order to establish its suitability for these purposes. The interfering effect of EDTA was also investigated, and utilised in order to enable the total dissolution of zinc sulphide at the working pH of 5.2. The EDTA also acts as a masking reagent for other cations which form insoluble sulphides. The results of these investigations appear in Table 3.

Table 2. Effect of foreign ions on the spectrofluorimetric determination of sulphide (amount of sulphide taken = 0.35 μg ml^{-1})

Ion added	Tolerance limit/μg ml^{-1}
Anions—	
Acetate	2000
Chloride, bromide, sulphate	1000
Carbonate	500
Tetraborate, arsenate, orthophosphate, tartrate	200
Nitrate, oxalate	100
Citrate	50
Cyanide	50 (100)*
Thiosulphate	20
Iodide, thiocyanate	5
Nitrite	2
Iodate, chlorate	0.5
Sulphite	0.4 (2)†
Periodate	0.3
Cations—	
Na^{I}, K^{I}	2000
NH_4^{I}	100
Ca^{II}, Mg^{II}	50
Cd^{II}	0.2 (30)*
Cu^{II}, Mn^{II}	0.1 (10)*
Zn^{II}, Fe^{III}	0.1 (2)*

* With addition of EDTA to the sample, fixed with zinc acetate.
† With addition of chlorate to the sample, fixed with zinc acetate.

Table 3. Recovery of sulphide in the presence of zinc acetate and/or EDTA

Substance added (μmol per 25 ml of sample)		Sulphide recovered (μmol per 25 ml of sample)
Zinc(II)	EDTA	
—	—	0.32
1.53	—	<0.01
0.19	—	0.27
0.03	—	0.32
—	268.8	0.18
—	107.5	0.27
—	53.8	0.33
3.82	53.8	0.18
2.29	53.8	0.32
1.15	53.8	0.32

From these results, it is concluded that: (*a*) only 0.03 μmol of zinc(II) can be tolerated in the determination of sulphide without EDTA in the medium; (*b*) no interference was seen when 53.80 μmol of EDTA were added (which represents a 168-fold molar excess) to the determination of the above amount of sulphide; and (*c*) using 53.80 μmol of EDTA, as masking and dissolving agent, 0.15 μmol of zinc(II) (a 3.6-fold molar excess) can now be tolerated. Therefore, zinc acetate can be used at the level given under Procedure as preserving agent and as a collector of hydrogen sulphide.

Under these new conditions, the effect of foreign interfering cations was studied again. Now, a 30-fold mass excess of cadmium(II), a 10-fold excess of manganese(II) and copper(II), and a 2-fold excess of zinc(II) and iron(III) can be tolerated. However, the tolerance limit for cyanide is also greater (now 100 μg ml^{-1}, previously 50 μg ml^{-1}) due to the complexing action of zinc(II) on this anion (Table 2, values in parentheses).

Determination of Sulphide in Waters

Based on the experimental work, two methods are reported for the spectrofluorimetric determination of sulphide ion in natural waters and wastewaters.

Table 4. Determination of sulphide in natural waters and wastewaters. A, river water; B, dock river water; C, industrial wastewater; and D, municipal wastewater

Type	Location of sampling	Sulphide found*/μg ml^{-1} Proposed method	Methylene Blue method†
A	Guadalquivir River	0.02 ± 0.01†	0.02 ± 0.01
B	Guadalquivir Dock (sampling point no. 1)	0.05 ± 0.01‡	0.04 ± 0.01
	Guadalquivir Dock (sampling point no. 2, commercial port)	0.10 ± 0.01‡	0.11 ± 0.01
	Guadalquivir Dock (sampling point no. 3, commercial port)	0.12 ± 0.01‡	0.15 ± 0.01
C	Effluent from a pulp industry	0.21 ± 0.03†	0.21 ± 0.01
D	Untreated sewage	0.74 ± 0.01†	0.71 ± 0.03
	Effluent from a sewage treatment plant (primary sedimentation)	0.48 ± 0.02†	0.47 ± 0.03
	Effluent from a sewage treatment plant (activated sludge)	0.08 ± 0.01†	0.08 ± 0.01

* Average of three separate determinations.
† Determination with prior distillation.
‡ Direct determination.

(*a*) *Direct method*

The sulphide in the sample is fixed with zinc acetate and treated with NS at pH 5.2 in the presence of EDTA, to enable the dissolution of zinc sulphide and other insoluble sulphides. From data reported above (under Spectrofluorimetric determination of sulphide), it is concluded that the major interferences are caused by reducing agents, whereas other substances can be tolerated at the levels normally present in natural waters and wastewaters. The addition of chlorate was found to increase the tolerance level for sulphite. When 2.5 ml of 0.1 M chlorate solution are added to the sample suspension (with sulphide fixed), up to 2 μg ml^{-1} of sulphite can be tolerated (Table 3).

A calibration graph for the range 0.08–0.48 μg ml^{-1} was prepared using standard solutions of sulphide ion treated in the same manner as the samples. The coefficients of variation calculated for replicate analyses of 0.25 and 0.12 μg ml^{-1} sulphide solutions were 3.20 and 4.39%, respectively.

(*b*) *Distillation method*

In order to assess possible analytical applications of the determination of sulphide in the presence of interfering substances or when the samples contain suspended solids, or to attain greater sensitivity by concentration of the analyte, it appears that prior separation of the sulphide from interferents may be useful. Most interfering substances can be removed by distilling the sulphide, as hydrogen sulphide which is collected on zinc acetate at pH 5.2 from acidic media. The efficiency of the collection was tested by distillation of a series of standard sulphide solutions under the conditions described under Experimental and using the Methylene Blue method as a control. Quantitative recoveries were obtained.

The possible interference from some anions (Br^-, I^-, Cl^-, $C_2O_4^{2-}$, PO_4^{3-}, SO_4^{2-}, CH_3COO^-, CN^- and SCN^-) which may also be carried over by the distillation was investigated. The tolerance limits of these anions under the distillation conditions (presence of zinc as collector in the receiver flask and addition of EDTA to aid dissolution and masking) were very similar to those reported in Table 3, which shows that the procedure is highly selective.

The calibration graph was prepared for the range between 0.04 and 0.24 μg ml^{-1}, under the conditions described under Procedure, using a 200-ml volume of sample. For samples with lower concentrations than 0.02 μg ml^{-1}, a calibration graph between 0.01 and 0.12 μg ml^{-1} was prepared, using a 400-ml volume of sample. The coefficient of variation of the method ($p = 0.10$) is 3.70%.

Table 5. Characteristics of the other reagents used for the spectrofluorimetric determination of sulphide

Reagents	pH/alkalinity conditions	$\lambda_{ex}/\lambda_{em}$/nm	Sensitivity/ μg per 100 ml of sample	Interferences*	References
1,2-Naphthoquinone-4-sulphonate					
Without distillation	5.0–5.7	235/475	4–48	Zn, Fe, SO_3^{2-}, NO_2^-	This work
With distillation	5.0–5.7	235/475	1–24	SO_3^{2-}, NO_2^-	This work
Di-(acetoxymercurio)fluorescein†	0.1 M NaOH	499/519	0.1–1	Co, Ni, Fe, I^-‡	18
3,4,5,6-Tetrachlorofluorescein-mercury†	6.4–7.0	496/550	0–400	SCN^-, $S_2O_3^{2-}$‡	19
Cu^{II} + 2-(*o*-hydroxyphenyl)-benzoxazole†	0.01 M NaOH	355/459	0.1–10	CN^-	20
Hg^{II}-2,2′-pyridylbenzimidazole	6.2–7.3	311/381	0.3–3.2	CN^-, SCN^-	21
Homovanillic + H_2O_2 + peroxidase†	8.5	—	3–320	Mn, Fe, Co, CN^-	22
Thiamine + permanganate†	7.7	375/440	0.3–2	Cd, Co, Mn, Hg, SO_3^{2-}, PO_4^{3-}, EDTA‡	23
Me-*p*-toluenesulphonate + taurine + *o*-phthalaldehyde	8.5–9.0	338/450	1–160	Fe, Mn, Cu, CN^-, $S_2O_3^{2-}$	24

* Reported substances exhibiting interferences at levels lower than a 5-fold mass excess, with respect to sulphide.
† Based on the inhibitory action of sulphide ion on the fluorescence of the system.
‡ Interference of cyanide was not reported.

Analysis of natural water and wastewaters

The proposed methods were applied successfully to the determination of trace amounts of sulphide in natural waters and wastewaters.

The results are given in Table 4 together with those obtained using the Methylene Blue method as reference. However the Methylene Blue method could not be applied directly, but only after distillation under the same conditions as for the proposed procedure, because the presence of interfering substances always prevented formation of the characteristic blue colour.

The proposed method was applied directly, and also by distillation of H_2S (depending on sulphide content and/or the interfering substances and suspended solids, present in the samples). Thus, the direct method was applied for the determination of three samples taken from Guadalquivir Dock at Seville, and the distillation method for samples from the Guadalquivir River and from municipal and industrial effluents. The results showed that the accuracy for the determination of sulphide was satisfactory.

Conclusions

Two sensitive and selective procedures for the determination of sulphide ion in waters have been established, based on the fluorescent reaction of this ion with the NS reagent at pH 5.2. The first procedure relies directly on the reaction between sulphide and NS and the second involves prior distillation as H_2S. Hence, the over-all determination time is longer, however, the method has lower determination limits and turbid waters can also be processed.

The proposed method is highly selective. The main interferents are sulphite and nitrite ions, which may also be carried over by the distillation procedure. The elimination of these interferents, if necessary (for a ratio of interferent to sulphide greater than 5 to 1), is very simple. Co-distilled SO_2 can be removed using a filter impregnated with $KHCO_3$[23] and NO_2^- can be removed by adding several drops of urea solution[25] into the receiver flask.

Many other reagents have been proposed for the spectrofluorimetric determination of sulphide (Table 5). Most of these methods are based on the inhibitory action of sulphide on a fluorescent system,[18–23] which represents a severe disadvantage in relation to their reliability. It is noticeable that their direct applicability to water samples is often limited by the interference of trace amounts of metals precipitating with the sulphide or as hydroxide due to the high alkalinity employed in the procedures. In contrast, the direct procedure [procedure (*a*)] does not suffer from the above limitations (as it is not based on fluorescence quenching) and EDTA addition and pH of the medium minimise the interference from metal ions. Many of the other methods in Table 5[18–21] are based on substitution reactions (reactions between sulphide ion and a cation that initially forms a chelate with an organic reagent) which have high sensitivities, but are less selective over-all with respect to other competitive complexing anions. For example, CN^- seems to be a strong interferent for the substitution and other methods but the proposed method tolerates a concentration of CN^- that is 286-fold in excess of that of the sulphide ion.

The proposed method is not as sensitive as some other methods, even when the distillation technique is considered. Nevertheless, the applicability of other methods to real samples has not been substantiated, and has only been tested with sulphide standards. The method of Bark and Rixon[21] always involves distillation. The method of Grünert *et al.*[18] is highly sensitive, but also involves a complicated procedure and is particularly recommended for the determination of trace amounts of sulphur in organic substances after hydrogenation.

Sano and Takitani[24] applied the fluorogenic reaction of alkylated sulphide ion with taurine and *o*-phthalaldehyde to the determination of sulphide in natural spiked waters. At present it is the only method for the determination of sulphide based on the appearance of fluorescence, but it also has the inconvenience of having to heat the solutions to 60 °C for 30 min and the method suffers interference from cyanide and some cations.

The standard Methylene Blue method for the determination of sulphide in waters[1] is less selective and 3–10 times less sensitive than the proposed method and it suffers from the practical disadvantage, that the rate of colour formation is dependent on the concentration of sulphide.

The proposed method, according to the above considerations and the satisfactory results obtained for various real samples, provides a useful tool for the determination of sulphide ion in natural waters and in both municipal and industrial wastewaters. The method shows excellent selectivity, sensitivity, reproducibility and versatility and may be used directly, or with prior distillation of H_2S.

References

1. "Standard Methods for Examination of Water and Wastewater," Fifteenth Edition, American Public Health Association, American Water Works Association, Water Pollution Control Federation, Washington, DC, 1980, pp. 1132–1151.
2. Smirnov, E. V., *Morsk. Girdofyz. Issled*, 1971, 195. *Chem. Abstr.*, 1972, **77**, 38951p.
3. Kloster, M. B., and King, M. P., *J. Am. Water Works Assoc.*, 1977, **69**, 544.
4. Wood, C. F., and Marr, I. L., *Analyst*, 1988, **113**, 1635.
5. Bahat, S. R., Eckert, J. H., Gibson, R., and Goyer, J. M., *Anal. Chim. Acta*, 1979, **108**, 293.
6. Lewin, K., Walsh, J. N., and Miles, D. L., *J. Anal. At. Spectrom.*, 1987, **2**, 249.
7. Hawke, D. J., Lloyd, A., Martinson, D. M., Slater, P. G., and Excell, C., *Analyst*, 1985, **110**, 269.
8. Caron, F., and Kramer, J. R., *Anal. Chem.*, 1989, **61**, 114.
9. Goodwin, L. R., Francom, D., Urso, A., and Dieken, F. P., *Anal. Chem.*, 1988, **60**, 216.
10. Haddad, P. R., and Hockenberg, A. L., *J. Chromatogr.*, 1988, **447**, 415.
11. Glaister, M. G., Moody, G. J., and Thomas, J. D. R., *Analyst*, 1985, **110**, 113.
12. Clysters, H., Adams, F., and Verbeck, F., *Anal. Chim. Acta*. 1976, **83**, 27.
13. Luther, G. W., Giblin, A. E., and Varsolona, R., *Limnol. Oceanogr.*, 1975, **30**, 727.
14. Leung, L. K., and Bartak, D. E., *Anal. Chim. Acta*, 1981, **131**, 167.
15. Shimizu, K., and Osteryoung, R. A., *Anal. Chem.*, 1981, **53**, 584.
16. Jaya, S., Rao, T. P., and Rao, G. P., *Analyst*, 1986, **111**, 717.
17. Wronski, M., *Fresenius Z. Anal. Chem.*, 1961, **180**, 185.
18. Grünert, A., Ballschmiter, K., and Tölg, G., *Talanta*, 1968, **15**, 451.
19. Mori, I., Fujita, Y., Goto, M., Furuya, S., and Enoki, T., *Bunseki Kagaku*, 1980, **29**, 145.
20. Vernon, F., and Whitham, P., *Anal. Chim. Acta*, 1972, **59**, 155.
21. Bark, L. S., and Rixon, A., *Analyst*, 1970, **95**, 786.
22. Guilbault, G. G., Brignac, P., and Zimmer, M., *Anal. Chem.*, 1968, **40**, 190.
23. Holzbecher, J., and Ryan, D. E., *Anal. Chim. Acta*, 174, **68**, 454.
24. Sano, A., and Takitani, S., *Anal. Sci.*, 1986, **2**, 357.
25. "The Testing of Water," Merck, Darmstadt (R.F.A.), 1974, pp. 193 and 194.
26. Punta, A., Barragan, F. J., Ternero, M., and Guiraum, A., *Int. J. Environ. Anal. Chem.*, in the press.
27. De Moerloose, P., and Baeyens, W., *Ver. Koninkl. Gen. Belg.*, 1976, **38**, 252.
28. Pomeroy, R., *Anal. Chem.*, 1954, **26**, 571.

Paper 9/04965G
Received November 20th, 1989
Accepted May 30th, 1990

Enhanced Luminescence of the Europium(III) - Terbium(III) - Dibenzoylmethane - Ammonia - Acetone System and its Application to the Determination of Europium

Yang Jinghe, Ren Xuezhen, Zou Huabin and Shi Ruiping
Department of Chemistry, Shandong University, Jinan, People's Republic of China

The enhanced luminescence of the Eu - dibenzoylmethane(DBM) - NH_3 system in the presence of Tb^{3+} and the effect of solvents on that system in the absence of Tb^{3+} were studied. The optimum conditions for co-luminescence of the Eu - Tb - DBM - NH_3 system were examined. The optimised procedure was applied to the determination of trace amounts of Eu. The detection limit is 4.0×10^{-11} M, which is about two orders of magnitude lower than that of the system in the absence of Tb. An intermolecular transfer of energy from the enhancing complex to the fluorescing complex is proposed.

Keywords: *Fluorescence enhancement; europium determination; terbium; spectrofluorimetry; intermolecular energy transfer*

The determination of Eu using the Eu - dibenzoylmethane (DBM) - diethylamine(DEA) fluorescence system has been reported.[1] However, it was not investigated in detail. During an in-depth study of the system we found that fluorescence enhancement effects were observed when La^{3+} and Lu^{3+} were added to the system in the absence of DEA. The enhancement was much greater for Tb^{3+} and Y^{3+} and still greater for Gd^{3+}. This is known as a co-luminescence effect.[2]

In this paper, the co-luminescence effect of the complex formed by Eu^{3+} with DBM and NH_3 in the presence of Tb^{3+} is reported and a spectrofluorimetric method for the determination of ultratrace amounts of Eu is described. The detection limit of Eu^{3+} with the Eu - Tb - DBM - NH_3 complex in acetone - Gum Acacia is 4.0×10^{-11} M, which is *ca.* two orders of magnitude lower than that of the system in the absence of Tb.

Experimental

Reagents

All chemicals used were of analytical-reagent grade, and distilled, de-ionised water was used to prepare the solutions. Stock solutions (1.00×10^{-2} M) of lanthanides were prepared by dissolving the oxides (99.9% or better) (Yuelong Chemical Plant, Shanghai, China) in dilute hydrochloric acid. Working solutions were prepared by appropriate dilution with water. A 2.0×10^{-3} M DBM (Beijing Chemical Plant, China) solution was prepared by dissolving the appropriate amount of the reagent in acetone. A 1.0 M NH_3 - 1.0 M NH_4Cl solution was used as a buffer.

Apparatus

All fluorescence intensity measurements were made on an RF-540 spectrofluorimeter (Shimadzu) with a 150-W Xe arc lamp as the excitation source.

General Procedure

To each of a series of 25-ml test-tubes, add the solutions in the following order: working solutions of Eu^{3+}, Tb^{3+}, DBM and buffer solutions. Dilute the mixture to 10 ml, shake and allow to stand for 15 min. Measure the fluorescence intensity in a 1-cm quartz cell at excitation and emission wavelengths of 400 and 612 nm, respectively. To study the effect of pH on the fluorescence intensity, dilute hydrochloric acid or sodium hydroxide is added after the addition of buffer to adjust the pH of the solution. When the effect of solvents is to be studied, the DBM solution is prepared by dissolving DBM in the corresponding solvent to be tested.

Results and Discussion

Fluorescence Spectra

The excitation and emission spectra of the Eu - DBM - DEA (pH = 9.25), Eu - DBM - DEA - buffer, Eu - DBM - buffer - acetone, Eu - DBM - DEA - buffer - acetone, Eu - DBM - buffer - ethanol and Eu - DBM - buffer - methanol systems are shown in Fig. 1. From the excitation spectra it can be seen that the excitation peak of the Eu - DBM - DEA system shifted after the addition of the NH_3 - NH_4Cl buffer. This may be due to the formation of a ternary complex between NH_3, DBM and Eu^{3+}.

Experiments showed that when organic solvents such as methanol, ethanol and acetone were added to the Eu - DBM - DEA - buffer system the fluorescence intensity greatly increased. From Fig. 1 it can be seen that when organic solvents were added in the absence of DEA the fluorescence intensity increased to a much greater extent (methanol>acetone>ethanol). Therefore, in subsequent experiments DEA was not added. Because of the low solubility of DBM in methanol, the solution was too turbid to determine the fluorescence intensity reliably; hence acetone was selected as the solvent, even though the greatest fluorescence intensity was obtained by the addition of methanol.

Fig. 2 shows the excitation and emission spectra of the Eu - DBM - NH_3, Tb - DBM - NH_3 and Eu - Tb - DBM - NH_3 systems. It can be seen that the intrinsic Eu^{3+} emission of the Eu - DBM - NH_3 system is weak, whereas the addition of Tb^{3+} causes a marked increase in the fluorescence intensity. The excitation and emission spectra of the Eu - DBM - NH_3 system in the presence and absence of Tb^{3+} are similar, and show the intrinsic emission of Eu^{3+} at 612 nm. Both systems show an excitation peak at 400 nm. The weak intrinsic emission peak (612 nm) of Eu^{3+} in the Tb - DBM - NH_3 system is caused by the presence of ultratrace amounts of Eu in the Tb_4O_7 used to prepare the solution.

Factors Affecting the Co-luminescence Intensity

The variation in the co-luminescence intensity was investigated as a function of the concentration of Tb^{3+} in a fixed amount of Eu^{3+} (see Fig. 3). The concentrations of Eu^{3+} employed were 1.0×10^{-7} and 1.0×10^{-8} M. From Fig. 3 it can be seen that at different concentrations of Eu^{3+} the maximum

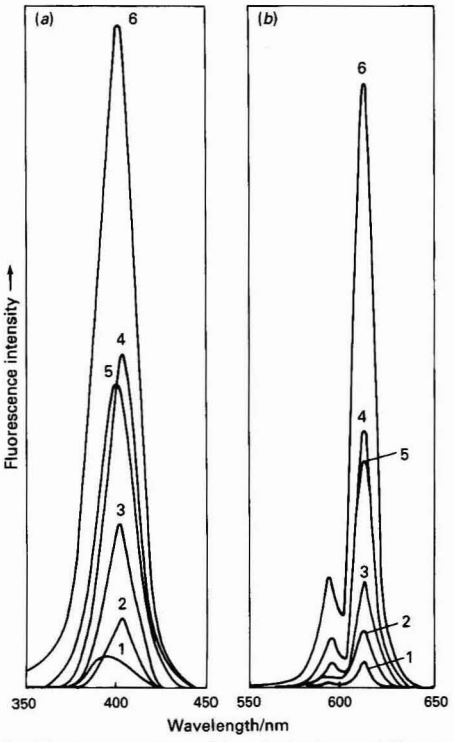

Fig. 1. Fluorescence spectra: (*a*) excitation $\lambda_{em.}$ = 612 nm; and (*b*) emission $\lambda_{ex.}$ = 400 nm. 1, Eu - DBM - DEA (pH = 9.25); 2, Eu - DBM - DEA - buffer; 3, Eu - DBM - DEA - buffer - acetone; 4, Eu - DBM - buffer - acetone; 5, Eu - DBM - buffer - ethanol; and 6, Eu - DBM - buffer - methanol. Conditions: 1.0×10^{-6} M Eu^{3+}; 4.0×10^{-4} M DBM; 0.1 M DEA; buffer, 1 ml; acetone, 20% v/v; methanol, 20% v/v; and ethanol, 20% v/v

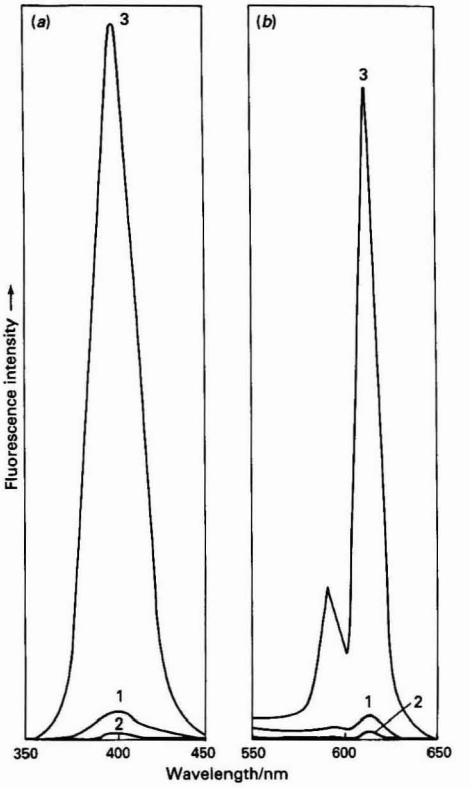

Fig. 2. Fluorescence spectra of the Eu - Tb - DBM - NH_3 - acetone system. (*a*) Excitation $\lambda_{em.}$ = 612 nm; and (*b*) emission $\lambda_{ex.}$ = 400 nm. 1, Eu - DBM - NH_3 - acetone; 2, Tb - DBM - NH_3 - acetone; and 3, Eu - Tb - DBM - NH_3 - acetone. Conditions: 1.0×10^{-7} M Eu^{3+}; 1.5×10^{-5} M Tb^{3+}; 4.0×10^{-4} M DBM; buffer, 1 ml; and acetone, 20% v/v

intensity occurs at *ca.* 1.5×10^{-5} M Tb. This result indicates that for efficient enhancement of the fluorescence intensity a specific concentration of Tb should be maintained and that no new complex is formed after the addition of Tb^{3+}.

The effect of solvents was examined. From Table 1 it can be seen that for the Eu - Tb - DBM - NH_3 system in those solvents that are immiscible with water (benzene and butanol), no enhancement of fluorescence was observed. In contrast, in those solvents that are miscible with water (methanol, ethanol, acetone, propan-2-ol and dimethyl sulphoxide), an enhancement of fluorescence was observed; further, when the concentrations of these solvents were greater than 20%, the enhancement effect decreased with an increase in solvent concentrations and was not observed at all when their concentrations were greater than 70, 60, 60, 50 and 50%, respectively.

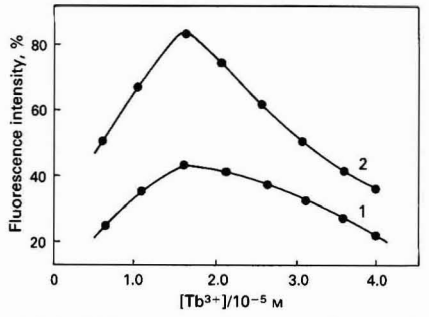

Fig. 3. Effect of Tb^{3+} concentration on co-luminescence intensity. [Eu^{3+}]: 1, 1.0×10^{-8}; and 2, 1.0×10^{-7} M. Conditions: 4.0×10^{-4} M DBM; buffer, 1 ml; and acetone, 20% v/v

Optimisation of the Eu - Tb - DBM - NH_3 - Acetone System

From the above results, it can be seen that the strong fluorescence of the Eu - Tb - DBM - NH_3 - acetone system may provide the basis for the sensitive determination of trace amounts of Eu, in addition to constituting an adequate means of studying the co-luminescence effect. Therefore, all the reaction variables were carefully considered.

The fluorescence intensity of 1.0×10^{-7} M Eu^{3+} with 1.5×10^{-7} M Tb^{3+} was measured over the pH range 8.5–9.8, using NH_3 - NH_4Cl as buffer solution (Fig. 4). Maximum fluorescence intensity was obtained over the pH range 8.5–10.0. When the amount of NH_3 - NH_4Cl solution added was between 0.5 and 3.0 ml, the maximum fluorescence intensity did not vary. The effects of DBM and acetone concentrations on the fluorescence intensity were investigated. The concentration ranges that gave the greatest intensity were 3.0×10^{-4}–8.0×10^{-4} M and 10–30% v/v, respectively. The intensity reached its highest value at room temperature after 15 min and lasted for about 1 h, after which it decreased with time due to aggregation and deposition of the minute particles of the fluorescent precipitate.

The effect of Gum Acacia on the Eu - Tb - DBM - NH_3 system was studied in the range 0.02–0.1% (m/v). It was found that in the Eu - Tb - DBM - NH_3 - acetone system the fluorescence intensity increased *ca.* 10-fold when 0.05% Gum

Table 1. Effect of solvents on fluorescence intensity. The reference intensity (100%) is that of the Eu - DBM - NH_3 system in the corresponding solvent. $[Eu^{3+}] = 1.0 \times 10^{-7}$ M

	[Methanol], % v/v			[Ethanol], % v/v			[Acetone], % v/v			[Propan-2-ol], % v/v			[DMSO*], % v/v			
	20	50	70	20	50	60	20	50	60	20	50	60	20	50	Benzene	Butanol
Eu - DBM - NH_3 - solvent	100	100	100	100	100	100	100	100	100	100	100	100	100	100	100	100
Eu - Tb - DBM - NH_3 - solvent	7500	300	99	4000	320	60	8000	500	80	1000	100	100	150	100	85	100

* DMSO = Dimethyl sulphoxide.

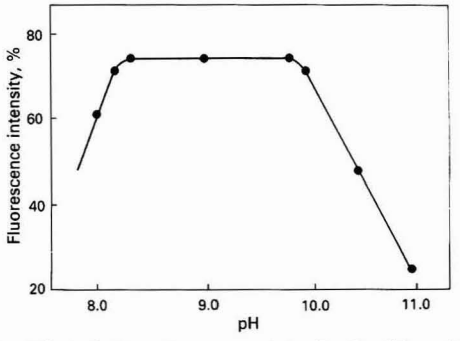

Fig. 4. Effect of pH on fluorescence intensity. Conditions: 1.0×10^{-7} M Eu^{3+}; 1.5×10^{-5} M Tb^{3+}; 4.0×10^{-4} M DBM; buffer, 1 ml; and acetone, 20% v/v

Table 2. Determination of Eu by the standard additions method

*Synthetic sample**—

Europium added/ng	Europium found/ng	Mean ± standard deviation/ng
20	19.1, 22.1, 22.2, 19.6, 20.4	20.7 ± 1.4

Standard sample†—

Standard value of Eu_2O_3,%	Determined value of Eu_2O_3,%	Mean ± standard deviation,%
0.23	0.22, 0.24, 0.24, 0.21, 0.21, 0.20	0.22 ± 0.02

* The amount of each lanthanide ion (μg) per 100 ml of the synthetic sample was as follows: La(190), Ce(440), Pr(56), Nd(240), Sm(105), Eu(10), Gd(63), Tb(10), Dy(43), Ho(12), Er(24), Tm(2.1), Yb(26), Lu(7) and Y(310).

† The standard sample was obtained from the Baotou Institute of Rare Earths, Baotou, China. Its composition (%) is as follows: La_2O_3(27.11), Ce_2O_3(49.21), Pr_6O_{11}(5.18), Nd_2O_3(16.75), Sm_2O_3(1.29), Eu_2O_3(0.23), Gd_2O_3(0.40), Tb_4O_7(0.03), Dy_2O_3(0.09) and Y_2O_3(0.27).

Acacia was added, whereas in the Eu - Tb - DBM - NH_3 - methanol (or ethanol) system the fluorescence intensity decreased when Gum Acacia was added. The stability of the Eu - Tb - DBM - NH_3 - acetone system was greatly improved after the addition of Gum Acacia. The system reached maximum fluorescence intensity in 15 min at room temperature after the solutions were mixed, and lasted for at least 3 h.

Analytical Characteristics

The fluorescence intensity of the Eu - Tb - DBM - NH_3 - acetone system is a linear function of the Eu^{3+} concentration in the range 5.0×10^{-7}–1.0×10^{-9} M under the optimised conditions. The detection limit [signal to noise (S/N) ratio = 3] is 1.5×10^{-10} M, which is *ca.* two orders of magnitude less than that of the Eu - DBM - NH_3 - acetone system. In the presence of Gum Acacia the detection limit (S/N = 3) is 4×10^{-11} M.

The effect of other lanthanide ions was studied for 1.0×10^{-7} M Eu^{3+}. The highest molar excesses that caused a variation of ±5% in the fluorescence intensity were as follows: Y^{3+} and Gd^{3+}, 40-fold; La^{3+} and Lu^{3+}, 20-fold; Sm^{3+}, 10-fold; Dy^{3+} and Yb^{3+}, 5-fold; and other ions, an equivalent molar excess. Higher concentrations decreased the intensity. Therefore, the standard additions method was employed for the determination of Eu. The results obtained (Table 2) for synthetic mixtures, which were prepared on the basis of the amount of each rare earth element in the Earth's crust,[3] indicate that the procedure is suitable for the determination of trace amounts of Eu.

Enhancement Mechanism

Fig. 2 shows that the excitation spectrum of the Eu - Tb - DBM - NH_3 system is similar to that of the system without Tb. Fig. 3 shows that there is no constant molar ratio of Eu^{3+} to Tb^{3+}. These results indicate that Tb does not form a new complex with the Eu - DBM - NH_3 system. Assuming the formation of the ternary $Eu(DBM)_3.DEA$ complex[1] in the Eu - DBM - DEA system, we believe that the ternary $Eu(DBM)_3.NH_3$ and $Tb(DBM)_3.NH_3$ complexes are both formed in the Eu - Tb - DBM - NH_3 system, and that they exist in water in the form of a solid-solution because of the similarity of their chemical properties and their low solubilities.

The DBM molecules in the ternary complexes are excited to an excited singlet state after they have absorbed light energy, after which they go to the triplet state through a radiationless transition. Because the luminescence level ($^5D_4$) of Tb^{3+}(20430 cm^{-1}, reference 4) is higher than that of the excited triplet state of DBM (20300 cm^{-1}, reference 5), it appears that the excited DBM molecules cannot transfer their energy to Tb^{3+} through an intramolecular transfer of energy, but can transfer their energy to Eu^{3+} in the $Eu(DBM)_3.NH_3$ complex, which is very similar to the $Tb(DBM)_3.NH_3$ complex, through an intermolecular transfer of energy. The concentration of the Tb complex is much greater than that of the Eu complex and each $Eu(DBM)_3.NH_3$ molecule is surrounded by many $Tb(DBM)_3.NH_3$ molecules. Therefore, the fluorescence intensity of Eu^{3+} is considerably enhanced. With the instrumentation available it was not possible to investigate the mechanism further, by the use of fluorescence lifetime measurements.

The proposed intermolecular energy transfer mechanism is well supported by the effect of solvents on the system. In organic solvents that are immiscible with water and in mixed solvents containing an organic solvent and water (in which the volume ratios are large), $Eu(DBM)_3.NH_3$ and $Tb(DBM)_3.NH_3$ exist as single molecules. The distance between $Eu(DBM)_3.NH_3$ and $Tb(DBM)_3.NH_3$ would be large and it would be difficult for the intermolecular transfer of energy to occur; hence enhancement of the fluorescence is not observed.

References

1. Tishchenko, M. A., Zheltvai, I. L., Poluektov, N. S., and Bakshun, I. V., *Zavod. Lab.*, 1973, **39**, 671.
2. Yang, J.-H., and Zhu, G.-Y., *J. Shandong Univ. (Nat. Sci. Ed.)*, 1986, **21**, 133.
3. Huang, H.-G., Liou, E.-B., and Duan, W.-Z., *Fenxi Shiyanshi*, 1985, **4**, 1.
4. Crosby, G. A., Whan, R. E., and Alire, R. A., *J. Chem. Phys.*, 1961, **34**, 743.
5. Sager, W. F., Filipeseu, N., and Serafin, F. A., *J. Phys. Chem.*, 1965, **69**, 1092.

Paper 0/01145B
Received March 15th, 1990
Accepted June 26th, 1990

BOOK REVIEWS

Spectroscopic Properties of Inorganic and Organometallic Compounds. Volume 22. Specialist Periodical Reports. G. Davidson and E. A. Ebsworth. Pp. xiv + 480. Royal Society of Chemistry. 1989. Price £130; $253.00. ISBN 0 85186 203 9.

This review of the recent literature up to late 1988 follows the same pattern as previous volumes. Individual chapters cover NMR (193 pp.), NQR (28 pp.) and rotational spectroscopies (21 pp.), 3 chapters deal with the IR spectra of main group compounds, transition element compounds and co-ordinated ligands (120 pp.), and there are two chapters of Mössbauer spectroscopy (99 pp.) and gas-phase electron diffraction (19 pp.). As usual, the information is comprehensive, with extensive references (6074 in all), and the series continues to be an invaluable reference work for inorganic chemists.

Alan Townshend

Heavy Metals in Soils
Edited by B. J. Alloway. Pp. xiii + 339. Blackie. 1990. Price £59.00. ISBN 0 216 92698 X; 0 470 21598 4 (USA and Canada).

The problem with many multi-authored books on topics such as heavy metals in soils is that they rapidly become mere catalogues of references to the ageing primary literature, with little attempt to place the subject in overall context and perspective, both scientific and historical. This book, however, edited by B. J. Alloway, takes steps to at least partially avoid this problem.

It is organised into three main sections. The first, General Principles, 80 pages long, contain four chapters: Introduction; Soil processes and the behaviour of metals; The origins of heavy metals in soils (all by Alloway); and an especially authoritative, readable and comprehensive 312-reference Methods of analysis for heavy metals in soils (by Ure). These neatly and concisely lay down the general foundations of fundamental soil chemistry, heavy metal sources and analysis which enables more effective use of the detailed information in the ten review chapters of the succeeding section on Individual Elements.

The chapters of the second section, each about 20 pages long, focus on Arsenic (O'Neill), Cadmium (Alloway), Chromium and nickel (McGrath and S. Smith), Copper (Baker), Lead (Davies), Manganese and cobalt (K. A. Smith), Mercury (Steinnes), Selenium (Neal), Zinc (Kiekens) and Other metals and metalloids (antimony, gold, molybdenum, silver, thallium, uranium and vanadium) (Jones, Lepp and Obbard). I particularly liked the sub-sectional structure common to most of the first nine of these chapters, usually introduction, geochemical occurrence, origin (soil parent, agricultural, atmospheric deposition, sewage sludges and other sources), chemical behaviour in the soil, soil - plant relationships, polluted soils and concluding comments, although Davies and K. A. Smith were clearly permitted some latitude in deviating slightly from this format. The individual authors have shown a critical discrimination in the selection of references, which range from 47 on arsenic to 151 on chromium and nickel. The amount of post-1985 material varies from 5 per cent. of the 340 references on the multi-element chapter. Other metals and metalloids, to 43 per cent. for arsenic.

The book is nicely rounded off by a useful final section of seven appendices containing summary tables of metal concentration data and regulatory limits for soils, plants and sewage sludges as well as analytical data for Certified Reference Materials.

The many sources, wide environmental distribution, diverse beneficial and harmful roles and complex behaviour of heavy metals have made them the subject of intensive investigation by research chemists, geochemists, soil scientists, agricultural chemists and environmental scientists, for whom this volume is intended. I feel that postgraduate students will find it a useful source of reference but its value for advanced undergraduates may be restricted to the overview of Section 1. At £59 it represents a good investment for the library and the committed researcher but not for the general environmental reader or typically impoverished student.

John G. Farmer

Chromatography/Fourier Transform Infrared Spectroscopy and Its Applications
Robert White, *Practical Spectroscopy Series. Volume 10.* Pp. vi + 328. Marcel Dekker. Price $99.75 (USA and Canada); $119.50 (Export). ISBN 0 8247 8191 0.

Interfacing chromatography with Fourier transform infrared spectroscopy (FTIR) has received a large amount of research attention in the past few years. The development of these hyphenated techniques has proved to be a powerful analytical tool and has significantly increased the applicability of IR spectroscopy to the analysis of complex mixtures. A book which deals with this topical issue in such a detailed and comprehensive manner, therefore, is to be welcomed.

The introductory chapter serves to summarise the basic theories and advantages of the various chromatographic techniques coupled with IR spectroscopy and discusses how chromatographic efficiency and IR spectroscopy are affected by the methods of connecting the two. There then follow three chapters, each dealing with the theory and instrumentation of a particular hyphenated technique: GC - FTIR, LC - FTIR and TLC - FTIR. Of the three techniques, only GC - FTIR has attained commercial maturity and this is reflected in the depth of coverage in this central section of the book and in the last section, dealing with industrial applications.

In Chapter 2, a full account of the instrumentation is given and a comparison of interface characteristics is made for three GC - FTIR methodologies: light-pipe, matrix isolation (MI) and sub-ambient. The trade-offs between sensitivity and expense are discussed in each instance. The less common LC - FTIR technique is dealt with in Chapter 3. Methods of dealing with the lack of IR-transparent solvents and their effects on resolution degradation are discussed. Some space is also devoted in this chapter to SFC - FTIR and its limitations. Chapter 4 deals with TLC - and HPTLC - FTIR. The two sampling techniques used, DRIFT and PAS, are discussed in relation to their lack of sensitivity and susceptibility to spectral distortion.

In the remaining two chapters, the author looks at the problems of computer-aided structure elucidation in chromatography - FTIR. Various methods are described, with most emphasis on library searching programs but with some mention of expert systems. Industrial applications of chromatography - FTIR interfaces are also discussed, although as mentioned earlier, most are in the better known GC - FTIR area.

The author's intention is to produce an up-to-date reference source for those familiar with chromatography - FTIR methods, and an introduction to the techniques and applications for those interested in future uses for chromatography - FTIR. He has largely succeeded in these aims, so that the book is a useful addition to the literature in this area.

O. M. Lacy

Trace Element Analytical Chemistry in Medicine and Biology. Volume 5. Proceedings of the Fifth International Workshop Neuherberg, Federal Republic of Germany, April 1988

Edited by Peter Brätter and Peter Schramel. Pp. xvii + 666. de Gruyter. 1988. Price DM330. ISBN 3 11 011340 6.

The fifth volume in this series of international workshop proceedings is arranged in 8 sections and reports 12 plenary papers (up to 3 per section) plus 62 presented papers. The sections are newer analytical techniques, pre-analytical treatment of samples, speciation, physiological levels and reference data, aluminium and platinum (as two elements of special interest), nutrition, pathology and metabolic processes.

The section on newer analytical methods is introduced by Tölg whose review encompasses a wide range of analytical techniques but which concentrates mainly on atomic/mass spectrometric methods. These methods dominate this section with papers on HGAAS and ETAAS, LEI spectroscopy, XRF and NAA. The last two of these papers seem to offer little which is new. It was also disappointing to find no discussion of recent advances in electrochemical techniques although this was probably due to the omission of Stoeppler's paper.

Sample preparation procedures are excellently reviewed by Knapp, who with others in this section provides much useful data on sample collection and preparation for analysis.

The section on specification is (for me) the most interesting and stimulating part of the book. A superb, comprehensive review of Duneman and Brätter ranges from speciation in natural waters to bioavailability of metals from soils to plants, to detailed studies of Ni and Zn in soya bean flour. Procedures are outlined for sample preparation, separation and elemental and protein analysis. There follows some excellent applications in which AAS, ICP-AES, ICP-MS and NAA analyses are combined with separation techniques such as HPLC, FPLC, polyacrylamide gel electrophoresis, gel filtration and anion-exchange chromatography. These studies provide data for ten elements, Ca, Cd, Cr, Cu, Fe, Mg, Mn, Ni, Se and Zn and metal-binding species including citrate, metallothieneins and proteins of high relative molecular mass.

The clinical importance of Pt and Al justifies their special attention. Alt's paper reviews the methods currently available for measuring Pt. This is followed by using an RNAA method for measuring down to 8 ng l^{-1} in urine and 5 ng kg^{-1} in liver specimens. Caroli *et al.*, combined HPLC with ICP-AES for the separation and measurement of cisplatin and carboplatin in pharmacokinetic studies. The papers on Al are concerned mainly with the application of ETAAS to the analysis of urine, serum, tissue specimens and ultrafilterable fractions from serum and with the use of ^{67}Ga as a model for Al in bioavailability studies.

The analysis and classification of dietary fibre reported by van Soest and Jones is excellent being both concise and informative. They explain the absence of effect of dietary fibre on bioavailablity of trace elements in terms of initial impairment of GI absorption by complexation followed by a later colonic fermentation yielding short chain fatty acids which transport metal ions across the colon. The remainder of this section on food/nutrition contains much valuable information on total elemental concentrations as well as speciation. The sections on pathological states and diagnosis, and on physiological levels and reference values contain little of analytical interest but have a wealth of data on trace element concentrations in healthy and diseased states.

Aggett's plenary paper gives an excellent review of the changes in pregnancy of the metabolic processes associated with trace element species, with emphasis on Cu, Zn, Se and Cr. The remainder of this section also contains good data on total trace elements and trace element speciation.

The editors claim that the workshop was "more orientated towards the state-of-the-art of trace element analytical techniques." However, the emphasis of the book is more towards the acquisition and presentation of biochemical data rather than towards new analytical procedures. The book will therefore appeal more to the biochemist/clinical scientist than it will to those concerned more with analytical developments.

There are a few typographical errors and pages 44 and 42 are interchanged. Even so this does not detract from the value of this book.

H. T. Delves

Mass Spectrometry of Biological Materials

Edited by Charles N. McEwen and Barbara S. Larsen. *Practical Spectroscopy Series. Volume 8.* Pp. xiii + 515. Marcel Dekker. 1990. Price $125.00 (USA and Canada); $150.00 (Export). ISBN 0 8247 8182 1.

I opened the package that contained this book and my heart sank. Yet another collection of standard reviews, by yet another set of internationally respected authors, I thought. But it would be unfair and unkind to view the book in this light, even though the list of contents would give this impression. There are 15 contributions, by 38 authors, with the emphasis on the isolation and mass spectrometric analysis of peptides (6 chapters). Other topics covered are glycoproteins, biogenic amines, lipids, steroids and bile acids (2 chapters), pesticide metabolites, porphyrin photosensitisers, isotope dilution methods, GC - MS, and LC - MS. The book ends with a subject index. So, what sets this book apart from other collections of reports? As a volume of the Practical Spectroscopy Series, the book often uses a didactic approach and gives many practical hints.

Biemann's considered overview of the applications of mass spectrometry to peptides carefully avoids exaggerated claims for the technique. I particularly enjoyed the lively chapter (62 pages) on strategies for the isolation and structural analysis of peptides by Shively and Paxton. Replete with many practical insights into the topic, it succeeds in alerting the protein chemist to the needs of the mass spectrometrist and *vice versa*. Given that mass spectrometry plays a major role when the Edman method fails, reviews on post-translationally modified peptides and glycoproteins are valuable inclusions.

The non-peptidic part of the text is inevitably limited in scope but the areas chosen for discussion are sensible and worthwhile. The articles vary from conventional reviews to virtual instruction manuals. Most contributions, however, hit the happy medium. At 9 pages, the primer on sterols is too brief but it is followed by a more substantial chapter on hormonal steroids and bile acids (81 pages). Weintraub admirably squeezes a representative examination of lipids into 30 pages. The last three technique-led chapters on isotope dilution, GC - MS and LC - MS are necessarily very selective. Wisely, the authors concentrate on their own expertise and experience. Henion and Lee steer the reader carefully through the myriad approaches to LC - MS, stressing the undoubted versatility of atmospheric pressure ionisation mass spectrometry in coupling with both HPLC and SFC.

Multi-author books are prone to problems such as duplication, missing topics, variable quality, inconsistent jargon and so on. This volume avoids most of the pitfalls but I still had a few grumbles. For instance, the important topics of continuous-flow FAB mass spectrometry, capillary electrophoresis and electrospray mass spectrometry are either hardly covered or not at all. In the peptide section of the book, fragmentation nomenclature is defined in three separate chapters and several other unfortunate overlaps also occur. I found it difficult to fathom the reason for the order of some of the chapters. There

is some loose language: abundant ions are often referred to as "strong" or "intense" (conjuring up images of muscular, emotionally charged entities!), and in one chapter the amounts given as "sensitivity" are presumably limits of detection. Potential purchasers of the book should also note that its price will make a sizeable hole in their budgets.

Life sciences is one of the areas that has benefited by recent innovations in mass spectrometry, especially in ionisation methods and extended mass ranges. Such developments ensure increasing applications of the technique to biological materials and make it worthwile for the mass spectrometrist to reserve a place on his/her shelf for this well balanced, amply illustrated and acid-free book.

M. E. Rose

Chemical Analysis of Polycyclic Aromatic Compounds
Edited by Tuan Vo-Dinh. *Volume 101 in Chemical Analysis: A Series of Monographs on Analytical Chemistry and Its Applications.* Pp. xxiv + 494. Wiley-Interscience. 1990. Price £70.00. ISBN 0 471 62889 1.

This is an important book as polycyclic aromatic compounds (PAC) are ubiquitous pollutants and represent the largest class of known chemical carcinogens; it follows that an up-to-date account of current developments in the analysis of PAC is required reading for all chemists engaged in environmental analysis.

The book consists of 15 chapters by a total of 27 authors, all but three with US addresses and includes many of the acknowledged leaders in the field. After an introductory chapter by the Editor, there are chapters on chromatography (gas and liquid by J. C. Fetzer; supercritical fluid chromatography by B. W. Wright and R. D. Smith) and immunological methods (by R. M. Santella and M. Stefanidis), and then chapters describing a variety of spectroscopic procedures. Interesting chapters on the novel techniques of micelle-mediated methodologies, multi-dimensional resonance mass spectrometry, and photothermal spectroscopy are contributed, respectively, by W. L. Hinze and co-workers, S. J. Weeks and colleagues and M. D. Morris.

It has to be said that this is very much a book for the specialist, with the emphasis clearly on techniques. Analysts wishing to find established and reliable procedures for determining PAC in, say, food, dust or engine exhausts will find it more useful to consult earlier texts (see, for example references 1 and 2). However, those looking for a survey of modern directions in PAC analysis, with the emphasis on spectroscopic methods, will find much of interest.

Within this framework, the coverage is a little uneven, with few clues as to the relative values of different approaches; thus, over 60 pages are devoted to laser multiphoton ionisation spectroscopy (K. Siomos) whereas, gas and liquid chromatography, surely the methods most often applied, merit fewer pages, a consequence perhaps, of the maturity of the latter techniques. On the other hand, the thought-provoking chapter by D. A. Lane on the fate of PAC in the atmosphere and during sampling, and the thorough coverage of mass spectrometric analysis of PAC by R. A. Hites, are both model reviews. Similarly, the two chapters on electronic spectroscopy (by M. Zander, and L. B. McGown and K. Nithipatikom) and those on infrared and Raman spectroscopy (by P. Stout and G. Mamantov, D. L. Gerrard and H. J. Bowley, and T. Vo-Dinh) together provide the most complete coverage yet attempted of the spectroscopic analysis of PAC.

Overall, the style and presentation of the book are pleasing with only occasional inconsistencies in PAC nomenclature; the principles behind the more innovative methods are clearly explained, and most chapters emphasise their relevance to the special problems of PAC analysis.

Highly recommended!

References

1. Bjørseth, A., and Randal, T., *Editors*, "Handbook of Polycyclic Aromatic Hydrocarbons," Volume 1, Marcel Dekker, New York, 1983.
2. Bjørseth, A., and Randal, T., *Editors*, "Handbook of Polycyclic Aromatic Hydrocarbons," Volume 2, Marcel Dekker, New York, 1985.
3. Bjørseth, A., and Becher, G., "PAC in Workplace Atmospheres: Occurrence and Determination," CRC Press, Boca Raton, 1986.

K. D. Bartle

CUMULATIVE AUTHOR INDEX

JANUARY–NOVEMBER 1990

The XXVII Colloquium Spectroscopicum Internationale

XXVII CSI

1991
NORWAY

will be held in

Grieg Hall, Bergen, Norway
June 9–14 1991

IUPAC

This traditional biennial conference in analytical spectroscopy will once again provide a forum for atomic, nuclear and molecular spectroscopists worldwide to encourage personal contact and the exchange of experience.

Participants are invited to submit papers for presentation at the XXVII CSI, dealing with the following topics:

Basic theory and instrumentation of—

- Atomic spectroscopy (emission, absorption, fluorescence)
- Molecular spectroscopy (UV, VIS and IR)
- X-ray spectroscopy
- Gamma spectroscopy
- Mass spectrometry (inorganic and organic)
- Electron spectroscopy
- Raman spectroscopy
- Mössbauer spectroscopy
- Nuclear magnetic resonance spectrometry
- Methods of surface analysis and depth profiling
- Photoacoustic spectroscopy

Application of spectroscopy in the analysis of—

- Metals and alloys
- Geological materials
- Industrial products
- Biological samples
- Food and agricultural products

Special emphasis will be given to trace analysis, environmental pollutants and standard reference materials.
The scientific programme will consist of both plenary lectures and parallel sessions of oral presentation. Specific times will be reserved for poster sessions.

PRE- AND POST-SYMPOSIA

In connection with the XXVII CSI the following symposia will be organised:

Pre-symposia—

I. GRAPHITE ATOMISER TECHNIQUES IN ANALYTICAL SPECTROSCOPY
June 6–8, 1991, Hotel Ullensvang, Lofthus, Norway.

II. CHARACTERISATION OF OIL COMPONENTS USING SPECTROSCOPIC METHODS
June 6–8, 1991, Hotel Hardangerfjord, Øystese, Norway.

III. MEASUREMENT OF RADIO-NUCLIDES AFTER THE CHERNOBYL ACCIDENT
June 6–8, 1991, Hotel Solstrand, Bergen, Norway.

Post-symposium—

IV. SPECIATION OF ELEMENTS IN ENVIRONMENTAL AND BIOLOGICAL SCIENCES
June 17–19, 1991, Hotel Alexandra, Loen, Norway.

For further information contact:

THE SECRETARIAT
XXVII CSI
HSD Congress-Conference
P.O. Box 1721 Nordnes
N-5024 Bergen, Norway.
Tel. 47-5-318414, Telex 42607 hsd n, Telefax 47-5-324555

FIRST FOLD HERE

THE ANALYST READER ENQUIRY SERVICE

For further information about any of the products featured in the advertisements in this issue, write the appropriate number on the postcard, detach and post.

FOLD HERE

THE ANALYST READER ENQUIRY SERVICE

NOV'90

For further information about any of the products featured in the advertisements in this issue, please write the appropriate number in one of the boxes below.
Postage paid if posted in the British Isles but overseas readers must affix a stamp.

PLEASE USE BLOCK CAPITALS LEAVING A SPACE BETWEEN WORDS *Valid 12 months*

1 NAME

2 COMPANY

PLEASE GIVE YOUR BUSINESS ADDRESS IF POSSIBLE. IF NOT, PLEASE TICK HERE ☐

3 STREET

4 TOWN

5 COUNTY
POST CODE

6 COUNTRY

7 DEPARTMENT/
DIVISION

8 YOUR JOB TITLE/
POSITION

9 TELEPHONE NO

OFFICE USE ONLY REC'D PROC'D

FOLD HERE

Postage will be paid by Licensee

Do not affix Postage Stamps if posted in Gt. Britain, Channel Islands, N. Ireland or the Isle of Man

BUSINESS REPLY SERVICE
Licence No. WD 106

Reader Enquiry Service
The Analyst
The Royal Society of Chemistry
Burlington House, Piccadilly
LONDON
W1E 6WF
England

ANALAO 115(11) 1397–1516 (1990) November 1990

The Analyst

The Analytical Journal of The Royal Society of Chemistry

CONTENTS

Typeset and printed by Black Bear Press Limited, Cambridge, England